

UNIVERSITY OF CRETE
SCHOOL OF SCIENCE AND ENGINEERING
DEPARTMENT OF CHEMISTRY



Department of Chemistry

Supervisor: Dr. Kelly Velonia

Dr. Emmanouil Stratakis

Masters Thesis

**“Synthesis of red shifted azobenzenes as precursors in
photopharmacology”**

Petros Mandriotis

(AM: 1002)

Curriculum Vitae

Petros Mandriotis

Location: Limassol

Telephone: 99071348

Email: Petros.mandriotis@gmail.com

Education

- **MSc** University of Crete (10/2018 – 03/2021)
- **BCs** University of Crete (2014 – 2018)
 - **Degree subject** – Chemistry 7.33

- **School** Laniteio lyceum A (2009 – 2012)
 - **Apolytyrion** – 18.7

Research experience

Undergraduate research

02 /2018- 08 /2018

Functional protein-porphyrin biohybrids

Aiming to combine proteins with supramolecular catalysts, I focused on synthesizing precisely defined, mono- and multi- protein-porphyrin biohybrids.

Post graduate research

10 /2018- 03/2021 present

Synthesis of red shifted azobenzenes as precursors in photopharmacology

Aimed at synthesizing azobenzene molecules that could undergo isomerization under visible light and more specifically, under bioluminescence.

Publications

1. Oxygen tolerant, photoinduced controlled radical polymerization approach for the synthesis of giant amphiphiles. A. Theodorou, P. Mandriotis, A. Anastasaki, K. Velonia *Polym. Chem.*, **2021**, DOI: 10.1039/D0PY01608J

Languages and technologies

- Greek, Native speaker
- English, Native speaker (Dual Nationality: English/Cypriot), (IGCSE, Cambridge certificate)

Computer skills

- Office Suite: MS Office (MS Word, MS Excel, MS PowerPoint), LibreOffice
- Scientific Suite: Chemdraw, Origin, LabVIEW, MestreNova, UV Probe.

Military service

Served 24 months in the Cypriot National Guard.

“Aut viam inveniam aut faciam”

Hannibal

Acknowledgments

I would first like to thank my thesis advisor Dr. Kelly Velonia whose door was always open whenever I ran into a trouble spot or had a question about my research or writing. She consistently allowed this paper to be my own work, but steered me in the right the direction whenever she thought I needed it

I would also like to thank Dr. Charis Gryparis and Dr. Alexis Theodorou for their guidance and friendship over the last 2 years.

I would also like to acknowledge the thesis examination committee Professor Emmanouil Stratakis, Professor Ioulia Smonou. I am grateful for the valuable comments on the thesis.

Finally, I must express my very profound gratitude to my parents for providing me with unfailing support and continuous encouragement throughout my years of study and through the process of researching and writing this thesis. This accomplishment would not have been possible without them.

Table of Contents

Curriculum Vitae	2
Acknowledgments	5
Summary	1
Περίληψη	4
1 Introduction	7
1.1 Use of light in pharmacotherapy.....	7
1.2 Designing azo-based pharmaceuticals	11
Isomeric ratio	12
Wavelength optimization	13
Cis isomer half-life.....	14
Biological stability	14
Toxicity	15
1.3 Photoswitchable drugs.....	16
Photoswitchable antibiotics.....	16
Photoswitchable anticancer agents.....	17
Photoswitches in medicine	18
1.4 Bioluminescence as a tool for pharmacology	20
Aim of the Thesis.....	23
2 Results and discussion	25
2.1 Initial Design.....	25
Tetrahalogenated azobenzene 2 - Synthesis and Spectroscopic Study	26
Tetrahalogenated azobenzene 4 - Synthesis and Spectroscopic Study	30
Trihalogenated azobenzenes	32
Wavelength tuning for blue light isomerization	37

2.2 Design and synthesis of mono- and di-fluorinated azobenzenes as precursors for amination	37
2.3 Synthesis and spectroscopic evaluation of aminated azobenzenes.....	43
UV-Vis spectroscopic studies on azobenzene 15	49
UV-Vis spectroscopic studies on azobenzene 16	50
Effect of water on the cis half-life of azobenzene 16	53
2.4 Bromination studies	55
2.5 Bioluminescence studies	65
2.5.1 Bioluminescent cultures	65
3 Conclusions	71
4 References	73
5 Experimental Section	76
Instruments and methods.....	76
UV/Vis Spectra and Photoisomerization:.....	76
Substrate synthesis	77
Compound 1	77
Compound 2	77
Compound 3	78
Compound.....	79
Synthetic approaches toward the azobenzene derivative 5	80
Synthetic approaches toward the azobenzene derivative 8	81
Compound 6	82
Compounds 7 & 8	82
Compound.....	83
Compound 10	84
Compound 11	85

Synthetic approach toward the azobenzene derivative 12	86
Compound 13	86
Compound 14	87
Compounds 15 & 16	87
Synthetic approaches toward the azobenzene derivative 17	88
Compound 18	90
Compound 19	90
Compound 20	91
Synthetic approaches toward the azobenzene derivative 21	92
Compound 22	92
Synthetic approaches toward the azobenzene derivative 23	93
Molar extinction coefficient measurements	93
Bacterial cultures	94
Bacterial luciferase induces isomerization	94
Supplementary information.....	95

Summary

Aim of this study was the synthesis of red shifted azobenzenes in order for isomerization in the visible range of the spectrum to be achieved, avoiding the toxic UV light. Azobenzenes were chosen since they are pivotal molecules in photopharmacology, a clinical approach that uses light as a mean for drug activation. In addition to this, we examined the possibility of isomerization using bioluminescence, as it is widely applied in the pharmaceutical area and in particular in bioluminescent imaging.

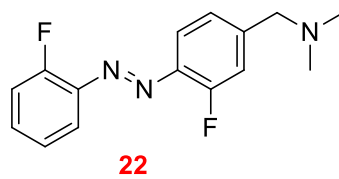
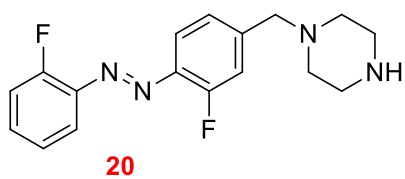
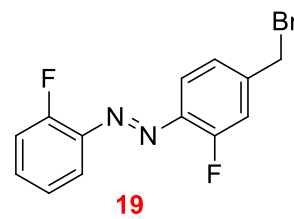
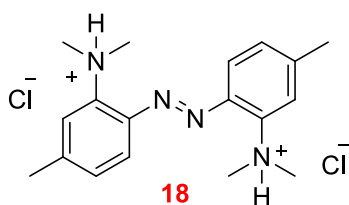
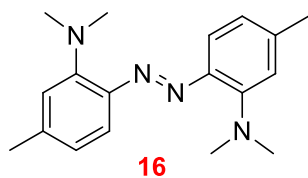
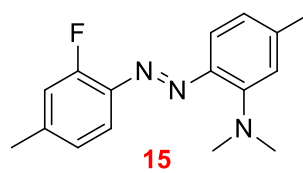
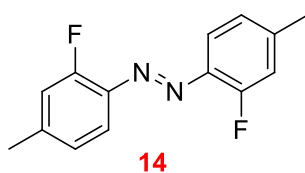
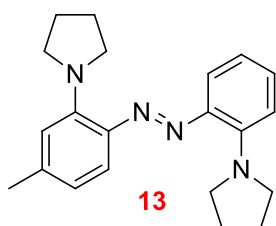
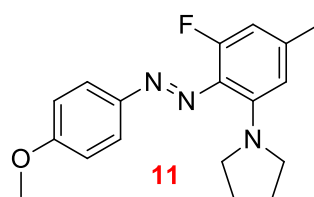
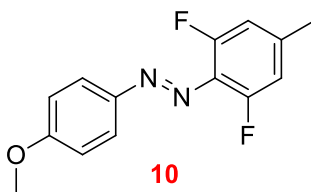
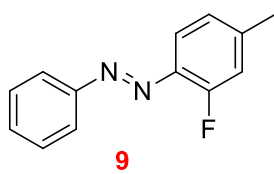
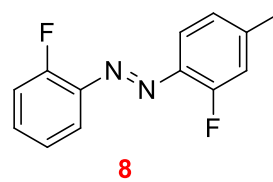
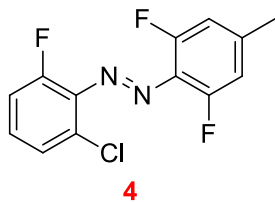
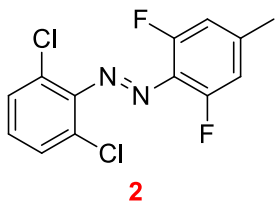
Our efforts to synthesize red shifted azobenzenes were initially based on tetrahalogenated azobenzenes reported in literature, according to which the tetra-ortho-fluoro azobenzene undergoes isomerization in the green region of the spectrum, while the tetra-ortho-chloro azobenzene undergoes isomerization in the red region of the visible spectrum. With the intention of synthesizing an azobenzene derivative that undergoes isomerization in the yellow region of the visible spectrum, in order to investigate the possibility of isomerization with firefly bioluminescence, we prepared two tetrahalogenated derivatives bearing a combination of ortho- fluoro and ortho- chloro substituents. This study led to the conclusion that when comparing tetrahalogenated azobenzene derivatives, the fluoro substituent had a dominant effect over the chlorine in determining the red shifted nature of azobenzenes. This conclusion was based on the fact that the azobenzenes **2** and **4** bearing two and three fluorine substituents respectively, exhibited isomerization solely in the green part of the visible spectrum. For this reason, we decided to attempt the synthesis of a trihalogenated azo compound bearing two chlorine substituents and just one fluorine substituent for two reasons. Firstly, we aimed to investigate the red shifted nature of the compound and secondly to attempt nucleophilic aromatic substitution reactions on the fluorinated ring to investigate the effect of various nucleophiles.

As efforts at wavelength optimization in the yellow region of the spectrum weren't successful, we opted to synthesize azobenzene derivatives designed to undergo blue light induced isomerization in order to investigate the possibility of isomerization using bacterial bioluminescence. For this purpose, we synthesized a series of mono- and di- ortho substituted azobenzenes as precursors for nucleophilic aromatic substitution to screen various nucleophiles for red shifted behaviours. It was found in literature that ortho

aminated azobenzenes fitted our requirements, as these derivatives absorb in the visible range, possess a small *cis* lifetime and are not reduced by glutathione. The ortho amination reactions, however, were not straightforward as our attempt of nucleophilic aromatic substitution, using pyrrolidine as a nucleophile, yielded a non-photostable azobenzene. Considering other alternatives, we attempted ortho amination using a simpler amine, dimethylamine, in an effort to test photostability. Ortho amination using dimethylamine was partly based on literature, taking advantage of the hydroxide assisted thermal decomposition of DMF into dimethylamine and formate. As the reaction did not proceed under the reported conditions, we optimized both the apparatus and conditions to ortho aminated products for possible blue light isomerization. Spectrophotometric studies proved that the ortho aminated derivative **16** displayed poor solubility in water. In an effort to increase overall solubility in water we studied the substitution of the azo compound with a polar/water soluble group, such as piperazine. We carried out various reactions including a combination of benzylic bromination, nucleophilic aromatic substitution and benzylic S_N2 reactions that did not result in the expected product.

In the final part of the Thesis, we investigated the possibility of bacterial luciferase induced isomerization. For this purpose, we isolated blue light emitting bioluminescent bacteria from fresh sea shrimp and cultivated them on agar plates containing LA medium. We then proceeded with bioluminescent photometric studies by recording UV-Vis spectra before and after irradiation with bioluminescent bacteria in order to gain a qualitative understanding of the effect that bacterial bioluminescence has on azobenzene isomerization.

In summary, 14 new azobenzene derivatives were synthesized. The azobenzenes **2** and **4** showed isomerization under green light irradiation. The azobenzenes **15** and **16** showed isomerization under blue light irradiation and specifically azobenzene **16** was shown to undergo partial isomerization with bacterial bioluminescence.



Abstract Scheme

Περίληψη

Στόχος της παρούσας εργασίας ήταν η σύνθεση υποκατεστημένων αζωβενζολίων με βαθυχρωμική μετατόπιση, προς αποφυγή της τοξικής UV ακτινοβολίας, καθώς τα μόρια αυτά, συζευγμένα με φαρμακευτικά μόρια, προσελκύουν το ενδιαφέρον στον τομέα της φωτοφαρμακολογίας η οποία περιλαμβάνει την ενεργοποίηση φαρμάκων με την χρήση του φωτός. Επίσης δευτερεύων στόχος της παρούσας εργασίας ήταν η διερεύνηση πιθανού ισομερισμού των υποκατεστημένων αζωβενζολίων με την χρήση την βιοφωταύγειας, καθώς χρησιμοποιείται ευρέως στην Ιατρική με την μέθοδο της απεικόνισης βιοφωταύγειας.

Στη παρούσα εργασία ασχοληθήκαμε με την σύνθεση αζωβενζολίων που σχεδιάστηκαν ώστε να παρουσιάζουν βαθυχρωμική συμπεριφορά. Το πρώτο κομμάτι της μεταπτυχιακής εργασίας εστιάζει στη σύνθεση τέτρα-ορθο αλογονωμένων αζωβενζολίων καθώς υπάρχει βιβλιογραφική αναφορά ότι το τετρα-ορθο-φθόρο υποκατεστημένο παράγωγο ισομερίζεται στην πράσινη περιοχή του ορατού ενώ το τετρα-ορθο-χλώρο παράγωγο ισομερίζεται στην κόκκινη περιοχή του ορατού φάσματος. Στοχεύοντας στη σύνθεση αζωβενζολίων που ισομεριώνονται στην κίτρινη περιοχή του φάσματος, θελήσαμε να ερευνήσουμε την πιθανή ισομερίωσή τους χρησιμοποιώντας την βιοφωταύγεια της πυγολαμπίδας. Για τον σκοπό αυτό συνθέσαμε δύο τετραλογονωμένα παράγωγα που φέρουν υποκαταστάτες φθορίου και χλωρίου στις ορθο- θέσεις. Παρατηρήσαμε ότι η υποκατάσταση με άτομα φθορίου καθορίζει την βαθυχρωμική μετατόπιση των αζωβενζολίων, σε σύγκριση με την αντίστοιχα χλωρο- υποκατεστημένα αζωβενζόλια, καθώς τα αζωβενζόλια **2** και **4** παρουσίαζαν ισομερίωση στην πράσινη περιοχή του ορατού. Για αυτό τον λόγο έγινε προσπάθεια σύνθεσης ενός τριαλογονωμένου παραγώγου που φέρει δύο άτομα χλωρίου και ένα άτομο φθορίου σαν υποκαταστάτες σε ορθο θέσεις. Η προσπάθεια σύνθεσης αυτού του παραγώγου έγινε τόσο για να μελετήσουμε την βαθυχρωμική μετατόπιση του τριαλογονωμένου αζωβενζολίου, όσο και για να συντεθεί ένα υπόστρωμα κατάλληλο για πυρηνόφιλη αρωματική υποκατάσταση με μια ποικιλία πυρηνόφιλων αντιδραστηρίων, χρησιμοποιώντας το φθόριο σαν αποχωρούσα ομάδα. Η

μελέτη της βαθυχρωμικής μετατόπισης των παραγόμενων προϊόντων αποτελεί επίσης στόχο αυτής της προσπάθειας.

Καθώς η προσαρμογή του μήκους κύματος στην κίτρινη περιοχή του ορατού δεν ήταν εφικτή, επιλέξαμε τη μπλε περιοχή για να ερευνήσουμε την πιθανή ισομερίωση των υποκατεστημένων βενζολίων, χρησιμοποιώντας την βακτηριακή βιοφωταύγεια. Για αυτό τον λόγο συνθέσαμε μία σειρά από ορθο- υποκατεστημένα μονο- και δι-φθορο αζωβενζόλια ως πρόδρομες ενώσεις για την πυρηνόφιλη αρωματική υποκατάσταση με μία σειρά πυρηνόφιλων αντιδραστηρίων. Αναφέρεται στη βιβλιογραφία πως η ορθο αμίνωση πληρούσε τις προϋποθέσεις για την σύνθεση των επιθυμητών αζωβενζολίων, καθώς τα ορθο αμινωμένα παράγωγα απορροφούν στο ορατό, εμφανίζουν γρήγορη θερμική χαλάρωση στην *trans* μορφή και δεν ανάγονται από γλουταθειόνη.

Η ορθο αμίνωση ωστόσο επιφύλασσε συγκεκριμένες δυσκολίες, καθώς χρησιμοποιώντας την πυρολιδίνη σαν πυρηνόφιλο βασισμένοι στην βιβλιογραφία, είχαμε ενδείξεις φωτοαποικοδόμησης του μορίου. Ψάχνοντας για εναλλακτικούς τρόπους σύνθεσης, χρησιμοποιήσαμε μια πιο απλή αμίνη, την διμεθυλαμίνη με σκοπό να εξετάσουμε το τελικό αζωβενζόλιο για την φωτοσταθερότητα του. Η ορθο αμίνωση χρησιμοποιώντας την διμεθυλαμίνη σαν πυρηνόφιλο βασίστηκε εν μέρει στην βιβλιογραφία, όπου αναφέρεται η πυρηνόφιλη αρωματική υποκατάσταση μέσω της *in situ* αποικοδόμησης του DMF σε διμεθυλαμίνη και φορμικό οξύ, παρουσία βάσης. Η συγκεκριμένη αντίδραση αρχικά δεν έδωσε τα επιθυμητά προϊόντα. Εξετάζοντας τους πιθανούς λόγους αποτυχίας, σχεδιάσαμε μια νέα πειραματική διάταξη που επέτρεψε την μελέτη των παραμέτρων που επηρεάζουν την αντίδραση και ταυτοποιήσαμε σαν βέλτιστη θερμοκρασία τους 70°C. Έπειτα από επιτυχή αντίδραση προχωρήσαμε σε μελέτες ισομερίωσης των προϊόντων με τη βοήθεια φασματοσκοπίας NMR και UV χρησιμοποιώντας την μπλε περιοχή του ορατού.

Κατά την διάρκεια των φασματοσκοπικών μελετών αποδείξαμε τον ισομερισμό *cis/trans* παρουσία μπλε φωτός αλλά ταυτόχρονα παρατηρήσαμε ελάχιστη υδατοδιαλυτότητα του αμινωμένου παραγώγου. Σε μια προσπάθεια να καταστήσουμε το μόριο πιο υδατοδιαλυτό, θελήσαμε να προσθέσουμε στο αζωβενζόλιο έναν πιο πολικό/υδατοδιαλυτό υποκαταστάτη, όπως η πιπεραζίνη, η οποία αποτελεί δομική μονάδα

πολλών φαρμακευτικών ενώσεων. Προχωρήσαμε σε μία σειρά από αντιδράσεις που βασίστηκαν σε συνδυασμό βενζυλικής βρωμίωσης, S_N2 και πυρηνόφιλης αρωματικής υποκατάστασης, οι οποίες όμως δεν οδήγησαν στο επιθυμητό προϊόν.

Για το τελικό μέρος της εργασίας εξετάσαμε την πιθανή ισομερίωση του παραγώγου **16** με την χρήση βακτηριακής βιοφωταύγειας. Για αυτό τον λόγο απομονώσαμε τα κατάλληλα βακτήρια από γαρίδες και τα αναπτύξαμε σε στερεή καλλιέργεια, χρησιμοποιώντας θρεπτικό μέσο Luminescent Agar (LA). Τέλος πραγματοποιήσαμε φασματοσκοπικές μελέτες UV-Vis παίρνοντας με βακτηριακή βιοφωταύγεια.

Συνοψίζοντας, συντέθηκαν 14 νέα υποκατεστημένα αζωβενζόλια. Τα αζωβενζόλια **2** και **4** παρουσίασαν ισομερισμό στην πράσινη περιοχή του ορατού. Τα αζωβενζόλια **15** και **16** παρουσίασαν ισομερισμό στην μπλέ περιοχή του ορατού και πιο συγκεκριμένα το αζωβενζόλιο **16** παρουσίασε μερικό ισομερισμό με τη χρήση βακτηριακής βιοφωταύγειας.

1 Introduction

Pharmacotherapy is a pillar of modern medicine used to cure diseases through the administration of drugs. There are however several drug related issues such as poor drug selectivity which can result in side effects^{1,2} and, less often, drug resistance that hinder the efficacy of pharmacotherapy.³

Drug selectivity relates to affinity of a drug to various targets other than its own. Many anticancer agents for example are known for their dreadful side effects and because of this, efforts have been made towards more targeted therapies. Poor selectivity on the other hand, severely limits the therapeutic window which leads to a decrease in allowed dosage. This is a major concern in drug development as roughly 85 % of small molecule drugs developed and researched are discontinued due to poor selectivity.⁵ Another concern in modern day medicine is drug resistance which is notable in antibacterial molecules due to the rise of resistant bacterial strains. Resistance can be attributed to the build-up of antibiotic molecules in the environment which kill-off of sensitive bacteria promoting the growth of more resilient strains. This is also an example of poor selectivity as the drug is not only active following administration, but also after excretion.^{1,6}

Poor selectivity is a consequence of drugs being active at unwanted times and sites both in the body and in the environment. Photopharmacology offers a new approach for controlling drug activity. Unlike chemicals, photons do not contaminate and show low to no toxicity in subject studies. Furthermore, light of a given intensity and wavelength can be delivered with immense precision which is key to a more targeted therapy.¹

1.1 Use of light in pharmacotherapy

Light has been used in medicine over the past years in methods such as optogenetics and photodynamic therapy. Optogenetics, mainly applied in neuroscience, involve synthetic biology approaches for the expression of photoresponsive proteins.⁷ Photodynamic therapy is a widely applied method which involves light and a photosensitizing agent used in conjunction with molecular oxygen to generate singlet oxygen thus, causing cell death.⁸ Photodynamic therapy has proven to be effective against microbial cells including bacteria, fungi and viruses. It is also used to treat tumours including brain, neck, lung and skin cancer.

Its applications however are limited to situations where cell death is necessary. Photopharmacology on the other hand offers the opportunity to induce a biological response without causing cell death (Figure 1).

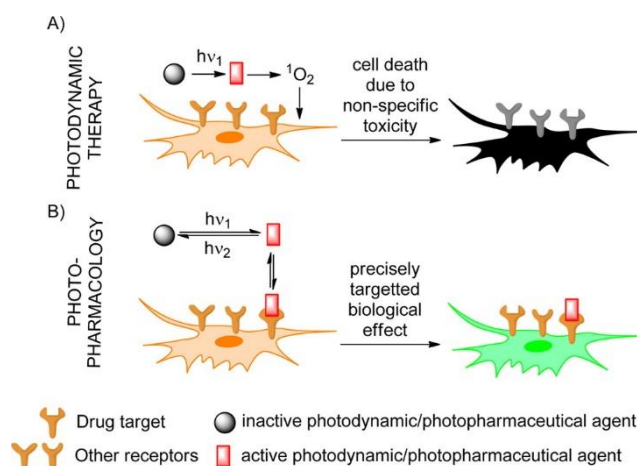


Figure 1 A. Photodynamic therapy resulting in cell death; B. Photopharmacology inducing a biological response.¹ Reprinted with permission from *J. Am. Chem. Soc.* 2014, 136, 6, 2178–2191. Copyright (2014) American Chemical Society.

Photopharmacology revolves around the insertion of a photoswitchable bioactive molecule added either as an extension to the compound under study (*e.g.* a drug) or built into its backbone. Dynamic control of the activity of this compound is thus achieved through a photoswitchable unit. This method is revolutionary in medical applications yielding high selectivity drugs with full temporal and spatial control.¹

Molecular photoswitches are compounds that undergo a reversible change in structure and properties when irradiated with light. Over the years many types of photoswitches have been developed, though two types have been of most interest in the field of photopharmacology, namely azobenzenes and diarylethenes (Figure 2).¹

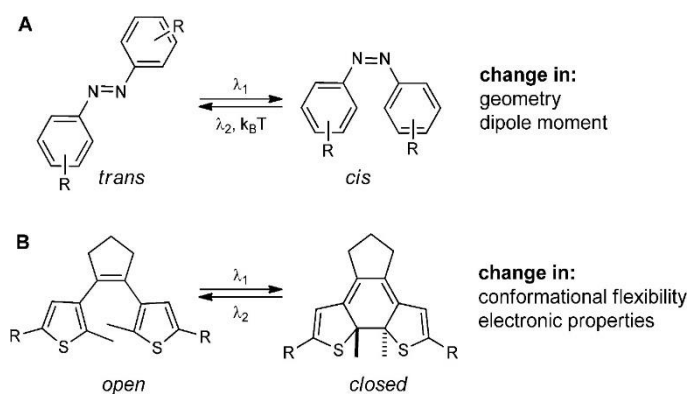


Figure 2 Photochemical conversion of azobenzenes and diarylethanes.¹ Reprinted with permission from *J. Am. Chem. Soc.* **2014**, *136*, **6**, 2178-2191. Copyright (2014) American Chemical Society.

Diarylethanes, consisting of a hexatriene frame, can undergo a reversible, photochemical cyclization altering the electronic properties as well as the rigidity of the molecule. Both isomers are thermodynamically stable and can be switched from the open to the closed (rigid) isomer using light of different wavelengths (Figure 2).⁹

The *trans/cis* photoisomerization of azobenzenes results in a large change in both geometry and polarity. This fact has led to extensive research and development of azo-containing photoswitchable drugs.¹ It should be noted that the main objective of this thesis focuses solely on the development of new azobenzene switches. The *trans (E)/cis (Z)* isomerization of azobenzene takes place upon irradiation with UV-visible (UV-Vis) light, mechanical stress or electrostatic stimulation while the *cis/trans* isomerization arises spontaneously in the dark due to the thermodynamic stability of the *trans* isomer.¹⁰

The *trans* azobenzene UV-Vis spectrum contains two bands in the UV-visible region (Figure 3). The strong absorption band with λ_{max} ca. 320 nm arises from the symmetry allowed $\pi\text{-}\pi^*$ transition. The weak visible region band (λ_{max} ca. 450 nm) arises from the forbidden $n\text{-}\pi^*$ transition. The $\pi\text{-}\pi^*$ transition of the *cis* azobenzene (λ_{max} ca. 270 nm) is weaker while the $n\text{-}\pi^*$ transition (λ_{max} ca. 450 nm) is stronger than those of the *trans* isomer. This allows for the qualitative characterization of isomerization via UV-Vis spectroscopy.¹⁰

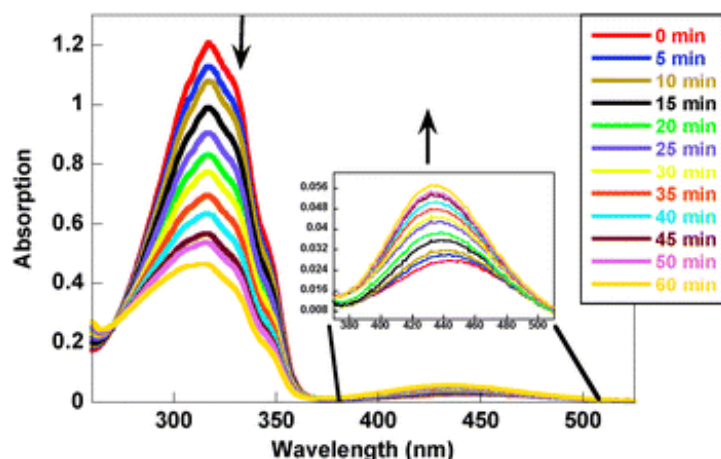


Figure 3 UV-Vis spectrum of azobenzene.¹⁰ Reproduced from Ref. 10 with permission from The Royal Society of Chemistry.

The azobenzene ground state is a singlet state (S_0), with S_1 and S_2 being the first and second singlet excited states. The S_1 state arises by direct $S_1 \leftarrow S_0$ excitation or intersystem crossing between S_2 and S_1 states (*i.e.* relaxation of the S_2 state). The S_1 and S_2 states differ in energy and conformation in the *cis* and *trans* isomers. The $n \rightarrow \pi^*$ and $\pi \rightarrow \pi^*$ transitions correlate to the $S_1(n\pi^*)$ and $S_2(\pi\pi^*)$ states, respectively. *Cis/trans* isomerization and vice versa can be achieved by irradiating at either transition. *Trans* azobenzene undergoes *trans/cis* isomerization following $S_1 \leftarrow S_2$ and $S_2 \leftarrow S_0$ excitation (Figure 4). In the same manner, the *cis* azobenzene converts to the *trans* isomer by excitation to the S_1 or S_2 state (Figure 4).

10

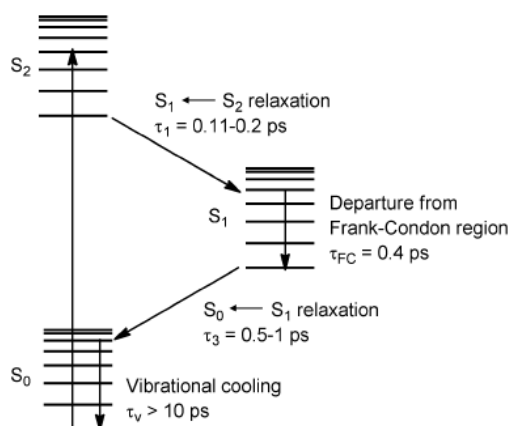


Figure 4 Simplified Jablonski energy diagram of *trans*-azobenzene. Reproduced from Ref. 10 with permission from The Royal Society of Chemistry.

The isomerization mechanism is not yet completely understood but four possible pathways have been proposed and reported in literature (Figure 5), namely:^{11,12,13,14}

10

- The rotational mechanism which assumes that the N=N bond breaks allowing free rotation around the N-N bond.
- The inversion mechanism that involves a sp hybridized N atom where the N=N-C angle is increased to 180° while, the C-N=N-C dihedral angle is fixed at 0°.
- The converted mechanism that requires both C-N=N-C angles to increase to 180° forming a linear transition state.
- The inversion mechanism that involves both large changes in the C-N=N-C dihedral angle and smaller changes in the N=N-C angle occurring simultaneously.

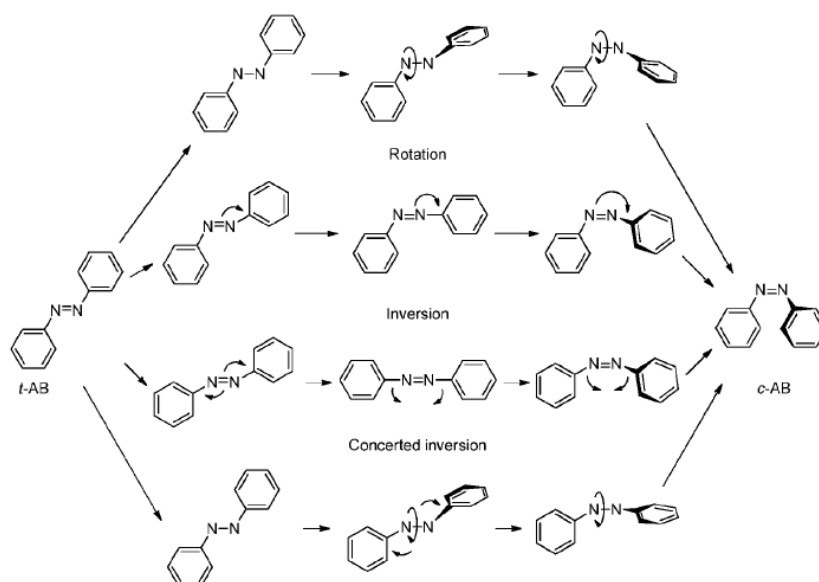


Figure 1 The four mechanisms proposed for azobenzene isomerization. Reproduced from Ref. 10 with permission from The Royal Society of Chemistry.

1.2 Designing azo-based pharmaceuticals

Pharmacokinetics and pharmacodynamics are crucial factors of pharmacology as they determine the effect the drug will have on the target as well as on the rest of the body.¹⁵ Pharmacokinetics concern drug absorption, distribution, metabolism, and excretion and can be evaluated on the basis of factors such as polarity, lyophilicity and size of bioactive compound. Since the photoisomerization of azobenzenes causes a shift in polarity, the incorporation of this molecular switch on a bioactive compound can be used to achieve dynamic control. The change in the geometry and polarity of a drug at different time-points during its distribution can be beneficial when concerning the increase of its effectiveness.

Two methods have deployed shift in polarity as means of altering drug efficacy.¹ The first approach, reported by the groups of Trauner¹⁶ and Feringa,¹⁷ involves the insertion of a photoswitchable molecule within the pharmacophore backbone (Figure 6A). The second method reported by Y. Zhang et al.,¹⁸ is applicable for multivalent drugs and involves addition of a photoswitch between two ligands (Figure 6B).

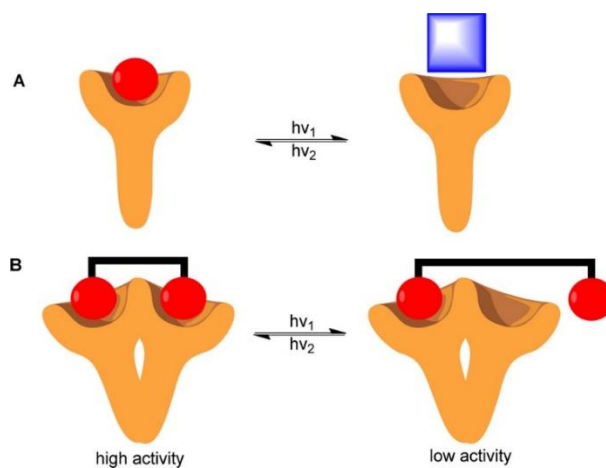


Figure 6 Representation of photoswitch insertion on to pharmacophore A and insertion between two ligands that interact with a multivalent target B.¹ Reprinted with permission from *J. Am. Chem. Soc.* **2014**, *136*, **6**, 2178-2191. Copyright 2014 American Chemical Society.

When designing azo-based pharmaceuticals, one must take into consideration factors such as isomeric ratio, wavelength optimization, *cis* isomer half-life, biological stability and toxicity. These factors are discussed in more detail below.

Isomeric ratio

The structures of drugs are mostly optimized through clinical research feedback. Introducing an additional unit on to the structure of a proven drug may disturb its pharmacokinetics and pharmacodynamics resulting in alteration or loss of activity.¹⁹ A photocontrolled drug thus has to be designed so as to maintain its activity in one or both isomeric states and have little to no effect off-target. In azobenzene molecules, irradiation of the *trans* isomer -which is up to 10 kcal/mol more stable than the *cis*-isomer²⁰ with the correct wavelength, converts a modest to substantial amount of the *trans* isomer population to *cis* isomer depending on the switch.²¹ The *trans/cis* isomer ratio is crucial at all times since a drug must be active on the site of action and inactive off-target.

Wavelength optimization

In order to achieve the desired isomeric ratio, UV light irradiation is mostly required in the case of azobenzenes.¹⁰ During irradiation, the parent compound undergoes *trans/cis* isomerization. However, the toxicity of UV light has been thoroughly studied and UV irradiation has been shown to be carcinogenic and mutagenic.^{22,23} To avoid the use of UV irradiation, the synthesis of red shifted azobenzenes has been proposed. The wavelength window for in-body activation using an exogenic light source is reported to be between 600 and 1200 nm, with haemoglobin absorbing at the lower and water at the higher-end wavelengths.²⁴ Tissue penetration for this wavelength window is reported to be between 1 and 2 cm.²⁵ These windows of limitation could however be avoided with the use of an endogenous light source that could activate the drug on-site.



Figure 7 Time courses of possible therapeutic pathways that can be followed during “on” and “off” switching of photoswitchable drugs with light of different wavelengths. Activity profile of (A) a conventional drug not metabolized in the body; (B) a conventional drug metabolized in the body. Photoactivation of (C) a switchable drug on the site of action, followed by inactivation with clearance; (D) a switchable drug prior to administration, followed by inactivation with clearance. (E) Inactivation of a switchable drug prior to administration, followed by activation at the site of action, and final inactivation at clearance.¹ Reprinted with permission from *J. Am. Chem. Soc.* 2014, 136, 6, 2178-2191. Copyright 2014 American Chemical Society.

The possible routes a drug could follow during the therapeutic time course between administration and excretion are presented in Figure 7.¹ Especially beneficial is the case of photoswitchable antibiotic drugs in which activation ceases upon excretion (Figure 7, Plot D) avoiding thus an antibiotic build-up in the environment. Our approach focused more on targeting site-diseases *e.g.*, cancer and therefore aiming at a variation of Plot C (Figure 7)

which incorporates thermal relaxation as a means for drug deactivation rather than a second stimuli as seen in the chapter below.

Cis isomer half-life

The *cis/trans* isomerization can be achieved either upon irradiation or, spontaneously (*vide supra*). This offers tremendous prospects for dynamic and spatial control of a photoswitchable drug as demonstrated in the plots depicted in Figure 8 describing various routes to utilize and profit from the half-life of the *cis* isomer.¹ Plot A describes the activity time course of a photocontrolled drug which is activated prior to administration and deactivated with time reaching zero activity upon excretion. Similarly to Plot A, Plot B describes the activity of a drug that is activated on the target site. Plot C describes the activity of a drug that is repeatedly activated on the target site. Plot D describes the activity of a drug that is deactivated prior to administration and through thermal relaxation shows increased activity. Plot E describes the activity a drug that is deactivated both prior to administration and excretion.¹

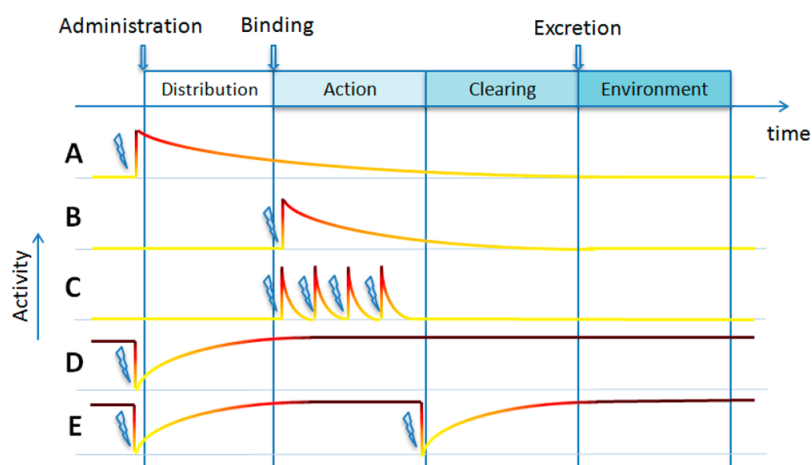


Figure 8 Time course scenarios on photocontrolled drugs.¹ Reprinted with permission from J. Am. Chem. Soc. 2014, 136, 6, 2178-2191. Copyright 2014 American Chemical Society.

In all pathways described in Figure 8, regardless whether the pharmacologically active form is in the *cis* or the *trans* geometric isomer, the importance of a tuneable *trans/cis* half-life is key to dynamic and spatial control of the drug in the body.

Biological stability

Before designing a bioactive switch, one must access the biological stability of the target compound. A major concern when using azobenzene derivatives for drug development lies

in their *in vivo* stability and more specifically, in cellular stability. Azobenzenes are susceptible to reduction via glutathione (GSH)²⁶ and enzymatic degradation.²⁷ Significant attention has been given to azobenzene reduction since glutathione concentration in cells is up to 10 mM. L. Morder and C. Renner reported that reduction of azobenzenes using GSH occurs spontaneously at neutral and basic pHs with the reduction rate of the *cis* isomer being 100 times faster compared to that of the *trans* isomer.²⁸ E.Krosower and H.Kanety-Londer further reported on the mechanism involving nucleophilic attack of the thiolate on the diazo bond which subsequently reacts with GSH to afford a hydrazo compound (Figure 9).²⁹

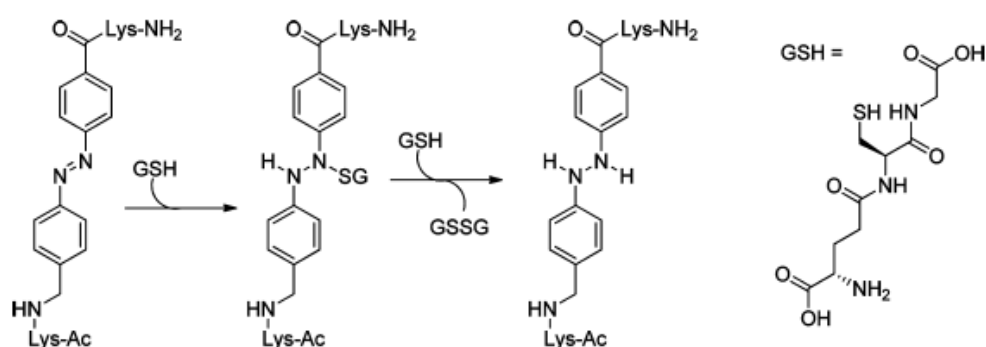


Figure 9 Glutathione promoted reduction of azobenzene.²⁹ from *J. Am. Chem. Soc.* 2014, **136**, 6, 2178-2191. Copyright 2014 American Chemical Society.

The incorporation of electron donating groups on the aromatic rings of an azobenzene however, could prevent the thiolate nucleophilic attack on the diazo group by decreasing its electrophilicity. This was elegantly demonstrated with the incorporation of amido³⁰ or methyl thiol³¹ groups on the aromatic moiety of azobenzenes. To further support this, when electron withdrawing methoxy groups were incorporated in the azobenzene rings, thiolate attack was reported.³²

Toxicity

The only remaining factor to pencil in when evaluating the *in vivo* toxicity of azobenzene derivatives is toxicity. Azobenzenes are not only extensively used in the dye industry but have also been used in food and cosmetic industry.³³ In all applications however, azobenzene derivatives must be carefully engineered as the above-mentioned *in vivo* degradation pathways can lead to dangerous by-products such as aromatic amines that bind

to genetic material. Oxidation leading to toxic species or diazonium salts must be avoided at all cost when designing an azobenzene-based drug.³⁴

The fact that azobenzene derivatives can be engineered in a sense of wavelength, half-life and substituent tuning, only strengthens the aspect of their potential for pharmaceutical applications.

1.3 Photoswitchable drugs

The first studies in photopharmacology were reported in the 1960's when Erlanger and Nachmansohn investigated azobenzene-based inhibitors of acetylcholinesterase.^{35 36} The following decades showed significant advances in the synthesis of photoswitchable drugs. Few notable azobenzene switches with antibacterial or anti-cancer action will be shortly discussed.

Photoswitchable antibiotics

The emergence of antibacterial resistance has driven research to breakthroughs on photoswitchable antibiotics with indicative examples photoswitchable quinolones reported by Valema et al. and a photoswitchable trimethoprim derivative reported by Wegener et al..^{37, 38}

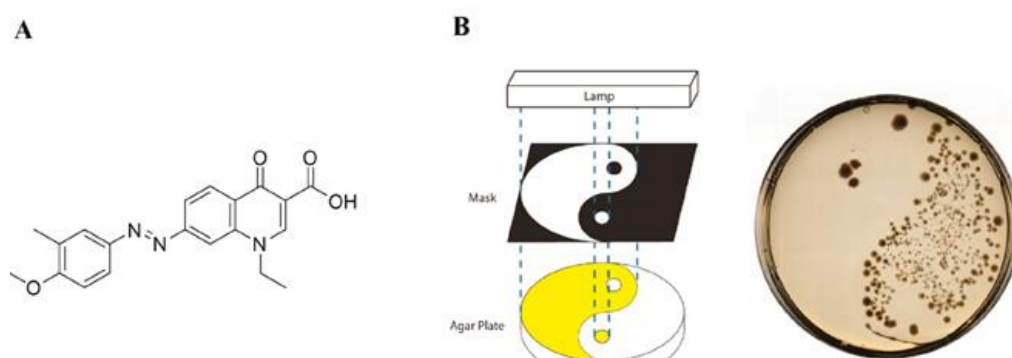


Figure 10 (A) Photoswitchable quinolone derivative reported by Feringa et al.; (B) Bacterial growth inhibition in the presence of the active *cis* isomer of the photoswitchable drug.³⁷ From W. A. Valema, J. P. van der Berg, M. J. Hansen, W. Szymanski, A. J. M. Driessen, B. L. Feringa, *Nature Chem*, **2013**, 5, 924–928. Copyright © 2013, Nature Publishing Group

Quinolones are broad spectrum antibiotics often used to treat infections. W. A. Valema et al. incorporated an azobenzene bearing different substituents in the structure of a

quinolone and tested against quinolone sensitive bacteria (Figure 10A).³⁷ It was discovered that the *cis* isomer of the antibiotic with a half-life of 2 hours displayed an activity up to 8 times higher of that of the *trans* isomer. This means that during *in vivo* use, the increased activity would be lost before excretion preventing the build-up of antibiotics in the environment. This example is representative of how *cis/trans* isomerization can be utilized for a time dependant loss in biological activity.³⁷

Another notable example of photoswitchable antibiotics are the trimethoprim based photoswitches reported by N. Wegner et al..³⁸ This research group reported on the synthesis of photoswitchable azobenzene-based antibiotics which could be activated with green and red light, in the presence of bacteria. Importantly, the red light activated derivative exhibited 8-fold increase in activity following irradiation, demonstrating that the activation of the drug could be accomplished within the light therapeutic window.³⁸

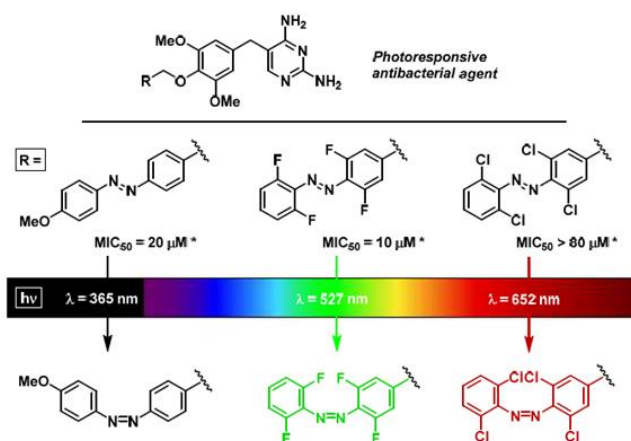


Figure 11 Photoswitchable derivatives of trimethoprim activated upon green and red light irradiation.³⁸ From *J. Am. Chem. Soc.* 2017, 139, 49, 17979-17986. Copyright © 2017, American Chemical Society.

Photoswitchable anticancer agents

Significant advancements have also been achieved in the synthesis of photoswitchable anti-cancer agents. M. J. Hansen et al. reported on bortezomib-based photoswitchable inhibitors which exhibit activity changes upon irradiation with visible and UV light (Figure12).³⁹ A strong proteasome inhibition was induced by the *trans* isomer while a weak proteasome inhibition with the *cis* isomer.³⁹

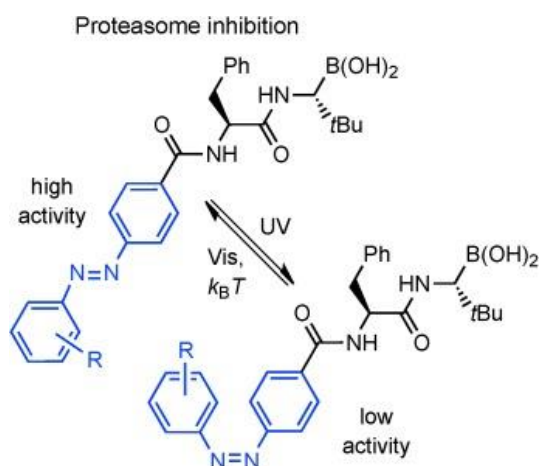


Figure 12 Photoswitchable diazobenzene derivative of bortezomib.³⁹ From M. J. Hansen, W. A. Velema, G. de Bruin, H. S. Overkleeft, W. Szymanski, B. L. Feringa, *ChemBioChem*, **2014**, 15, 2053-2057. © 2014 WILEY-VCH Verlag GmbH & Co. KGaA, Weinheim

A promising strategy for cancer therapy involves interfering with mitosis. In these lines, N.N. Mafy et al. reported on a photoswitchable inhibitor of the microtubule-dependent motor centromere-associated protein E (CENP-E), a mitotic kinesin required for chromosome transportation.⁴⁰ The inhibitor (Figure 13) was found to undergo reversible isomerization under visible and UV light. Interestingly, a 10-fold increase in inhibition was observed for the active trans isomer form of the drug.⁴⁰

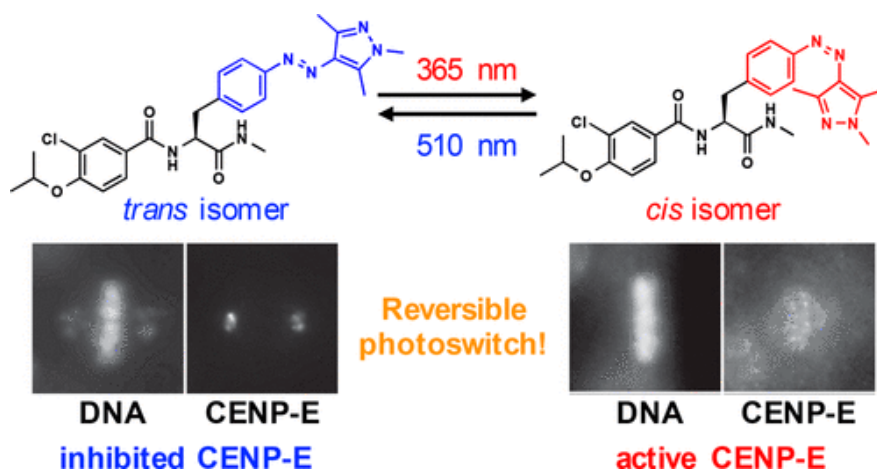


Figure 13 Photoswitchable CENP-E inhibitor.⁴⁰ From *J. Am. Chem. Soc.* **2020**, 142, 1763-1767. Copyright © 2020, American Chemical Society.

Photoswitches in medicine

Although research on photoswitches largely focuses on antibiotics and anticancer agents, photoswitches have also been prepared for treatment of a variety of other diseases. F.

Riefolo et al. for example, reported on a photoswitchable azo-modified muscarinic acetylcholine receptor M_2 (M_2 mAChR) agonist that modulates cardiac function.⁴¹ This photoswitchable agonist was found to activate M_2 muscarinic receptors through a two-photon excitation using near-IR light which offers opportunities for *in vivo* control of the cardiac function.⁴¹

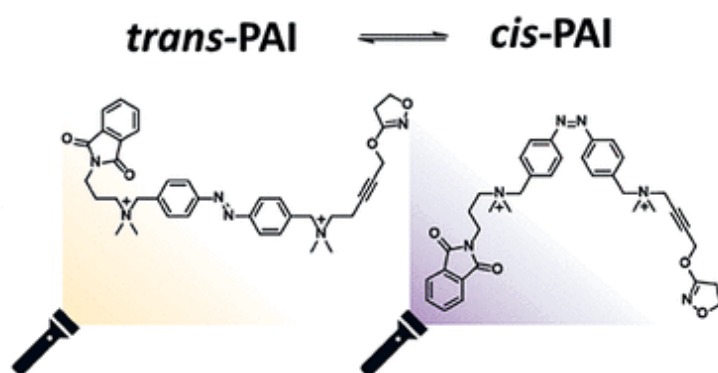


Figure 14 Photoswitchable M_2 mAChR agonist.⁴¹ From *J. Am. Chem. Soc.* **2019**, 141, 7628-7636. Copyright © 2019, American Chemical Society.

Photopharmacology has also been applied in the study of Alzheimer's disease target proteins mainly via using photoswitches to investigate the functions of acetylcholinesterase, muscarinic acetylcholine, cannabinoid, and N-Methyl-D-aspartate (NMDA) receptors.³⁹ Rodríguez-Soacha et al. reported the synthesis of a photoswitchable dual-esteric ligand shown in Figure 15 where the azobenzene is chemically bonded to both an allosteric modulator (Indigo circle, Figure 15) and a non-selective agonist (Purple circle, Figure 15).⁴²

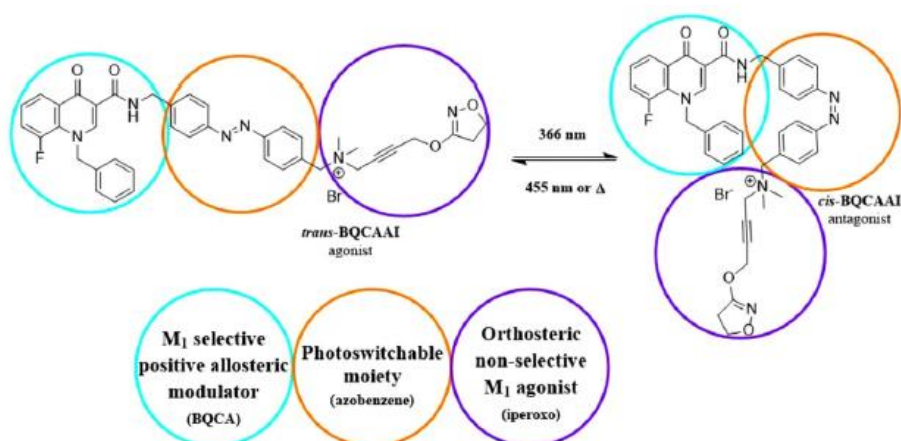


Figure 15 Photoswitchable dual-esteric ligand for the M_1 receptor.⁴² From *Adv. Therap.*, **2018**, 1, 180037. © 2018 WILEY-VCH Verlag GmbH & Co. KGaA, Weinheim.

1.4 Bioluminescence as a tool for pharmacology

Bioluminescence is the production and emission of light by a living organism - a form of chemiluminescence. The light emitted by a bioluminescent organism is produced by energy released by a chemical reaction which involves a light emitting molecule, generally called luciferin, and an enzyme called luciferase. All bioluminescent reactions require molecular oxygen for the production of light and energy carrying molecules such as ATP. In some species, cofactors such as calcium and magnesium ions are also required. Bioluminescence occurs widely in marine vertebrates and invertebrates as well as fungi, bacteria and terrestrial arthropods.⁴³

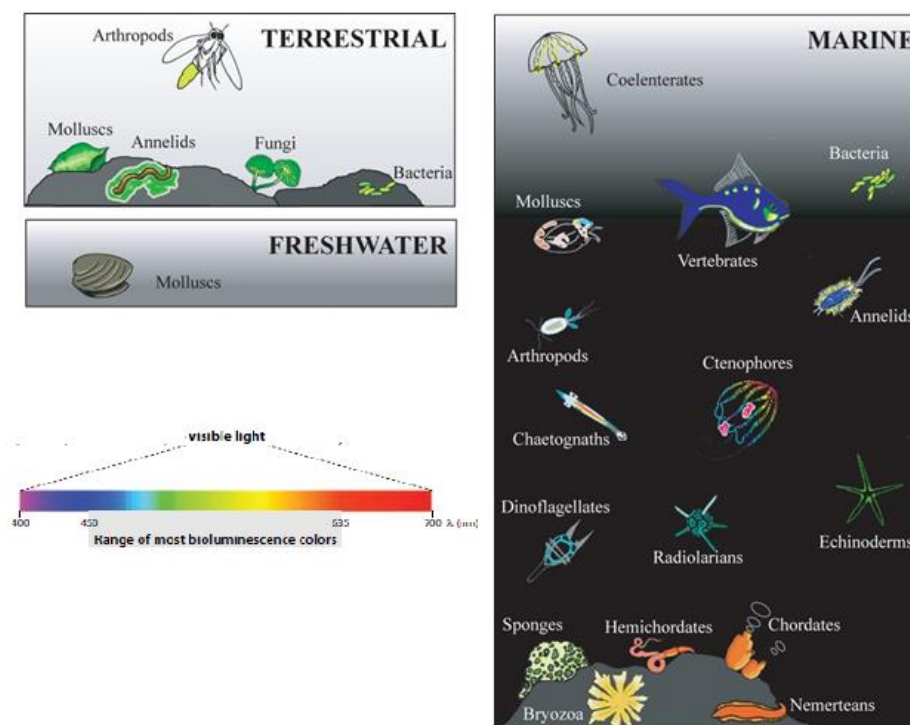


Figure 16 Diversity of bioluminescent organisms and wavelength span of light produced by different organisms.⁴⁴ Reprinted from *J. Cell. Mol. Med.*, **2013**, 17, 1582-1838, open access article distributed under the terms of the Creative Commons CC BY license.

What makes bioluminescence so fascinating is the diversity of organisms that produce light, the reasons they produce light *e.g.*, to communicate or for self-defence, and importantly, the wavelengths they produce. The wavelength span of bioluminescence lies between 450 and 630 nm.⁴³

A vast range of analytical techniques has been developed based on bioluminescence including immunoassays, gene expression assays, drug screening, bioimaging of live

organisms and, the investigation of cancer and infectious diseases.⁴⁵ One promising technique in cancer research for example is Bioluminescent Activated Destruction referred to as BLADe.⁴⁶ This technique utilizes both bioluminescence and Photodynamic Therapy (PTD) by activating the generation of singlet oxygen ($^1\text{O}_2$) with bioluminescence in an effort to access deep penetrated cancer tumors. Theodossiou et al. reported on the activation of Rose Bengal (RB) by intracellular generation of light in luciferase-transfected NIH 3T3 murine fibroblasts.⁴⁶

Photopharmacology can benefit modern medicine if drug activation is achieved through the use of bioluminescence. Biophotopharmacology could also exceed the BLADe technique, since PTD can only be used to induce cell death while photopharmacology aims at biological responses. This could be advantageous in cancer destruction, as PTD is dependent on tissue and tumour oxygenation, therefore tumours surrounded by necrotic or dense masses where oxygen levels are low, pose an issue in PTD treatment.⁴⁷ Photopharmacology on the contrary, does not rely on tissue oxygenation and could therefore be a viable alternative.

One possible way of implementing *in vivo* biophotopharmacology is with the aid of bioluminescent imaging. Bioluminescent imaging is a technique used to visualize molecular and cellular processes through the administration of bioluminescent reporters into small animals, followed by injection of bioluminescent substrate to initiate imaging (Figure 17).⁴⁸

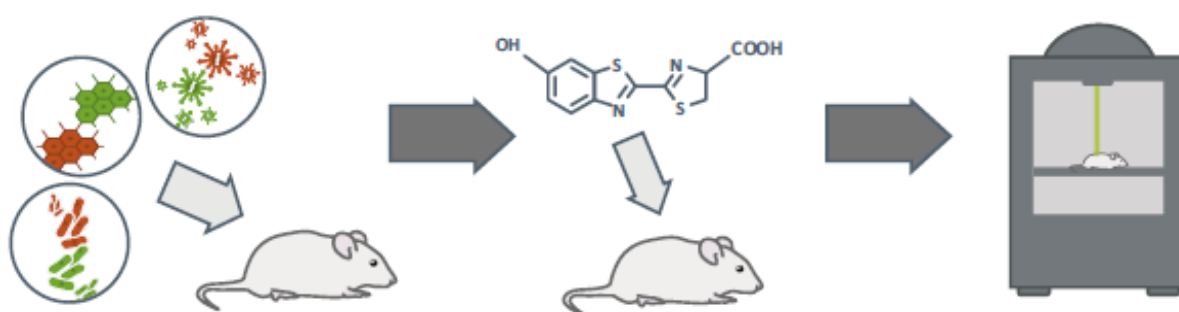


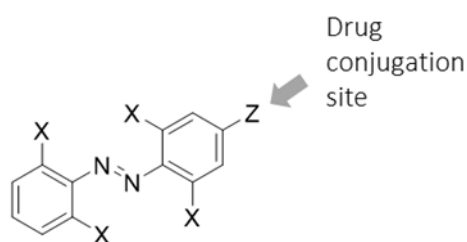
Figure 17 Schematic representation of bioluminescent imaging principle (a) reporter genes are transferred to small animals, (b) luciferin is injected to the animals and, (c) acquisition of light signals and data processing.⁴⁹ From *Trends in Biotechnology*, **2017**, 35, 640-652 © 2017 Elsevier Ltd. All rights reserved.

This method can be altered so cancer targeting viral vectors carrying the luciferase genes,⁵⁰ or cancer homing bacteria carrying the luciferase genes can be used to light up the target tissue.⁵¹ As for the use of luciferin, recent advancements have led to the production of autonomous bioluminescent systems without the need to inject luciferin into the system. It was previously considered that bioluminescence in human cells was impossible suggesting that all mammalian reporter systems required the addition of a chemical substrate in order to produce light. This was disproven however as Close et al. reported an engineered lux operon derived from bioluminescent bacteria that operates in eukaryotic human cells and does not require the addition of a chemical substrate in order to produce light.⁵²

Aim of the Thesis

Azobenzenes are pivotal molecules in the area of photopharmacology. Azobenzene geometrical isomers -*cis* and *trans*- exhibit different geometry and dipole moment affecting their properties.¹⁰ When azobenzenes are chemically bonded to pharmaceuticals either isomeric state could cause a shift in the activity of the parent pharmaceutical offering a plethora of alternatives to use them as regulators (molecular switches) in photopharmacology.¹ The drawback of azobenzene application in pharmacology however, lies in the fact that the *trans/cis* isomerization takes place with UV light which has toxic and carcinogenic effects.

Taking this into account, in this Thesis we aimed at the synthesis of red shifted azobenzene molecular switches that would exhibit bioluminescence induced *trans/cis* isomerization combined with a fast *cis/trans* thermal relaxation. The *trans/cis* isomerization is necessary for a possible photoinduced activation of an azobenzene-drug derivative on the target site while the *cis/trans* thermal relaxation, for fast deactivation away from the target site/light source. The system would ideally provide a non-interfering functional site to conjugate potential drugs (Scheme 1).



Scheme 1 Target azobenzenes designed to bear ortho substituents and a functional group aimed for drug conjugation. X= Cl, F or Z=methyl.

While designing the target azobenzenes, the two major factors which must be taken into consideration when designing molecular photoswitches, *i.e.*, isomerization wavelength and thermal relaxation rate (Paragraph 1.2) were taken into account. The former is crucial as it allows use of nontoxic irradiation, while the latter offers control on temporal activity.¹ The initial design therefore revolved around the synthesis of tetrahalogenated azobenzenes as their red shifted properties are known in literature.^{30-32, 38} Additionally, such azobenzenes are not prone to glutathione reduction. More specifically, a previously reported tetra-ortho-

fluorinated azobenzene derivative was shown to isomerize in the green region of the spectrum while, a tetra-ortho-chlorinated azobenzene derivative was shown to isomerize in the red region of the spectrum (Figure 11).³⁸ Taking this into consideration we opted to synthesize mixed ortho-halogenated azobenzene derivatives and study whether *trans/cis* isomerization could be induced under yellow light. This light-source was selected as, in a subsequent step, firefly bioluminescence could also be used to induce the desired *trans/cis* isomerization.

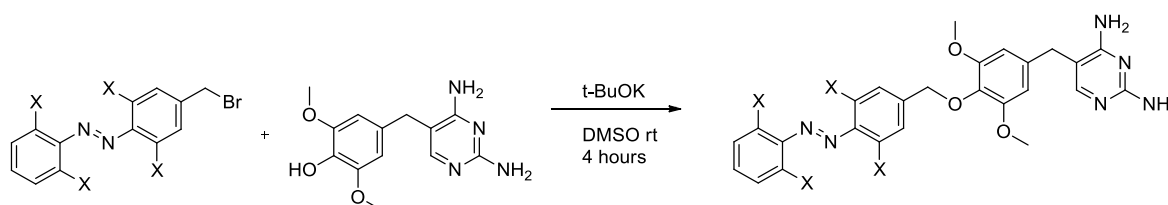
A second design focused on blue light isomerization and more specifically bacterial bioluminescence induced isomerization. This approach included the synthesis of ortho-substituted azobenzenes as precursors for nucleophilic aromatic substitution during which, different nucleophiles could be introduced on the aromatic rings. Literature reports demonstrated that ortho-aminated azobenzenes displayed increased molar absorptivity in the visible region of the spectrum, combined with low *cis*- half life and resistance to glutathione reduction.⁵⁸ Taking these reports into account, we designed molecular precursors that would allow investigating the suitability of various amines as nucleophiles. and study whether blue light isomerization could be induced.⁶⁶

2 Results and discussion

As mentioned before, the purpose of this Thesis was the synthesis of red-shifted azobenzene molecular switches designed to accomplish *trans/cis* isomerization with the aid of bioluminescence and *cis/trans* isomerization thermally, in a matter of seconds. The target azobenzenes (Scheme 1) should additionally provide a conjugation site to attach potential pharmaceuticals. New azobenzene derivatives (*i.e.*, compounds which have not previously been described in the literature) will appear in red numbering throughout this section.

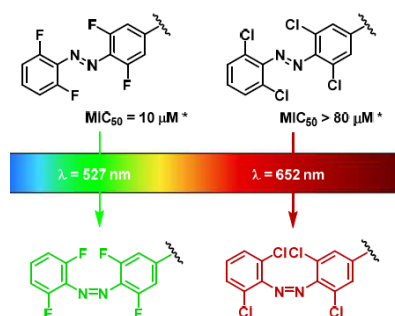
2.1 Initial Design

Feringa and co-workers reported red shifted azobenzene photoswitches that could isomerize upon irradiation with visible light.³⁸ The photoswitches bearing a toluoyl group in para position offered the opportunity for benzylic bromination and subsequent conjugation to a bioactive compound through an S_N2 reaction (Scheme 2).



Scheme 2 Conjugation of azobenzene to Trimethoprim via S_N2 reaction.

In a comparative study, the same investigators reported that tetra-ortho-fluoro-azobenzenes underwent *trans/cis* isomerization upon irradiation under green light, while tetra-ortho-chloro-azobenzenes underwent *trans-cis* isomerization upon irradiation with red light (Scheme 3).³⁸

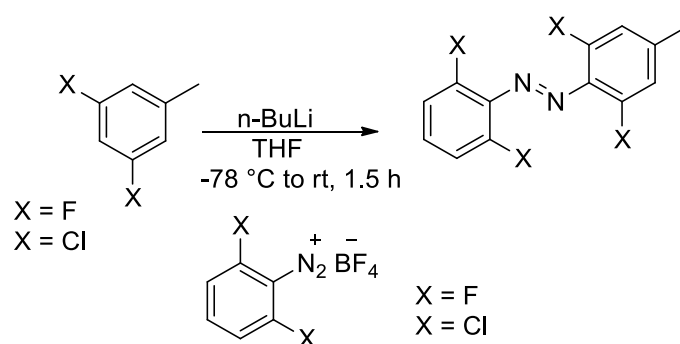


Scheme 3 Red shifted halogenated azobenzenes.³⁸ From *J. Am. Chem. Soc.* **2017**, **139**, **49**, **17979-17986**. Copyright © 2017, American Chemical Society.

Considering the fact that tetra-ortho-fluoro- and tetra-ortho-chloro- substituted azobenzenes exhibit isomerization in the visible portion of the spectrum, green for the former and red for the latter, and, taking into account the fact that the optimal wavelength window that allows for skin penetration lies between 600 and 1000 nm, we opted to synthesize unsymmetrical tetra-ortho- substituted azobenzenes combining chlorine and fluorine in the ortho positions (Scheme 1). The synthesis of unsymmetrical azobenzenes was considered to be crucial, as the toluoyl group located in the para position in respect to the azo group would later be used for conjugation with bioactive compounds. Aim of this design was to allow tuning of the isomerization wavelength towards the yellow-orange region of the spectrum, in order to perform *in vivo trans/cis* isomerization using the firefly luciferase.

Tetrahalogenated azobenzene 2 - Synthesis and Spectroscopic Study

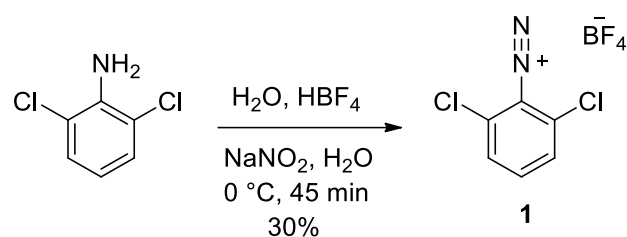
A general synthetic methodology found in literature involved a deprotonation of an aryl compound using *n*-butyllithium (*n*-BuLi) and subsequent nucleophilic attack on the diazo group of a second aryl compound (Scheme 4).⁴⁸ This method was used for the synthesis of the compounds (E)-1-(2,6-dichlorophenyl)-2-(2,6-difluoro-4-methylphenyl)diazene **2** and, (E)-1-(2-chloro-6-fluorophenyl)-2-(2,6-difluoro-4-methylphenyl)diazene **4**, aiming to investigate *trans/cis* isomerization under yellow LED light.



Scheme 4 General methodology of asymmetric azobenzene synthesis.⁴⁸

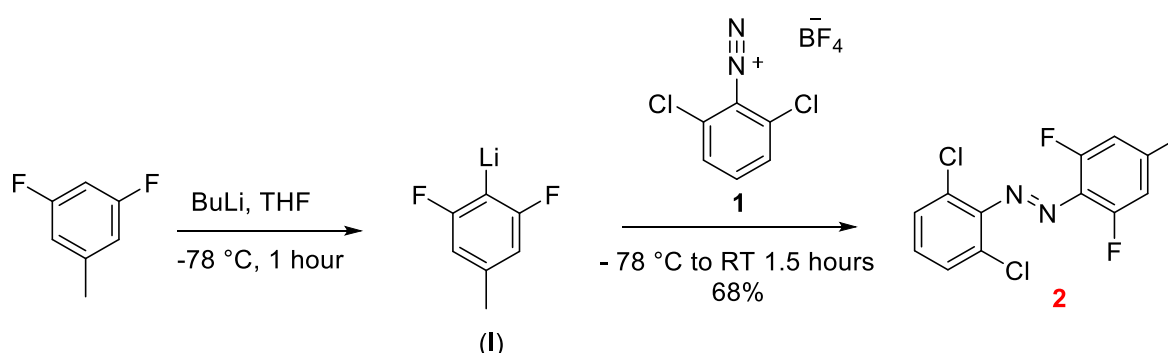
The synthesis of an ortho substituted diazonium salt could be achieved from its corresponding amine precursor according to M. J. Hansen et al.⁵³ Following this approach, the diazonium salt **1** was prepared by reacting the corresponding aniline, 2,6-

dichloroaniline, with HBF_4 and NaNO_2 in an aqueous solution at $0\text{ }^\circ\text{C}$ with yields up to 30 % (Scheme 5).



Scheme 5 Synthesis of the diortho-chloro-diazonium salt **1**.

The freshly prepared diazonium salt **1** was subsequently reacted with the lithiated aryl intermediate (**I**) at $-78\text{ }^\circ\text{C}$ to afford compound **2** with yields up to 68% (Scheme 6).



Scheme 6 Synthesis of ortho-halogen-tetra-substituted azobenzene **2**.

The $^1\text{H-NMR}$ spectrum of the azobenzene **2** (Figure 18) was recorded without subjecting the sample to any thermal relaxation prior to measurement though sample preparation and transfer was performed under light. Therefore, both isomeric forms could be identified in the spectrum with the *trans* isomer being the major isomer. The aromatic protons form an interesting doublet-triplet-doublet motif for the *trans* isomer: the doublet at 7.41 ppm corresponds to the *meta* to the azo group **a** protons of the phenyl ring, the triplet at 7.198 ppm corresponds to the *para* to the azo group **b** protons of the phenyl ring and the doublet at 6.91 ppm corresponds to the *meta* to the azo group **c** protons of the toluoyl moiety. The methyl **d** protons of the toluoyl ring appear in the aliphatic area as a sharp singlet at 2.43 ppm for the *trans* isomer of **2**. The *cis* isomer of **2** being the minor product, was identified through the methyl group **d** protons which are clearly visible in the aliphatic region at 2.30 ppm. The corresponding aromatic protons of the *cis* isomer are also present as minor peaks in the aromatic region. $^1\text{H-NMR}$ spectroscopy was conveniently used

(*vide infra*) to quantify the photoinduced *trans/cis* isomerization through the integrals of the singlet peaks of the *trans* and *cis* isomer methyl protons in the aliphatic region.³⁸

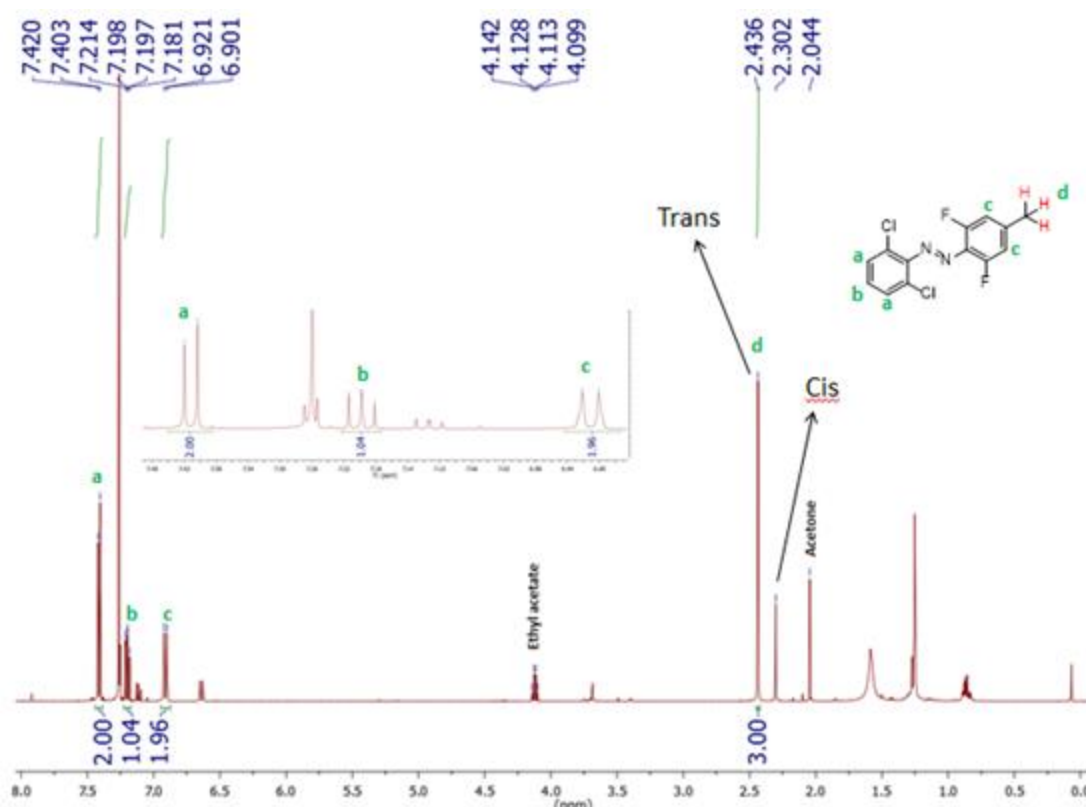


Figure 18 ¹H-NMR spectrum of compound **2** in CDCl₃.

To obtain a qualitative understanding of the optimal wavelength required to induce *trans/cis* isomerization, a solution of compound **2**, (ca. 30mM in DMSO), was irradiated with different light sources and studied using UV-Vis spectroscopy (Figure 19). Red, blue, green or yellow LED light was used during these studies and qualitative results on the *trans/cis* isomerization were obtained by comparing the absorption of the π - π^* (at 300 nm) transition with that of the n - π^* (at 438 nm) transition.¹⁰ As shown in Figure 19, only the green LED light was found to induce *trans/cis* isomerization that was observed via a decrease of the π - π^* absorption band accompanied by an increase of the n - π^* absorption band. A minor blue shift for both absorption bands (11 nm) was observed upon *trans/cis* isomerization. These findings indicate that the asymmetric ortho-halogen-tetra-substituted azobenzene **2** bearing two chlorine- substituents on the phenyl and two fluorine substituents on the toluoyl moiety does not give rise to the desired red shift in the yellow region of the visible region of the spectrum.

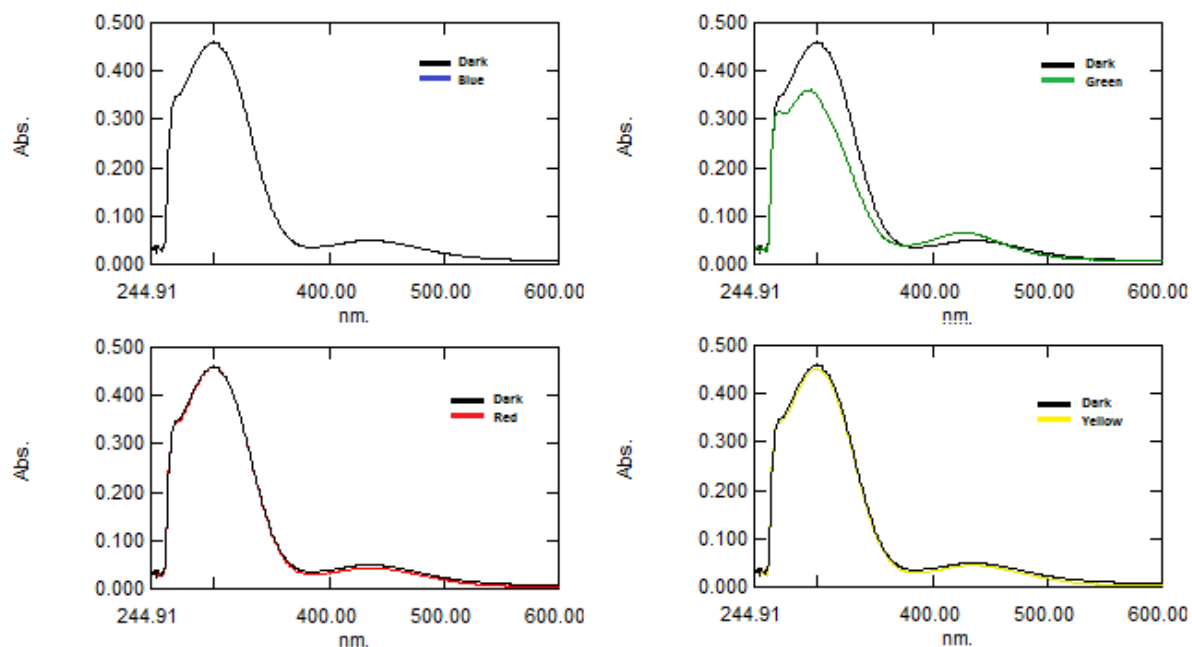


Figure 19 UV/Vis spectra of compound **2** in DMSO ($C \approx 30\text{mM}$) prior and upon 5-minute irradiation with a LED light source (light source indicated in each spectrum).

The *trans/cis* isomeric ratio for compound **2** was determined by $^1\text{H-NMR}$ spectroscopy given that geometric isomers can be easily distinguished through protons resonating with different chemical shifts due to differences in their chemical environment. The spectral window displayed in Figure 20, depicts the signals corresponding to the methyl group protons of the para-toluoyl substituent of **2**. As shown in Figure 20, the $^1\text{H-NMR}$ spectrum of the partially dark-adapted azobenzene **2** (*i.e.*, azobenzene allowed to relax back to the thermodynamically stable *trans* isomer), and the spectra of the azobenzene **2** upon irradiation with light of different wavelengths, exhibit distinct differences in terms of isomer population, specifically in the aliphatic region where the methyl proton peaks is shifted by ca 0.1 ppm. More specifically, an isomeric ratio of *cis/trans* 25/75 was determined for the partially dark adapted azobenzene. Irradiation with red light resulted in an isomeric *cis/trans* ratio of 40/60, ultraviolet light resulted in *cis/trans* ratio of 20/80, yellow light in *cis/trans* ratio of 45/55, green light in *cis/trans* ratio of 80/20 and blue light in *cis/trans* ratio of 25/75. Partial relaxation was unavoidable between irradiation and acquisition of the NMR spectra.

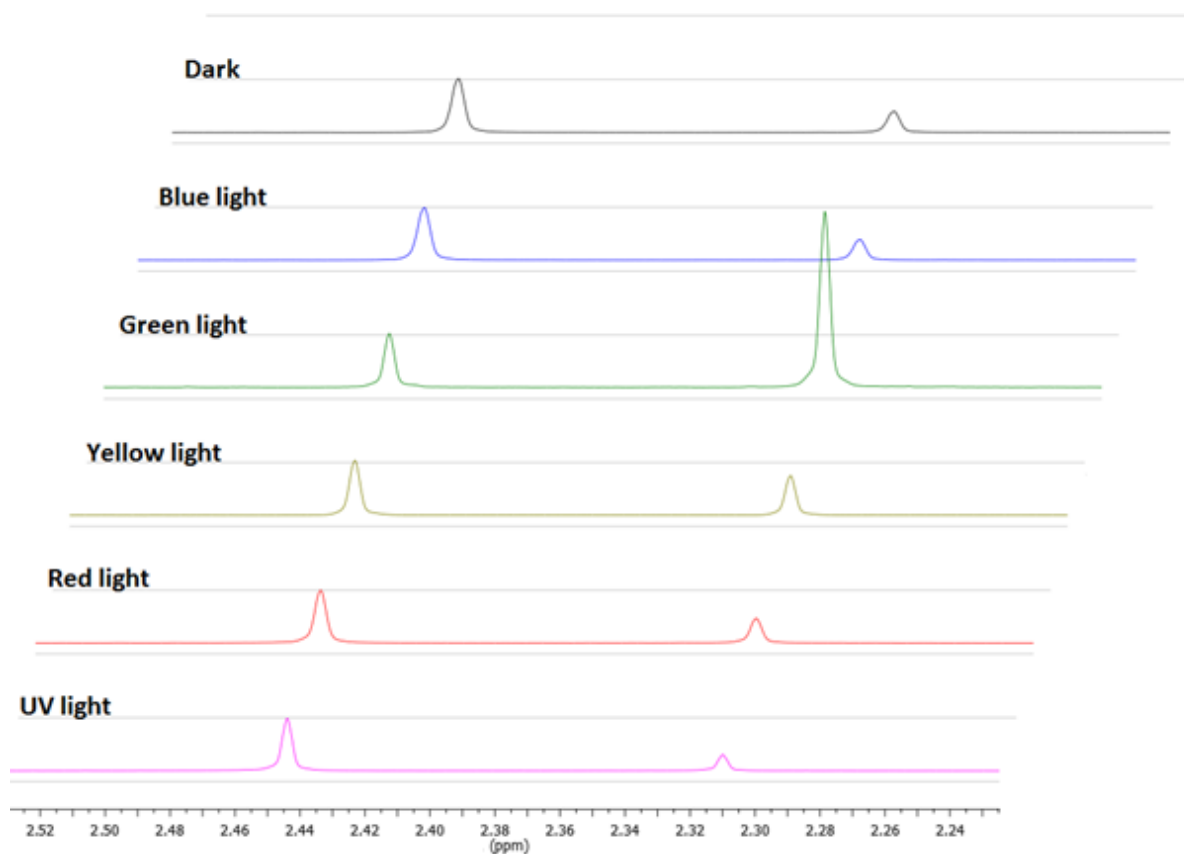
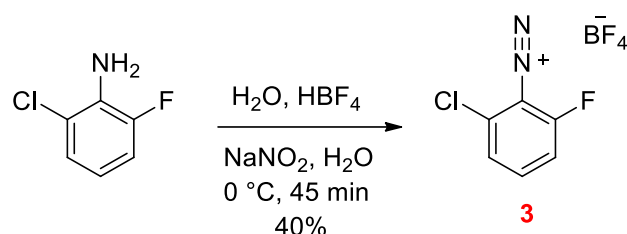


Figure 20 Aliphatic (2.5 to 2.25 ppm) region of the ^1H -NMR spectra acquired for azobenzene **2** after a 10-minute irradiation with the appropriate LED light source. The red spectrum corresponds to red light irradiation, the violet spectrum to ultraviolet light irradiation, the yellow spectrum to yellow light irradiation, the green spectrum to green light irradiation, the blue spectrum to blue light irradiation and the black spectrum corresponds to the partially dark-adapted azobenzene.

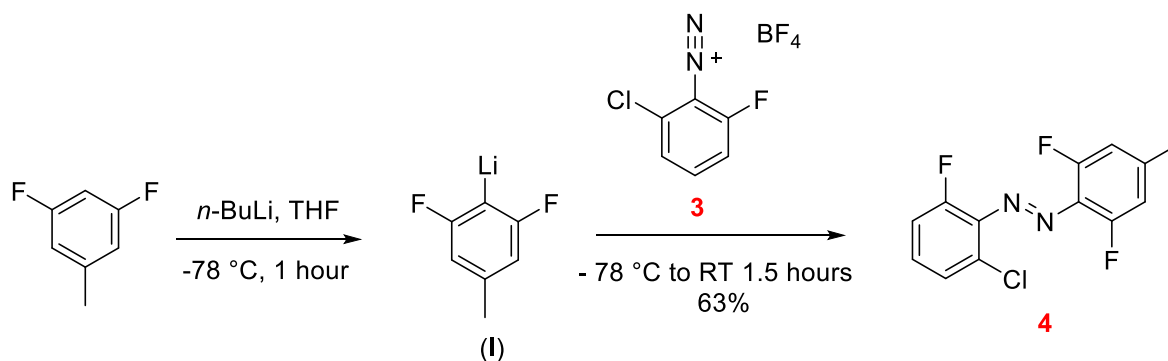
These findings are in full agreement with the spectrophometric studies proving that the asymmetric ortho-halogen-tetra-substituted azobenzene **2** does not give rise to the desired red shift in the yellow region of the visible region of the spectrum.

Tetrahalogenated azobenzene 4 - Synthesis and Spectroscopic Study

In order to investigate the effect of fluorine and chlorine substitution on the azobenzene light induced isomerization, the azobenzene derivative **4** was prepared following the synthetic approach used for compound **2**. The synthesis of the precursor diazonium salt **3** was achieved with yields of up to 40 % (Scheme 7), while the reaction of diazonium salt **3** with the lithiated aryl intermediate (**I**) afforded the desired azobenzene **4** with up to 63% yields (Scheme 8).



Scheme 7 Synthesis of the asymmetric ortho-chloro-ortho-fluoro-diazonium salt **3**.



Scheme 8 Synthesis of the asymmetric azobenzene **4**.

The asymmetric azobenzene **4** was studied with UV-Vis spectroscopy upon irradiation under different light sources, in order to obtain a qualitative understanding of the optimal wavelength required for the *trans/cis* isomerization. Similarly to the azobenzene **2**, red, blue, green and yellow LEDs were used as irradiation source. As shown in Figure 21, only green LED light causes *trans/cis* isomerization as seen via a decrease in the π - π^* absorption band accompanied by an increase in the n - π^* absorption band. A minor blue shift for both bands (ca. 15 nm) was observed upon *trans/cis* isomerization. These findings indicate that the ortho-halogenation of an azobenzene to yield a compound bearing one chlorine and one fluorine on the phenyl and two fluorines on the toluoyl moiety, does not give rise to the desired red shift in the yellow region of the visible spectrum.

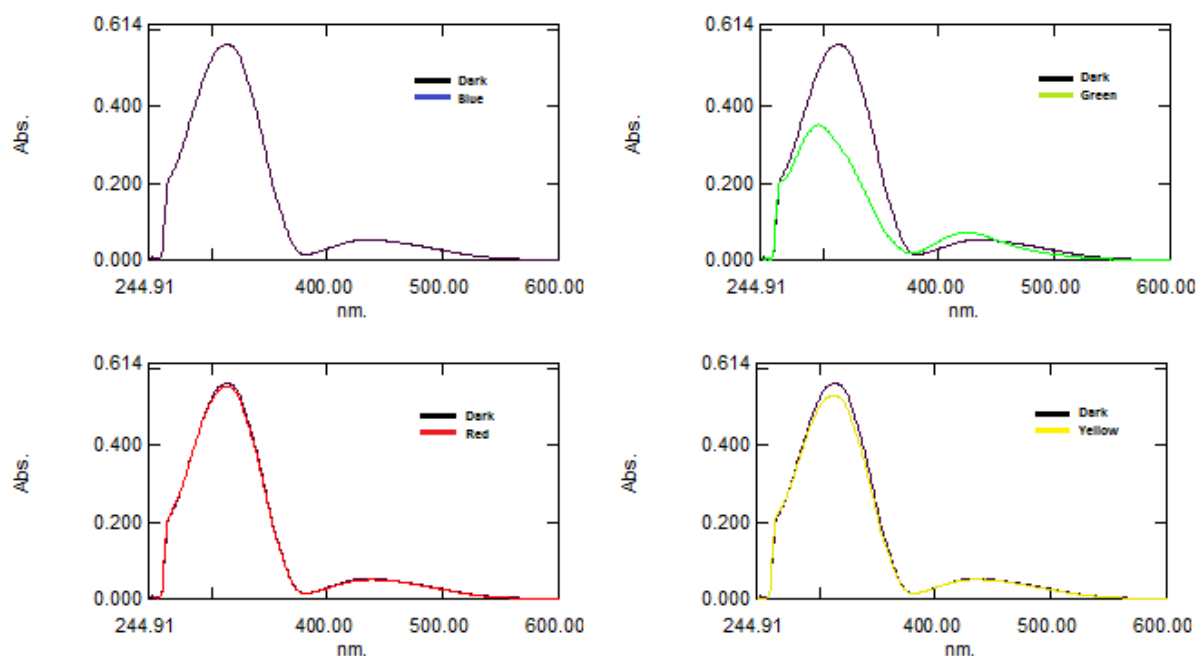


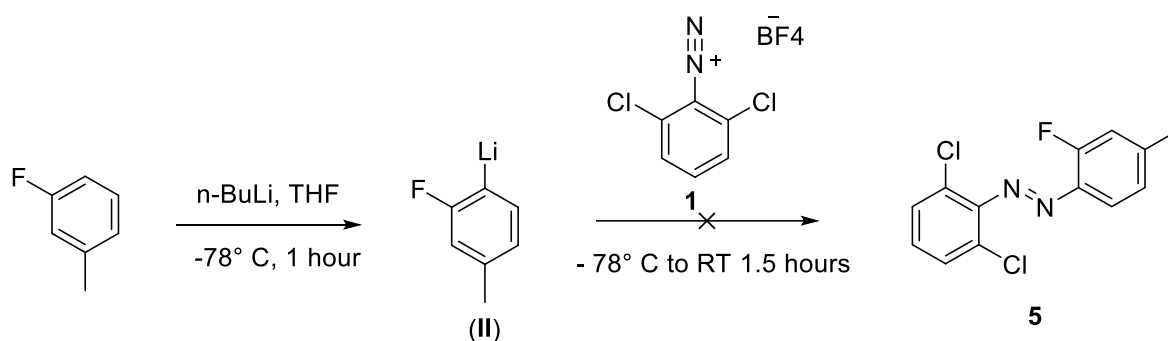
Figure 21 UV/Vis spectra of compound **4** in DMSO ($C \approx 40\text{mM}$) prior and upon 5-minute irradiation with a LED light source (light source indicated in each spectrum).

To summarize, UV-Vis spectrophotometric studies revealed that *trans/cis* isomerization of the azobenzenes **2** and **4** occurs exclusively upon irradiation with green light, while red, blue or yellow light displayed minimal effect. This study proved that though tetra-ortho-chloro- azobenzenes exhibit *trans/cis* isomerization in the red region,³⁸ and tetra-ortho-fluorosubstituted azobenzenes exhibit *trans/cis* isomerization in the green region of the visible spectrum,³⁸ the designed molecules combining ortho-fluoro- and ortho-chloro- substitution did not result in the predicted red shift in the yellow region of the spectrum.

Trihalogenated azobenzenes

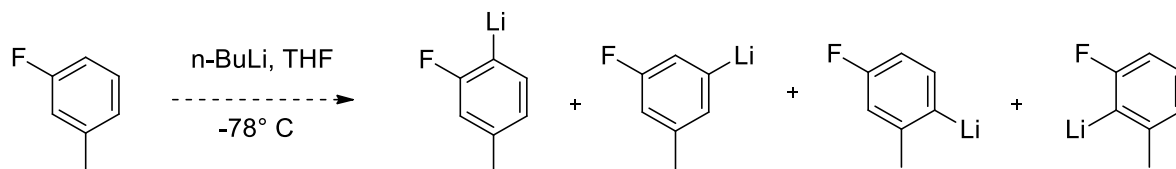
Based on the study of the tetra-halogenated derivatives **2** and **4** proving that *trans/cis* isomerization is limited in the green region of the spectrum, we opted to synthesize a tri-halogenated derivative and more specifically (E)-1-(2,6-dichlorophenyl)-2-(2-fluoro-4-methylphenyl)diazene (compound **5**, Scheme 9) bearing one fluorine atom on the toluoyl moiety and two chlorine atoms on the phenyl moiety. We were interested to perform a spectrophotometric investigation of the proposed dichloro- monofluoro- derivative upon irradiation with appropriate light sources, to identify the isomerization inducing wavelength. Additionally, compound **5** was expected to be prone to nucleophilic aromatic

substitution on the fluorinated ring which would allow further tuning. Following the approach used to synthesize the azobenzene derivatives **2** and **4**, the aryl diazonium salts **1** and **3** did not afford the expected product with the lithiated aryl intermediate (**II**) (Scheme 9) as evidenced by NMR-spectroscopy.



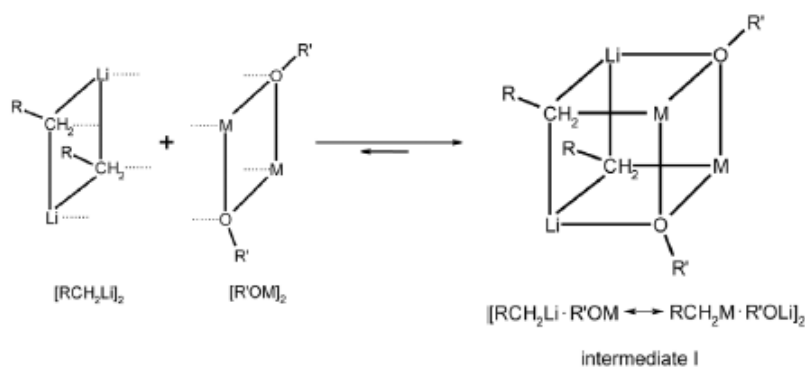
Scheme 9 Synthetic approach followed for the synthesis of compound **5**.

This outcome could possibly be attributed to the fact that *n*-BuLi might not be selective for the desired ortho-lithiation as it was in the case of 3,5-difluorotoluene (Scheme 8),⁵⁴ leading to a plethora of possible byproducts (Scheme 10).



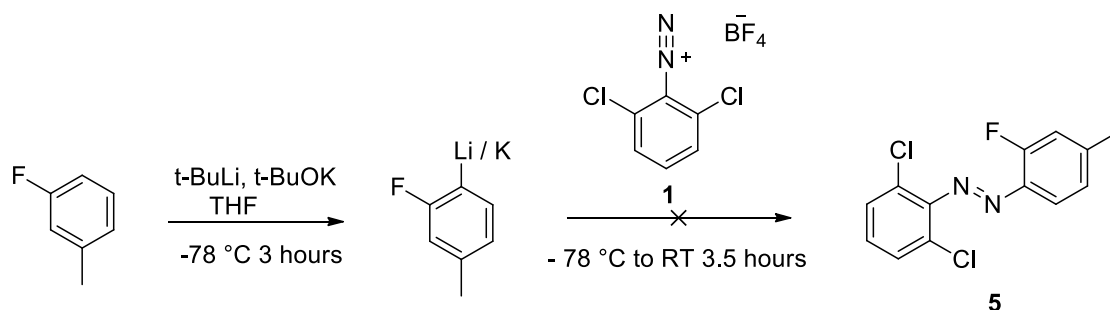
Scheme 10 Possible by-products of a non-selective lithiation.

To avoid non-specific lithiation we utilized the method developed by Schlosser and Geneste to achieve ortho lithiation on 3-fluoro-toluene during their synthesis of ibuprofen.⁵⁴ More specifically, they reported that deprotonation of the ortho position of 3-fluoro-toluene could be achieved by using a superbases mixture consisting of *n*-BuLi (or *t*-BuLi) and *t*-BuOK where, the metal clusters formed between the two reagents drive the selectivity towards the less hindered ortho position (Scheme 11).



Scheme 11 Superbase metal cluster formation from organo-lithium and alkoxide compounds.⁵⁵ This article is licensed under a [Creative Commons Attribution-NonCommercial 3.0 Unported Licence](https://creativecommons.org/licenses/by-nc/3.0/).

In a slightly altered experimental approach, as compared to the ortho lithiation methodology used with *n*-Buli (Scheme 9), *t*-Buli and *t*-BuOK were added to dry THF accordingly to the protocol proposed by Schlosser,⁵⁴ prior to the addition of *t*-BuLi. The *t*-Buli and *t*-BuOK system was specifically used to afford the clusters and simultaneously deprotonate the less hindered ortho position (Scheme 12).



Scheme 12 Proposed synthetic approach for compound **5** following Schlosser's protocol.⁴⁹

Following this approach, we observed release of a gas upon the addition of the diazonium salt **1**. The product expected from the addition could not be identified in the ¹H-NMR spectrum of the crude reaction mixture. Assuming that a reaction of *t*-BuOK with the diazonium salt could take place before the desired nucleophile attack, several efforts to drive the reaction to the desired product were performed by utilizing a two-fold increased concentration of the diazonium salt. All efforts led to the same by-products which could not be characterized by ¹H-NMR spectroscopy (Figure 22). More specifically, the ¹H-NMR spectrum of the reaction product revealed a plethora of peaks corresponding to aromatic protons while, no peaks could be attributed to the toluoyl methyl group (in the expected range between 2.2 and 2.6 ppm). It was noted in literature that excess of *n*-Buli in the reaction with the aryldiazonium salt caused liberation of nitrogen.⁵² Since the N₂

group is brittle in the presence of *t*-BuOK and *t*-BuLi leading to loss of nitrogen and emergence of free radicals, a similar outcome could be assumed for our reaction.

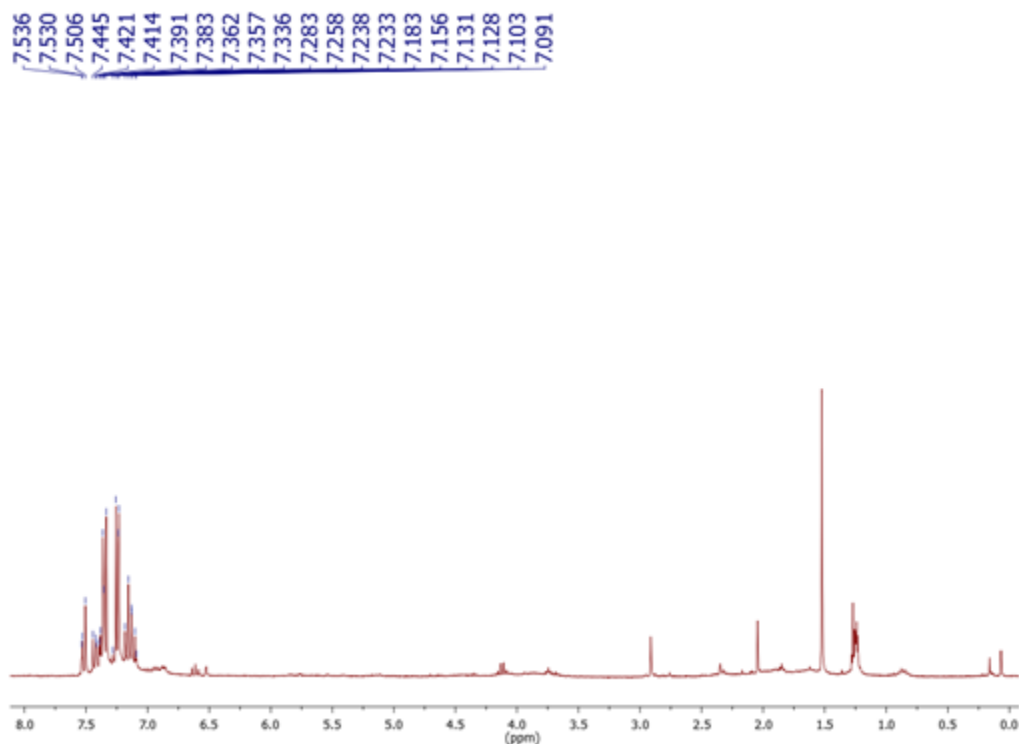
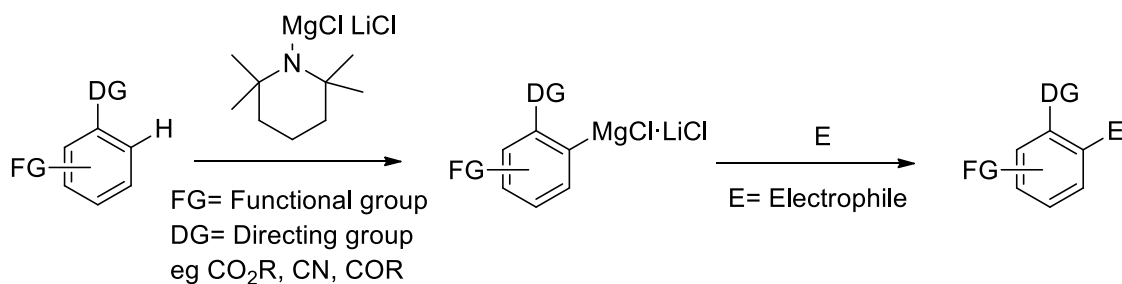


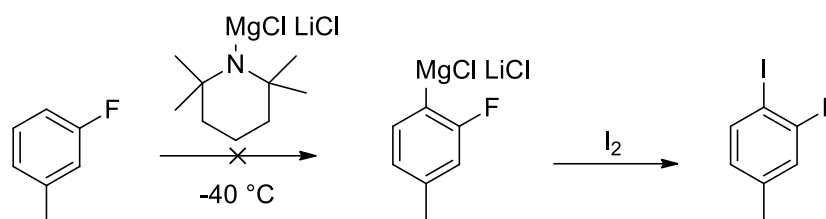
Figure 22 $^1\text{H-NMR}$ spectrum of the uncharacterized products of the superbases metal cluster mediated approach toward the synthesis of azobenzene **5**.

Taking into consideration that ortho lithiation was not feasible through the implementation of the selected superbases conditions; we investigated another approach for this reaction. Knochel and co-workers had reported on the regioselective generation of aryl and heteroaryl magnesium compounds using mixed Mg/Li compounds (Scheme 13).⁵⁶ In their report, the necessity of two substituents on the aryl compound, a directing and a functional group was rationalized (Scheme 13).



Scheme 13 Knochel's methodology for regioselective deprotonation.⁵¹

Considering this methodology milder than the superbases approach, we used a substrate bearing a fluorine substituent as the directing group, and a methyl substituent as a functional group (Scheme 14).



Scheme 14 Synthetic approach toward the organometallic intermediate.⁵¹

The reaction was performed at four different temperatures, -40, -20, -10 and 0 °C. Reaction fractions were withdrawn, quenched with an Iodine solution and characterized with Gas Chromatography–Mass Spectrometry (GC-MS). No reaction took place at -40, -20 and -10 °C while, a side reaction took place at 0 °C, leading to an undesired product as evidenced via the representative GC-MS shown in Figure 23.

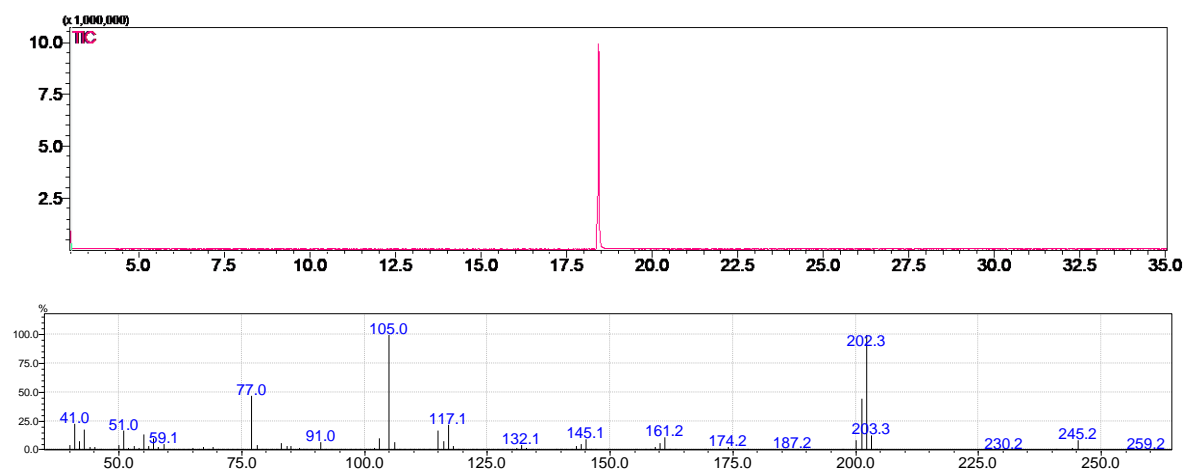


Figure 23 A. GC chromatogram and, B. MS spectrum of the product of the reaction aiming at the organometallic intermediate at 0° C.

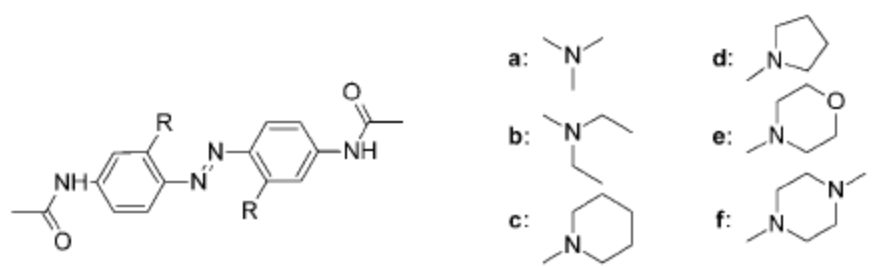
Taking into account that the *trans/cis* isomerization of the tetra-halogenated azobenzenes **2** and **4** upon irradiation with yellow light was either insufficient or not feasible and the preparation of tri-halogenated azobenzenes, and more specifically of the azobenzene **5**, with the chemicals at our disposal was not possible, more feasible approaches were considered using different ortho substituents in order to tune the isomerization wavelength.

Wavelength tuning for blue light isomerization

The firefly luciferase system requires luciferin as an external substrate to produce light while, a flux system producing blue light encodes for both the light producing enzyme and substrate.^{40,47} Therefore, blue light induced isomerization was also considered as it could prove beneficial and possibly even increase the opportunities for *in vivo* isomerization. We focused our attention to the synthesis of azobenzene derivatives which could combine easy wavelength and thermal relaxation tuning based on the findings of O. Sadovski and Z. Ahmed^{57, 58}

2.2 Design and synthesis of mono- and di-fluorinated azobenzenes as precursors for amination

Wooley and co-workers reported on the synthesis of a series of ortho-amino substituted azobenzene derivatives, in which longer switching wavelengths (up to 530 nm) were combined with relatively slow thermal relaxation rates and high *cis* isomer yields (Figure 24).⁵⁷ Based on these properties, we reasoned that the reported azobenzenes can be used as effective, long wavelength photoswitches to drive conformational photocontrol in biochemical systems.⁵⁷



The figure shows a general structure of an azobenzene derivative with two ortho-amino groups and substituents R. Below it are six specific substituents labeled a through f:

- a: N,N-dimethylamino group
- b: N-ethyl-N-(2-(dimethylamino)ethyl)amino group
- c: N-methylpiperidine ring
- d: N-methylpyrrolidine ring
- e: N-methylmorpholine ring
- f: N-methylpiperazine ring

Photoswitch	λ_{\max} [nm] ^[a]	ϵ ^[a] [M ⁻¹ cm ⁻¹]	$\tau_{1/2}$ ^[a] [s]	$\tau_{1/2}$ ^[b] [s]
5a	470	13 900	3.3 ± 0.3	–
5b	488	13 000	0.8 ± 0.1	–
5c	445	10 180	6.0 ± 0.2	–
5d	513/537	–	0.7 ± 0.1	–
5e	435	9 610	302 ± 4	8.1 ± 0.2
5f	437	10 440	207 ± 10	27 ± 1

Figure 24 Photometric studies and properties of photoswitches **a-f** reported by O. Sadovski, A. A. Beharry, F. Zhang, G. A. Woolley, *Angew. Chem., Int. Ed.* **2009**, 48, 1484-148.⁵⁷

Furthermore, we took into account the work of Z. Ahmed et al. reporting on a series of visible light absorbing azobenzene photoswitches with *cis* lifetimes varying from one second to a few days (Figure 25).⁵⁸ This was achieved by combining ortho- fluorination and ortho- amination where, the former was found to control *cis* life time, whereas the latter to boost visible light absorption. The synthesis was accomplished by selectively replacing one or more ortho- fluorines with amines on azobenzene precursors.⁵⁸

Compd	λ_{\max} (nm)	ϵ ($M^{-1} \text{ cm}^{-1}$)	τ (s h ⁻¹)	<i>cis</i> -% at PSS ^c
1	357/432	29110/3608	41.8 ± 1.3 h ^a	93
2	359/432	25810/3185	60.2 ± 0.5 h ^a	93
3	350/432	24652/2286	430 ± 150 h ^{ab}	94
4	340/462	12693/12749	15.2 ± 0.1 s	73
5	341/402	14924/10075	9.1 ± 0.3 h	75
6	344/479	13777/15042	258 ± 30 s	71
7	488/514	3701/3456	1.21 ± 0.01 s	62
9	335/411/454	16739/8006/7792	72 ± 8 h ^a	80

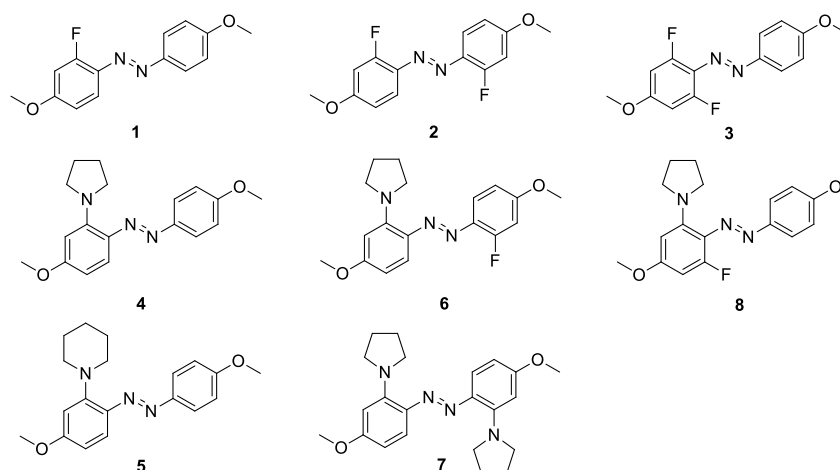
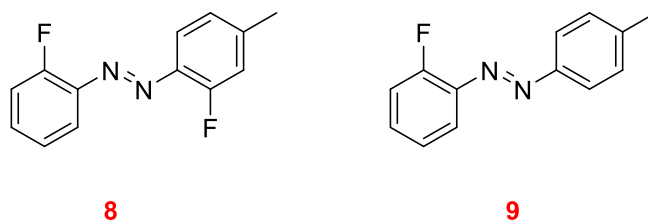


Figure 25 (A) UV-Vis spectra and, (B) photometric data for the ortho substituted azobenzenes reported by Z. Ahmed et al.⁵⁸ This article is licensed under a [Creative Commons Attribution-NonCommercial 3.0 Unported Licence](https://creativecommons.org/licenses/by-nc/3.0/).

Taking into consideration that ortho-amination offers the opportunity to tune both isomerization wavelength and thermal relaxation life times, a hypothesis was formed that an analogue of Z. Ahmed's molecule 7 shown in Figure 25, which exhibits a λ_{\max} of 488/514 nm and a *cis* half-life of 1.21 seconds, could possibly be effectively utilized in our approach. We aimed to design an azobenzene derivative which could, in principle, be conjugated to an anticancer agent in order to achieve a therapeutic scenario where activation would occur

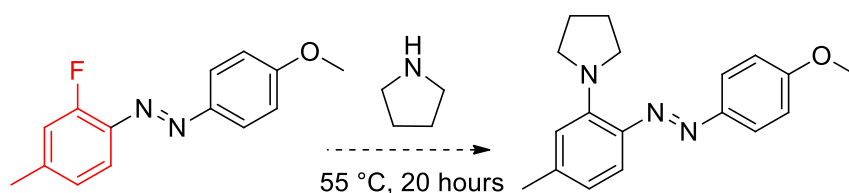
repetitively on the tumour,¹ by a light source such as bioluminescent bacteria *vibrio fischeri*. With the aim to evaluate this hypothesis, the preparation of ortho fluorinated azobenzenes (E)-1-(2-fluoro-4-methylphenyl)-2-(2-fluorophenyl)diazene **8** and, (E)-1-(2-fluorophenyl)-2-(p-tolyl)diazene **9** was judged to be essential, since they could serve as precursors for an ortho amination.



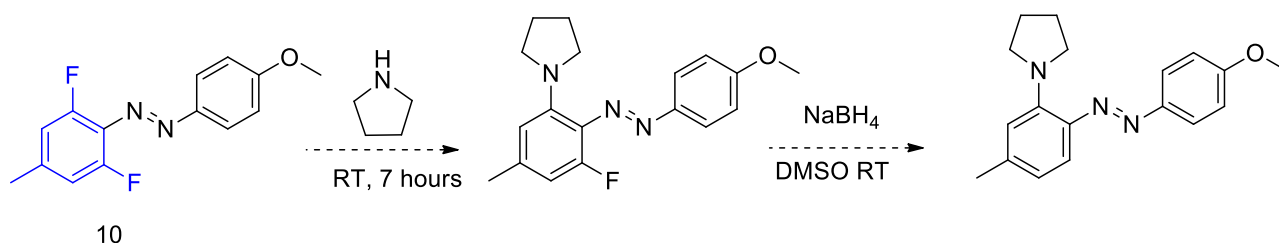
Scheme 16 Ortho-fluorinated azobenzene derivatives **8** and **9**.

Since aryl lithiation for the synthesis of a mono fluorinated azobenzene proved unsuccessful in previous synthetic approaches used during the course of this thesis, and taking into account that lithiation of 3,5-difluorotoluene was relatively an easy process we reasoned that the cleavage of one fluorine atom at a later stage would be possible and could afford the same result.

Following this rationale, instead of using the proposed 3-fluorotoluene (marked in red colour in Scheme 17) we reasoned it could be possible to use 3,5-difluorotoluene (marked in blue in Scheme 18) to synthesize an ortho fluorinated azobenzene, perform selective ortho amination,⁵⁸ and subsequently use a hydride source such as Sodium Borohydride (NaBH₄) to perform an aromatic nucleophilic substitution. Sodium Borohydride was judged to be an appropriate hydride source as, according to literature, it does not cause reduction of the azo group,⁵⁹ and can therefore be used for fluorine elimination via hydride aromatic substitution.

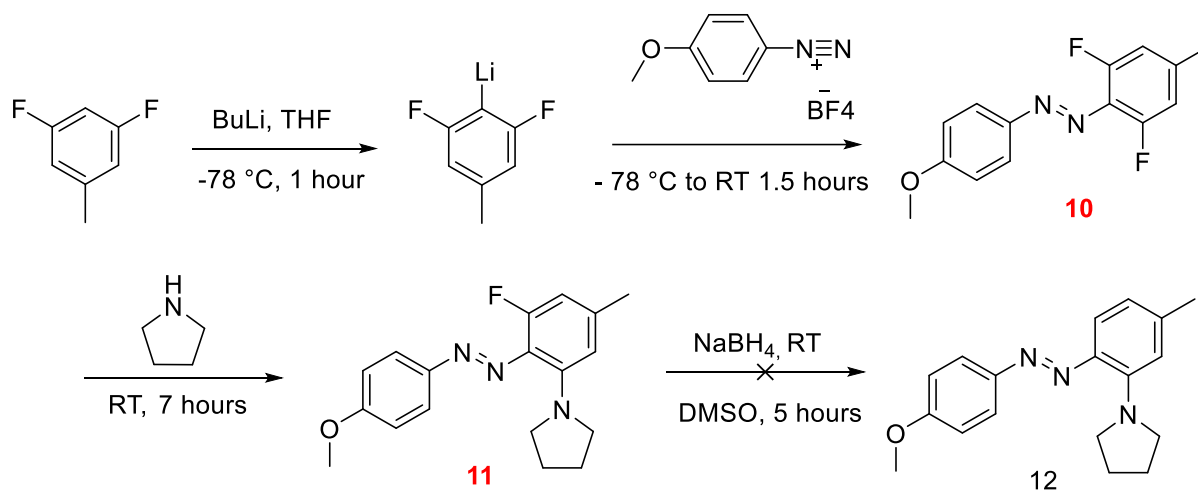


Scheme 17 Reaction scheme using as starting material 3-fluorotoluene. According to our studies, this azobenzene precursor cannot be synthesized via aryl lithiation.



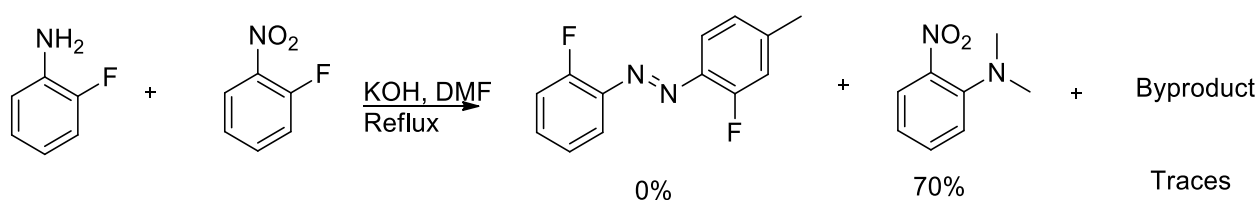
Scheme 18 Proposed reaction scheme using as starting material 3,5-difluorotoluene.

The synthesis of (E)-1-(2,6-difluoro-4-methylphenyl)-2-(4-methoxyphenyl)diazene **10**, was performed following the general methodology previously used for the synthesis of compounds **2** and **4**, with yields of up to 70%. The selective amination of **10** led to (E)-1-(3-fluoro-2-((4-methoxyphenyl)diazenyl)-5-methylphenyl)pyrrolidine **11** with yields of up to 90%. The hydride aromatic substitution using NaBH₄ however; yielded no reaction therefore we searched for possible synthetic alternatives in literature.



Scheme 19 Synthetic scheme for hydride aromatic substitution.

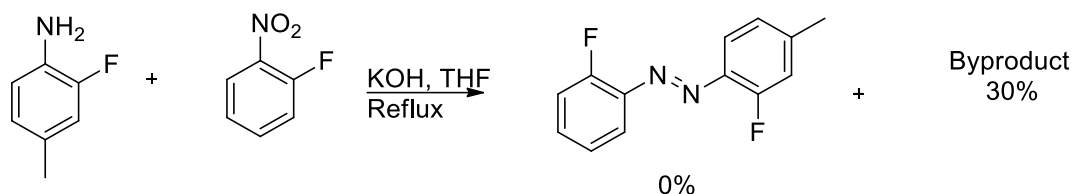
The first alternative route we evaluated was based on a report from C. Zhang et al. in which, nitro aromatics were reacted with substituted anilines to yield azobenzenes in moderate to good yields.⁶⁰



Scheme 20 Condensation of 2-fluoro-4-methyl-aniline and 2-fluoro-nitrobenzene in DMF.

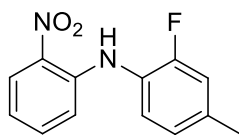
When DMF was used as a solvent (Scheme 20), the expected azobenzene was not formed. Instead, a nucleophilic aromatic substitution took place due to the thermal

decomposition of DMF. A minor by-product was also formed during this reaction suggesting a S_NAr reaction of the aniline onto the nitro aromatic ring. To avoid the production of dimethylamine and gain a more clear picture of the outcomes of this reaction, THF was used as solvent as reported in literature for an alternative reaction solvent.⁶⁰



Scheme 21 Condensation of 2-fluoro-4 methyl-aniline and 2-fluoro-nitrobenzene in THF.

The reaction in THF did not afford the desired product but yielded instead a by-product in yields of up to 30%. Preliminary studies using $^1\text{H-NMR}$ spectroscopy (Figure 26) indicated that the aniline amino group could have acted as a nucleophile performing S_NAr onto the nitro aromatic ring (Scheme 22).



Scheme 22 Possible by-product of the heterocoupling reaction between 2-fluoro-4 methyl-aniline and 2-fluoro-nitrobenzene.

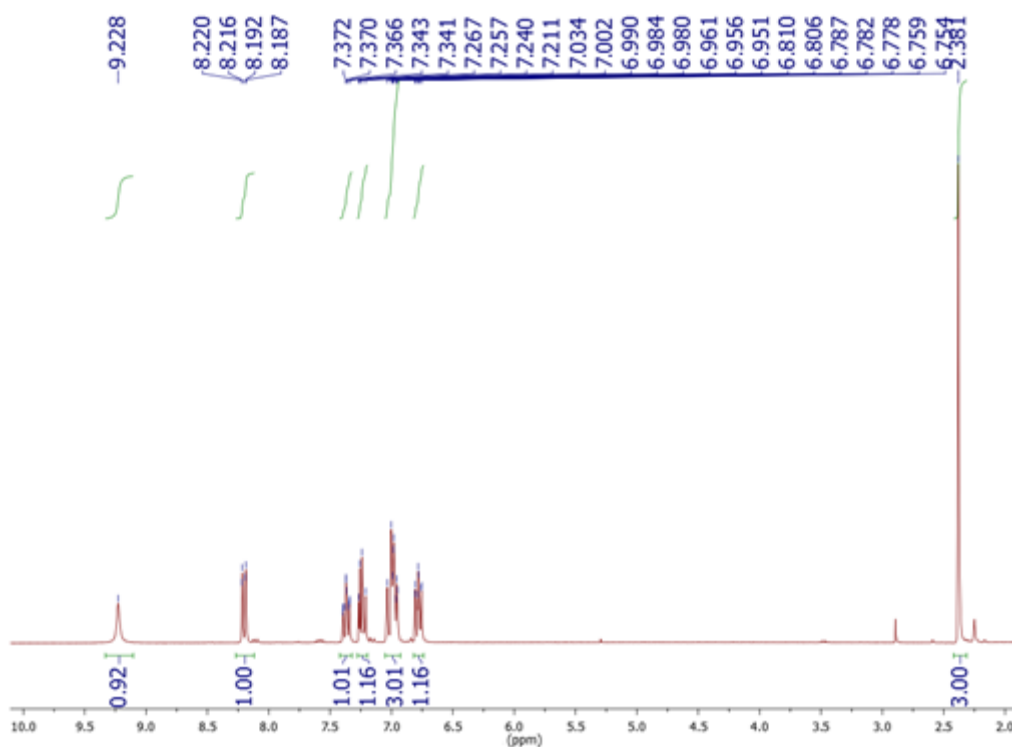
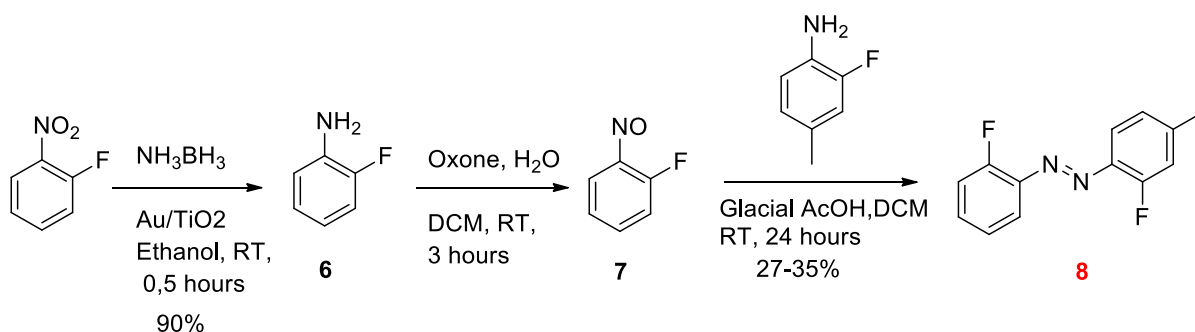


Figure 26 $^1\text{H-NMR}$ spectrum of the product of the condensation reaction between 2-fluoro-4 methyl-aniline and 2-fluoro-nitrobenzene in THF (Scheme 21).

More specifically, aromatic region in the $^1\text{H-NMR}$ spectrum of the product isolated after the condensation reaction, reveals a product bearing seven aromatic protons (8.3 to 6.8 ppm) and possibly the presence of a NH proton resonating in a broad peak at 9.2 ppm. The methyl group of the toluoyl moiety the aliphatic region (2.3 ppm) only strengthens a hypothesis of heterocoupling *i.e.* an $\text{S}_{\text{N}}\text{Ar}$ reaction between the aniline amino group and the fluorinated nitro compound. Further studies need to be performed to verify this assumption.

Another alternative route to synthesize asymmetric fluorinated azo compounds we considered was through the Mills reaction⁶¹ which involves condensation of an aniline and a nitroso compound at room temperature. To convert a fluorinated nitro compound into the corresponding fluorinated nitroso compound two relatively easy extra steps were necessary as shown in Scheme 23.



Scheme 23 Synthesis of the azobenzene **8**.

The reduction of 2-fluoro-nitrobenzene to 2-fluoro-aniline was performed as reported by E. Vasilikogiannaki et al.⁶² to yield compound **6** in 90% yield as evidenced by $^1\text{H-NMR}$ spectroscopy. A colour loss was observed in the product within a short period of time upon isolation so the next step was carried out with freshly prepared product. Following the oxidation of the aniline to the corresponding nitroso compound **7**, a colour loss during chromatography (silica) was also observed therefore we decided to perform the final step without purification. The Mills reaction was performed according to literature in the presence of residual dichloromethane (DCM),⁶³ and compound **8** was synthesized with relative ease, in moderate to low yields of 25-35 % over a total of 3 steps.

The asymmetry of the azobenzene **8** is expressed in a particularly interesting ^{19}F NMR spectrum where the fluorine substituents can be distinguished (Figure 27) with the fluorine **a** of the phenyl group showing multiplet resonance at -124.4 ppm and the toluoyl fluorine **b** a doublet of doublets at -124.7 ppm.

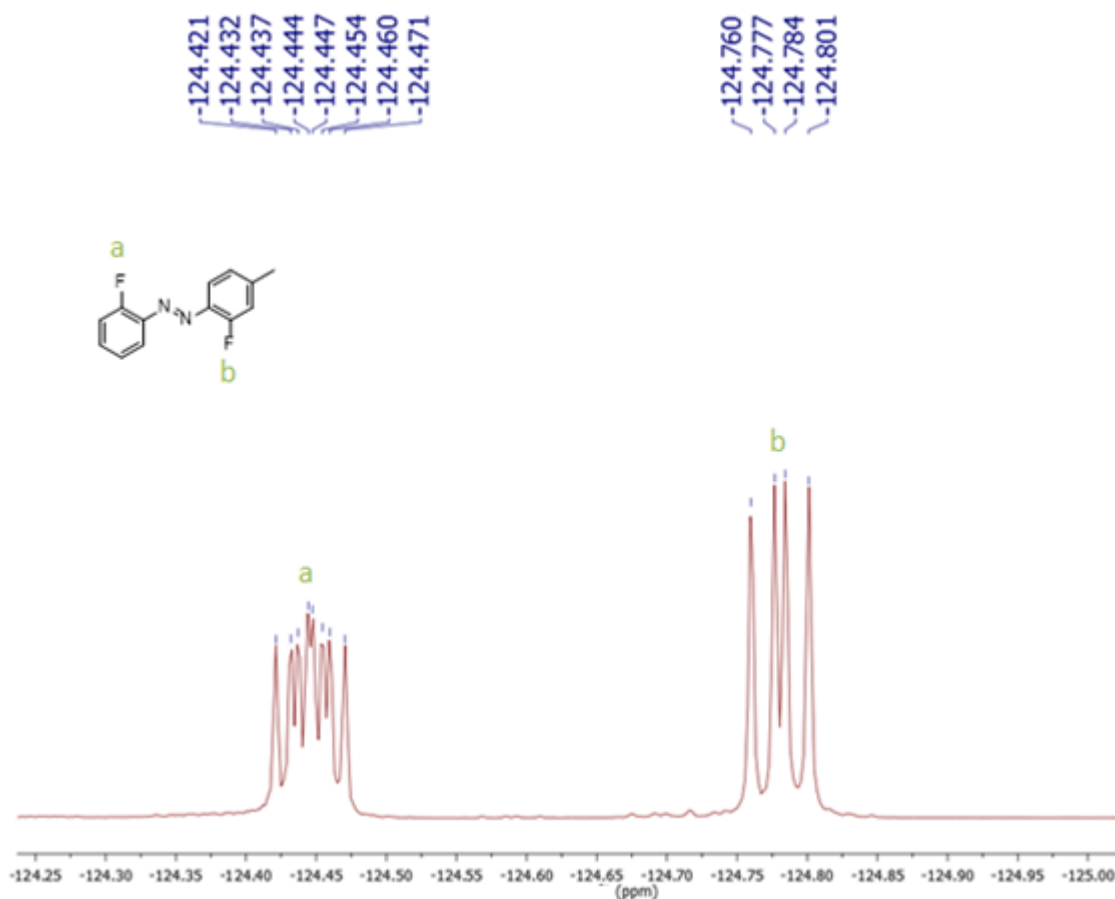
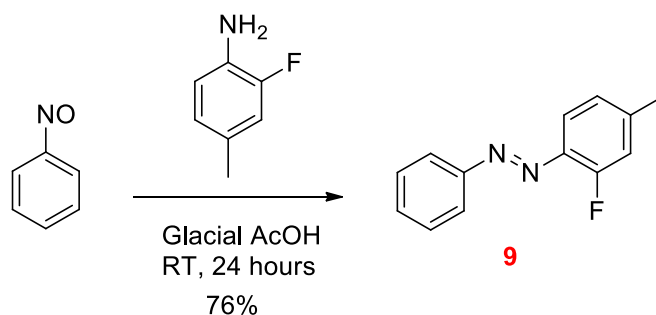


Figure 27 Aromatic region (-124.2 to 125.0 ppm) of the ^{19}F NMR of azobenzene **8** in CDCl_3 .

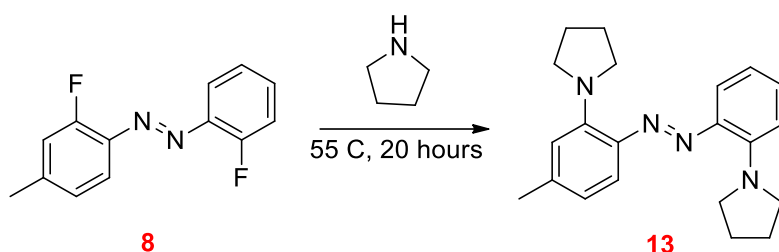
Similarly to the difluorinated azobenzene **8**, the monofluorinated azobenzene derivative **9** was prepared in a one-step reaction and characterized with NMR spectroscopy.



Scheme 24 Synthesis of the azobenzene **9**.

2.3 Synthesis and spectroscopic evaluation of aminated azobenzenes

Nucleophilic aromatic substitution of the azo fluoride derivative **8** with pyrrolidine was performed according to Z. Ahmed et al.⁵⁸ yielding (E)-1-(5-methyl-2-((2-(pyrrolidin-1-yl)phenyl)diazanyl)phenyl)pyrrolidine **13** up to 60 % yield.



Scheme 24 Synthesis of azobenzene derivative **13**.

In the UV-Vis spectrum of **13** in acetonitrile, a strong absorbance in the visible region (λ_{max} 488nm) was observed (Figure 28) as opposed to the non aminated molecule. This prompted us to study the effects of blue and green light irradiation on the *trans/cis* isomerization.

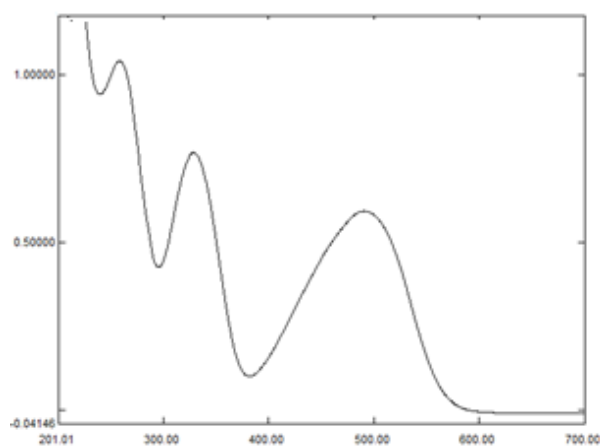


Figure 28 UV-Vis spectrum of azobenzene **13** in MeCN.

Photometric studies using green LED light irradiation initially indicated a short *cis* half-life as predicted by Z. Ahmed et al.,⁵⁸ nevertheless, under constant irradiation photodegradation was observed which could possibly lead to the conclusion that this compound might not be a good candidate for *in vivo* irradiation. To examine the extent of photodegradation in order to verify whether the derivative **13** would be of any use to our research we performed a kinetic experiment lasting 45 minutes (Figure 29). For the first minute the absorbance was recorded without irradiation and was found to be constant. The cuvette was then irradiated with green light for 40 minutes. Upon irradiation we observed a decrease in absorbance attributed to the isomerization to the *cis* isomer. The light was then switched off (41 minutes) to allow for relaxation to the *trans* state (Figure 28).

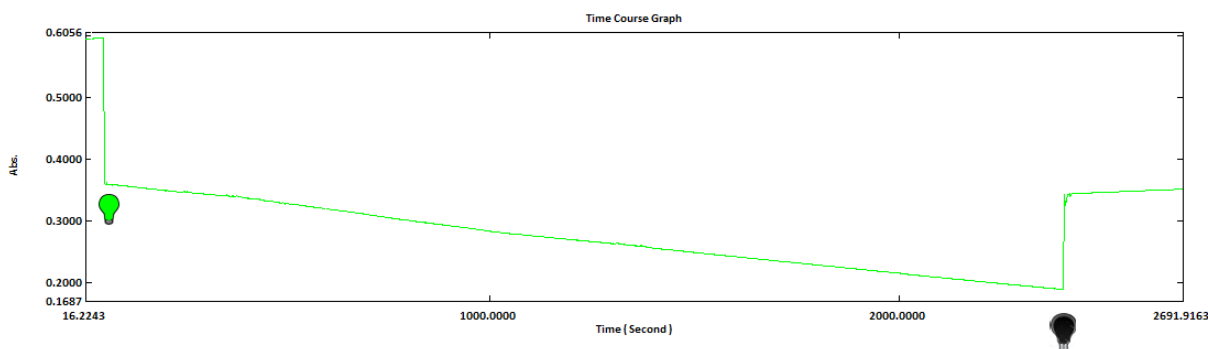
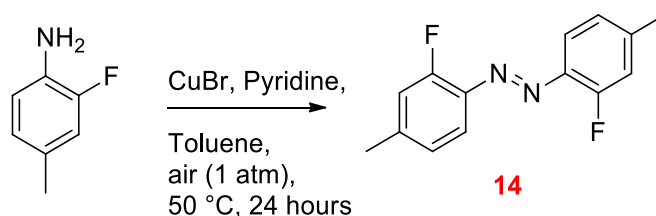


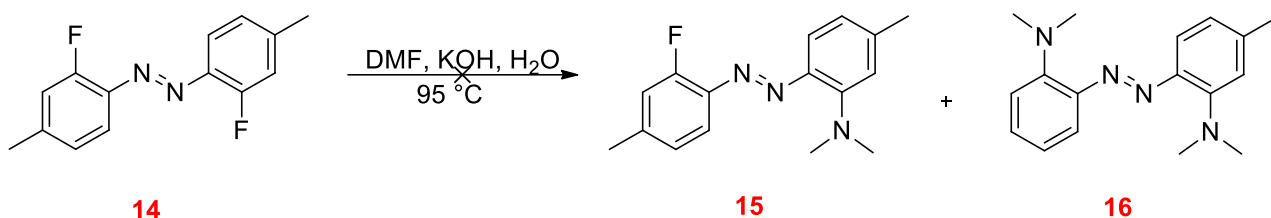
Figure 29 Kinetic photodegradation of azobenzene **13** studied by following the absorption at 465 nm with time.

According to literature, the more electron rich the system becomes, the more prone it is to photodegradation.⁶⁴ Taking this into account, we decided to perform nucleophilic aromatic substitution with alternative amines, and also synthesize a symmetrical analogue of compound **8**; compound **14** (Scheme 25). In addition to the expected higher yields, the inherent symmetry of derivative **14**, was expected to render NMR analysis easier when testing different amines as nucleophiles.⁶⁵



Scheme 25 Synthesis of the symmetric azobenzene **14**.

Out of the amines considered, dimethylamine was selected as it is an important group in pharmacology. Dimethylamine derivatives represent an important class of molecules that possess a range of biological activities including acting as central nervous system stimulants, antimicrobials, anti-cancer agents, anti-H1 AT2 receptor antagonists, progesterone receptor modulators, and rho kinase antagonists.⁶⁶ Since we had no access to dimethylamine gas or dimethylamine salt we used the knowledge gained in a previous experiment involving the thermal decomposition of DMF into dimethylamine (Scheme 20). A thorough search through literature lead us to a report by J. Garcia et al. on hydroxide assisted safe DMF thermal decomposition.⁶⁶



Scheme 26 Synthetic procedure followed to ortho aminate the azobenzene **14**.

The reaction based on the protocol proposed by J. Garcia et al.⁶⁶ yielded trace amounts of the expected products **15** and **16** while, a major by-product was formed. Preliminary analysis based on ¹H NMR spectroscopy indicated at the formation of a derivative bearing a nitrogen bound hydrogen that could agree with a possible N-demethylation. More specifically, the product was found to bear 6 aromatic protons (6.5 to 8 ppm), a singlet at 2.3 ppm indicating two aromatic methyl group moieties and, importantly, a singlet at 2.9 ppm indicating a nitrogen bound methyl moiety. The broad peak at 9.3 ppm could be attributed to a N-bound hydrogen.

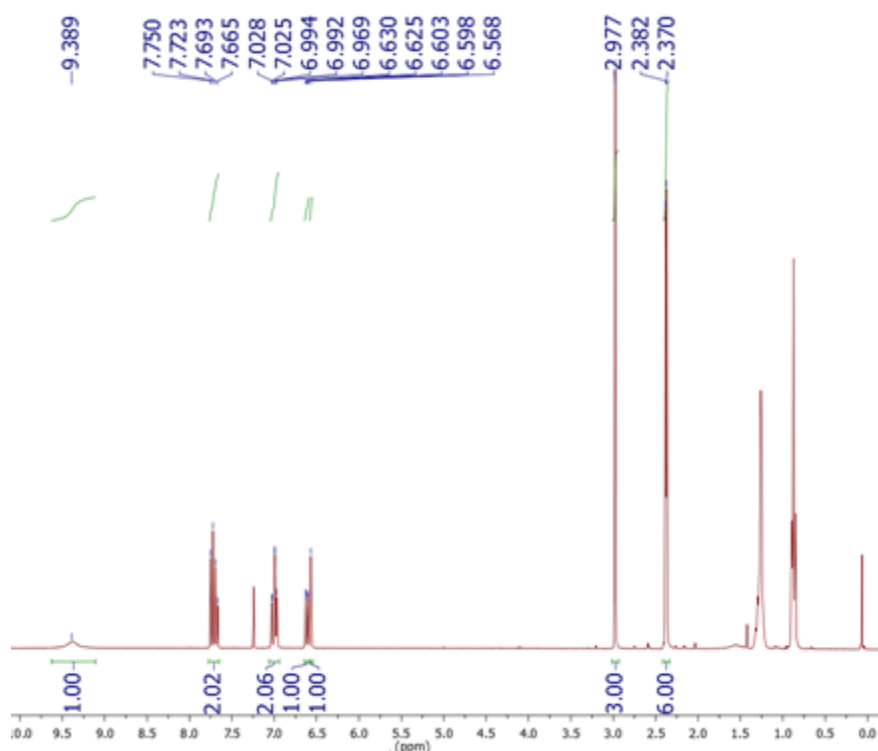
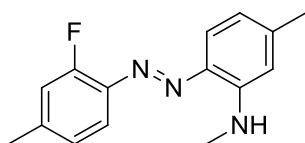


Figure 30 ¹H-NMR spectrum of the by-product isolated from the ortho amination reaction.

The structure of the byproduct proposed after this interpretation of the ¹H-NMR spectrum is shown in Scheme 27. Further studies need to be performed to unravel the structure and fully understand this reaction.



Scheme 27 Possible by-product of ortho amination.

Since the reason for a possible N-demethylation was unclear, we reasoned that the presence of a strong oxidizer, such as KOH, together with a reducing agent, such as the formate, should probably be avoided during handling of the azo compound. To achieve this, we used a two-pot reaction setup (Figure 31) enabling thermal decomposition of DMF in one flask and channelling the produced dimethylamine with the aid of nitrogen gas into a second flask containing the azobenzene solution.

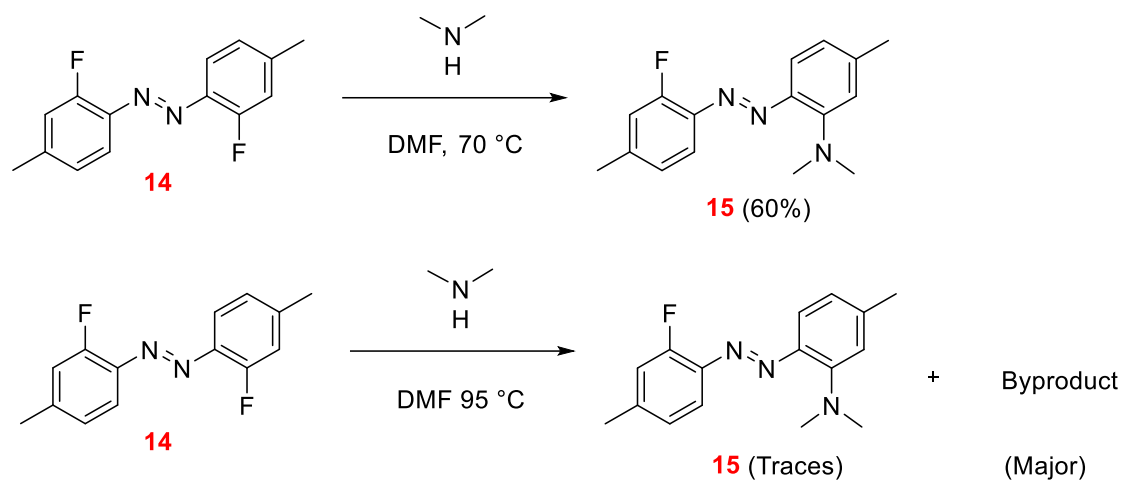


Figure 31 Two-pot dimethylamine channelling system.

When the azobenzene/DMF solution was heated at 70 °C, aromatic nucleophilic substitution took place only on the one aromatic ring affording product **15** with yields up to 60% (Scheme 28). This can be probably attributed to the fact that the addition of the first dimethylamino- group rendered the product more electron rich, making it less susceptible to a second aromatic nucleophilic substitution.

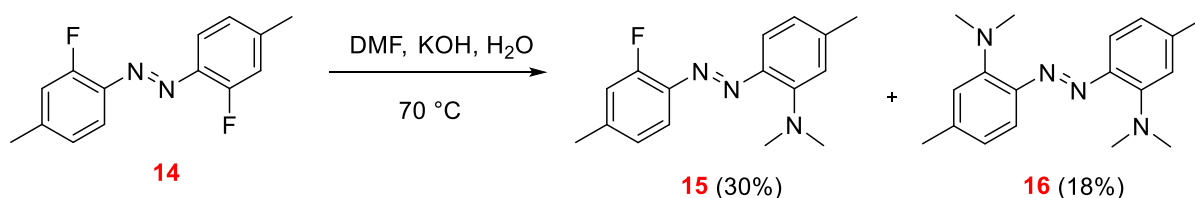
When the temperature was increased to 95 °C in an effort to achieve full amination, the monoaminated product resulted in a by-product resembling the by-product shown in

Scheme 27 *i.e.*, possibly a demethylation occurred (Scheme 28). Since the reaction was performed in a two-pot system to avoid a harsh oxidizing/reducing environment, the formation of the by-product can probably be attributed to the increased temperature. This can be possibly explained by hypothesizing that the monoaminated product **15** facilitates demethylation at high temperatures via a mechanism simulating the action of DEAD.⁶⁷



Scheme 28 Two-pot ortho amination of the symmetric azobenzene **14** via dimethylamine channelling.

Assuming that the two-pot experimental set-up did not allow for a high concentration of dimethylamine gas in the reaction vessel due to a constant bubbling with nitrogen gas, the reaction was performed in one pot. Several synthetic attempts were performed to achieve formation of the diaminated azobenzene **16** by altering the concentrations of all the reagents *i.e.*, potassium hydroxide, water and DMF and the reaction times while retaining the temperature under 75 °C to avoid the formation of the by-product. Via this optimization we achieved the formation of the desired azobenzenes **15** and **16** in relative low yields (up to 30% for the azobenzene **15** and up to 18% for the azobenzenes **16**, Scheme 29).



Scheme 29 Temperature and concentration optimized experimental procedure utilized for ortho amination of azobenzene **14**

UV-Vis spectroscopic studies on azobenzene **15**

To evaluate whether the azobenzene derivative **15** had the expected red shift, a UV-Vis spectrum was recorded in MeCN (Figure 32). The spectrum showed three peaks, two in the UV region at 257.0 and 333.0 nm and one broad peak in the visible (blue) part of the spectrum at 465.5 nm.

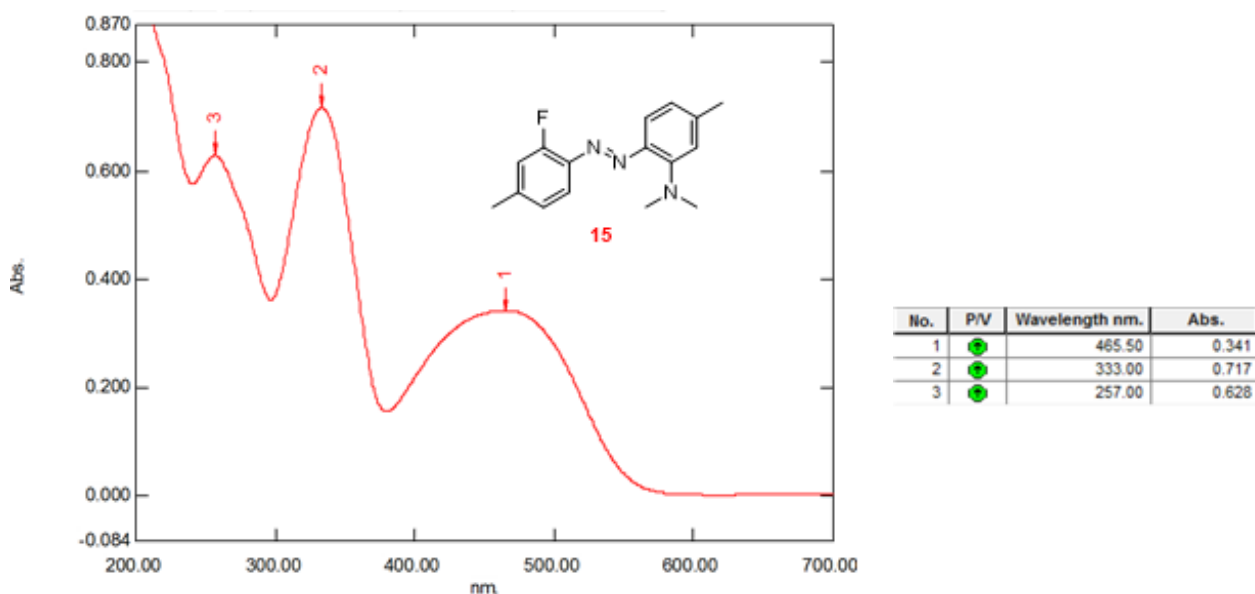
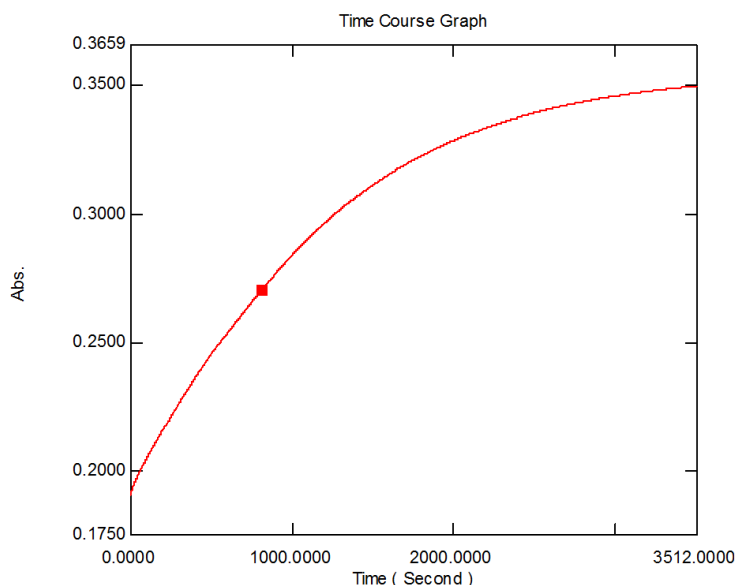


Figure 32 UV-Vis spectrum of azobenzene **15** in MeCN, $C \approx 0.045$ mM at 25 °C.

The broad peak in the visible part of the spectrum prompted us to investigate the *trans/cis* isomerization under blue LED lights. Considering the fact that isomerization is accompanied by a decrease in absorbance we performed a kinetic UV-Vis study (Figure 33) in which, after irradiating the cuvette containing compound **15** in MeCN with Blue LED light for 5 minutes, we followed the thermal relaxation of the *cis* isomer back to the *trans* with time at 465 nm (Figure 33).

The UV-Vis study following the relaxation of the *cis* azobenzene **15** formed upon blue LED light irradiation, revealed complete thermal relaxation within the duration of the experiment (3515 seconds). The *cis* half-life (thermal relaxation of half of the initial concentration of the *cis* isomer to the *trans* isomer) of azobenzene **15** was found to be 812 seconds (Figure 33).

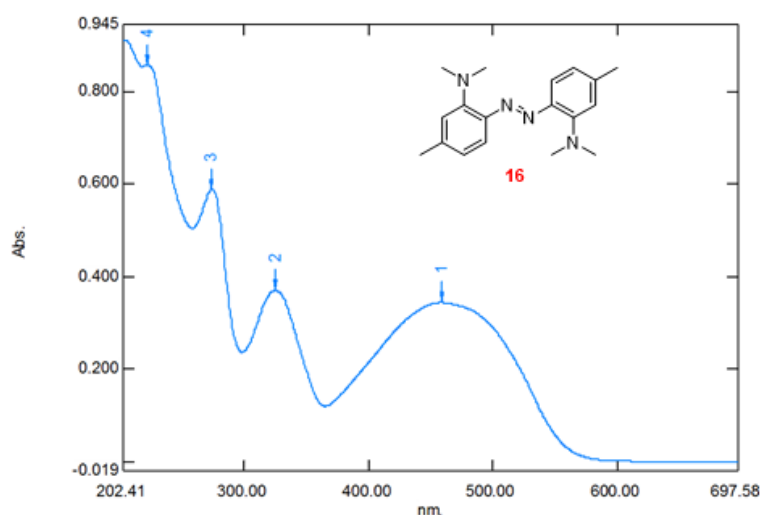


No.	Time (Second)	Absorbance
1	812.0000	0.2704
2		

Figure 33 Kinetics of the thermal relaxation of the *cis* isomer of azobenzene **15** in MeCN (C \approx 0.045 mM at 25 °C).

UV-Vis spectroscopic studies on azobenzene **16**

The UV-Vis spectrum of the azobenzene derivative **16** was recorded in MeCN to evaluate whether it was red shifted (Figure 34). The spectrum showed four peaks, three within the UV region at 221.5, 273.5 nm and 324.5 nm and one broad peak in the visible (blue) part of the spectrum at 459.0 nm.



No.	P/V	Wavelength nm.	Abs.
1	●	459.00	0.345
2	●	324.50	0.370
3	●	273.50	0.588
4	●	221.50	0.858

Figure 34 UV-Vis spectrum of azobenzene **16** in MeCN, C \approx 0.045 mM at 25 °C.

The broad peak in the visible part of the spectrum prompted us again to investigate *trans/cis* isomerization with the use of blue LED lights (Figure 35). A cuvette containing azobenzene **16** in MeCN was irradiated with Blue LED light for 5 minutes to afford the *cis*

isomer and its thermal relaxation back to the *trans* isomer was followed with time at 460 nm.

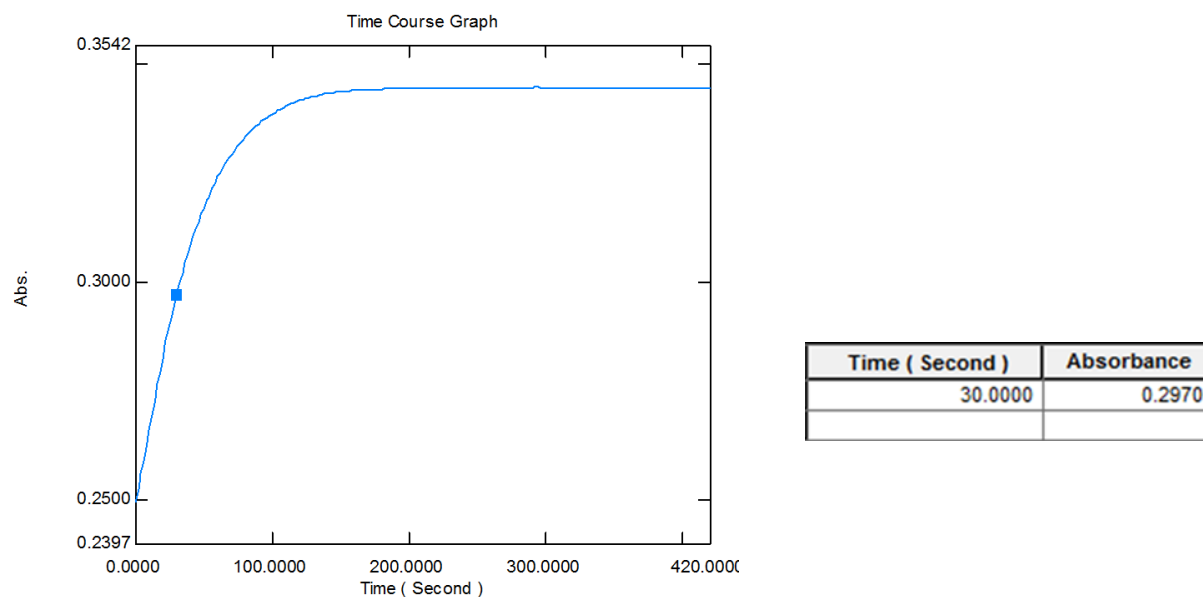


Figure 35 Kinetics of the thermal relaxation of the *cis* isomer of azobenzene **16** in MeCN ($C \approx 0.045$ mM at 25 °C).

A complete thermal relaxation of *cis* isomer of the azobenzene **16** was observed within 190 seconds with *cis* half-life (thermal relaxation of half of the *cis* isomer back to the *trans* isomer) was found to be 30 seconds (Figure 35).

In summary the half-lives of the *cis* isomers produced after irradiation with blue light at 25 °C were 812 seconds for azobenzene **15** (Figure 33) and, 30 seconds for azobenzene **16** (Figure 35) in MeCN. This represents a significant difference in the *cis* half-life in this solvent. These half-lives are indicative and do not directly correspond to the half-lives expected in water (the medium selected for our final studies), we would expect very different behaviour in water as the *cis* half-life is highly solvent sensitive.⁶⁸ Nevertheless, we opted to continue studying the azobenzene **16** due to its shorter *cis* half-life.

The molar absorption coefficient of the azobenzene **16** was determined to be $\epsilon_{460\text{nm}} = 7674 \text{ M}^{-1}\text{cm}^{-1}$ (as measured by UV-Vis and ¹H-NMR measurements, experimental details included in the Experimental Part). Importantly, the azobenzene **16** was found to be stable and showed no photodegradation under continuous irradiation with blue light for a period of 40 minutes. This was proven by following the change of the intensity of the absorption band at 460 nm with time while irradiating the sample at a 90-degree angle in the photometer. The irradiation started after 60 seconds and ended at 3000 seconds (Figure

36). The time course presented in Figure 36 shows fast *trans/cis* isomerization upon irradiation, and fast relaxation to the *trans* isomer at the end of irradiation without loss of intensity.

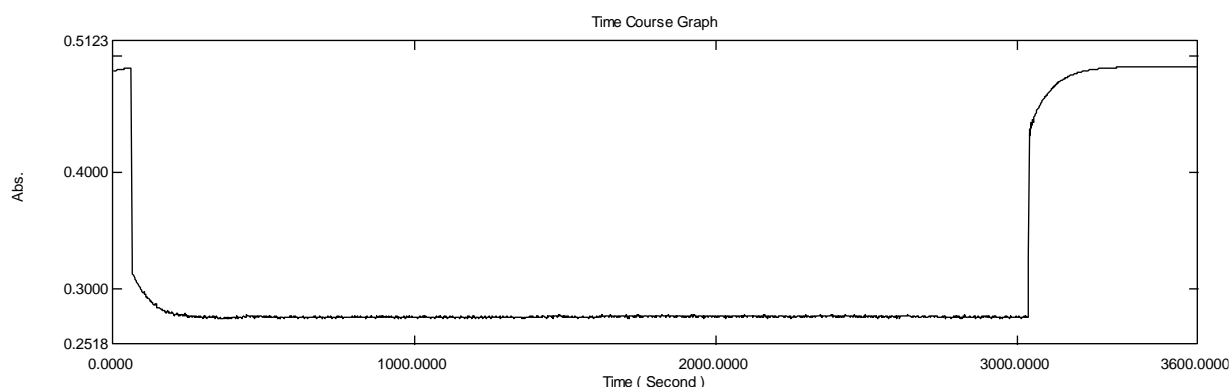


Figure 36 Photostability kinetics of azobenzene **16**: Absorption at 460 nm with time, irradiation started at 60 seconds and was terminated at 300 seconds.

These findings supported our assumption that the azobenzene **16** was a suitable candidate for the purposes of this research. However, due to its small *cis* half-life it was difficult to calculate the *cis/trans* ratio of the photoisomers. M. Kojima, S. Nebashi, K. Ogawa and et al. previously reported that the *cis* lifetime of azobenzenes could be increased in aromatic solvents.⁶⁸ A UV-Vis kinetic study measuring the absorbance at 460 nm and following the thermal relaxation of azobenzene **16** in benzene revealed a *cis* half-life of 2180 seconds (Figure 37) which was judged to be large enough to acquire an NMR spectrum before and after irradiation in deuterated benzene in order to get a rough approximation of the *cis/trans* ratio of the photoisomers (Figures 38, 39).

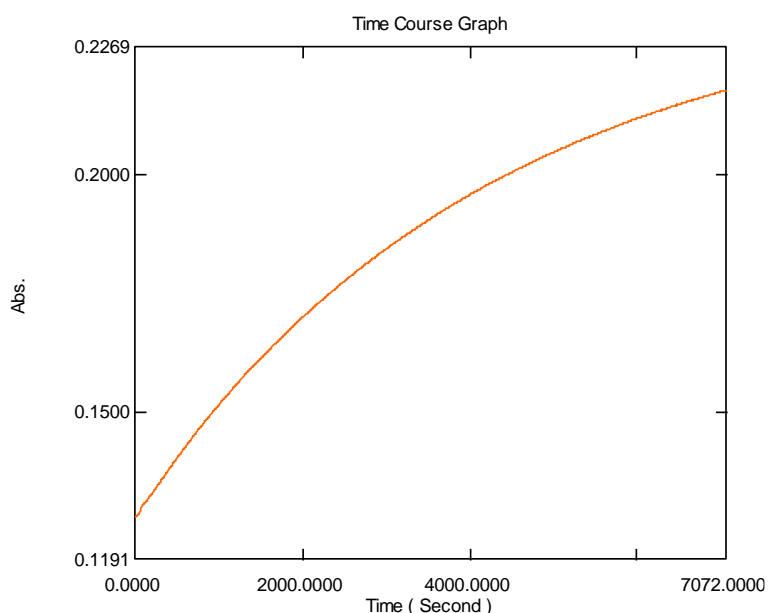


Figure 37 Kinetics of the thermal relaxation of the *cis* isomer of azobenzene **16** in benzene.

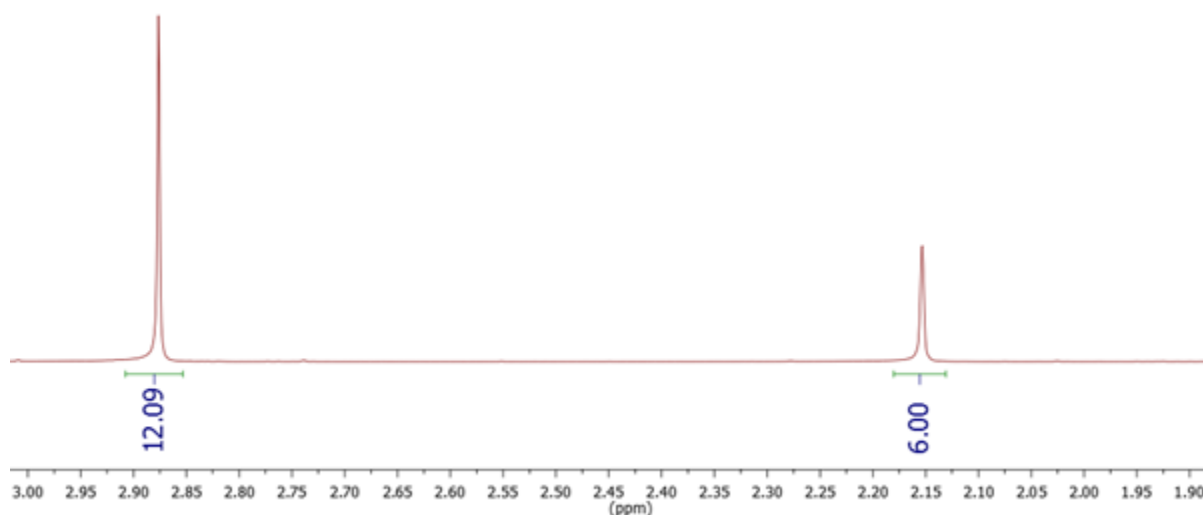


Figure 38 Aliphatic region of the $^1\text{H-NMR}$ spectrum of the azobenzene **16** in benzene- d_6 before irradiation with blue light.

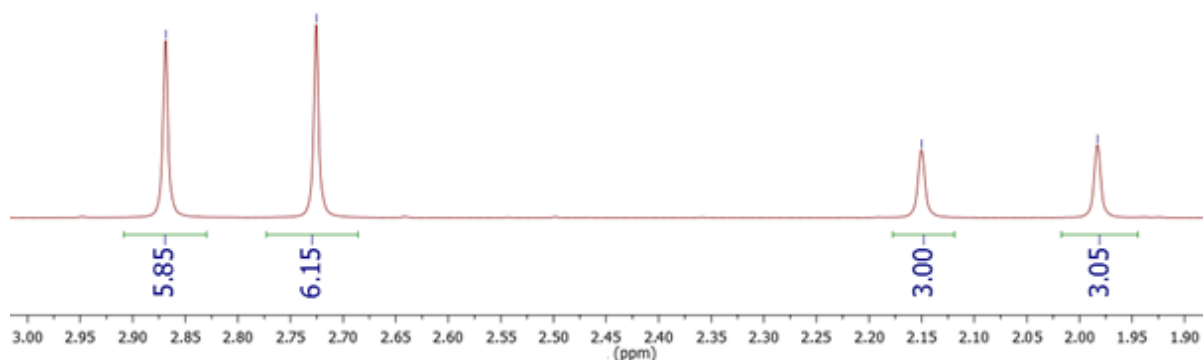


Figure 39 Aliphatic region of the $^1\text{H-NMR}$ spectrum of the azobenzene **16** in benzene- d_6 after irradiation with blue light.

Before irradiation no *cis* isomer was detected in the $^1\text{H-NMR}$ spectrum of the azobenzene **16** (Figure 38) while after irradiation with blue led light for one hour the *cis/trans* ratio was determined to be 49/51, as seen in Figure 39 indicating a substantial shift in the *cis* population at the photostationary state.

Effect of water on the cis half-life of azobenzene 16

The molecular photoswitches need to be fully operational in water in order to be considered for pharmaceutical use. The azobenzene switch **16** is not soluble in water. As its solubility would change upon functionalization (Scheme 1), we performed preliminary UV-Vis kinetic studies measuring the absorbance at 460 nm to determine the *cis* half-life in acetonitrile/water mixtures.

The kinetic study of the relaxation of a 0.04 Mm solution of azobenzene **16** in MeCN/H₂O = 7/3 at 25 °C proved to be difficult as the azobenzene did not exhibit excellent solubility in this solvent mixture (Figure 40).

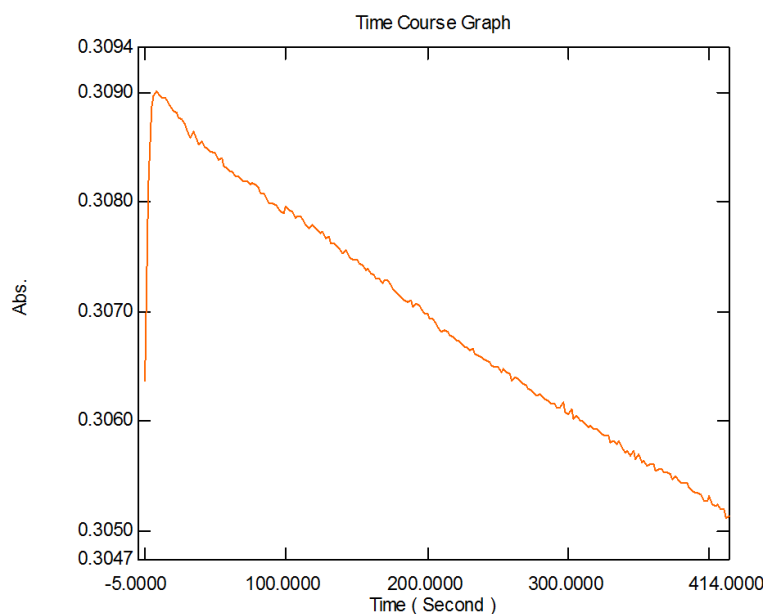


Figure 40 Kinetics of the thermal relaxation of a *ca.* 0.045 mM solution of the *cis* isomer of azobenzene **16** in MeCN/H₂O = 7/3.

As shown in Figure 40, when measuring a previously irradiated with blue light, solution of the azobenzene **16** we initially observed the expected fast thermal isomerization which after a certain concentration ($A_{460\text{nm}} \approx 0.31$ au), starts to decrease. This can be attributed to the fact that the *cis* isomer is more water soluble than the *trans* isomer so as the *trans* population increases, aggregates form and fall out of solution causing a decrease in the absorbance of the mixture. This was elegantly proven in a study by C. Brown et al. on azobenzene solubility as shown in Figure 41.⁶⁹



Figure 41 Differences in azobenzene solubility increases equilibrium *cis/trans* ratio in water due to the formation of aggregates.⁶⁹ Journal of Photochemistry and Photobiology A: Chemistry, 2017, 336, 140-145. © 2016 Elsevier B.V.

When the concentration of the azobenzene **16** was decreased to *ca.* 0.02 mM in the same solvent mixture, a more clear picture of the thermal relaxation could be obtained and a *cis* half-life of 3.6 seconds could be measured (Figure 42).

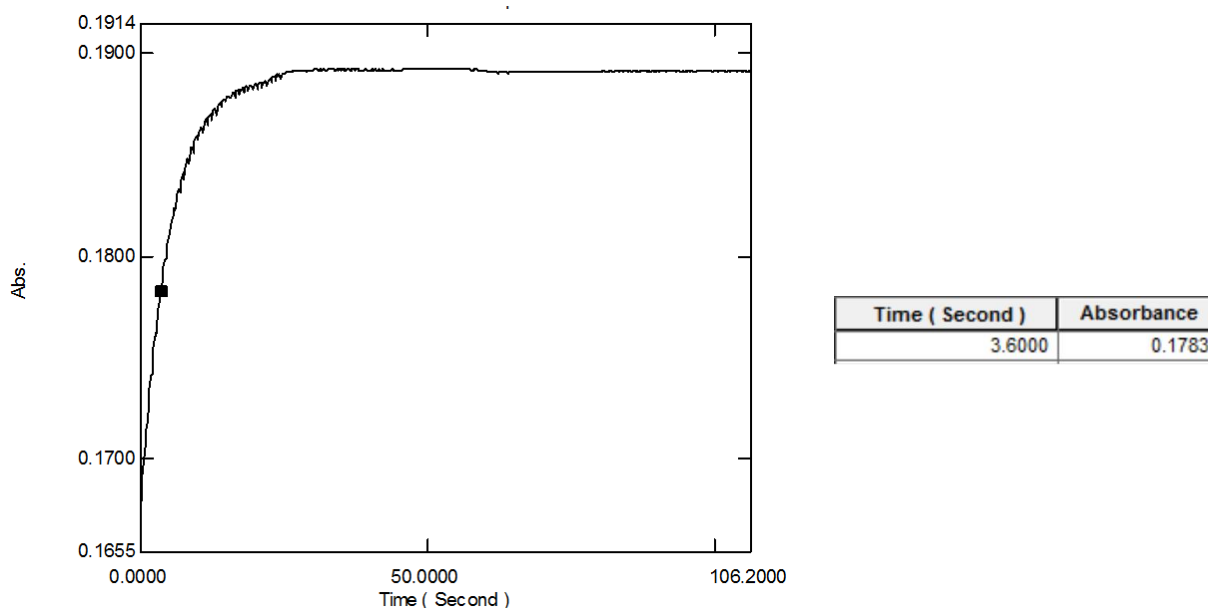


Figure 42 Kinetics of the thermal relaxation of a \sim 0.02 mM solution of the *cis* isomer of azobenzene **16** in MeCN/H₂O 7/3.

The results in acetonitrile and acetonitrile/water mixture are promising. Yet, our studies prove that the azobenzene should be at least partially soluble in water to study the *trans/cis* isomerization with the use bioluminescent bacteria. As proposed in Scheme 1, we proceeded to the functionalization of the methyl group in order to attach a more polar group that would ideally increase the solubility of the azobenzene.

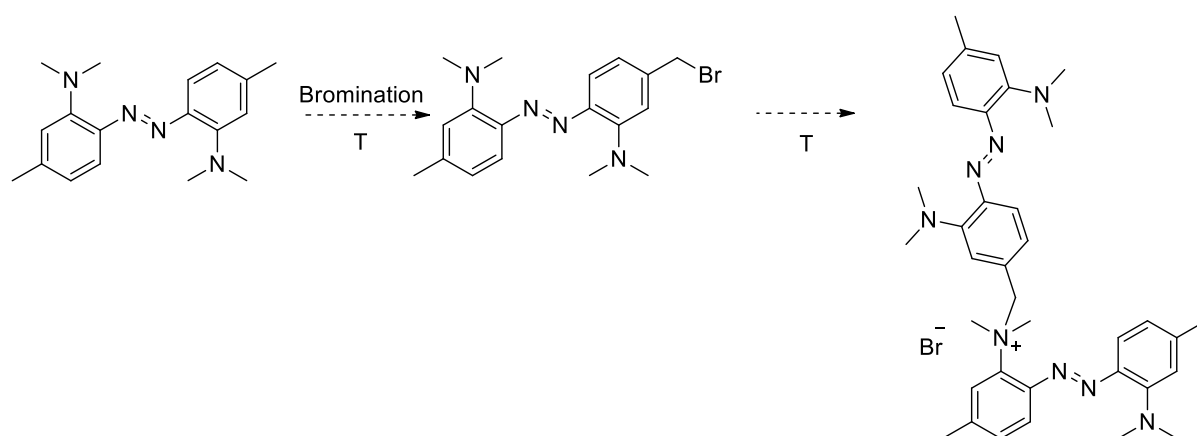
To create a promising pharmaceutical azobenzene precursor, we planned to introduce a spacer group that would make the molecule more water soluble, have a conjugation site for bioactive compounds (to be conjugated on later studies) and bear some pharmaceutical relevance. Piperazine was judged to be a good candidate due to the fact that it is widely used in a range of pharmaceuticals such as anticancer, antipsychotic, antiviral, antihistamine and imagine agents.⁷⁰

2.4 Bromination studies

In order to conjugate a piperazine on the azobenzene moiety, a few different approaches were considered. Oxidizing the methyl group to a carboxylic acid or an aldehyde, was avoided in order to preserve the dimethylamino groups. Oxidation of the

methyl group of the di-fluorinated azobenzene followed by amination, would result in reaction of the functional aldehyde or carboxylic acid with the amines. We therefore considered as a possible route a benzylic bromination of compound **16** followed by piperazine introduction through a nucleophilic attack.

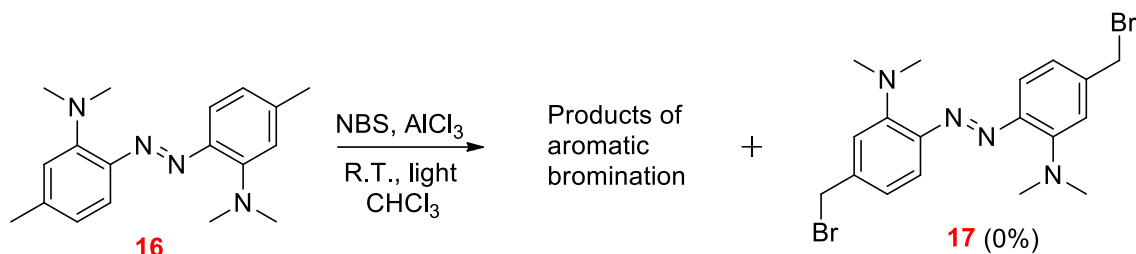
N. Wegner et al. had previously reported on a benzylic bromination of azobenzenes using 2,2'-azobis(isobutyronitrile) (AIBN),³⁸ while M. Kaiser et al. previously reported on a benzylic bromination with benzoyl peroxide.⁷¹ These methodologies require high temperatures for the activation of the radical initiators and would not be advantageous for our purposes as amine N-demethylation and quarterisation of the tertiary amines with the produced benzyl bromide would most probably occur as reported by Ten-Tsai Wang in his research involving tertiary amines and benzyl chloride.⁷²



Scheme 30 Representation of amine quarterisation and why high temperature should be avoided.

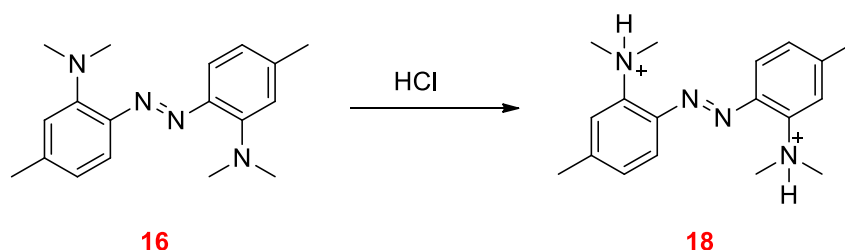
In order to achieve benzylic bromination of the azobenzene **16**, quarterisation of the dimethylamine groups should be avoided, we therefore proceeded to perform room temperature benzylic brominations. Our first synthetic attempt was conducted following the experimental procedure proposed by F. Riefolo et al. according to which, an azobenzene and NBS solution in MeCN was illuminated with white light at room temperature to achieve bromination in conventional azobenzenes.⁴¹ By following the course reaction by TLC, a quick disappearance of the starting material and the emergence of a new product was observed. ¹H-NMR spectroscopy revealed signs of aromatic bromination rather than benzylic bromination. The electron rich azobenzene **16** is, as reported in literature, susceptible to photodegradation.⁵⁷ Additionally, electron rich aromatics in general undergo aromatic bromination rather than benzylic bromination.⁷³

Since benzylic bromination is sensitive to heat and light, we performed an acid catalysed benzylic bromination according to the methodology proposed by Yamamoto et al.⁷³ The article explains that benzylic bromination can occur on slightly activated rings using a catalytic amount of a Lewis acid proving also that more electron rich substrates would afford both benzylic and aromatic bromination products.



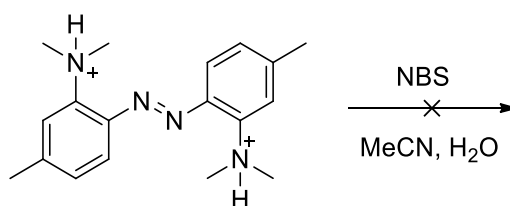
Scheme 31 Lewis acid catalysed assisted benzylic bromination of azobenzene **16**.

The Lewis acid catalyzed bromination of the azobenzene **16** afforded solely aromatic brominated by-product (Scheme 31). This can be attributed both to the electron rich nature of **16** as well as to the ability of aluminum chloride to act as activator for aromatic substitution. One possible way to overcome this problem would be to protonate the amine groups thus making the molecule electron poor.⁷⁴



Scheme 32 Amine protonation of azobenzene **16** to synthesize the electron poor azobenzene derivative **18**.

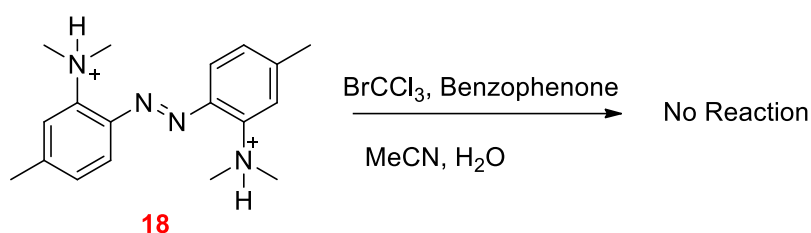
Protonation of the azo-switch **16** to azobenzene **18** was accomplished by adding a 3N solution of HCl to solid **16**, affording the soluble in water **18** that was partially soluble in MeCN and chloroform.



Scheme 33 Benzylic bromination of compound **18** using NBS.

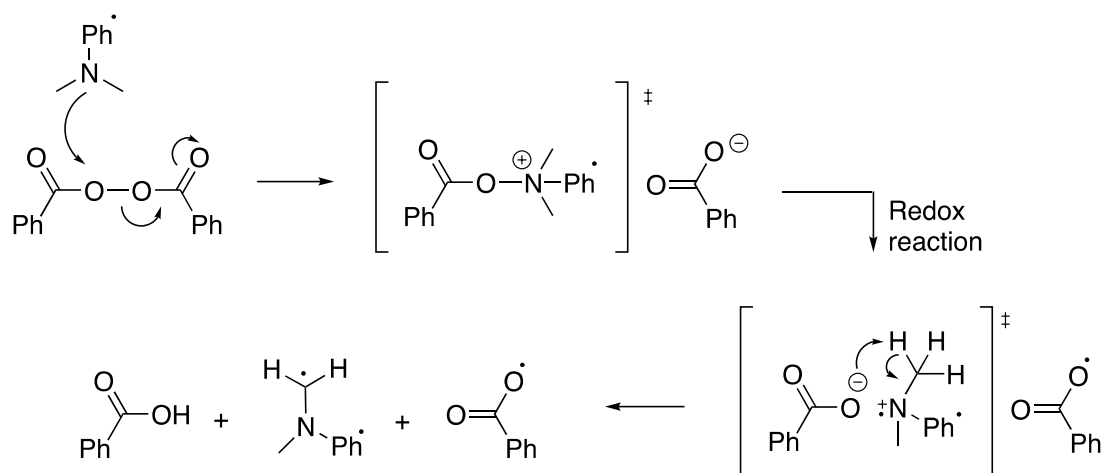
When the protonated azobenzene **18** was reacted with NBS, the reaction mixture instantly turned brown and no product could be observed. This could probably be caused by

NBS protonation. We proceeded to react the organic salt with BrCCl_3 as it was reported in literature to be an appropriate bromine source for benzylic bromination,⁷⁵ and more importantly a successful reagent for the benzylic bromination of activated aromatics. Unfortunately, no reaction was observed.



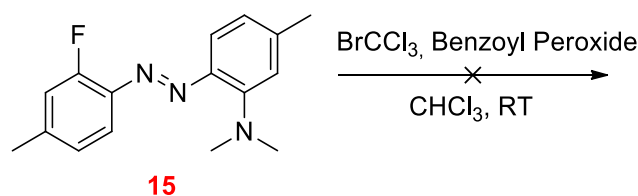
Scheme 34 Benzylic bromination of compound **18** using BrCCl_3 .

Our goal became to find a way to activate radical initiation with the electron rich azobenzene without using heat and/or light. A. Zoller et al. reported on a radical polymerization using a benzoyl peroxide/tertiary amine initiating system as shown in Scheme 35.⁷⁶



Scheme 35 Proposed mechanism of radical polymerization using the benzoyl peroxide/tertiary amine system.⁷⁶

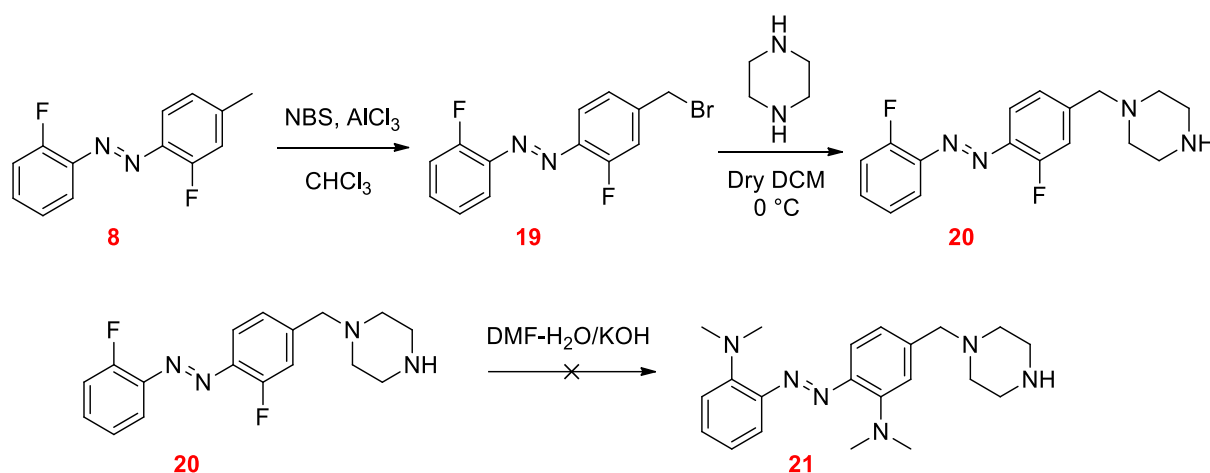
This reaction sequence consists of a nucleophilic attack of the tertiary amine on the peroxide bond followed by a redox reaction forming radical species, most interesting of which is the benzoyloxy radical which could possibly be used to initiate a bromination. We used this system to initiate bromination on the azobenzene **15** at the expense of a sacrificial small percentage of the starting material which would be lost as a radical. The azobenzene **15** was used in an effort to investigate the possibility of benzylic bromination on either or both methyl groups the one bearing an electron donor on one aromatic ring and the other an electron acceptor.



Scheme 36 Benzylic bromination using a benzoyl peroxide/tertiary amine radical initiation.

Only trace amounts of a non-desired by-product were observed probably formed by a redox reaction between the benzoyl peroxide and the aromatic amine.

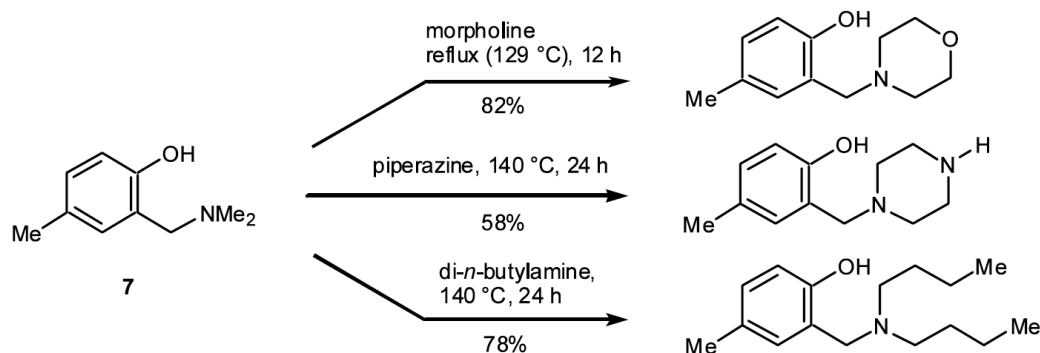
Having followed several different approaches to achieve benzylic bromination of the azobenzenes **15**, **16** and **18**, we decided to investigate benzylic bromination of the asymmetric fluorinated azobenzene **8** instead, proceed to piperazine conjugation to produce a photoswitchable drug, and then conduct amination as proposed in Scheme 37. The compatibility of the piperazine moiety with the harsh amination conditions, was not known.



Scheme 37 Proposed synthetic scheme for azobenzene **21**.

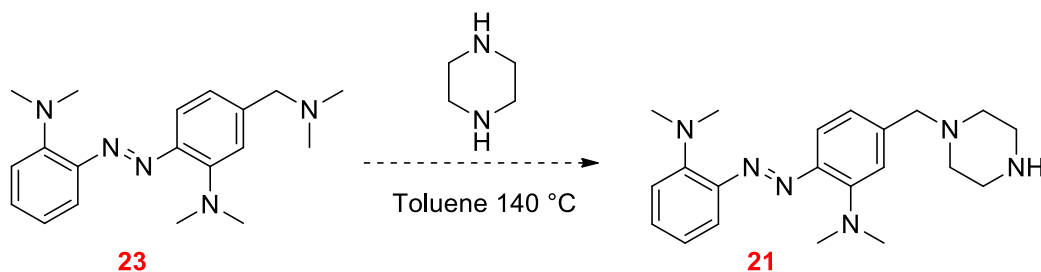
Acid catalysed bromination under green LED light irradiation for two hours afforded the brominated azobenzene **19** with up to 90 % yields.⁷³ Bromine substitution through an S_N2 reaction with piperazine was achieved with a 20-fold molar excess of piperazine over the azobenzene **19**, with yield of 90% for the azobenzene **20**.⁷⁷ However, amination of **20** did not yield the expected product. ¹H-NMR spectroscopy on the crude reaction mixture gave little to no indication concerning the structure of the by-products. After purification it was revealed that the major by-product either did not bear the piperazine or that it was modified on the piperazine moiety. Although this by-product was not studied any further, we invested time in researching the displacement of amines on benzylic carbons and found

a report by P. C. Bulman et al. on the benzylic position amine exchange, using amines such as dimethylamine and piperazine (Scheme 38).⁷⁸



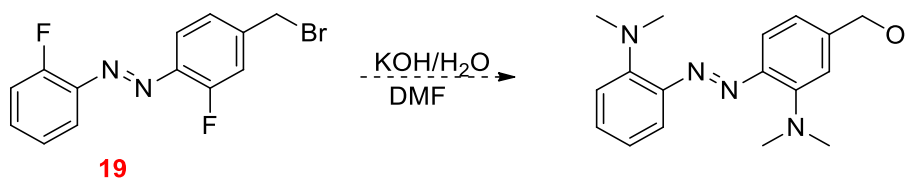
Scheme 38 Conditions for benzylic amine exchange reported by P. C. Bulman et al.⁷⁸ from P. C. B. Page, H. Heaney, M. J. McGrath, E. P. Sampler, R. F. Wilkins, *Tetrahedron Letters*, **2003**, 44, 2965-2970 Copyright © 2003 Elsevier Science Ltd. All rights reserved.

This was particularly interesting because we could adjust our approach accordingly, insert first the dimethylamino groups onto the azobenzene aromatic rings and subsequently perform an amine exchange on the benzylic dimethylamino group as proposed in Scheme 39.



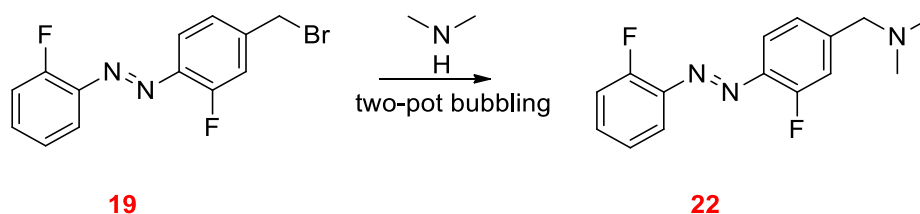
Scheme 39 Proposed amine exchange synthetic approach.

The preparation of compound **22** was not straightforward though, due to the fact that if amination was performed on the brominated difluoro- azobenzene **19**, the DMF-KOH/H₂O mixture would convert the benzylic bromide to the corresponding alkoxide as shown in Scheme 40.



Scheme 40 Product proposed for the base mediated DMF degradation demethylation of **19**.

E. Tayama et al. reported on the conversion of benzylic bromides to benzylic dimethylamino derivatives using aqueous dimethylamine and diethylether.⁷⁹ Following this approach, we considered using the two-pot system we previously used for thermal decomposition of DMF in the one flask and channelling of the produced dimethylamine into a second flask.



Scheme 41 Synthesis of azobenzene **22**.

We added both water and diethyl ether into the reaction flask creating a two-phase system (Figure 41) as water would trap dimethylamine and increase its concentration in the biphasic mixture.

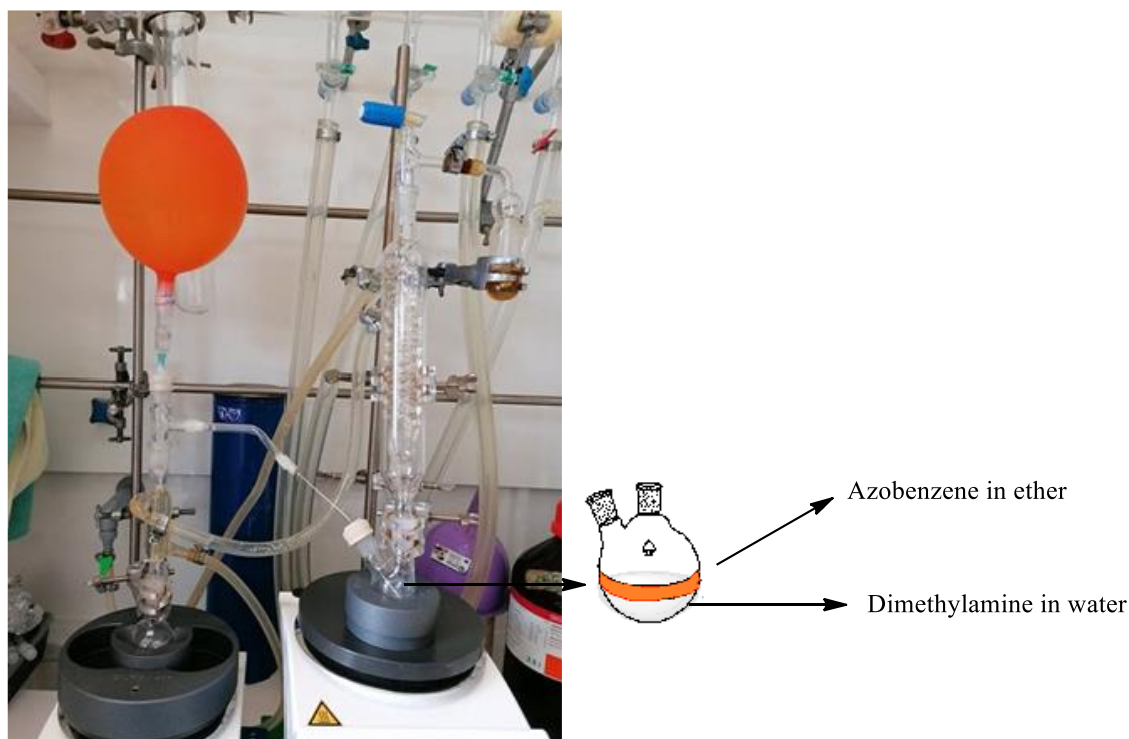
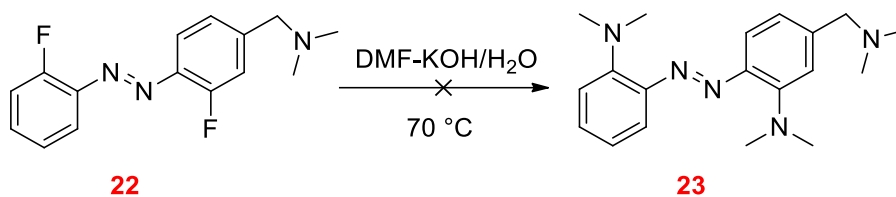


Figure 41 Two-pot dimethylamine channelling system: DMF degradation in pot A produces dimethylamine which is channelled to pot B where it reacts with azobenzene **19**.

After bubbling the two-pot reaction system with nitrogen gas for two hours, the system was disassembled and the two-neck reaction flask was left under vigorous stirring overnight. The reaction yielded the azobenzene **22** with yields of up to 60 %.

The subsequent step of ortho amination (Scheme 42) was performed according to the protocol previously used for the synthesis of azobenzene **16**. No product could be identified using NMR spectroscopy.



Scheme 42 DMF thermal degradation mediated amination.

Several experiments were performed for the synthesis of the azobenzene **23** using different molar excess and concentrations of aqueous KOH. Upon purification all reactions yielded the same product which, according to $^1\text{H-NMR}$ spectroscopy, most probably corresponds to the monoaminated isomers presented in Figure 42 with protons **a** corresponding to the benzylic carbon, protons **b** corresponding to the aromatic dimethylamine methyl groups and protons **c** corresponding to the benzylic dimethylamine methyl groups.

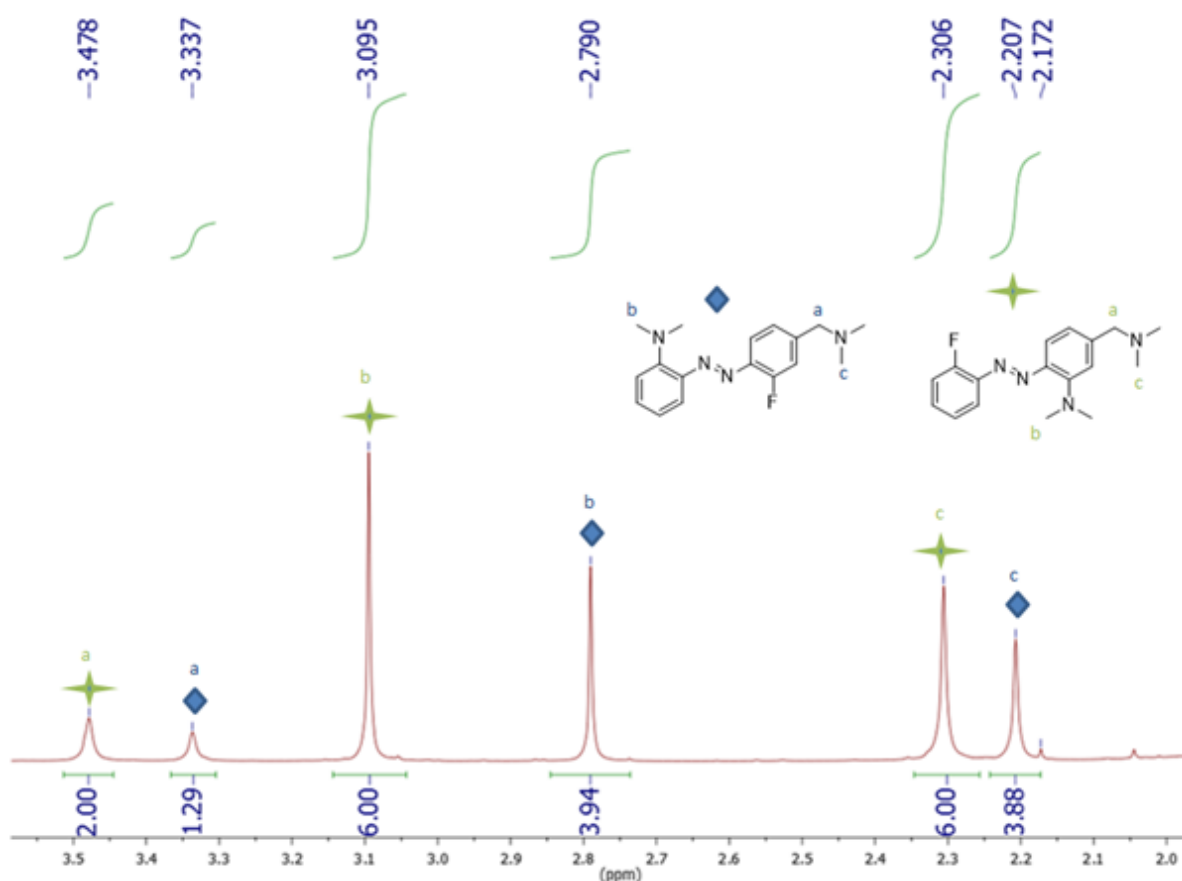


Figure 42 $^1\text{H-NMR}$ spectrum (aliphatic region) of the product isolated from the DMF thermal degradation mediated amination and possible structure of the product.

Further reaction of the above-mentioned product under the same conditions led to a single azobenzene derivative which arises from the conversion of the one possible isomer but not of the other (Figures 42 and 43). According to $^1\text{H-NMR}$ spectroscopy this azobenzene (Figure 43) with the protons **a** corresponding to the benzylic carbon, the protons **b** and **c** corresponding to the aromatic dimethylamine methyl groups and the protons **d** corresponding to benzylic dimethylamine methyl groups could be the desired product **23**. Unfortunately, the product was prone to decomposition during silica column chromatography purification and therefore was not studied any further.

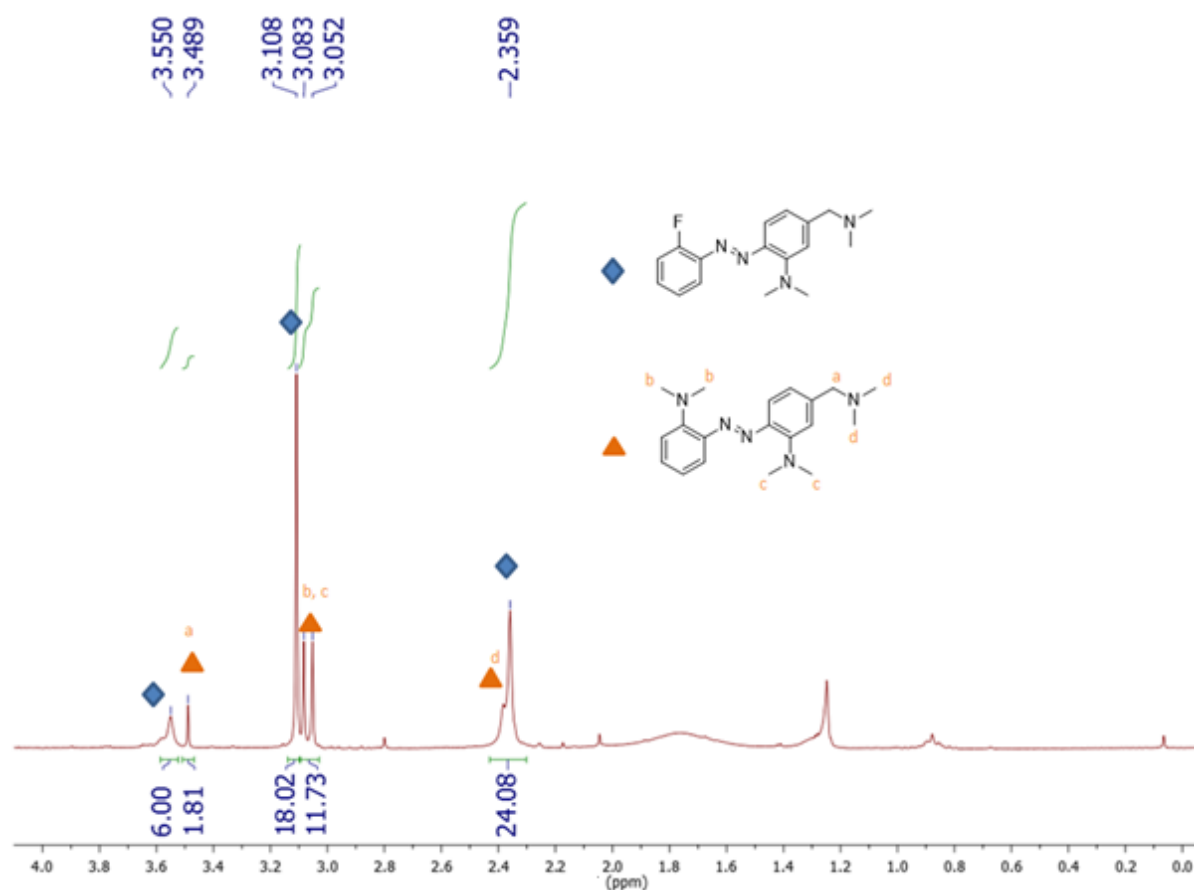


Figure 43 $^1\text{H-NMR}$ spectrum of the product of DMF mediated amination: the integration of the peaks of the aromatic and the methyl protons indicate formation of azobenzene **23**.

In a final attempt to minimize the by-products and obtain the diaminated azobenzene **23**, the reaction was performed using a mixture of aqueous dimethyl amine (produced by channelling DMF decomposition produced dimethyl amine in water through a two-pot experimental setup similar to that of Scheme 41) and DMF. The reaction flask was heated at $50\text{ }^\circ\text{C}$ for 24 hours and the extent of aromatic nucleophilic substitution was studied.⁸⁰ Analysis of $^1\text{H-NMR}$ spectra acquired during the course of this reaction, revealed

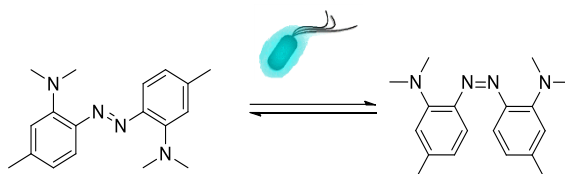
that the major component of the reaction mixture was starting material and the mixture contained traces of other species none of which were the product.

Since the designed azobenzene could not be transformed to a water-soluble derivative and due to limitations in time we decided to proceed to the final part of the project which included the bioluminescent studies with azobenzene **16**.

2.5 Bioluminescence studies

2.5.1 Bioluminescent cultures

In an effort to also conduct a proof of principle, blue light bioluminescence photochemical study, it was necessary to acquire a suitable luciferase system. Due to limited commercial availability of such systems we opted to proceed with bacterial luciferase, a system present in bioluminescent bacteria; easily isolated from fresh marine species such as squid and shrimp.



Scheme 43 Bacterial bioluminescence aided isomerization of azobenzene **16**.

Fresh shrimp from the region of Agios Nikolaos, Crete were bought from the local fish market in Heraklion and kept on ice. They were then carefully placed in a falcon containing a 3.0 % w/v NaCl solution so that the approximately 20% of the shrimp mass was above liquid level (Figure 44). The falcon was incubated at 18-20 °C overnight until luminous areas were observed.⁸¹



Figure 44 Falcon containing shrimps immersed in a 3.0 % w/v NaCl solution.

After 24 hours, bioluminescent spots were visible on the shrimp bodies. The next step was crucial as a suitable culture medium for the bioluminescent bacteria needed to be utilized. B. Danyluk et al. had investigated the difference of bioluminescent properties in bacteria in four common mediums namely, LA, BOSS, LM and NCBE media as seen in Figure 45 and, concluded that the best conditions for optimal bioluminescence involved incubation in LA medium at 20-22 °C for 36 hours. (Table 1).⁸²

LA medium	BOSS medium	LM medium	NCBE medium
NaCl 10 g Yeast extract 5 g Pepton (Bacto-peptone) 10 g Agar 15 g Made up with distilled water to 1000 ml	NaCl 30 g Glycerol 1 g Pepton (Bacto-peptone) 10 g Meat extract 3 g Made up with distilled water to 1000 ml	Yeast extract 3 g Glycerol 3 g CaCO ₃ 1 g Trypton 3 g Made up with sea water to* 1000 ml	Yeast extract 3 g Pepton (Bacto-peptone) 5 g distilled water 250 ml sea water* 750 ml

Figure 45 Commonly used mediums for marine bioluminescent bacteria.⁸²

Table 1 Mean bioluminescence values – relative light units (RLU) of examined microorganisms cultivated at temperature 20-22 °C.⁸²

Bacteria strain	Culture time h	Medium			
		LA	BOSS	LM	NCBE
<i>Vibrio fischeri</i>	12	1 280	17	9	817
	24	1 399	112	16	830
	36	1 488	117	11	901
	48	902	120	53	712
	120	880	184	189	453
<i>Vibrio harveyi</i>	12	316	10	10	13
	24	451	56	36	110
	36	850	73	48	215
	48	743	98	63	307
	120	283	118	43	289
<i>Photobacterium phosphoreum</i>	12	1 341	1 581	10	26
	24	1 386	1 611	51	204
	36	593	1 543	96	439
	48	310	1 281	198	706
	120	421	411	244	821
<i>Photobacterium luciferum</i>	12	31	11	251	110
	24	58	18	346	204
	36	381	43	307	520
	48	740	61	198	393
	120	861	160	364	756

Although the light intensity in these systems is significantly lower as compared to the bacterial bioluminescent systems cited in literature,^{52,83} we decided it would still be

interesting to investigate the isomerization of molecular switches with minimal biological light. According to the aforementioned protocols the bacteria from the shrimps were picked with a sterile toothpick and streaked across petri plates containing solid LA medium. The plates were monitored over 36 hours for bioluminescence (Figure 46).

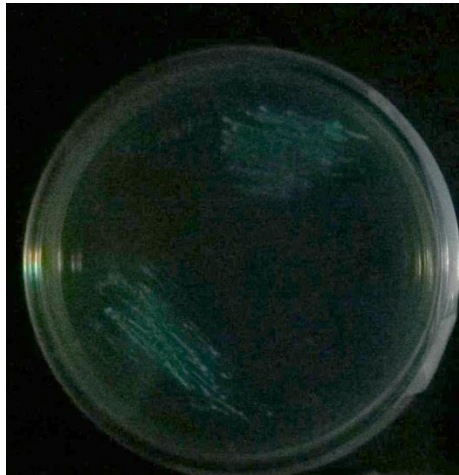


Figure 46 Petri dish containing LA medium, 36 hours after bioluminescent microorganisms were streaked.

According to B. Danyluk et al. the brightest colonies after 36 hours were *vibrio fischeri*.⁸² These colonies were then replated and monitored over 24 hours resulting in brighter bioluminescence (Figure 47).



Dark

With light

Figure 47 Petri dish replated with the brightest colonies of the first plating. Left as seen in dark and right as seen in a light.

There were certain practical difficulties involved in the way the experiment could be performed. Our initial thought was to prepare a liquid bacterial culture from the solid LA medium culture and mix amounts of the liquid culture and a solution of the azobenzene **16** in the cuvette to directly study isomerization as shown in Figure 48.

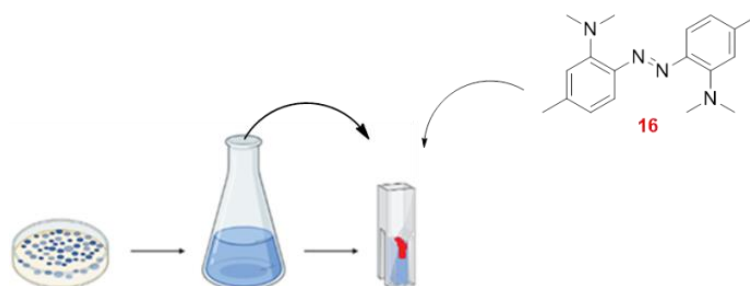


Figure 48 Proposed set-up for bioluminescence study of isomerization using UV-Vis spectroscopy with a mixture of liquid growth media and a solution of azobenzene **16**.

Since we previously determined that the solubility of **16** is limited in water, mixing it with a liquid bacterial growth medium would not be ideal.

The second approach we contemplated involved investigation through NMR spectroscopy. The advantage of this method was the existence of two separate mixtures, the liquid growth media and the azobenzene/benzene- d_6 NMR tube solution as seen in Figure 49.

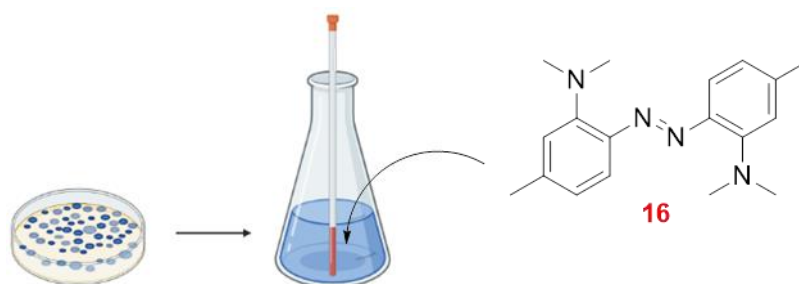


Figure 49 Proposed set-up for bioluminescence study of isomerization using NMR spectroscopy with the liquid culture as a light source.

The drawback with this system was that the combination of a dense NMR solution (> 1 mg in 0.4 ml) and the characteristically low intensity light produced by the bacteria, might not produce a reliable result.

In an effort to minimize the sample concentration and maximize the light irradiating the sample at the same time, it was decided to investigate possible isomerization using

UV-Vis spectroscopy by preparing a dilute sample of compound **16** in benzene and irradiating it with 2 bioluminescent petri dishes as shown in Figure 50

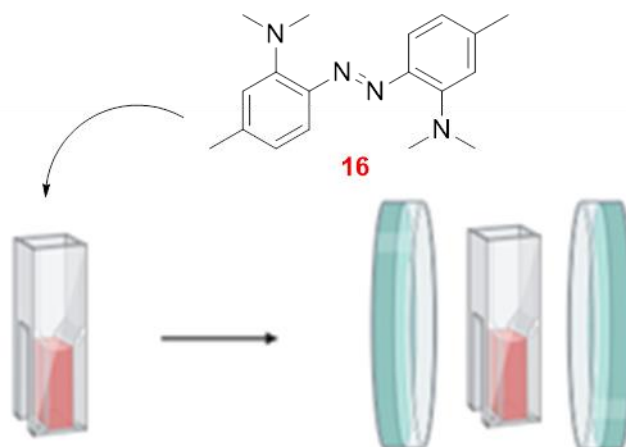


Figure 50 Set-up for bioluminescence study of isomerization using UV-Vis spectroscopy and the solid cultures as a light source.

Following the later approach, a solution of the azobenzene **16** in benzene ($C \approx 0.02$ mM) was prepared and a UV-Vis spectrum was recorded before illumination. The cuvette was then placed between 2 bioluminescent plates at a distance of 1 cm in complete darkness for 5 minutes and after which a UV-Vis spectrum was again recorded.

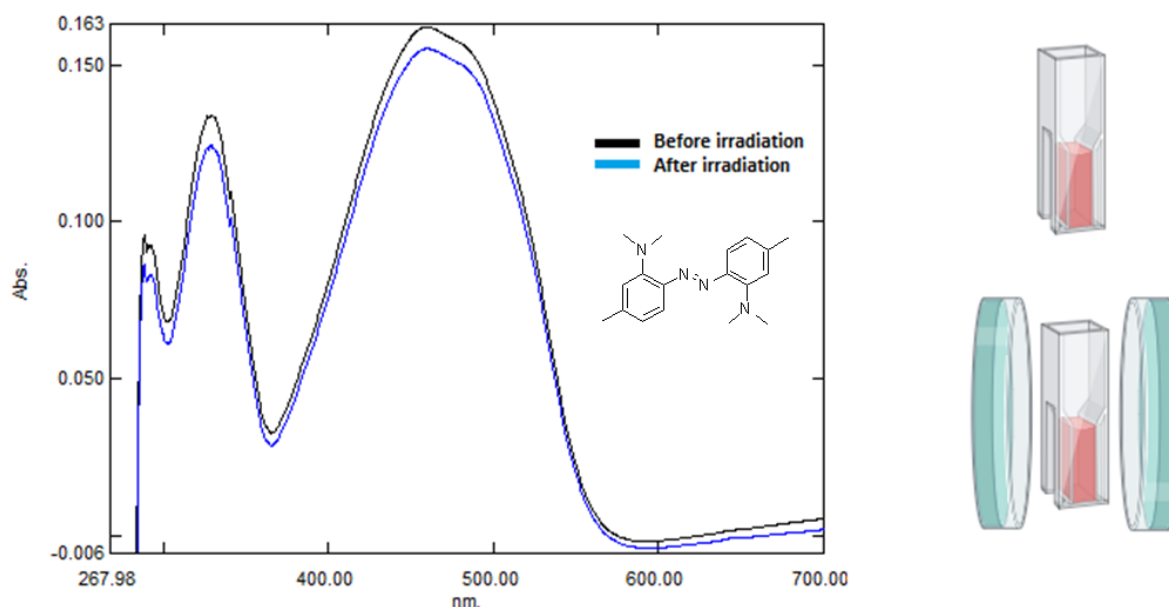


Figure 51 UV-Vis spectra of compound **16** in benzene before and after irradiation with bioluminescent plates.

Comparing the UV-Vis spectra (Figure 51) we did observe a minute degree of isomerization. Perhaps further isomerization could be seen by minimizing the distance of the bioluminescent cultures and the cuvette or by the synthesis of more water soluble

molecular switches which could be placed in a liquid medium containing the bioluminescent bacteria. The results however are encouraging taking into account the low intensity luxABCDE luciferase used and the distance between the agar and the quartz cuvette (1 cm). A brighter modified bacterial luciferase system⁸³ could be a good candidate in additional future experiments to further investigate the link between bioluminescence and photopharmacology.

3 Conclusions

During the yellow light wavelength tuning, the azobenzenes **2** and **4** exhibited *trans/cis* isomerization with the use of green light, similar to the tetra ortho-fluoro derivative reported in literature; despite introducing a new combination of fluoro- and chloro ortho substitution. These findings indicate a dominant effect of the fluoro substituent concerning the wavelength tuning in comparison to the chloro substituent. Attempts to synthesize a trihalogenated derivative with a halogen ratio of Cl/F = 2/1 in order to obtain a clearer picture of the effect of the chlorine atoms were unsuccessful due to the limited starting materials and sensitive chemistry involved.

In the second part of the project which involved the blue light wavelength tuning, the ortho-fluorinated precursors were prepared in moderate yields. Research was performed on the di-substituted fluoro derivatives **8** and **13** as a molecule with fluorine atoms on both rings made for a better candidate molecule to study the redshift effect with nucleophilic aromatic substitution. The aromatic nucleophilic substitution using pyrrolidine as a nucleophile yielded product **13** which presented loss in colour within a few hours of exposure to room light. A kinetic study was conducted measuring the absorbance while at the same time irradiating the sample with green light. As expected during irradiation a drop in absorbance was observed. These findings along with reports in literature indicate possible photodegradation. Dimethylamine was also chosen to be used as a nucleophile for comparison. It was found that ortho dimethylation proceeds best at temperatures not above 70 °C as above that temperature, demethylation and by-products were observed. At optimal conditions the reaction yields for products **15** and **16** were 30% and 18% respectively.

Photometric studies of products **15** and **16** revealed similarities concerning molar absorptivity in the visible range but substantial differences concerning the *cis* half-life. Product **15** exhibited a *cis* half-life of 812 seconds while product **16**, 30 seconds. This revealed that a variation of ortho substitution significantly affect the *cis* half-life, agreeing to reports in literature.

The *cis* half-life of compound **16** further showed a strong dependence on solvents as it was found to be 30 seconds in MeCN, 3.6 seconds in MeCN/H₂O = 7/3 and 2180 seconds

in benzene. The long half-life in benzenes was particularly interesting as we could investigate the isomeric ratio using benzene-d₆ without losing a substantial amount of the *cis* isomer during spectral recording. The isomeric ratio was found to be *trans/cis* = 51/49.

In an effort to conjugate azo switches to water soluble linkers to increase overall water solubility, benzylic bromination studies were conducted without success, which could be attributed to the electron rich nature of the ortho-dimethylated molecule. Benzylic bromination on the electron poor ortho fluorinated substrate **8** proceeded smoothly and in high yields. Substitution with the water soluble piperazino group also proceeded in high yields but the final stage; which included the nucleophilic aromatic substitution of dimethylamine was not successful. NMR spectroscopy showed evidence of piperazine degradation. In an effort to study this, dimethylamine was added to the sp² position yielding substrate **22** and nucleophilic aromatic substitution proceeded partially as indicated by NMR spectroscopy. Unfortunately, no product could be isolated probably be due to its basic nature

In an effort to investigate azobenzene isomerization with the use of bioluminescence, bioluminescent bacteria were extracted from fresh shrimps and cultured on solid LA medium according to literature. The low intensity of bioluminescence and the limited solubility of the azobenzene **16** in water made this study difficult. We nevertheless performed a preliminary study of the isomerization using UV-Vis spectroscopy and more specifically by recording spectra of **16** before and after irradiating the cuvette with bioluminescent petri dishes. A small difference in absorbance was observed, which could be attributed to a small shift in *trans/cis* population. This minute shift enhances our initial assumptions concerning the possibility of isomerization using bioluminescence and, encourages to the need for future studies in order to form a clearer conclusion.

4 References

- 1 W. A. Velema, W. Szymanski, B. L. Feringa *J. Am. Chem. Soc.* **2014**, 136, 2178–2191.
- 2 I. R. Edwards, J. K. Aronson *Lancet* **2000**, 356, 1255–1259.
- 3 J. Carlet, P. Collignon, D. Goldmann, H. Goossens, I. C. Gyssens, S. Harbarth, V. Jarlier, S. B. Levy, B. N’Doye, D. Pittet, R. Richtmann, W. H. Seto, J. W. M. van der Meer, A. Voss *Lancet* **2011**, 378, 369–371.
- 4 R. Langer *Nature* **1998**, 392 (6679 Suppl.), 5–10.
- 5 J. A Di Masi, L Feldman, A. Seckler, A Wilson, *Clin. Pharmacol. Ther.* **2010**, 87, 272–277.
- 6 A. J. Alanis *Arch. Med. Res.* **2005**, 36, 697.
- 7 Editorial: Method of the Year 2010, *Nat. Methods* **2011**, 8, 1.
- 8 R. C. Straight, J. D. Spikes, A. A. Frimer *In Singlet O2 Ed.; CRC Press: Boca Raton, FL, 1985*, 85-144.
- 9 M. Irie *Chem. Rev.* **2000**, 100, 1685–1716.
- 10 H. M. D. Bandarab, S. C. Burdette *Chem. Soc. Rev.*, **2012**, 41, 1809–1825.
- 11 H. Rau, E Lueddecke *J. Am. Chem. Soc.*, **1982**, 104, 1616–1620.
- 12 C. R. Crecca, A. E. Roitberg *J. Phys. Chem. A*, **2006**, 110, 8188–8203.
- 13 J. L. Magee, W. Shand Jr., H. Eyring *J. Am. Chem. Soc.*, **1941**, 63, 677–688.
- 14 D. Y. Curtin, E. J. Grubbs, C. G. McCarty *J. Am. Chem. Soc.*, **1966**, 88, 2775–2786.
- 15 D. E Mager *Adv. Drug Delivery Rev.* **2006**, 58, 1326–1356.
- 16 M. Stein, Simon, S. I. Middendorp, V. Carta, E. Pejo, D. E. Raines, S. A. Forman, E. Sigel D. Trauner *Angew. Chem., Int. Ed.* **2012**, 51, 10500–10504.
- 17 W. A. Velema, J. P. van der Berg, M. J. Hansen, W. Szymanski, A. J. M Driessen, B. L. Feringa *Nat. Chem.* **2013**, 5, 924–928.
- 18 Y. Zhang, F. Erdmann, G. Fischer *Nat. Chem. Biol.* **2009**, 5, 724–726.
- 19 J. P. Overington, B. Al-Lazikani, A. L. Hopkins *Nat. Rev. Drug Discov.* **2006**, 5, 993–996.
- 20 A. Dias, M. Dapiedada, J. Simoes, J. Simoni, C. Teixeira, H. Diogo, M. Yang, G. Pilcher *J. Chem. Thermodyn.* **1992**, 24, 439–447.
- 21 R. J. Mart, R. K. Allemann *Chem. Commun.*, **2016**, 52, 12262.
- 22 D. Brash, J. Rudolph, J. Simon, A. Lin, G. Mckenna, H. Baden, A. Halperin, J. Ponten *J. Proc. Natl. Acad. Sci. U.S.A.* **1991**, 88, 10124–10128.
- 23 M. Protic-Sabljić, N. Tuteja, P. Munson, J. Hauser, K. Kraemer, K. Dixon *Mol. Cell. Biol.*, **1986**, 6, 3349–3356.
- 24 K. Kalka, H. Merk, H. Mukhtar *J. Am. Acad. Dermatol.* **2000**, 42, 389–413.
- 25 C. C. Frazier *Int. J. Dermatol.* **1996**, 35, 312–316.
- 26 C. Boulègue, M. Löweneck, C. Renner, L. Moroder *ChemBioChem* **2007**, 8, 591–594.
- 27 S. Zbaida *Drug Metab. Rev.* **1995**, 27, 497–516.
- 28 C. Renner, L. Moroder *ChemBioChem* **2006**, 7, 868–878.
- 29 E. Kosower, H. Kanety-Londner *J. Am. Chem. Soc.* **1976**, 98, 3001–3007.
- 30 A. A. Beharry, L. Wong, V. Tropepe, G. A. Woolley *Angew. Chem., Int. Ed.* **2011**, 50, 1325–1327.
- 31 S. Samanta, T. M. McCormick, S. K. Schmidt, D. S. Seferosa, G. A. Woolley *Chem. Commun.* **2013**, 49, 10314–10316.

- 32 S. Samanta, A. A. Beharry, O. Sadovski, T. M McCormick, A. Babalhavaeji, V. Tropepe, G. A. Woolley *J. Am. Chem. Soc.* **2013**, 135, 9777–9784.
- 33 L. Abramsson-Zetterberg, N. Ilback *Food Chem. Toxicol.* **2013**, 59, 86-89
- 34 M. A. Brown, S. C. De Vito *Crit. Rev. Environ. Sci. Technol.*, **1993**, 23, 249–324.
- 35 J. Bieth, S. M. Vratsanos, N. Wassermann, B. F. Erlanger *Proc. Natl. Acad. Sci. U.S.A.*, **1969**, 64, 1103–1106.
- 36 W. J. Deal, B. F. Erlanger, D. Nachmansohn, *Proc. Natl. Acad. Sci. U.S.A.*, **1969**, 64, 1230–1234
- 37 W. A. Velema, J. P. van der Berg, M. J. Hansen, W. Szymanski, A. J. M. Driessen, B. L. Feringa *Nature Chem*, **2013**, 5, 924–928.
- 38 M. Wegener, M. J. Hansen, A. J. M. Driessen, W. Szymanski, B. L. Feringa *J. Am. Chem. Soc.* **2017**, 139, 17979–17986.
- 39 M. J. Hansen, W. A. Velema, G. de Bruin, H. S. Overkleeft, W. Szymanski, B. L. Feringa *ChemBioChem*, **2014**, 15, 2053-2057.
- 40 N. N. Mafy, K. Matsuo, S. Hiruma, R. Uehara, N. Tamaoki *J. Am. Chem. Soc.* **2020**, 142, 1763–1767.
- 41 F. Riefolo, C. Matera, A. Garrido-Charles, A. M. J. Gomila, R. Sortino, L. Agnetta, E. Claro, R. Masgrau, U. Holzgrabe, M. Batlle, M. Decker, E. Guasch, P. Gorostiza *J. Am. Chem. Soc.* **2019**, 141, 7628–7636.
- 42 D. A. Rodríguez-Soacha, M. Decker *Adv. Therap.*, **2018**, 1, 1800037.
- 43 “Bioluminescence: living lights, lights for living” Wilson, Thérèse and Hastings, J Woodland. Harvard University Press, Cambridge, MA (**2013**).
- 44 S. Roura, C. Gálvez-Montón A.Bayes-Genis *J. Cell. Mol. Med.*, **2013**, 17, 1582-1838.
- 45 C. L. Dybas *BioScience*, **2019**, 69, 487–495,
- 46 T. Theodossiou, J. S. Hothersall, E. A. Woods, K. Okkenhaug, J. Jacobson, A. J. MacRobert *Cancer Res*, **2003**, 63, 1818-1821.
- 47 G. M. F. Calixto, J. Bernegossi, L. M. De Freitas, C. R. Fontana, M. Chorilli *Molecules*, **2016**, 21, 342.
- 48 T. Xu, D. Close, W. Handagama, E. Marr, G. Sayler, S. Ripp *Front. Oncol.*, **2016**, 6.
- 49 L. Mezzanotte, M. van ‘t Root, H. Karatas, E. A. Goun, C. W. G. M. Löwik *Trends Biotechnol.*, **2017**, 35, 640-652.
- 50 Z. I. Pranjol, A. Hajitou, *Viruses*, **2015**, 7, 268-284.
- 51 C. K Baban, M. Cronin, A. R. Akin, A. O'Brien, X. Gao, S. Tabirca, K. P. Francis, M. Tangney *J. Vis. Exp.*, 2012, 69, e4318.
- 52 T. Xu, S. Ripp, G. S. Sayler, D. M. Close *PLoS ONE*, **2014**, 9, e96347.
- 53 M. J. Hansen, M. M. Lerch, W. Szymanski, B. L. Feringa *Angew. Chem. Int. Ed.*, **2016**, 55, 13514-13518.
- 54 M. Schlosser, H. Geneste *Chem. Eur. J.*, **1998**, 4, 1969-1973.
- 55 L. Lochman *Cent. Eur. J. Chem.*, **2014**, 12, 537-548
- 56 A. Krasovskiy, V. Krasovskaya, P. Knochel *Chem. Int. Ed.* **2006**, 45, 2958 –2961.
- 57 O. Sadovski, A. A. Beharry, F. Zhang, G. A. Woolley *Angew. Chem., Int. Ed.* **2009**, 48, 1484–1486.
- 58 Z. Ahmed, A. Siiskonen, M. Virkki, A. Priimagi *Chem. Commun.*, **2017**, 53, 12520-12523.
- 59 J. R. Brindle, J. L. Liard, N. Brub *Can. J. Chem.*, **1976**, 54, 871-877.

- 60 R. Zhao, C. Tan, Y. Xiea, C. Gao, H. Liu, Y. Jiang *Tetrahedron Letters*, **2011**, 52, 3805-3809.
- 61 P. Fatás, E. Longo, F. Rastrelli, M. Crisma, C. Toniolo, A. I. Jiménez, C. Cativiela, A. Moretto, *Chem. Eur. J.*, **2011**, 17, 12606-12611.
- 62 E. Vasilikogiannaki, C. Gryparis, V. Kotzabasak,i I. N. Lykakis, M. Stratakis *Adv. Synth. Catal.*, **2013**, 355, 907-911.
- 63 N. J. Hauwert, T. A. M. Mocking, D. Da Costa Pereira, K. Lion, Y, Huppelschoten, H. F. Vischer, I. J. P. De Esch, M. Wijtmans, R. Leurs *Angew. Chem. Int. Ed.*, **2019**, 58, 4531-4535.
- 64 M. Dong, A. Babalhavaeji, S. Samanta, A. A. Beharry, G. A. Woolley *Acc. Chem. Res.*, **2015**, 48, 2662–2670.
- 65 C. Zhang, N. Jiao *Angew. Chem., Int. Ed.*, **2010**, 49, 6174-6177.
- 66 J. Garcia, J. Sorrentino, E. J. Diller, D. Chapman, Z. R. Woydziak *Synth. Commun.*, **2015** 46, 475-481.
- 67 S. Thavaneswaran, K. McCamley, P. J. Scammells *Nat. Prod. Commun.*, **2006**, 1, 885 – 897.
- 68 M. Kojima, S. Nebashi, K. Ogawa, N. Kurita *J. Phys. Org. Chem.*, **2005**, 18, 994-1000.
- 69 C. Brown, S.K. Rastogi, S.L. Barrett, H.E. Anderson, E. Twichell, S. Gralinski, A. McDonald, W.J. Brittain *J. Photochem. Photobiol. A*, **2017**, 336, 140-145.
- 70 A. K. Rathi, R. Syed, Han-Seun Shin, R. V. Patel *Expert Opin. Ther. Pat.*, **2016**, 26, 777-797.
- 71 M. Kaiser, S. P. Leitner, C. Hirtenlehner, M. List, A. Gerisch, U. Monkowius *Dalton Trans.*, **2013**, 42, 14749-14756.
- 72 T.T Wang, T.C Huang *Chem. Eng. J. Biochem. Eng. J.*, **1993**, 53, 107-113.
- 73 K. Shibatomi, Y. Zhang, H. Yamamoto, *Chem.: Asian J.*, **2008**, 3, 1581-1584.
- 74 M. A. Cardona, D. Makuc, K. Szaciłowski, J. Plavec, D. C. Magri *ACS Omega*, **2017**, 2, 6159–6166.
- 75 Y. Otake, J. D. Williams, J. A. Rincón, O. de Frutos, C. Mateos, C. Oliver Kappe *Org. Biomol. Chem.*, **2019**, 17, 1384.
- 76 A. Zoller, D. Gígmes, Y. Guillaneuf *Polym. Chem.*, **2015**, 6, 5719-5727.
- 77 A. Zhou, H. Wu, J. Pan, X. Wang, J. Li, Z. Wu, A. Hui *Molecules*, **2015**, 20, 1304-1318.
- 78 P. C. B. Page, H. Heaney, M. J. McGrath, E. P. Sampler, R. F. Wilkins *Tetrahedron Letters*, **2003**, 44, 2965-2970.
- 79 E. Tayama, K. Takedachi, H. Iwamoto, E. Hasegawa *Tetrahedron*, **2010**, 66, 9389-9395.
- 80 N. A. Isley, R. T. H. Linstadt, S. M. Kelly, F. Gallou, B. H. Lipshutz *Org. Lett.*, **2015**, 17, 4734–4737.
- 81 R. Alias, J. Elangovan, H. M. Rathy, M. T. M. Zaid, S. H. Mohtar, Y. M. Yunus, R. Saadun, M. N. Lani *Journal of Built Environment, Technology and Engineering*, **2017**, 3.
- 82 B. Danyluk, W. Uchman, P. Konieczny, A. *Bilska Acta Sci. Pol., Technol. Aliment.*, **2007**, 6, 5-16.
- 83 C. Gregor, K. C. Gwosch, S. J. Sahl, S. W. *Proc. Natl. Acad. Sci. U.S.A.*, **2018**, 115, 962-967.

5 Experimental Section

Instruments and methods

The course of the reactions was monitored with Thin Layer Chromatography (TLC), Gas chromatography–mass spectrometry (GC-MS) and Nuclear Magnetic Resonance (NMR) spectroscopy. The NMR spectra were recorded on a 300 MHz DPX and a 500 MHz Bruker Avance III spectrometer. GC-MS spectra were recorded on a Shimadzu GC-MS QP5050 chromatograph/mass spectrometers equipped with a Supelco column (MDN-5, 30 mm × 25 μm film thickness) and a 5971A MS mass detector.

During product purification, the separation of the products from crude mixtures was achieved with column chromatography using silica as a static phase.

Various commonly used organic solvents were dried with several different drying agents. Dry THF was prepared over sodium–benzophenone ketyl.

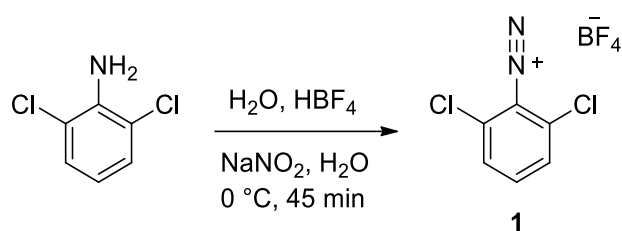
All photochemical studies were performed using LED lamp strips, bacterial bioluminescence photochemical studies were performed using the bacterial luciferase LuxABCDE system.

UV/Vis Spectra and Photoisomerization:

Ultraviolet absorbance spectra were recorded in Shimadzu 1900 UV–Vis spectrophotometer coupled with a temperature controlled cuvette Peltier holder. Irradiation of the sample, at 90 degree angle to the light source and the UV, was carried out using LED strips (Red, Blue, Green and Yellow). The rates of thermal *cis/trans* isomerization were measured by monitoring the changes in the maximum absorbance (λ_{\max}) determined for each compound after irradiation yielded the *cis* isomer. The light used for the absorbance measurement was of sufficiently low intensity to cause negligible isomerization. The isomerization percentage was calculated via $^1\text{H-NMR}$ spectroscopy before and after irradiation, using as a solvent chloroform- d for the tetrahalogenated azobenzenes and benzene- d_6 for the aminated azobenzenes. The isomerization using bioluminescent bacteria was achieved by comparing the UV-Vis spectrum of the non-irradiated compound **16** in benzene- d_6 with the spectrum of compound **16** upon irradiation with bioluminescence.

Substrate synthesis

Compound 1



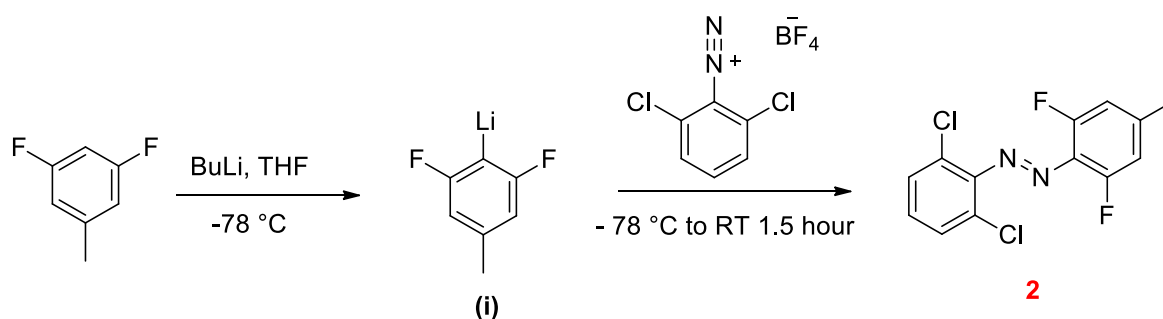
To a solution of aniline (162.02 mg, 1.00 mmol) in H_2O (0.4 mL) a 48 % w/w aqueous solution of HBF_4 (0.35 mL) was added and the mixture was stirred at 0°C . Subsequently, a solution of NaNO_2 (69.0 mg, 1.00 mmol) in H_2O (0.2 mL) was dropwise added. The reaction mixture was stirred for 45 minutes on ice and filtered. The solid was washed with Et_2O (4 x 20 mL) and dried under vacuum. The product **1** (32%) was stored in a dark vial in the refrigerator under N_2 atmosphere to prevent degradation.

^1H NMR (500 MHz, DMSO-d_6): δ = 8.15 (t, J = 8.5 Hz, 1H), 7.98 (d, J = 8.5 Hz, 2H).

^{13}C NMR (125 MHz, DMSO-d_6): δ = 144.27, 139.29, 132.14, 117.07.

^{19}F NMR (471MHz, DMSO-d_6): δ = -148.41 – -148.43 (m).

Compound 2



3,5-difluorotoluene (128 mg, 1.00 mmol) dissolved in 2 mL dry THF at -78°C was slowly treated with a solution of *n*-BuLi (2.4 M in hexane, 416 μL , 1.00 mmol) after which, stirring was continued at -78°C for 1 hour. Solid 2,6-dichlorobenzenediazonium tetrafluoroborate (260.8 mg, 1.00 mmol,) was then at once added to the mixture, which was then allowed to warm to room temperature over 1.5 hours. The reaction was quenched with saturated aqueous NaHCO_3 solution, extracted with EtOAc (3 x 5 mL), and the combined organic layers

were washed with brine, dried over Na₂SO₄ and concentrated under reduced pressure. After purification by flash chromatography (Petroleum Ether/EtOAc 100:0 → 99:1 → 98:2), the azobenzene derivative **2** was obtained as a dark-red crystalline solid (68%).

Trans isomer: ¹H NMR (500 MHz, CDCl₃): δ = 7.41 (d, J = 8 Hz, 2H), 7.20 (dd, J₁ = 8.5 Hz, J₂ = 8 Hz, 1H), 6.91 (d, J = 10.5 Hz, 2H), 2.44 (s, 3H).

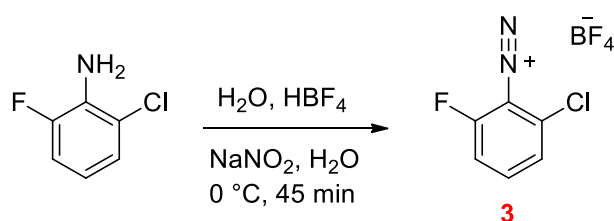
¹³C NMR (125 MHz, CDCl₃): δ = 156.0 (dd, J₁ = 261 Hz, J₂ = 5 Hz), 149.06, 144.67 (t, J = 10 Hz), 129.23, 128.96 (t, J = 20 Hz), 128.96, 126.86, 113.39 (dd, J₁ = 20 Hz, J₂ = 3.5 Hz), 21.99 (t, J = 1.5 Hz).

¹⁹F NMR (471 MHz, CDCl₃): δ = -120.53 (d, J = 10 Hz).

Cis isomer: ¹H NMR (500 MHz, CDCl₃): δ = 7.26 (d, J = 8 Hz, 2H), 7.11 (dd, J₁ = 8.5 Hz, J₂ = 7.5 Hz, 1H), 6.64 (d, J = 9.5 Hz, 2H), 2.30 (s, 3H).

¹⁹F NMR (471 MHz, CDCl₃): δ = -117.06 (d, J = 9 Hz).

Compound **3**



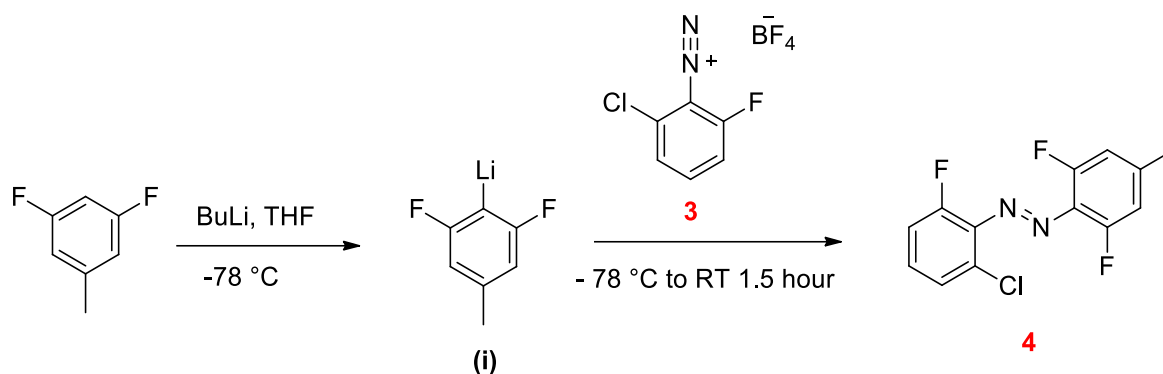
To a solution of aniline (145.56 mg, 1.00 mmol) in H₂O (0.4 mL) a 48 % w/w aqueous solution of HBF₄ (0.35 mL) was added and the mixture was stirred at 0 °C. Subsequently, a solution of NaNO₂ (69.0 mg, 1.00 mmol) in H₂O (0.2 mL) was dropwise added. The reaction mixture was stirred for 45 minutes on ice and filtered. The solid was washed with Et₂O (4 × 20 mL) and dried under vacuum. The product **3** (24%) was stored in a dark vial in the refrigerator under N₂ atmosphere to prevent degradation.

¹H NMR (500 MHz, DMSO-d₆): δ = 7.40 (dd, J₁ = 9.5 Hz, J₂ = 7.5 Hz, 1H), 6.63 (d, J = 9.5 Hz, 1H), 6.59 (d, J = 7.5 Hz, 1H).

¹³C NMR (125 MHz, DMSO-d₆): δ = 174.80, 138.24, 125.94, 121.23, 115.88.

^{19}F NMR (471MHz, DMSO-d6): $\delta = -148.25$.

Compound 4



3,5-difluorotoluene (128 mg, 1.00 mmol) dissolved in 2 mL dry THF at $-78\text{ }^\circ\text{C}$ was slowly treated with a solution of *n*-BuLi (2.4 M in hexane, 416 μL , 1.00 mmol) after which, stirring was continued at $-78\text{ }^\circ\text{C}$ for 1 hour. Solid 2-chloro-6-fluorobenzenediazonium tetrafluoroborate **3** (244.36 mg, 1.00 mmol) was then at once added to the mixture, which was then allowed to warm to room temperature over 1.5 hours. The reaction was quenched with saturated aqueous NaHCO_3 solution, extracted with EtOAc (3 \times 5 mL), and the combined organic layers were washed with brine, dried over Na_2SO_4 and concentrated under reduced pressure. After purification by flash chromatography (Petroleum Ether/EtOAc 100:0 \rightarrow 99:1 \rightarrow 98:2), the azobenzene **4** was obtained as a dark-red crystalline solid (65%)

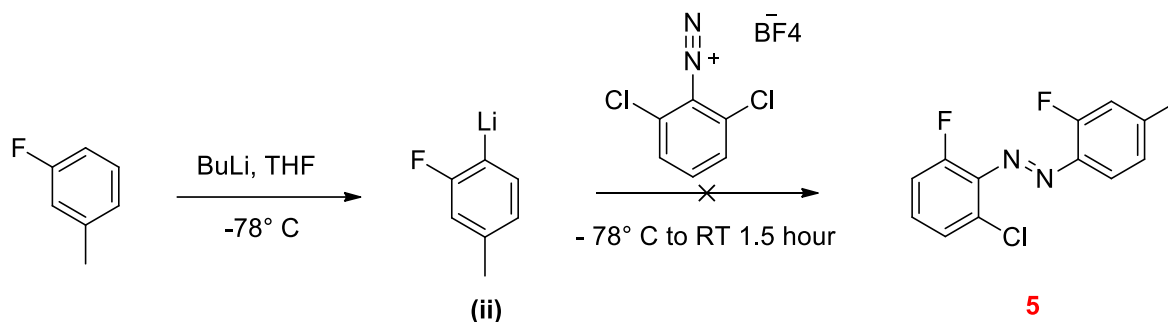
Trans isomer: ^1H NMR (500 MHz, CDCl_3): $\delta = 7.25$ (d, $J = 9$ Hz, 1H), 7.19-7.13(m, 1H), 6.85 (t, $J = 9$ Hz, 1H), 6.65 (d, $J = 9$ Hz, 2H), 2.30 (s, 3H).

^{13}C NMR (125 MHz, CDCl_3): $\delta = 151.86$ (dd, $J_1 = 252$ Hz, $J_2 = 6$ Hz), 148.72 (d, $J = 252$ Hz), 141.72 (t, $J = 9$ Hz), 140.30 (d, $J = 16.5$ Hz), 129.56 (d, $J = 8.5$ Hz), 129.47 (td, $J_1 = 17$ Hz, $J_2 = 1.5$ Hz), 128.92(d, $J = 4$ Hz), 126.24(d, $J = 3.5$ Hz), 114.78 (d, $J = 20.5$ Hz), 112.64 (dd, $J_1 = 19.5$ Hz, $J_2 = 3.5$ Hz), 21.53 (t, $J = 2$ Hz).

Cis isomer: ^1H NMR (500 MHz, CDCl_3): $\delta = 7.34$ (d, $J = 8$ Hz, 1H), 7.30-7.24 (m, 1H), 7.16-7.10 (m, 1H), 6.89 (d, $J = 10$ Hz, 2H), 2.42 (s, 3H).

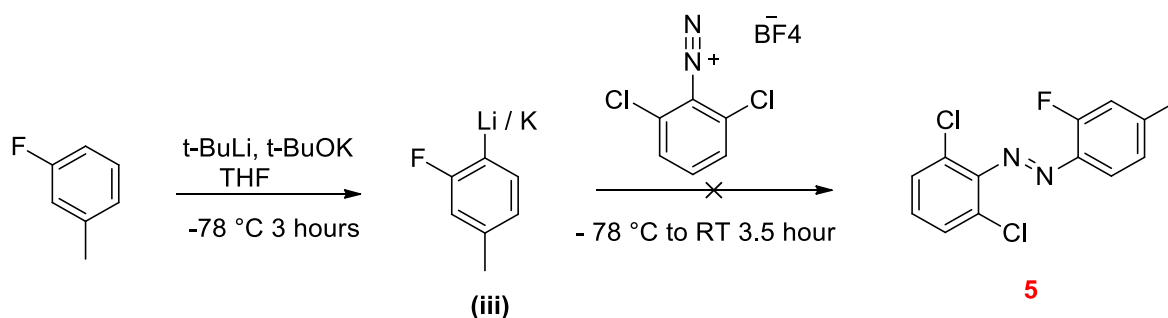
Synthetic approaches toward the azobenzene derivative **5**

First synthetic approach



3-fluorotoluene (111.1 μL , 1.00 mmol) dissolved in 2 mL dry THF at -78°C was slowly treated with a solution of *n*-BuLi (2.4 M in hexane, 416 μL , 1.00 mmol, 1 eq.) after which, stirring was continued at -78°C for 1 hour. Solid 2,6-dichlorobenzene diazonium tetrafluoroborate (260.8 mg, 1.00 mmol) was then at once added to the reaction mixture, which was subsequently allowed to warm to room temperature over 1.5 hours. The reaction was quenched with saturated aqueous NaHCO_3 solution, extracted with EtOAc (3×5 mL), and the combined organic layers were washed with brine, dried over Na_2SO_4 and concentrated under reduced pressure. NMR spectroscopy showed no product

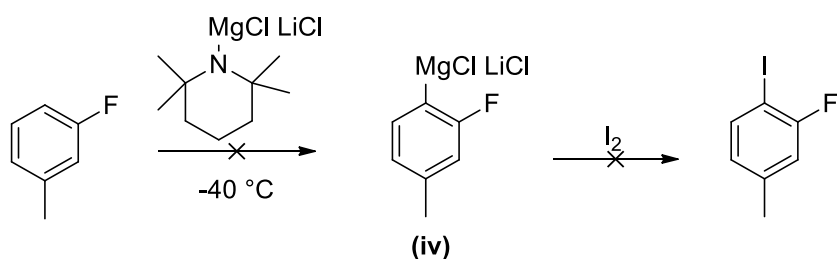
Second synthetic approach



To a flask containing dry THF (1 mL) cooled to -78°C , potassium *t*-BuOK (56 mg, 0.5 mmol) and *t*-Buli (1.7M in pentane, 294 μL , 0.5 mmol) were added. 3-fluorotoluene (55 μL , 0.5 mmol, 1 eq.) was then added and the mixture was allowed to stir at -78°C for 3 hours during which the colour of the reaction mixture gradually changed to pale orange. Solid 2,6-difluorobenzene diazonium tetrafluoroborate (130.4 mg, 0.5 mmol, 1 eq.) was then at once added to the reaction mixture, which was subsequently allowed to warm to room temperature over 3.5 hours. The reaction was quenched with saturated aqueous NaHCO_3 solution, extracted with EtOAc (3×5 mL), and the combined organic layers were washed

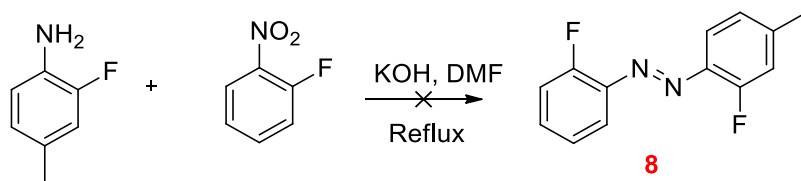
with brine, dried over Na₂SO₄ and concentrated under reduced pressure. NMR spectroscopy showed no product

Third synthetic approach



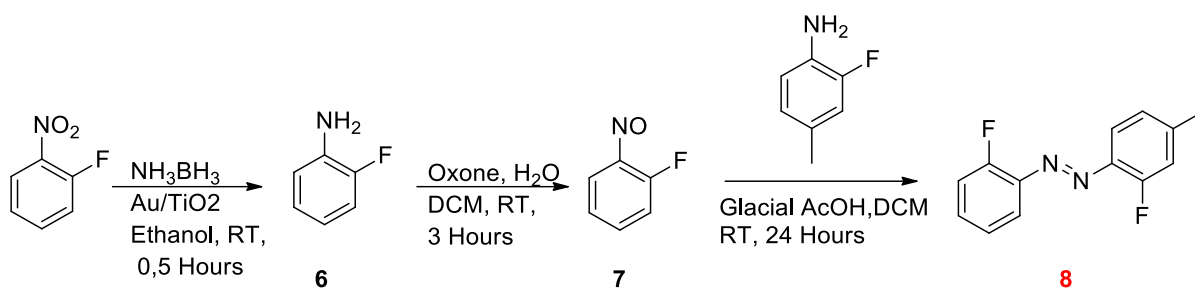
TMPMgCl•LiCl (1.2 mL, 1.0 M in THF and Toluene, 1.2 mmol) was added to a dry argon flushed Schlenk flask. 3-fluorotoluene (122 μ l, 1.1 mmol) in THF (1 mL) was added dropwise at -40 °C. The reaction was stirred at -40 °C and monitored with GC-MS by quenching reaction aliquots with an iodine solution in THF. No reaction could be observed at -40 °C, -20 °C, and 0 °C. At room temperature the starting material was converted to an uncharacterized product.

Synthetic approaches toward the azobenzene derivative **8**



To a solution of 1-fluoro-2-nitrobenzene (105.4 μ l, 1 mmol) in 5 ml DMF placed in a round-bottom flask, 2-fluoro-4-methyl-aniline (338.8 μ l, 3 mmol) and KOH (560.1 mg, 10 mmol) were added and vigorously stirred. The reaction mixture was heated to 150 °C for 24 h. The mixture was then washed several times with EtOAc and extracted with water and brine and the excess solvent was removed. NMR spectroscopy showed N,N Dimethylamine as a major product while no product was observed. The reaction was repeated using THF as solvent to avoid the thermal degradation of DMF but no product was observed.

Compound 6



To a flask containing 1-fluoro-2-nitro-benzene (421.6 μl , 4 mmol) and 8 mL ethanol, NH_3BH_3 (247 mg) and immediately after Au/TiO_2 (80 mg, 0.1 mol%) were added at room temperature in 2 doses of 40mg and 40 mg while the flask was in ice/water. The reaction was kept in an ice bath at the initial stages since the reactions are exothermic. To avoid the formation of minor oxidation by-products, inert atmosphere conditions were implemented. The slurry was filtered under a minor pressure through a short pad of silica gel with the aid of ethanol or methanol (16 mL) to withhold the supported catalyst and inorganic salts. The filtrate was evaporated under vacuum to afford compound **6** (90%) as seen by proton NMR spectroscopy. The product was used in the next step without further characterization.

Compounds 7 & 8

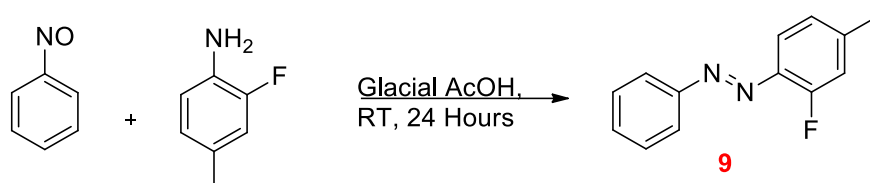
To a stirred solution of oxone™ (1.85 g, 3 mmol) in H_2O (12.5 mL), 2-fluoroaniline (289.6 μl , 3 mmol) dissolved in DCM (30 mL) was added. The obtained biphasic solution was vigorously stirred for 3 h after which the layers were separated. DCM (5 mL) was added to the organic phase, which was washed using 10% aq. sodium thiosulfate solution (5 mL), 1 M aq. HCl (5 mL) and aq. saturated NaHCO_3 (5 mL). The organic phase was transferred to a flask and 2-fluoro-4-methyl-aniline (180.7 μl , 1.6 mmol), was added. After 5 minutes, glacial acetic acid (3.2 mL) was added and the solution was stirred overnight at room temperature. The reaction mixture was the concentrated under reduced pressure. After purification by flash chromatography (Petroleum ether/EtOAc 100:0 \rightarrow 99:1 \rightarrow 98:2), the azobenzene **8** was obtained as an orange crystalline solid (28%)

Trans isomer: ^1H NMR (300 MHz, CDCl_3): δ = 7.76-7.58 (m, 2H), 7.43-7.30 (m, 1H), 7.23-7.08 (m, 2H) 6.99 (d, J = 11.5 Hz, 1H), 6.93 (d, J = 8.5 Hz, 1H), 2.33 (s, 3H).

^{13}C NMR (75 MHz, CDCl_3): δ = 160.48 (d, J = 256.5 Hz), 160.35 (d, J = 256 Hz), 144.71 (d, J = 8 Hz), 140.99 (d, J = 6.5 Hz), 138.88 (d, J = 6.5 Hz), 132.76 (d, J = 8.5 Hz), 125.33 (d, J = 3 Hz), 124.46 (d, J = 4 Hz), 118.00, 117.58, 117.52 (d, J = 19.5 Hz), 117.12 (d, J = 19.5 Hz), 21.72 (d, J = 1.5 Hz).

^{19}F NMR (471 MHz, CDCl_3): δ = -124.41 – -124.48 (m), -124.78 (dd, J_1 = 11.5 Hz, J_2 = 8 Hz).

Compound **9**



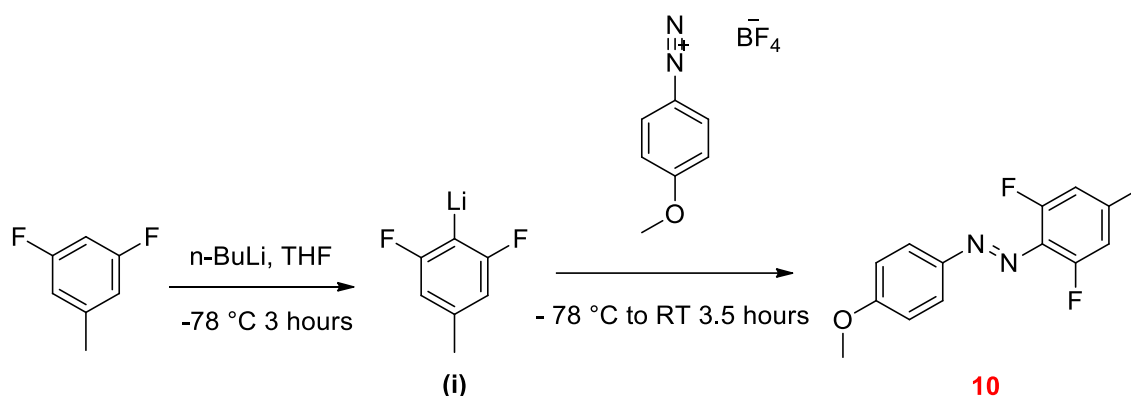
A solution of nitrosobenzene (107.11 mg, 1 mmol) in glacial acetic acid (1.1 mL) was added to a suspension of 2-fluoro-4-methyl-aniline (135.5 μl , 1.2 mmol) in glacial acetic acid (0.8 mL) and the mixture was stirred at room temperature for 24 h. The reaction mixture was then concentrated under reduced pressure. After purification by flash chromatography (Petroleum ether/EtOAc 100:0 \rightarrow 99:1 \rightarrow 98:2), the azobenzene derivative **9** was obtained as an orange crystalline solid (74%)

Trans isomer: ^1H NMR (500 MHz, CDCl_3): δ = 7.95-7.90 (m, 2H), 7.68 (t, J = 8 Hz, 1H), 7.54-7.45 (m, 3H), 7.08 (dd, J_1 = 11.5 Hz, J_2 = 1 Hz, 1H), 7.04-7.00 (m, 1H) 2.43 (s, 3H).

^{13}C NMR (75 MHz, CDCl_3): δ = 160.25 (d, J = 257.5 Hz), 152.98, 144.06 (d, J = 8 Hz), 138.67 (d, J = 7 Hz), 131.28, 129.23, 125.26 (d, J = 3 Hz), 123.14, 117.57 (d, J = 14.5 Hz), 117.44 (d, J = 4.5 Hz), 21.69 (d, J = 1.5 Hz).

^{19}F NMR (471 MHz, CDCl_3): δ = -125.16 (dd, J_1 = 11.5 Hz, J_2 = 8 Hz).

Compound **10**



3,5-difluorotoluene (128 mg, 1.00 mmol) dissolved in 2 mL dry THF at -78 °C was slowly treated with a solution of *n*-BuLi (2.4 M in hexane, 416 μ L, 1.00 mmol) after which, stirring was continued at -78 °C for 1 hour. Solid 4-methoxy-benzenediazonium tetrafluoroborate (222 mg, 1.00 mmol) was then at once added to the mixture, which was subsequently allowed to warm to room temperature over 1.5 hours. The reaction was quenched with saturated aqueous NaHCO₃ solution, extracted with EtOAc (3 \times 5 mL), and the combined organic layers were washed with brine, dried over Na₂SO₄ and concentrated under reduced pressure. After purification by flash chromatography (Petroleum ether/EtOAc 100:0 \rightarrow 99:1 \rightarrow 98:2), the azobenzene derivative **10** was obtained as an orange crystalline solid (71%)

Trans isomer: ¹H NMR (300 MHz, CDCl₃): δ = 7.92 (d, *J* = 9 Hz, 2H), 7.01 (d, *J* = 9 Hz, 2H), 6.84 (d, *J* = 10 Hz, 2H), 3.90 (s, 3H), 2.39 (s, 3H).

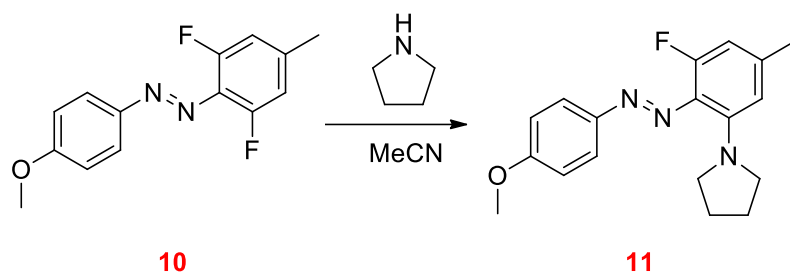
¹³C NMR (75 MHz, CDCl₃): δ = 162.72, 155.75 (dd, *J*₁ = 258 Hz, *J*₂ = 5.5 Hz), 147.93, 141.44 (t, *J* = 10 Hz), 129.10 (t, *J* = 10 Hz), 124.98, 114.32, 113.11 (dd, *J*₁ = 21 Hz, *J*₂ = 2.5 Hz), 55.76, 21.72, (t, *J* = 1.5 Hz).

¹⁹F NMR (471 MHz, CDCl₃): δ = -122.49 (d, *J* = 10 Hz).

Cis isomer: ¹H NMR (75 MHz, CDCl₃): δ = 7.01 (d, *J* = 9 Hz, 2H), 6.80 (d, *J* = 9 Hz, 2H), 6.63 (d, *J* = 8.5 Hz, 2H), 3.79 (s, 3H), 2.29 (s, 3H).

¹⁹F NMR (471 MHz, CDCl₃): δ = -122.49 (d, *J* = 8.5 Hz).

Compound **11**



To a solution of compound **10** (52.45 mg, 0.2 mmol) in MeCN (2 mL), pyrrolidine (80 μ L, 1 mmol) was added dropwise at room temperature. After 7.5 h, the reaction mixture was diluted with EtOAc (25 mL), washed with saturated NaHCO₃ (15 mL), dried over Na₂SO₄, filtered and evaporated. After purification by flash chromatography (Petroleum ether/EtOAc 95:5), the azobenzene derivative **11** was obtained as a dark-red crystalline solid (94%).

Trans isomer: ¹H NMR (300 MHz, CDCl₃): δ = 7.81 (d, J = 9 Hz, 2H), 6.99 (d, J = 9 Hz, 2H), 6.38 (s, 1H), 6.31 (dd, J_1 = 12.5 Hz, J_2 = 1.5 Hz, 1H), 3.88 (s, 3H), 3.50-3.38 (m, 4H), 2.30 (s, 3H), 1.94-1.88 (m, 4H).

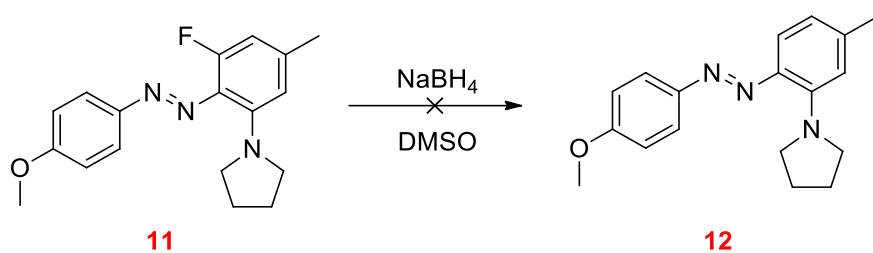
¹³C NMR (75 MHz, CDCl₃): δ = 161.52, 154.75, 151.36, 148.07, 146.82, (d, J = 4.95 Hz), 140.29 (d, J = 11.17 Hz), 128.76 (d, J = 7.57 Hz), 124.18, 114.26, 113.75 (d, J = 16.72 Hz), 110.89 (d, J = 2.47 Hz), 105.39 (d, J = 21.07 Hz), 55.69, 52.48, 25.96, 22.07 (d, J = 2 Hz).

¹⁹F NMR (471 MHz, CDCl₃): δ = -122.50 (d, J = 10 Hz).

Cis isomer: ¹H NMR (300 MHz, CDCl₃): δ = 7.92 (d, J = 9 Hz, 2H), 7.20 (d, J = 9 Hz, 2H), 6.26 (s, 1H), 6.00 (dd, J_1 = 11.0 Hz, J_2 = 1.0 Hz, 1H), 3.89 (s, 3H), 3.49-3.39 (m, 4H), 2.39 (s, 3H), 1.98-1.92 (br, 4H).

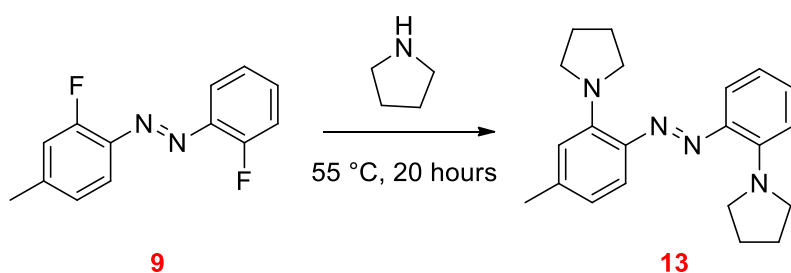
¹⁹F NMR (471 MHz, CDCl₃): δ = -120.71 (d, J = 8.5 Hz).

Synthetic approach toward the azobenzene derivative **12**



To a solution of compound **11** (31.33 mg, 0.1 mmol) in DMSO (1 mL), NaBH_4 (37.84 mg, 0.1 mmol) was added. The solution was left to stir for 7 hours and was then quenched with NaHCO_3 . The products was extracted with EtOAc (20 mL), dried over Na_2SO_4 and concentrated under reduced pressure. NMR spectroscopy showed no desired product.

Compound **13**

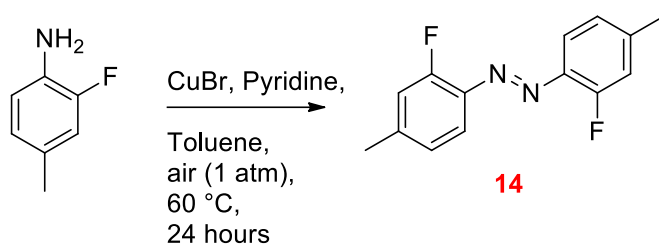


A mixture of compound **9** (20 mg, 0.086 mmol) and pyrrolidine (2 mL) was stirred at 55 °C for 20 hours. The reaction mixture was then cooled to room temperature and diluted with ethyl acetate (20 mL). The organic phase was thrice washed with water, dried over Na_2SO_4 and concentrated under reduced pressure. After purification by flash chromatography (Petroleum Ether/EtOAc 80:20), the azobenzene derivative **13** was obtained as a dark-red crystalline solid (62%).

Trans isomer: ^1H NMR (300 MHz, CDCl_3): δ = 7.55 (dd, $J_1 = 8$ Hz, $J_2 = 1.5$ Hz, 1H), 7.53 (d, $J = 8$ Hz, 1H), 7.21 (t, $J = 7.5$ Hz, 1H), 6.83 (d, $J = 8.5$ Hz, 1H), 6.69, (t, $J = 7.5$ Hz, 1H), 6.65 (s, 1H), 6.52, (d, $J = 8.5$ Hz, 1H), 3.72-3.60 (m, 8H), 2.34 (s, 3H), 2.06-1.90 (m, 8H).

^{13}C NMR (75 MHz, CDCl_3): Unidentified, due to compound instability.

Compound **14**



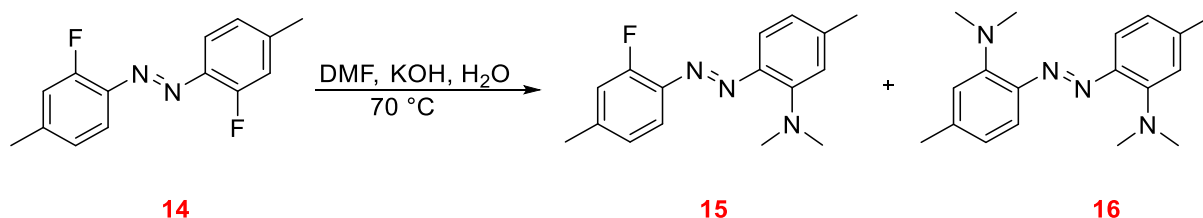
To a flask containing toluene (4mL), 2-fluoro-4-methyl-aniline (113 μL , 1mmol), CuBr (4.2 mg, 0.03 mmol) and pyridine (8.7 mg, 0.09 mmol) were added. The reaction was vigorously stirred at 60 $^\circ\text{C}$ for 20 hours under air (1 atm). The reaction was then cooled down to room temperature and concentrated under reduced pressure. After purification by flash chromatography (Petroleum Ether/EtOAc 100:0 \rightarrow 99:1 \rightarrow 98:2), the symmetric difluoro-azobenzene **14** was obtained as an orange crystalline solid (68%)

Trans isomer: $^1\text{H NMR}$ (300 MHz, CDCl_3): δ = 7.70 (t, J = 8 Hz, 2H), 7.07 (d, J = 11.5 Hz, 2H), 7.01 (d, J = 8 Hz, 2H), 2.42 (s, 6H).

$^{13}\text{C NMR}$ (75 MHz, CDCl_3): δ = 160.33 (d, J = 256 Hz), 144.27 (d, J = 8Hz), 138.93 (d, J = 7 Hz), 125.32 (d, J = 3 Hz), 117.62 (d, J = 1.5 Hz), 117.48 (d, J = 20.5 Hz), 21.71 (d, J = 1.5 Hz).

$^{19}\text{F NMR}$ (471 MHz, CDCl_3): δ = -125.14 (dd, J_1 = 11.5 Hz, J_2 = 8Hz).

Compounds **15** & **16**



A solution of compound **14** (123.1 mg, 0.5 mmol) in DMF (27.8 mmol, 2 mL) was heated to 70 $^\circ\text{C}$ at which point, 0.25 mL aqueous KOH, 20M was added on 20 minute intervals and DMF (1mL) was added on 80 minute intervals. After four hours of reaction (12 additions of aqueous KOH, 20M) the reaction mixture was cooled to room temperature and diluted with ethyl acetate (20 mL). The organic phase was washed five times with water, dried over Na_2SO_4 and concentrated under reduced pressure. After purification by flash chromatography (Petroleum Ether/EtOAc 100:0 \rightarrow 90:10), the azobenzene **15** was obtained

as a dark-red crystalline solid (37%). By increasing the polarity of the eluent during purification (Petroleum Ether/EtOAc 90:10 → 75:25), the symmetric azobenzene **16** was obtained as a dark-red crystalline solid (18%).

15 trans isomer: $^1\text{H NMR}$ (500 MHz, C_6D_6): δ = 8.02 (d, J = 8 Hz, 1H), 7.73 (t, J = 8.0 Hz, 1H), 6.77 (d, J = 11.5 Hz, 1H), 6.66 (d, J = 8 Hz, 1H), 6.60 (s, 1H), 6.54 (d, J = 8.5 Hz, 1H), 2.83 (s, 6H), 2.10 (s, 3H), 1.93 (s, 3H).

$^{13}\text{C NMR}$ (125 MHz, C_6D_6): δ = 160.36 (d, J = 254.5 Hz), 151.65, 142.62, 142.33 (d, J = 8 Hz), 142.22, 139.94 (d, J = 7 Hz), 125.25 (d, J = 2.5 Hz), 120.88, 118.33, 117.95 (2C), 117.68 (d, J = 19.5 Hz), 44.79, 21.86, 21.08 (br. s).

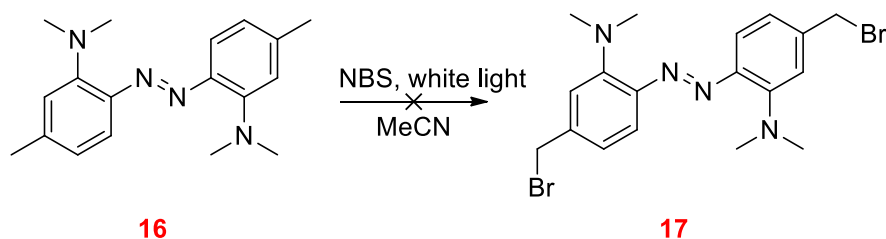
$^{19}\text{F NMR}$ (471 MHz, C_6D_6): δ = -125.09 (dd, J_1 = 11.5 Hz, J_2 = 8 Hz).

16 trans isomer: $^1\text{H NMR}$ (500 MHz, C_6D_6): δ = 7.94 (d, J = 8 Hz, 2H), 6.70 (s, 2H), 6.67 (d, J = 8 Hz), 2.88 (s, 12H), 2.15 (s, 6H).

$^{13}\text{C NMR}$ (125 MHz, C_6D_6): δ = 151.26, 143.16, 140.98, 121.08, 118.55, 117.87, 44.81, 21.78.

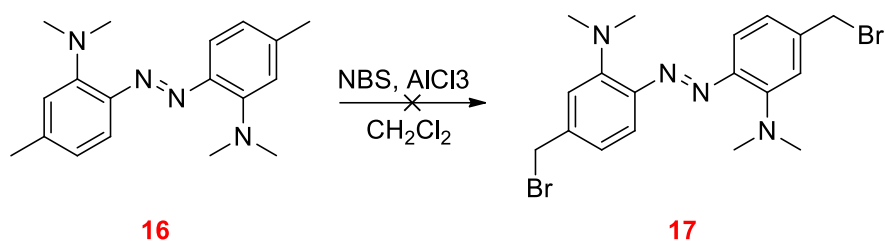
Synthetic approaches toward the azobenzene derivative **17**

First synthetic approach



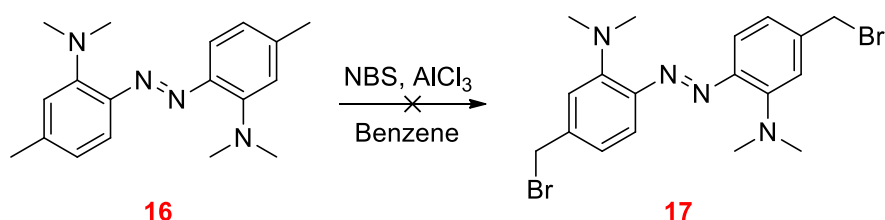
A solution of compound **16** (29.6 mg, 0.1 mmol) and *N*-bromosuccinimide (44.5 mg, 0.25 mmol) in MeCN (38 mL) was stirred at room temperature under white light illumination (300 watt lamp) for 5 hours. The course of the reaction was monitored by TLC and after 4 hours the starting material had completely disappeared. The expected product was not formed according to NMR spectroscopy.

Second synthetic approach



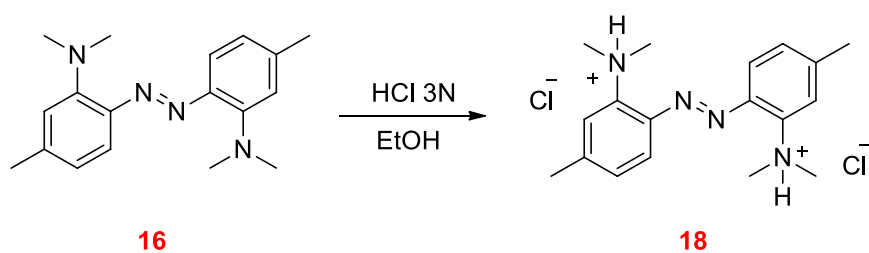
A solution of compound **16** (29.6 mg, 0.1 mmol) and NBS (89 mg, 0.5 mmol) in DCM (0.5 mL) was added to a suspension of AlCl₃ (0.133 mg, 0.01 mmol) in DCM (0.5 mL) at room temperature. The mixture was stirred for 2h at room temperature under ambient light. The reaction was quenched with saturated aqueous NaHCO₃, extracted with diethyl ether and concentrated under reduced pressure. NMR proton spectroscopy revealed that aromatic bromination had taken place instead of the desired benzylic bromination.

Third synthetic approach



To a solution of compound **16** (64.0 mg, 0.45 mmol) in benzene (0.25 mL), AlCl₃ (0.133 mg, 0.01 mmol) and *N*-bromosuccinimide (53.4 mg, 0.30 mmol) were added. The resulting mixture was exposed to standard hood fluorescent light and stirred until the starting material disappeared (1 hour). The reaction was quenched by adding a drop of water. The solvent was concentrated under reduced pressure and the residue was purified by flash chromatography. NMR spectroscopy revealed that aromatic bromination had taken place instead of the desired benzylic bromination.

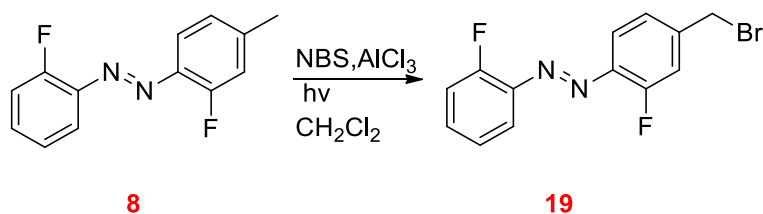
Compound **18**



To a flask containing solid compound **16** (10 mg, 0.07 mmol) in 0.5ml EtOH, HCl 3N was added while stirring until pH of around 3. A colour change from red to yellow was noticeable. The mixture was concentrated under reduced pressure to afford the salt **18** in pure form. Compound **18** could be reverted back to compound **16** by adding ethanol to the solid, deprotonating it and at the same time causing the colour to change back to red.

^1H NMR (300 MHz, D_2O): δ = 7.89 (d, J = 8.4 Hz, 1H), 7.76 (s, 1H), 7.49 (d, J = 8.5 Hz, 1H), 3.41 (s, 6H), 2.48 (s, 3H).

Compound **19**



A solution of compound **8** (23.2 mg, 0.1 mmol) and NBS (89 mg, 0.5 mmol) in DCM (0.5 mL) was added to a suspension of AlCl_3 (1.33 mg, 0.1 mmol) in DCM (0.5 mL) at room temperature. The mixture was stirred for 2 hours at room temperature under green LED light irradiation. The reaction was quenched with saturated aqueous NaHCO_3 , extracted with diethyl ether and concentrated under reduced pressure. After purification by flash chromatography (Petroleum ether/EtOAc 100:0 \rightarrow 90:10), the brominated azobenzene derivative **19** was obtained as an orange crystalline solid (37%).

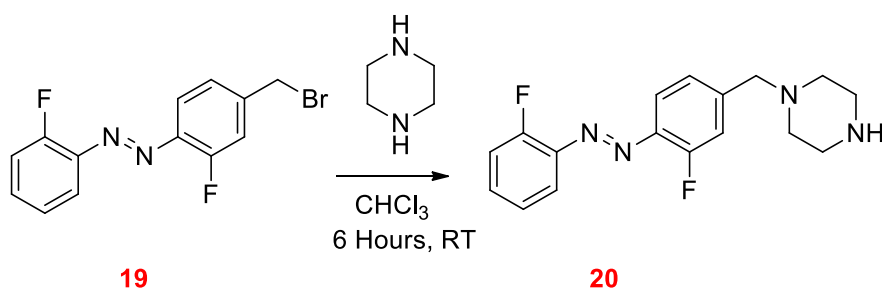
Trans isomer: ^1H NMR (500 MHz, CDCl_3): δ = 7.79 (td, J_1 = 8 Hz, J_2 = 1.5 Hz, 1H), 7.77 (t, J = 8 Hz, 1H), 7.51-7.45(m, 1H), 7.32 (dd, J_1 = 11 Hz, J_2 = 2 Hz, 1H), 7.30-7.20 (m, 3H), 4.50 (s, 2H).

^{13}C NMR (75 MHz, CDCl_3): δ = 159.60 (d, J = 257 Hz), 159.19 (d, J = 257.5 Hz), 142.17 (d, J = 8Hz), 139.93 (d, J = 6.5Hz), 139.57 (d, J = 6.5 Hz), 132.44 (d, J = 8.5 Hz), 124.21 (d, J = 3.5Hz),

123.54 (d, $J = 4\text{ Hz}$), 117.45, 116.95, 116.83 (d, $J = 20.5\text{ Hz}$), 116.27 (d, $J = 19.5\text{ Hz}$), 30.79 (d, $J = 1.5\text{ Hz}$).

^{19}F NMR (471 MHz, CDCl_3): $\delta = -123.17$ (dd, $J_1 = 11\text{ Hz}$, $J_2 = 7.5\text{ Hz}$), $-123.90 - -123.84$ (m).

Compound **20**



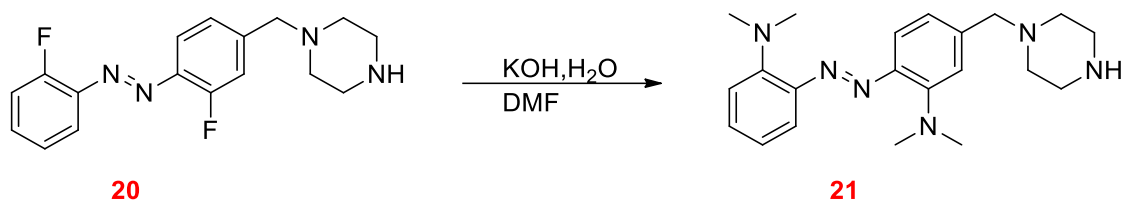
To a flask containing anhydrous piperazine (86.1 mg, 1 mmol) dissolved in chloroform (4 mL), a solution of compound **19** (15.5 mg, 0.05 mmol) in chloroform (3 mL) was added dropwise at 0 °C. The reaction mixture was stirred for six hours at room temperature. Then, the mixture was washed with a 5% K_2CO_3 solution (5 mL \times 2) and water (5 mL \times 4). The organic layer was dried over anhydrous Na_2SO_4 and concentrated under reduced pressure. After purification by flash chromatography (DCM/MeOH/ Et_3N 97:2:1). The azobenzene derivative **20** was obtained as an orange crystalline solid (90%).

Trans isomer: ^1H NMR (300 MHz, CDCl_3): $\delta = 7.78$ (td, $J_1 = 8\text{ Hz}$, $J_2 = 1.5\text{ Hz}$, 1H), 7.74 (t, $J = 8\text{ Hz}$), 7.51-7.41 (m, 1H), 7.34-7.14 (m, 4H), 3.53 (s, 2H), 2.91 (t, $J = 5\text{ Hz}$, 4H), 2.44 (br, 4H).

^{13}C NMR (75 MHz, CDCl_3): $\delta = 160.53$ (d, $J = 256.5\text{ Hz}$), 160.41 (d, $J = 256.5\text{ Hz}$), 145.16 (d, $J = 7.50\text{ Hz}$), 140.97 (d, $J = 7\text{ Hz}$), 139.90 (d, $J = 7\text{ Hz}$), 132.97 (d, $J = 8.5\text{ Hz}$), 124.82 (d, $J = 3.5\text{ Hz}$), 124.49 (d, $J = 4\text{ Hz}$), 117.97, 117.61, 117.24 (d, $J = 20\text{ Hz}$), 117.17 (d, $J = 19.5\text{ Hz}$), 62.94 (d, $J = 1.5\text{ Hz}$), 54.62, 46.17.

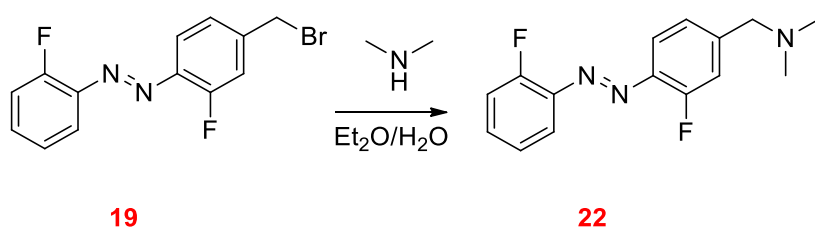
^{19}F NMR (471 MHz, CDCl_3): $\delta = -124.29 - -124.35$ (m), -124.42 (dd, $J_1 = 11.5$, $J_2 = 7.5\text{ Hz}$).

Synthetic approaches toward the azobenzene derivative **21**



A solution of compound **20** (158.18 mg, 0.5 mmol) in DMF (27.8 mmol, 2 mL) was heated to 70 °C at which point, 0.25 mL aqueous KOH 20 M was added on 20 minute intervals and DMF (1mL) on 80 minute intervals. After 4 hours of reaction (12 additions of aqueous KOH 20 M), the reaction mixture was cooled to room temperature and diluted with ethyl acetate (20 mL). The organic phase was washed with water (5×), dried over Na₂SO₄ and concentrated under reduced pressure. NMR spectroscopy did not reveal either product or starting material.

Compound **22**



To a solution of compound **19** (158.18 mg, 0.5 mmol) in ether (2mL), H₂O (2mL) was added. A syringe needle was fitted to the flask to allow gas to be pumped in. In a separate flask DMF (2mL) and aqueous KOH, 10M (0.5mL) were added and heated to 70 °C. A bent pipet was inserted on the outlet of the DMF degradation apparatus and connected to the syringe needle of the first flask, creating a system where the gaseous dimethylamine produced via the thermal degradation of DMF, could be channelled into the reaction mixture of the second flask (*i.e.* channelling gaseous dimethylamine in to the aqueous phase). Aqueous KOH 10M (0.5mL) was added to the DMF degradation flask on 20 minute intervals for a period of 2 hours after which the apparatus was disassembled. The flask containing the reaction mixture was left to vigorously stir (mixing of the aqueous dimethylamine and diethyl ether biphasic system) for 24 hours at room temperature. The organic phase was washed with water (4×), dried over Na₂SO₄ and concentrated under reduced pressure. After

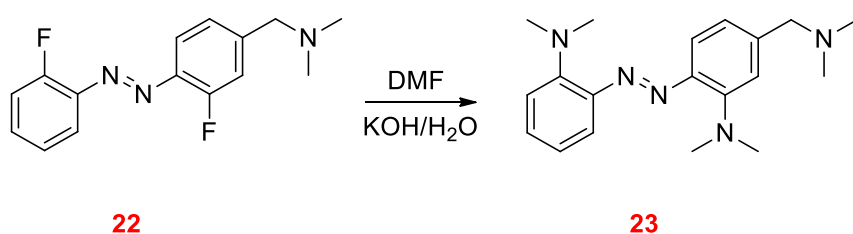
purification with flash chromatography (DCM/MeOH/Et₃N 98:1:1), the azobenzene **22** was obtained as an orange crystalline solid (72%).

Trans isomer: ¹H NMR (300 MHz, CDCl₃): δ = 7.78 (td, *J*₁ = 8 Hz, *J*₂ = 1.5 Hz, 1H), 7.75 (t, *J* = 8 Hz, 1H), 7.51-7.40 (m, 1H), 7.32-7.13 (m, 4H), 3.48 (s, 2H), 2.27 (s, 6H).

¹³C NMR (75 MHz, CDCl₃): δ = 160.52 (d, *J* = 257.5 Hz), 160.42 (d, *J* = 256.5 Hz), 145.57 (d, *J* = 7.5 Hz), 140.96 (d, *J* = 7 Hz), 139.92 (d, *J* = 7 Hz), 132.99 (d, *J* = 8.5 Hz), 124.82 (d, *J* = 3.5 Hz), 124.49 (d, *J* = 4 Hz), 117.96, 117.67, 117.31 (d, *J* = 20 Hz), 117.17 (d, *J* = 19.5 Hz), 63.73 (d, *J* = 1.5 Hz), 45.57.

¹⁹F NMR (471 MHz, CDCl₃): δ = -124.25 — -124.32 (m), -124.36 (dd, *J*₁ = 11.5 Hz, *J*₂ = 7.5 Hz).

Synthetic approaches toward the azobenzene derivative **23**



A solution of compound **22** (137.65 mg, 0.5 mmol) in DMF (27.8 mmol, 2 mL) was heated to 70 °C at which point 0.25 mL aqueous KOH, 20M was added on 20 minute intervals and DMF (1mL) on 80 minute intervals. After 4 hours reaction (12 additions of aqueous KOH, 20M) the reaction mixture was cooled to room temperature and diluted with ethyl acetate (20 mL). The organic phase was washed with water (5×), dried over Na₂SO₄ and concentrated under reduced pressure. NMR spectroscopy showed indicated at product formation but purification was unsuccessful.

Molar extinction coefficient measurements

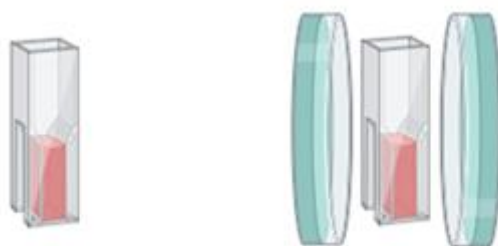
A NMR sample containing a mixture of a compound **16** and a known concentration of (10 μl) DCM in CDCl₃ was prepared. The concentration of compound **16** was measured by comparing the integrals of the peaks corresponding to the chemical shift of the methylene group of DCM at 5.3 ppm, with that of the methyl group of compound **16** at 2.15 ppm. The

NMR tube sample was then diluted in MeCN and UV-Vis spectra of the diluted samples were acquired.

Bacterial cultures

Fresh shrimps from the local fish market in Heraklion (fished from Agios Nikolaos, Crete) were placed on ice and transferred to the University. The shrimps were placed in a 50 mL falcon tubes containing enough 3.0 % w/w NaCl solution such that 20 % of the shrimp mass was above the level of the liquid. The tubes were incubated overnight at a temperature between 18 and 22 °C and monitored for luminous areas on the shrimp mass. When luminescence was observed, a sterile toothpick was used to gently scratch the luminous areas and streak agar plates containing LA medium. The agar plates were incubated at 18-22 °C for 36 hours and the brightest luminous colony was transferred to a new agar plate and incubated at 18-22 °C for 24 hours. The luminous plates were then used for photoisomerization studies.

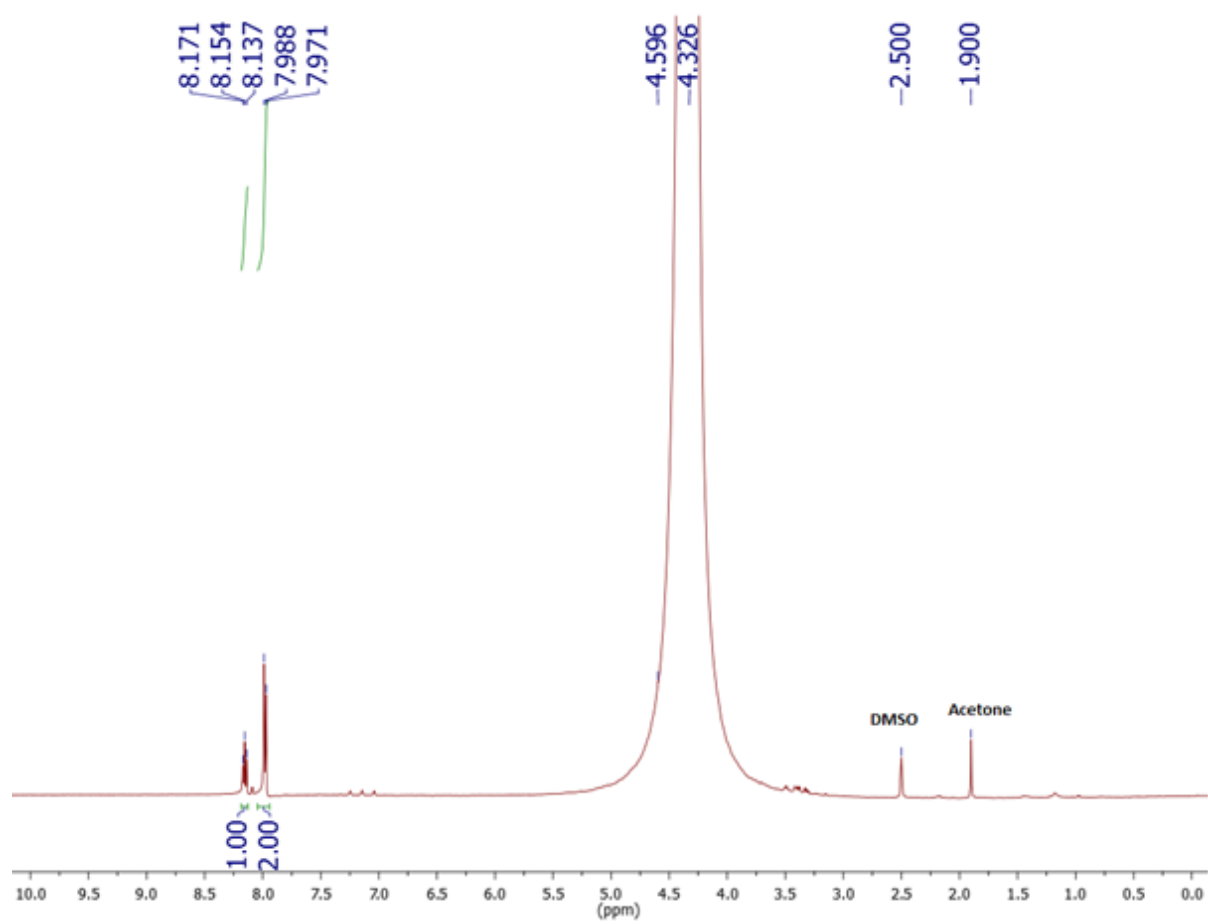
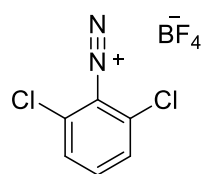
Bacterial luciferase induces isomerization



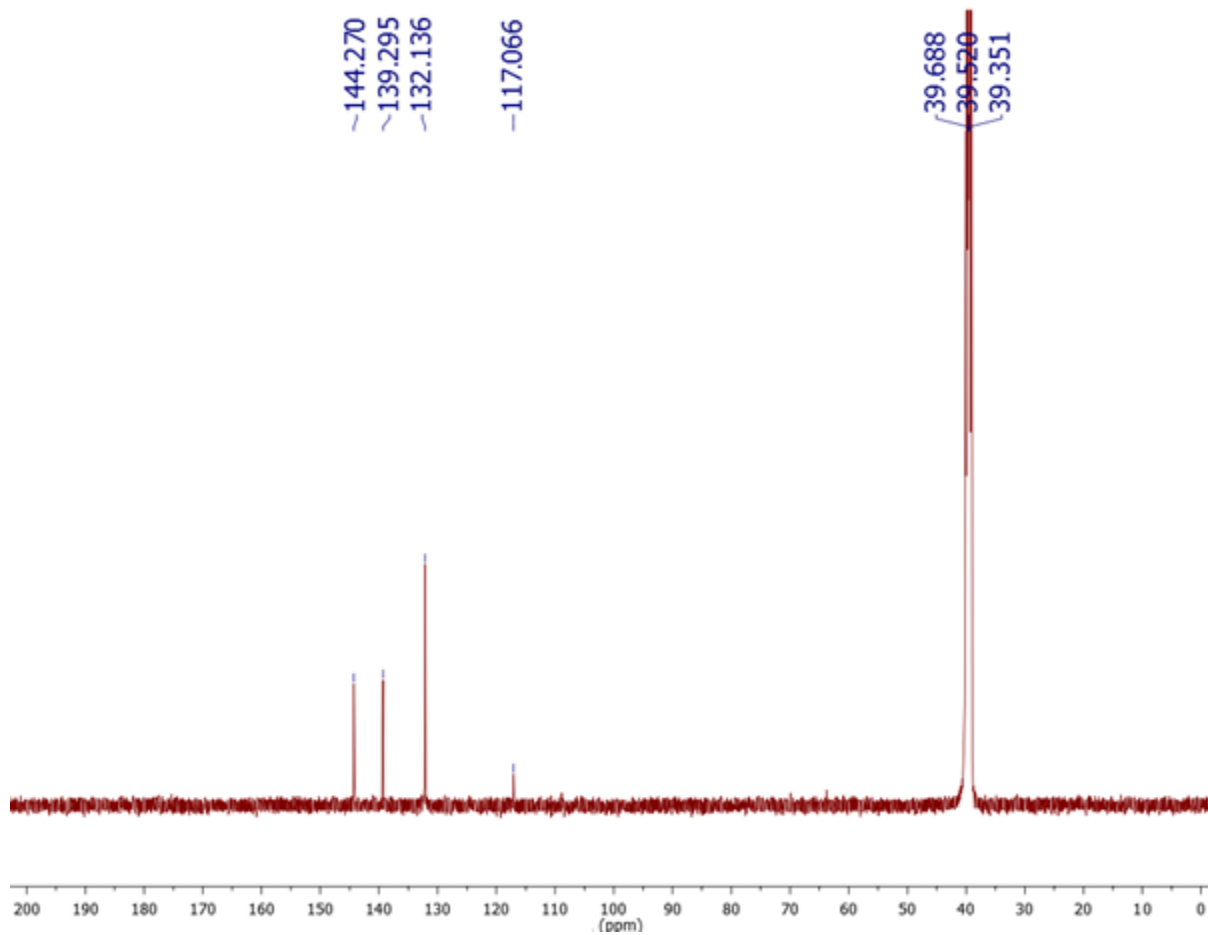
A solution of compound **16** in benzene ($C \approx 0.02$ mM) was placed in a quartz cuvette and the UV-Vis spectrum was recorded. The cuvette was then placed between 2 luminous plates at a distance of 2 cm for 5 minutes and a new UV-Vis spectrum was recorded. The 2 spectra were compared.

Supplementary information

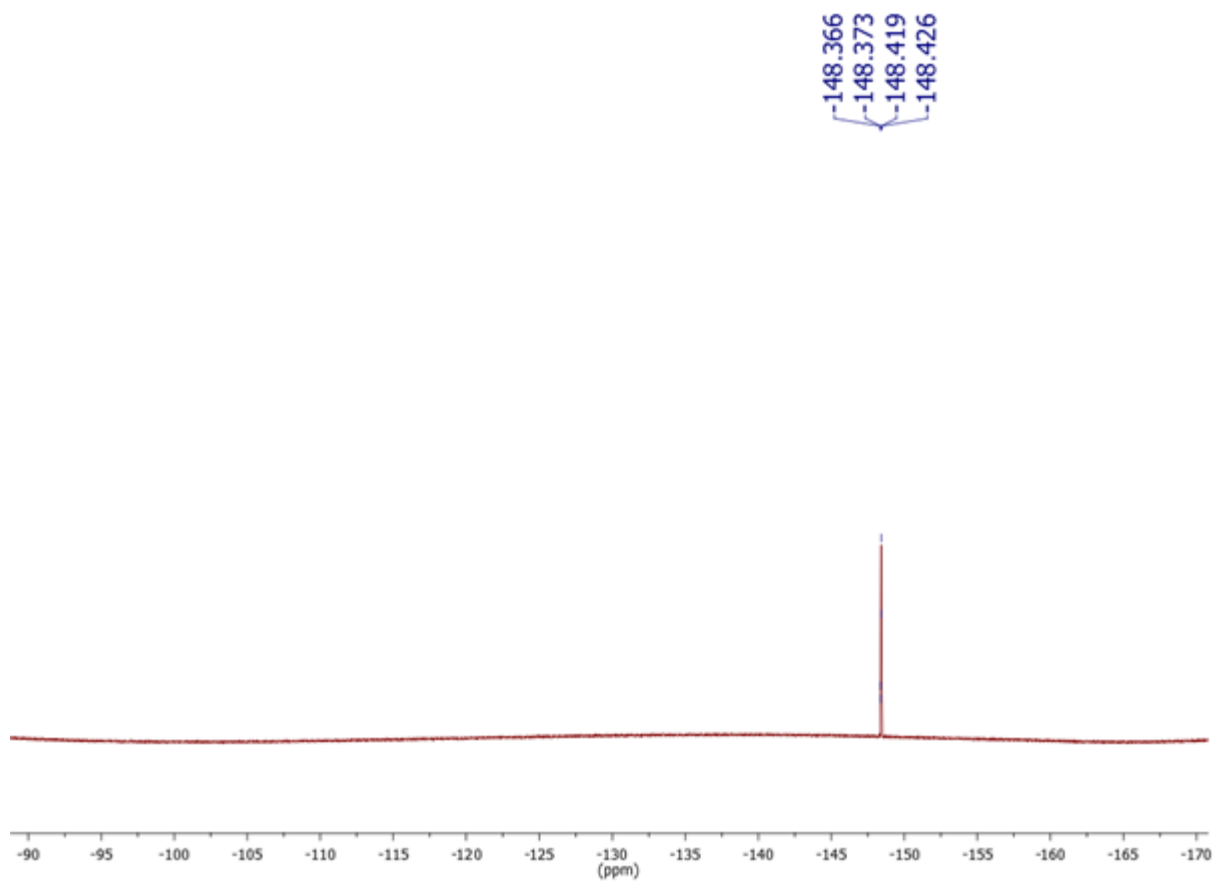
Compound 1



1H NMR (500 MHz, DMSO- d_6)

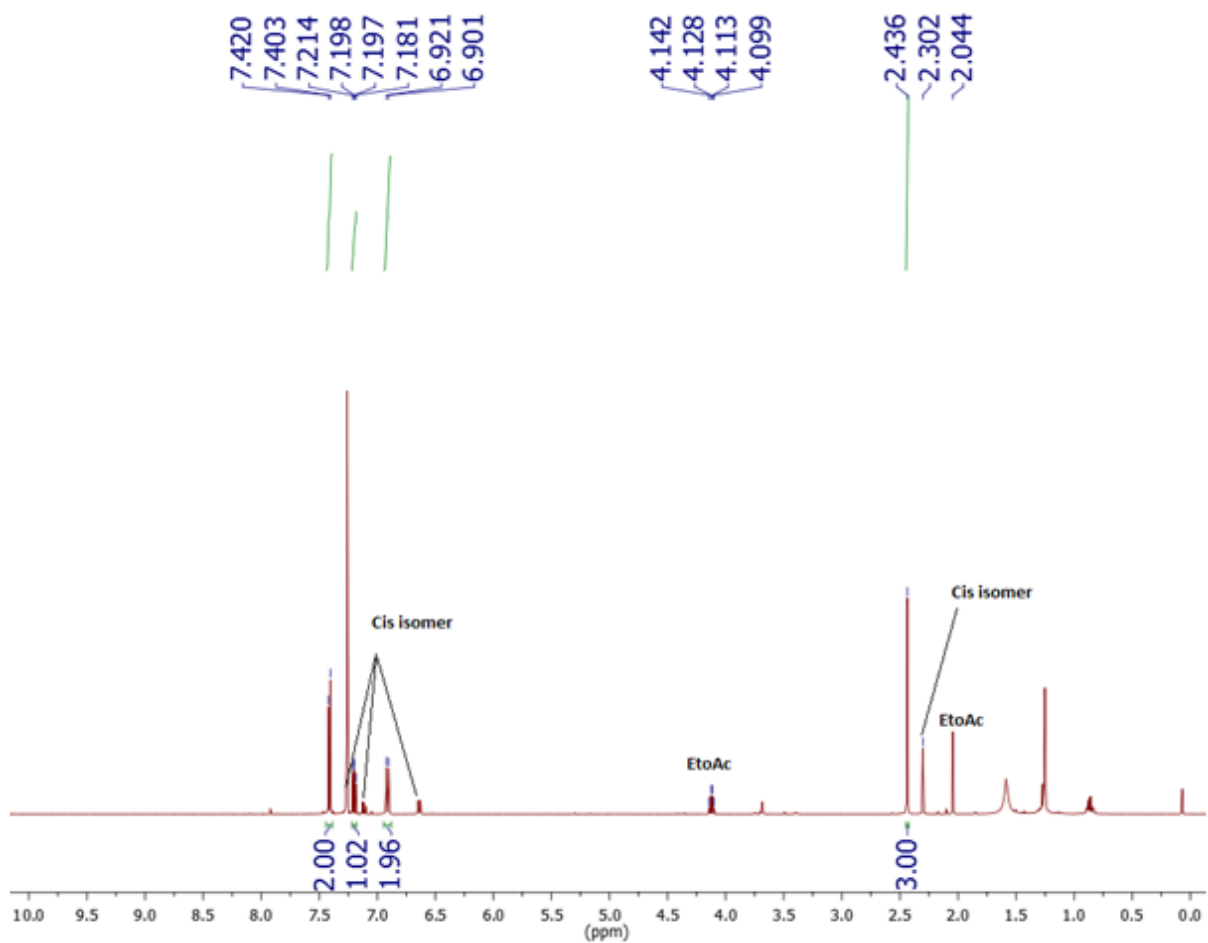
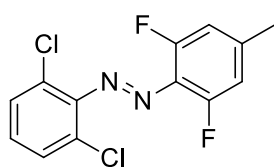


¹³C NMR (125 MHz, DMSO-d₆)

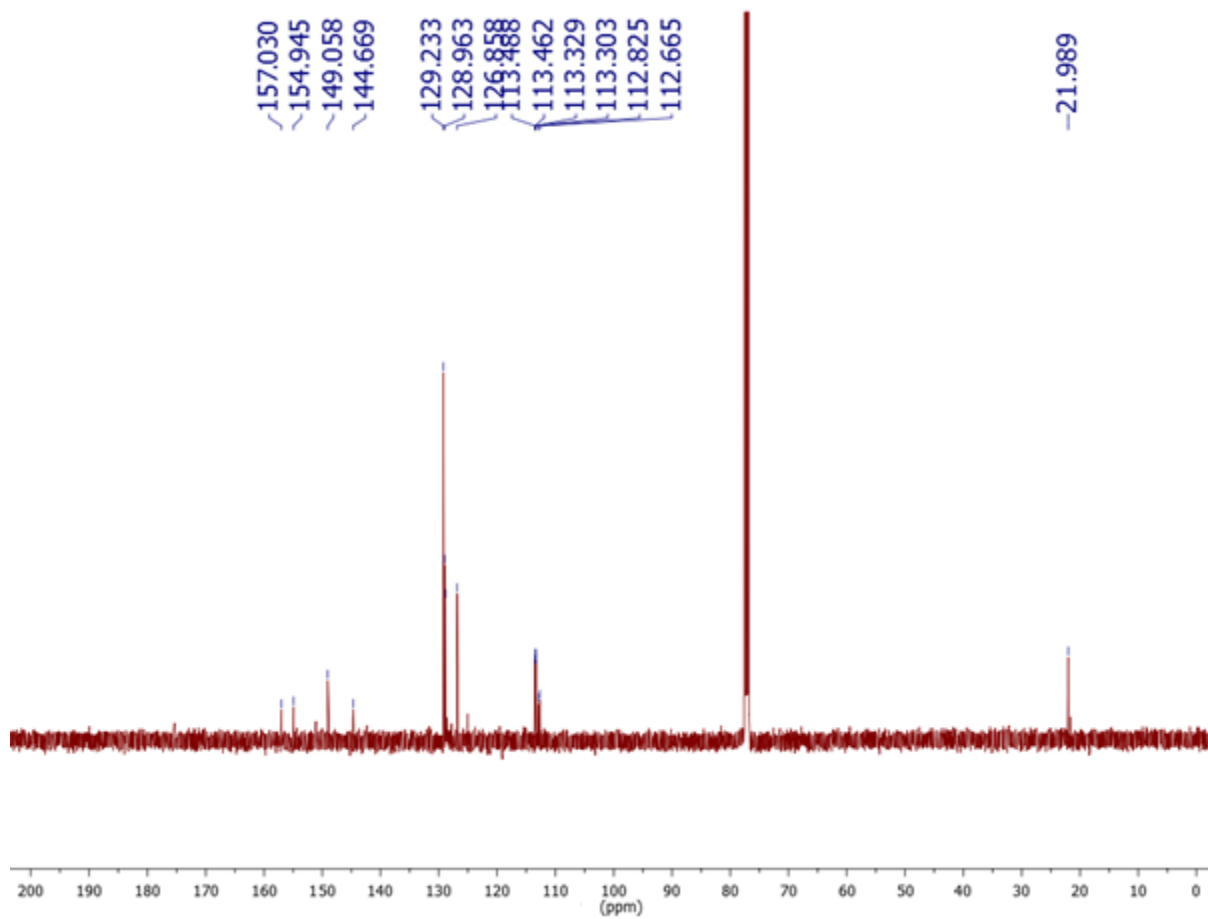


^{19}F NMR (471 MHz DMSO-d₆)

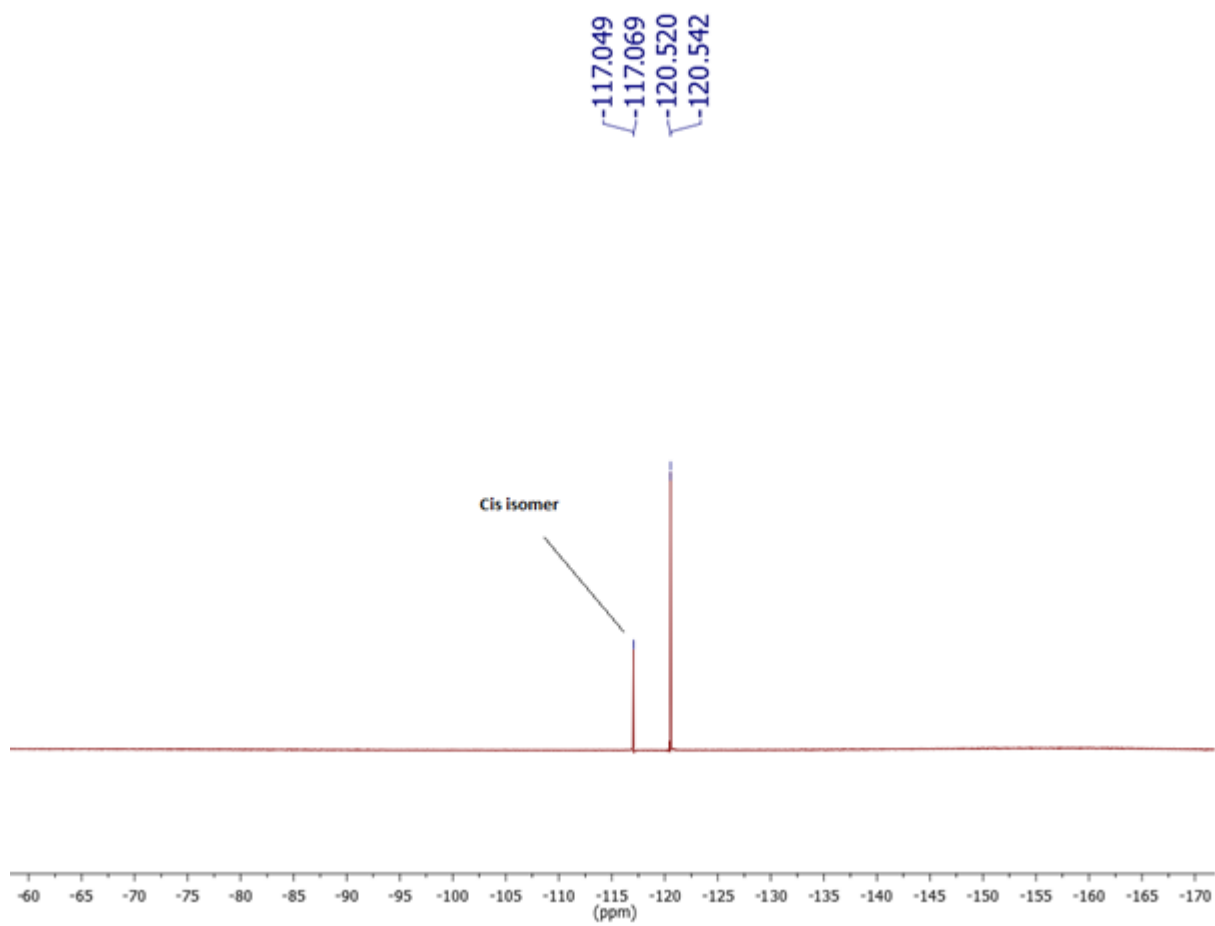
Compound 2



^1H NMR (500 MHz, CDCl_3)

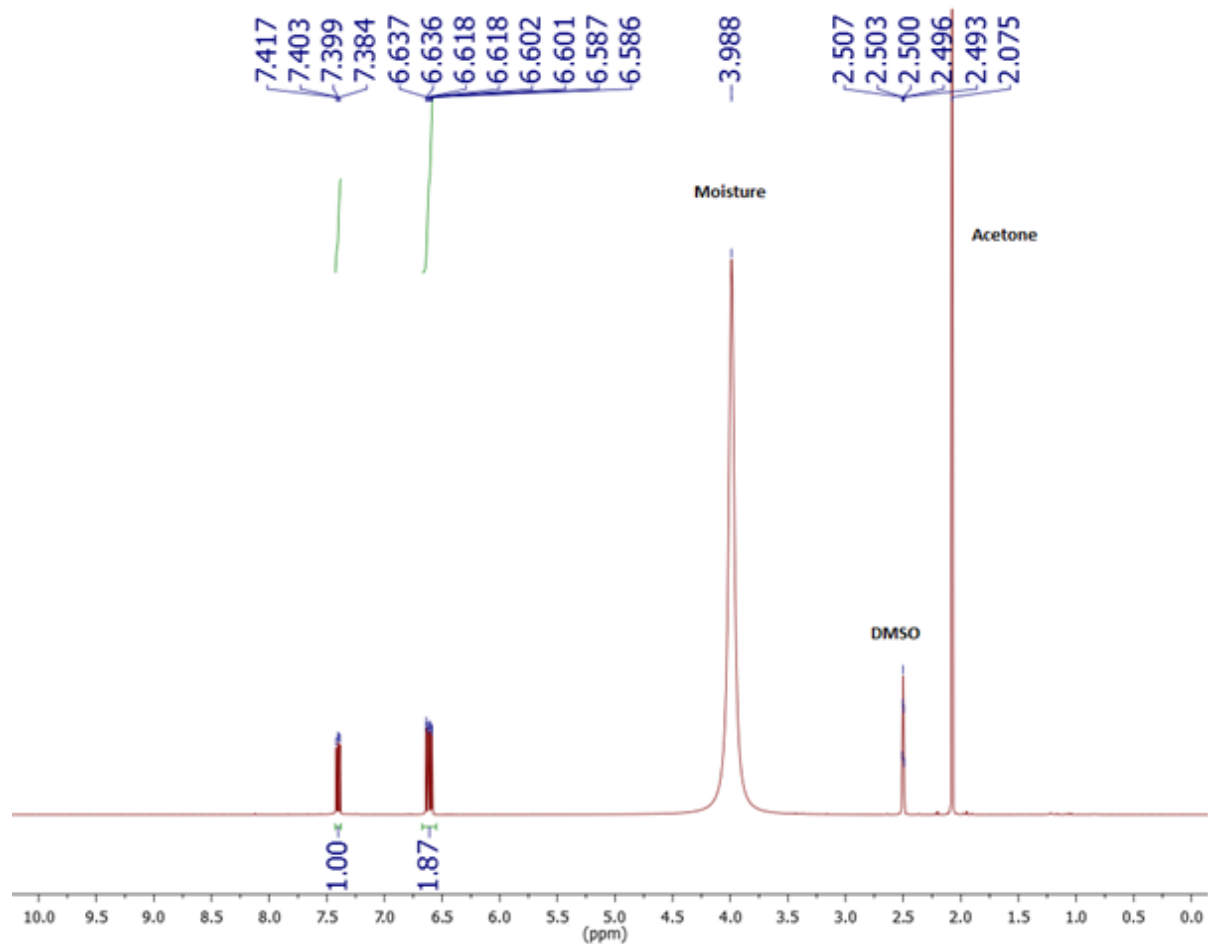
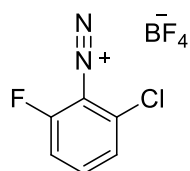


^{13}C NMR (125 MHz, CDCl_3)

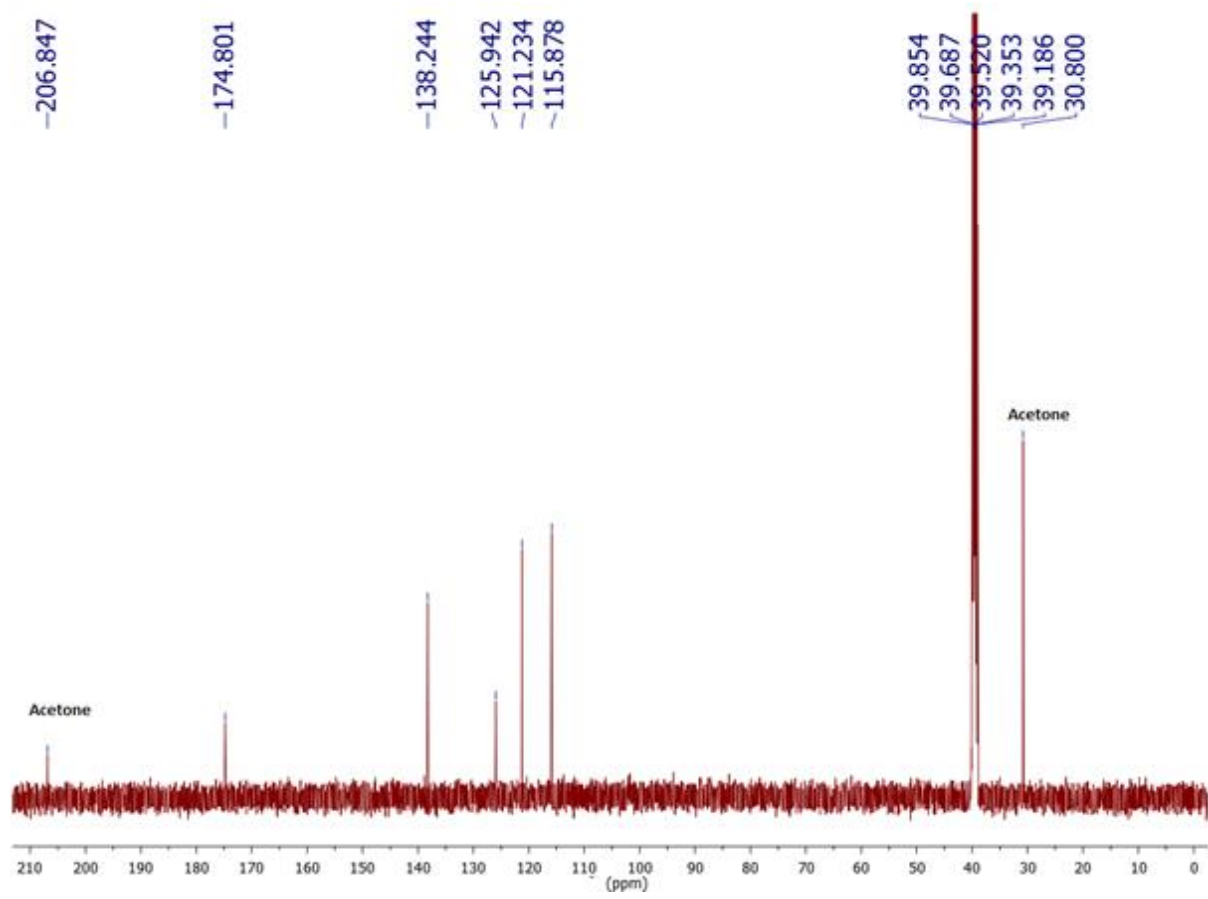


^{19}F NMR (471 MHz, CDCl_3)

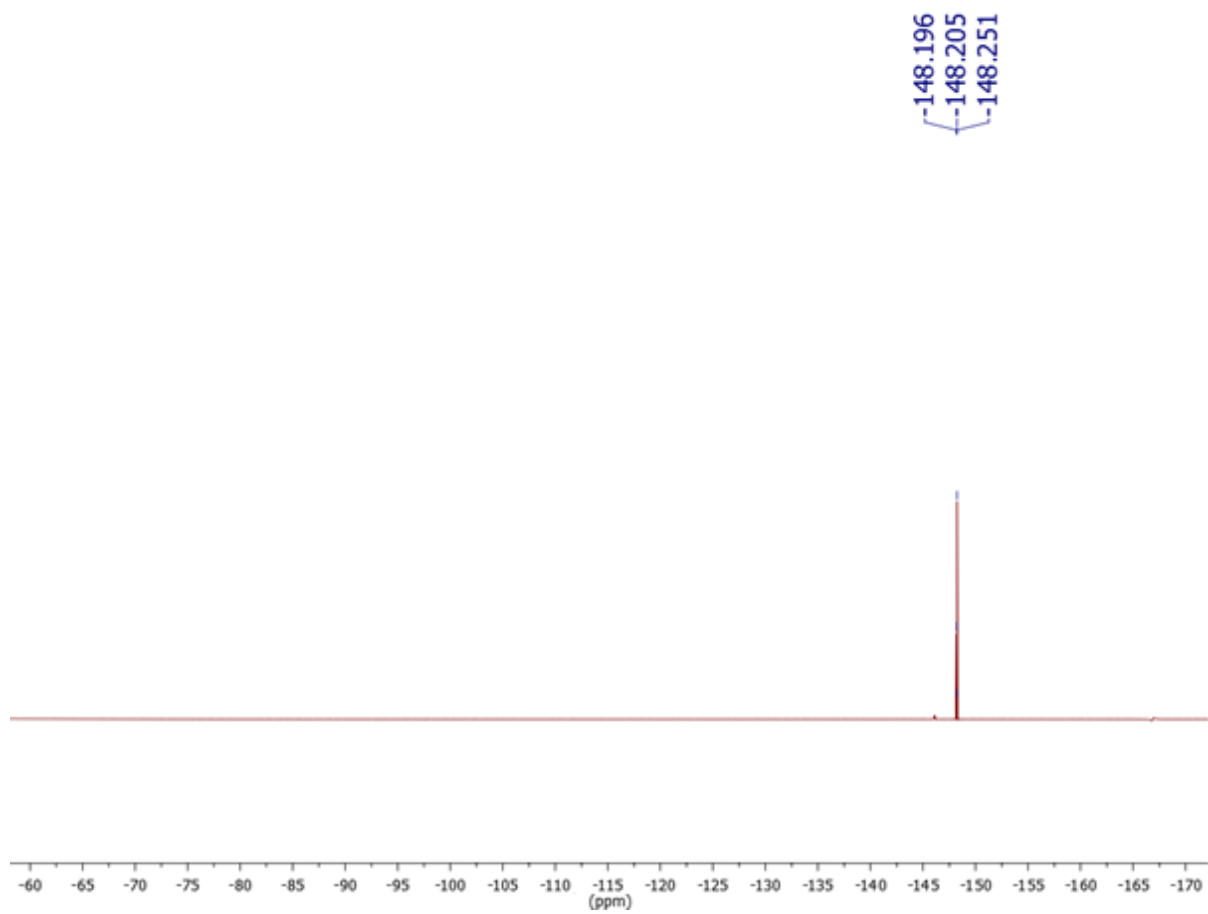
Compound 3



^1H NMR (500 MHz, DMSO-d_6)

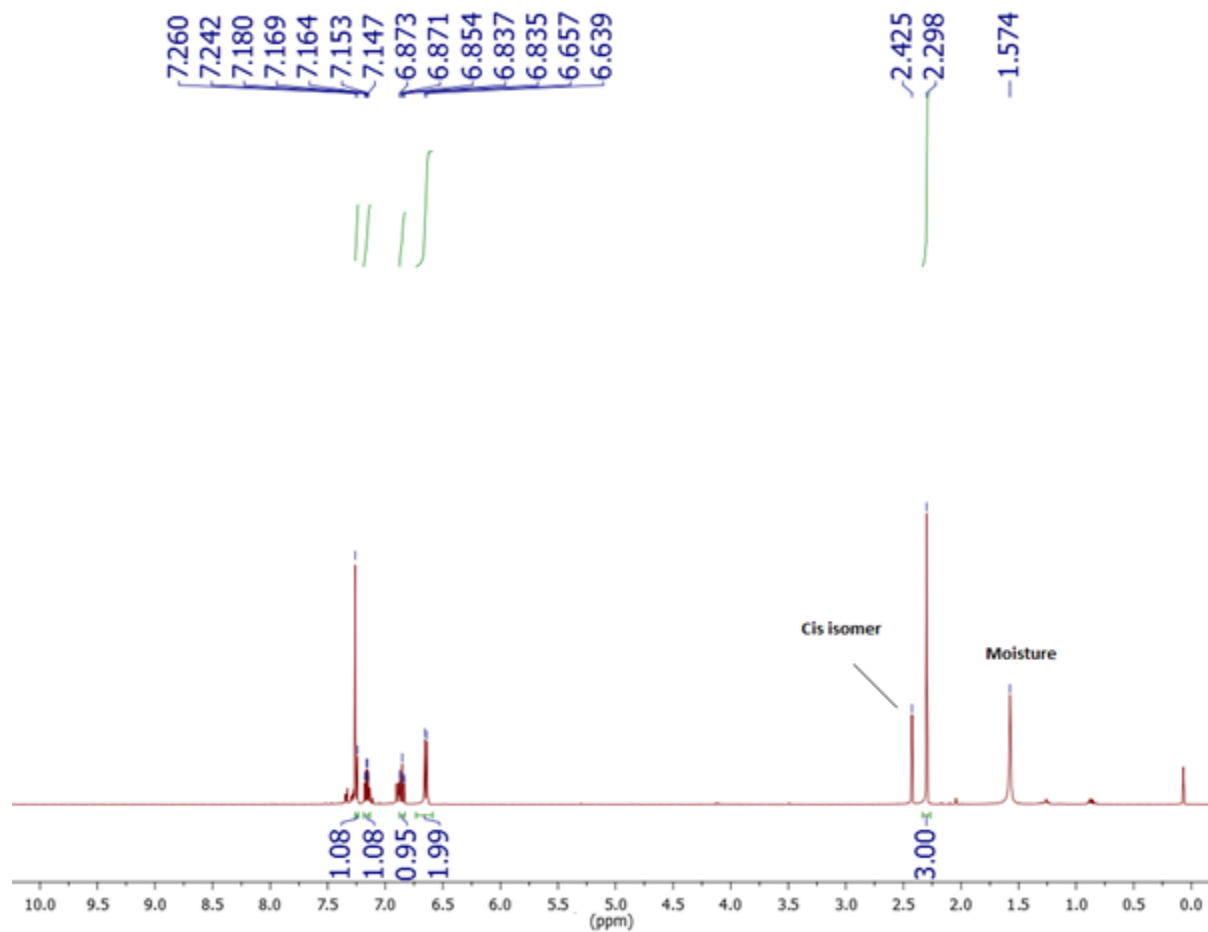
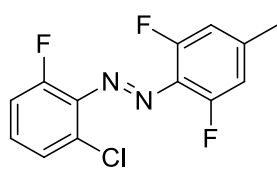


^{13}C NMR (125 MHz, DMSO-d_6)

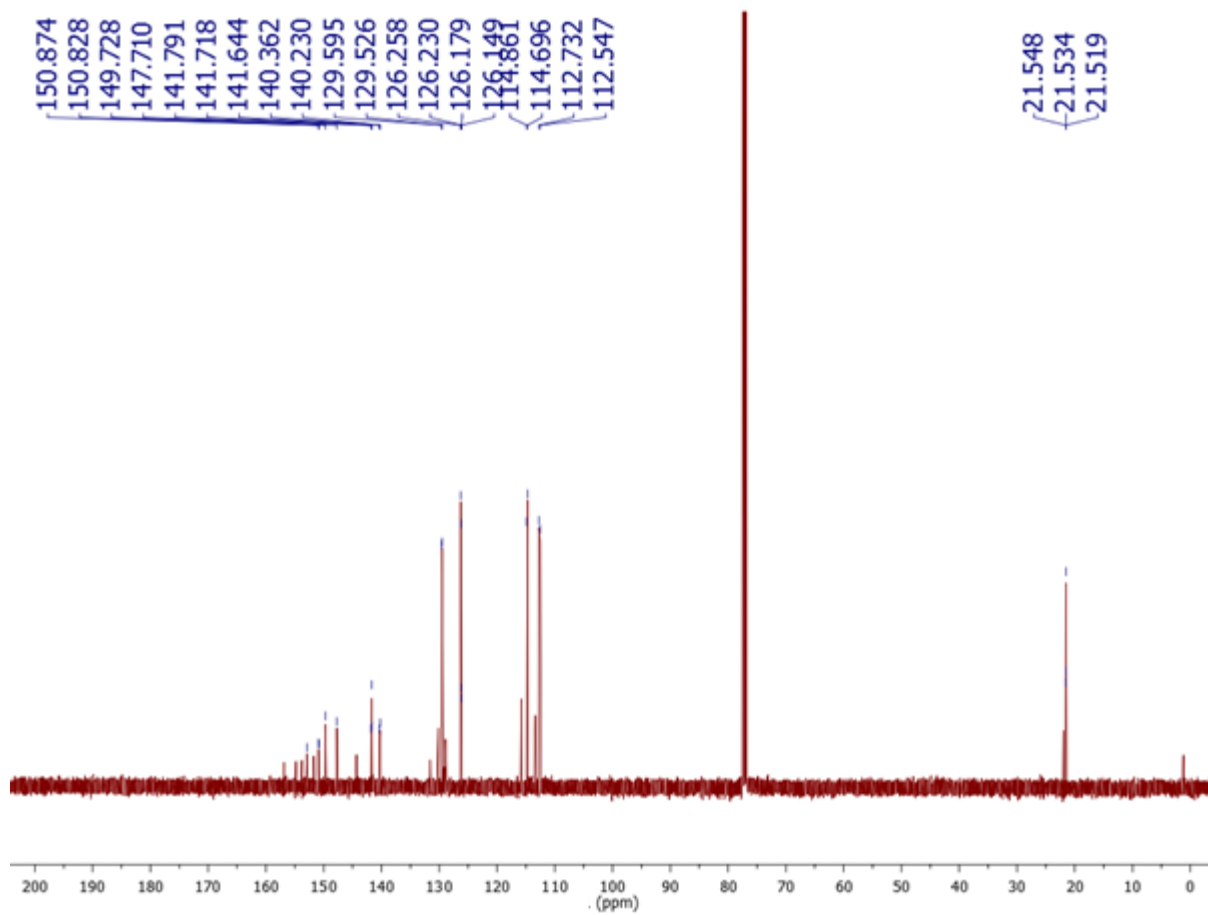


^{19}F NMR (471 MHz DMSO- d_6)

Compound 4

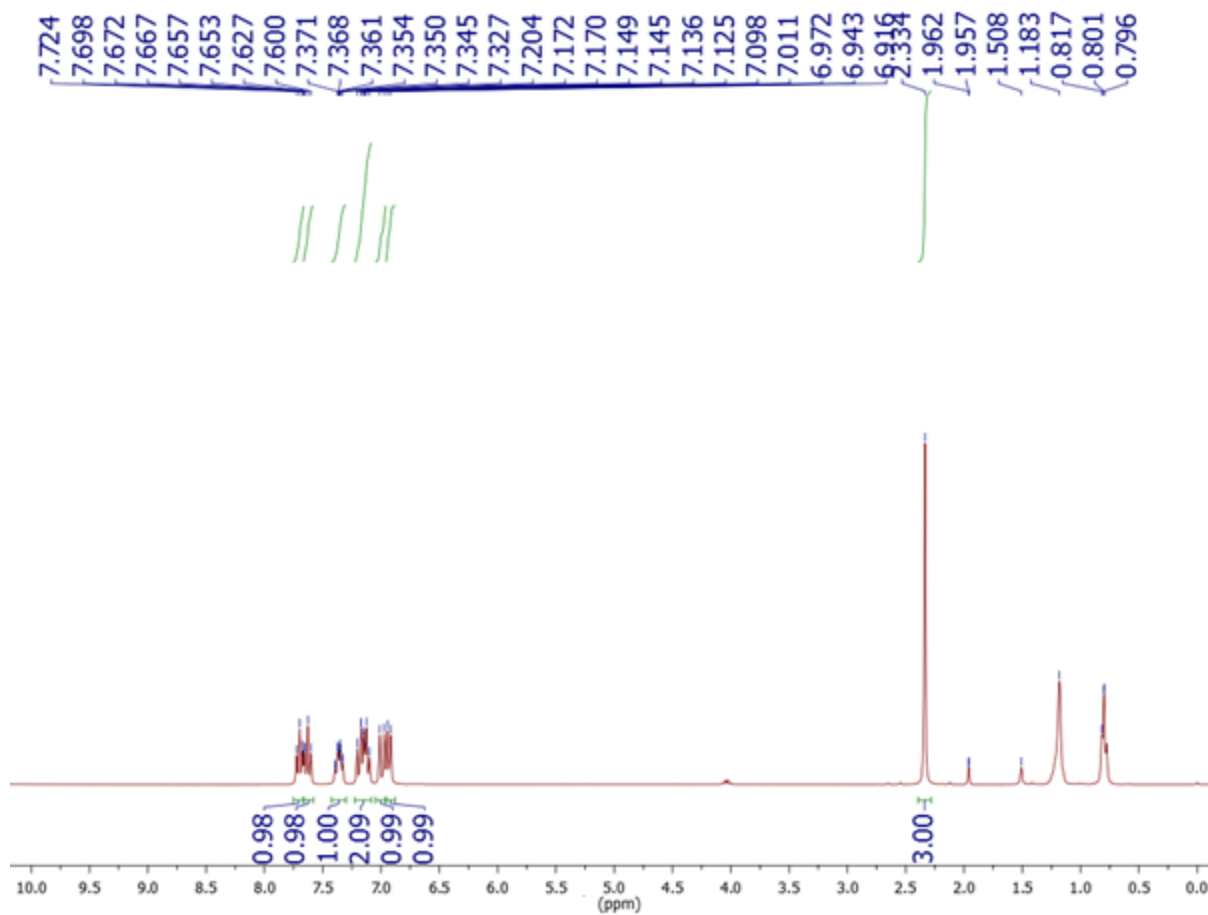
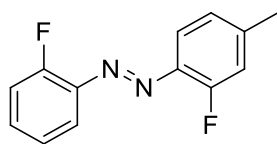


^1H NMR (500 MHz, CDCl_3)

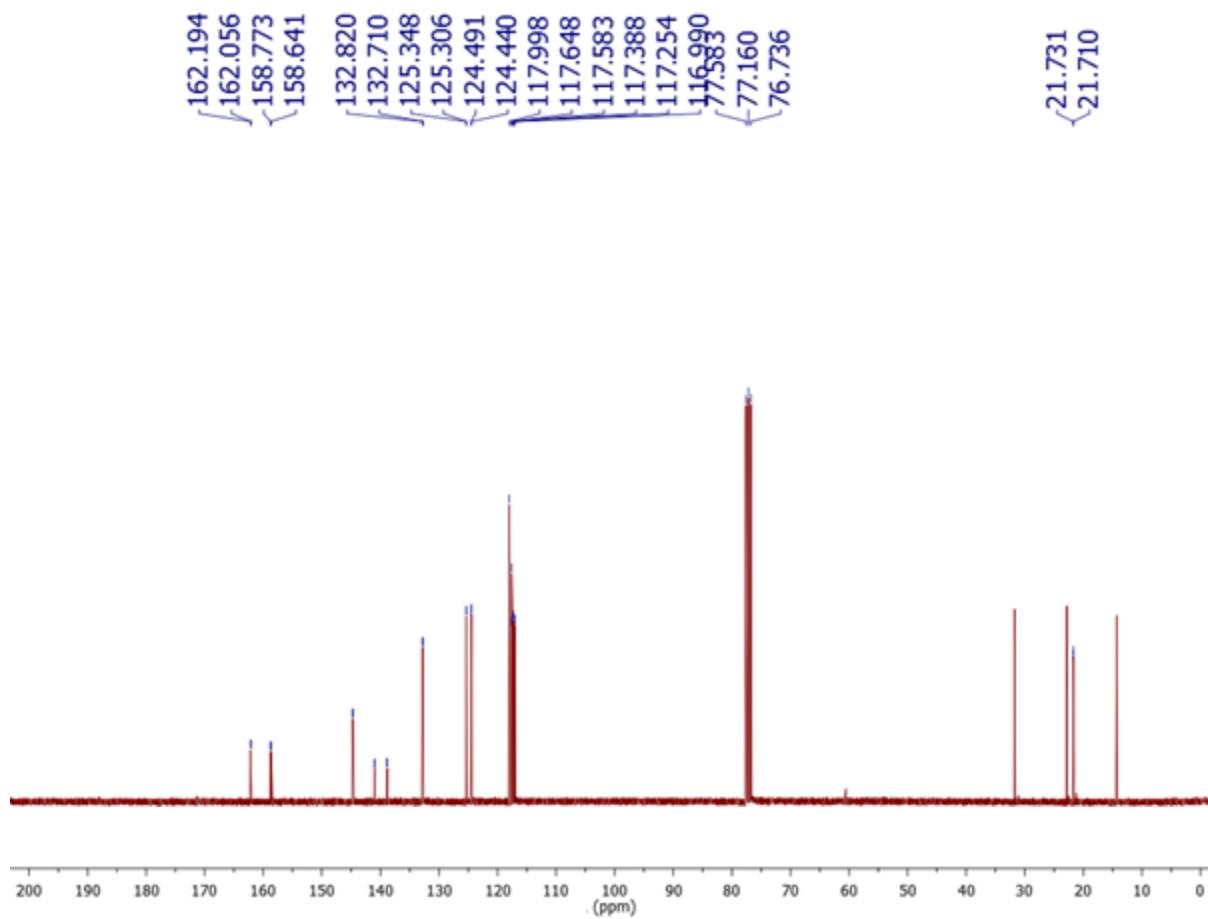


^{13}C NMR (125 MHz, CDCl_3)

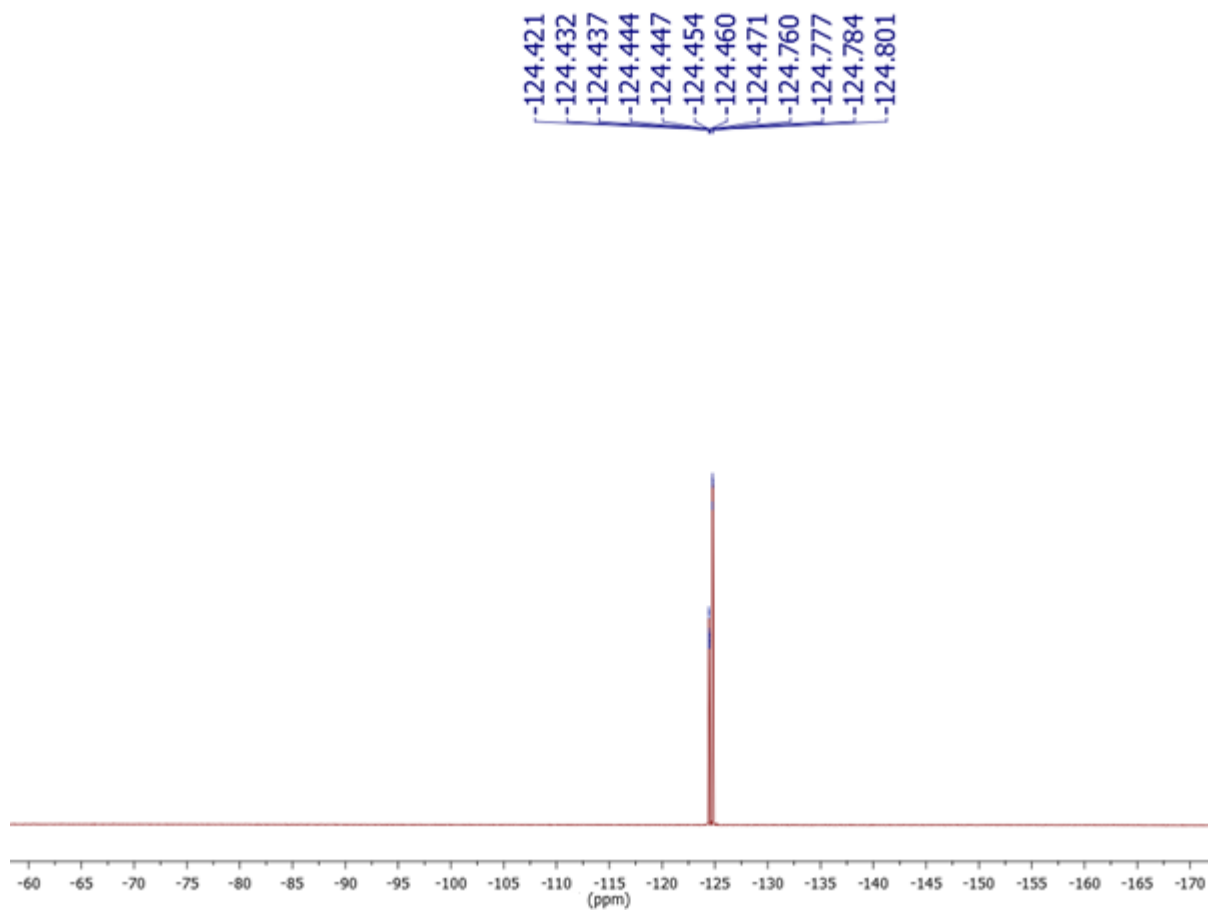
Compound 8



^1H NMR (300 MHz, CDCl_3)

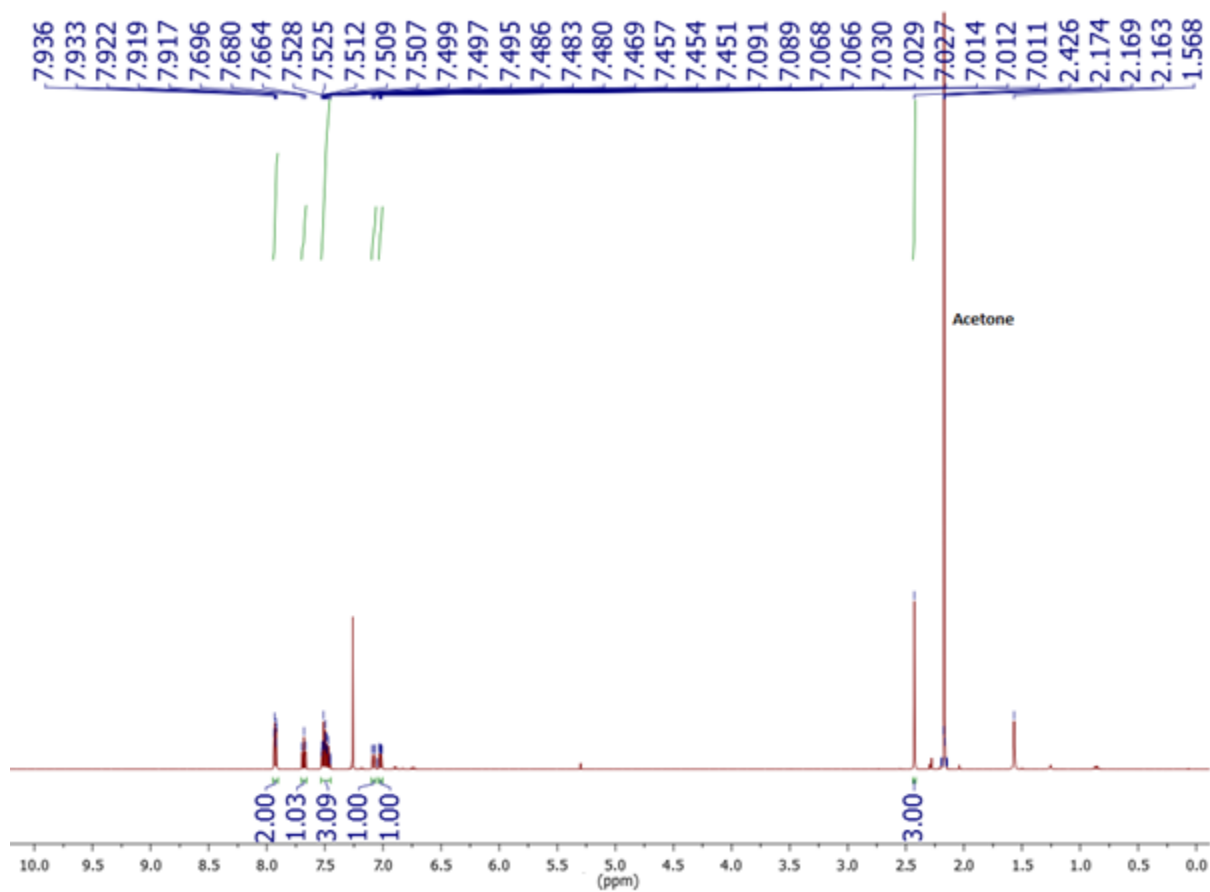
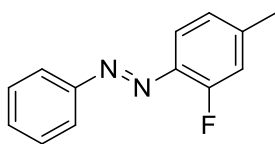


^{13}C NMR (75 MHz, CDCl_3)

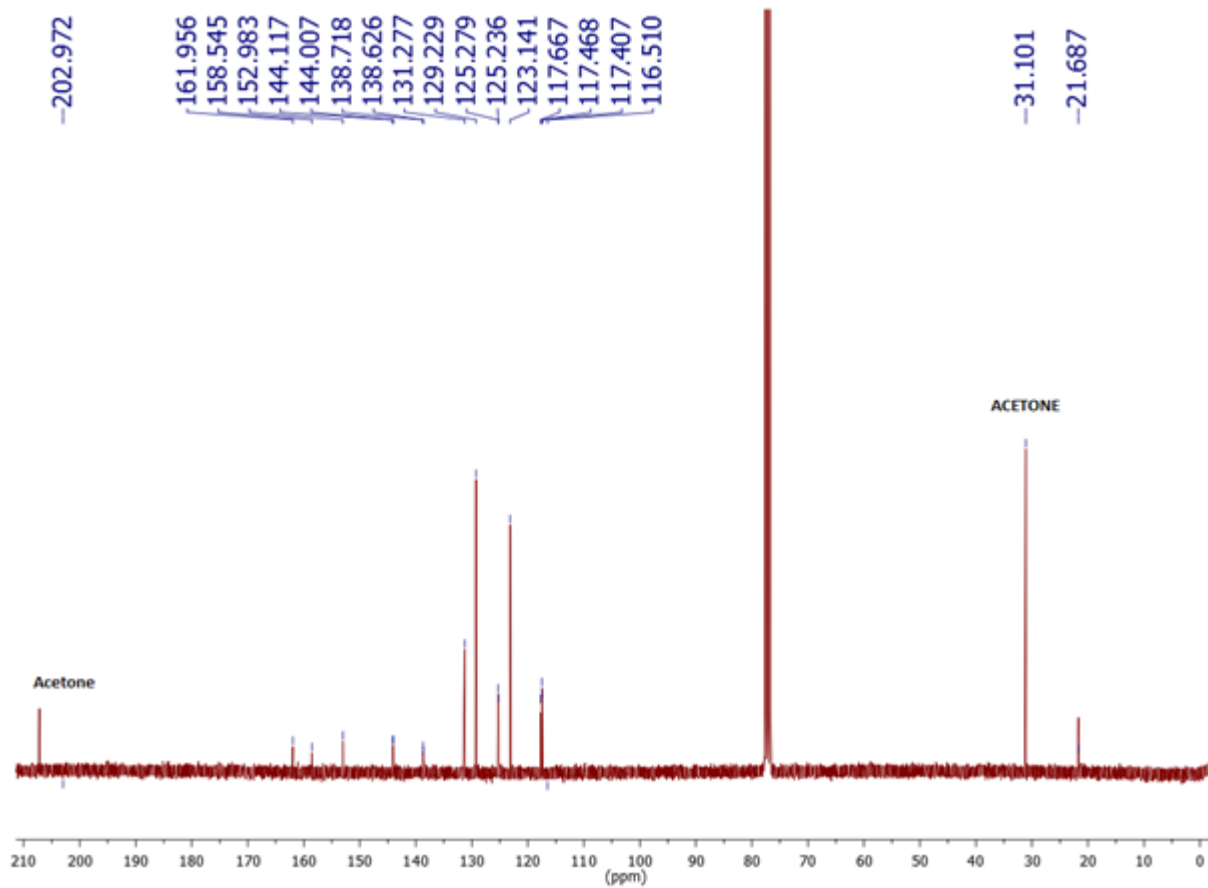


^{19}F NMR (471 MHz, CDCl_3)

Compound 9

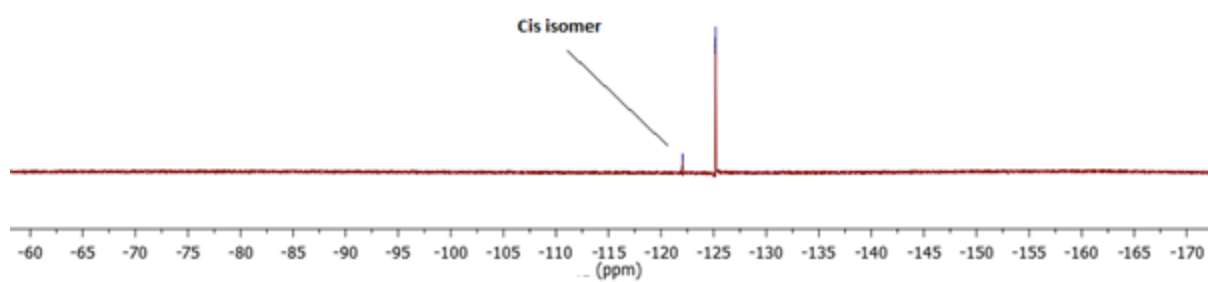


^1H NMR (500 MHz, CDCl_3)



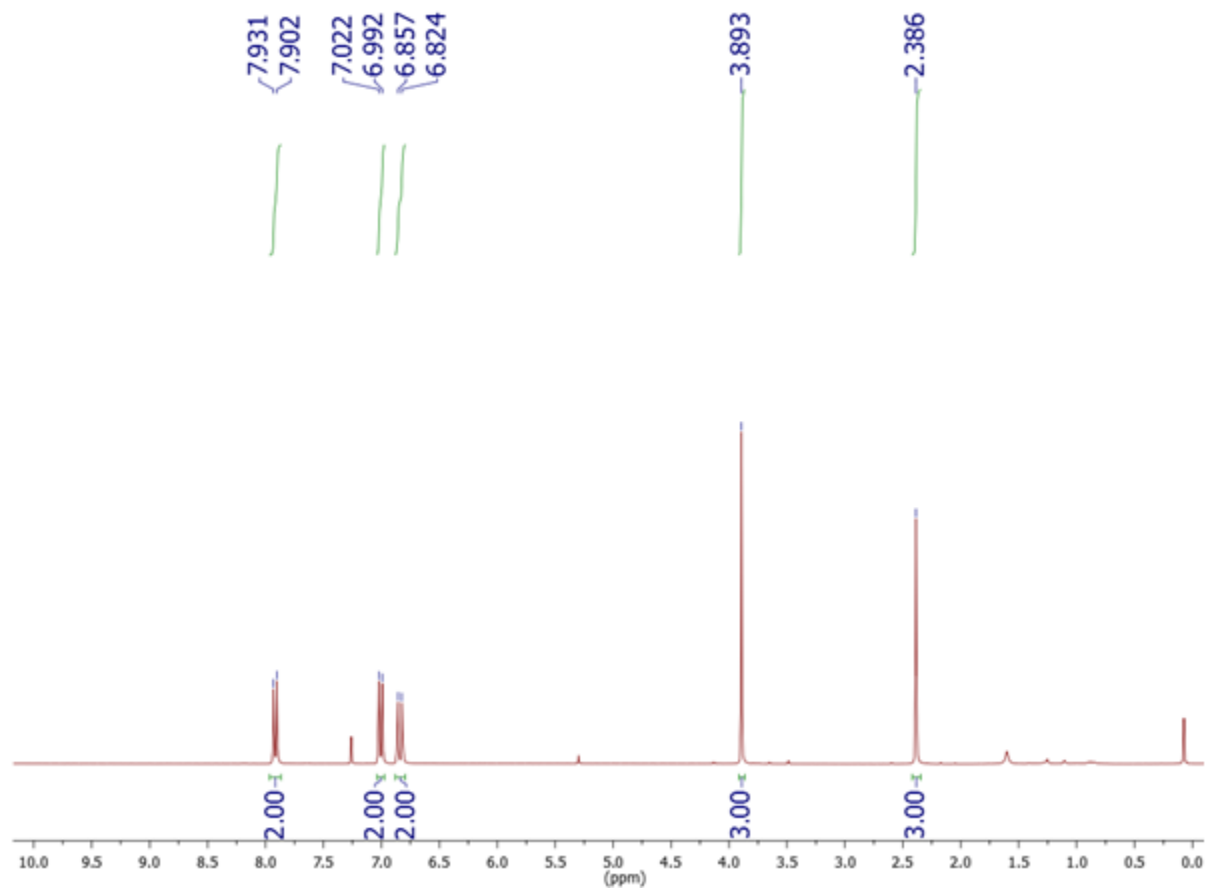
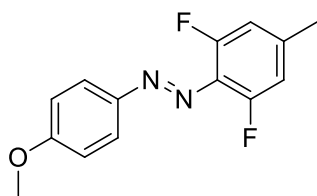
^{13}C NMR (75 MHz, CDCl_3)

-122.045
-122.068
-122.084
-125.136
-125.153
-125.160
-125.177

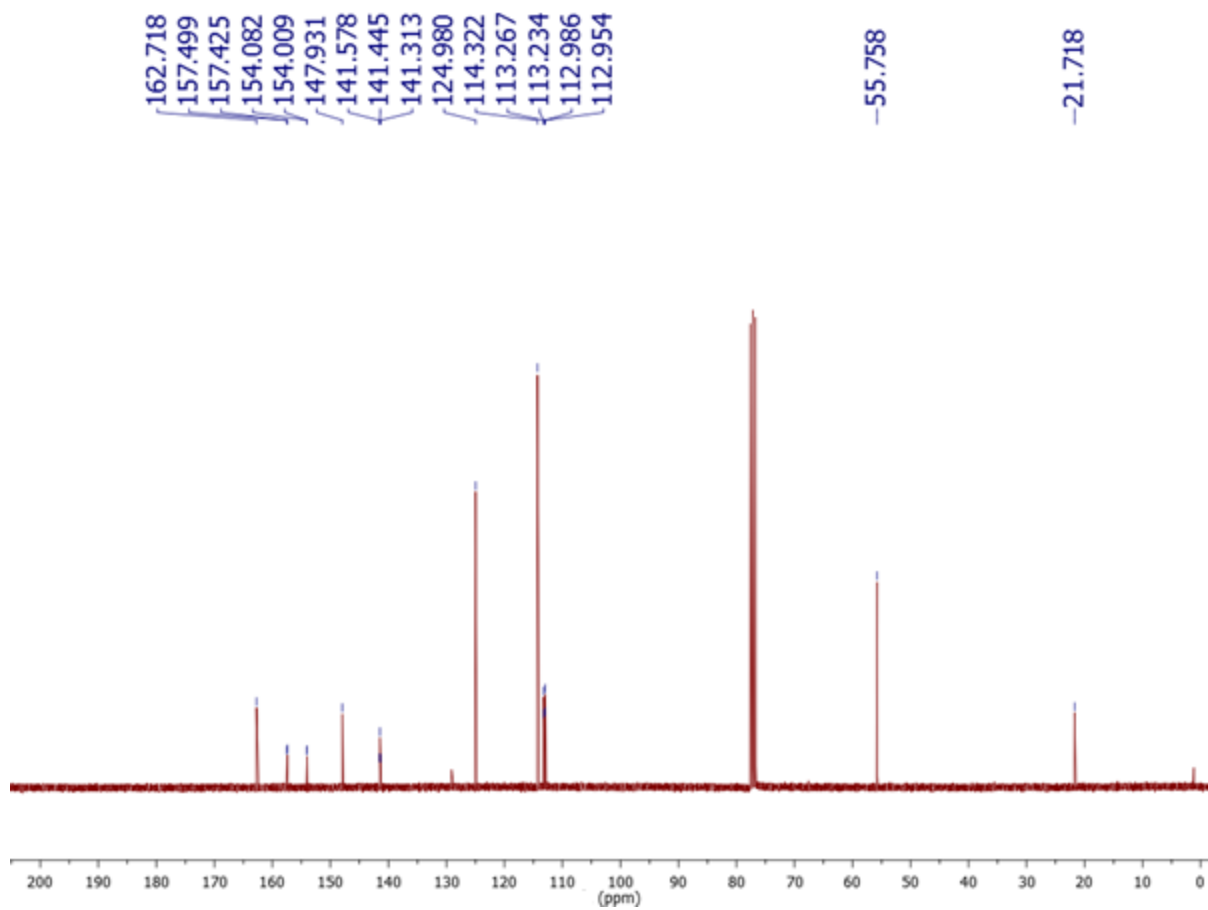


^{19}F NMR (471 MHz, CDCl_3)

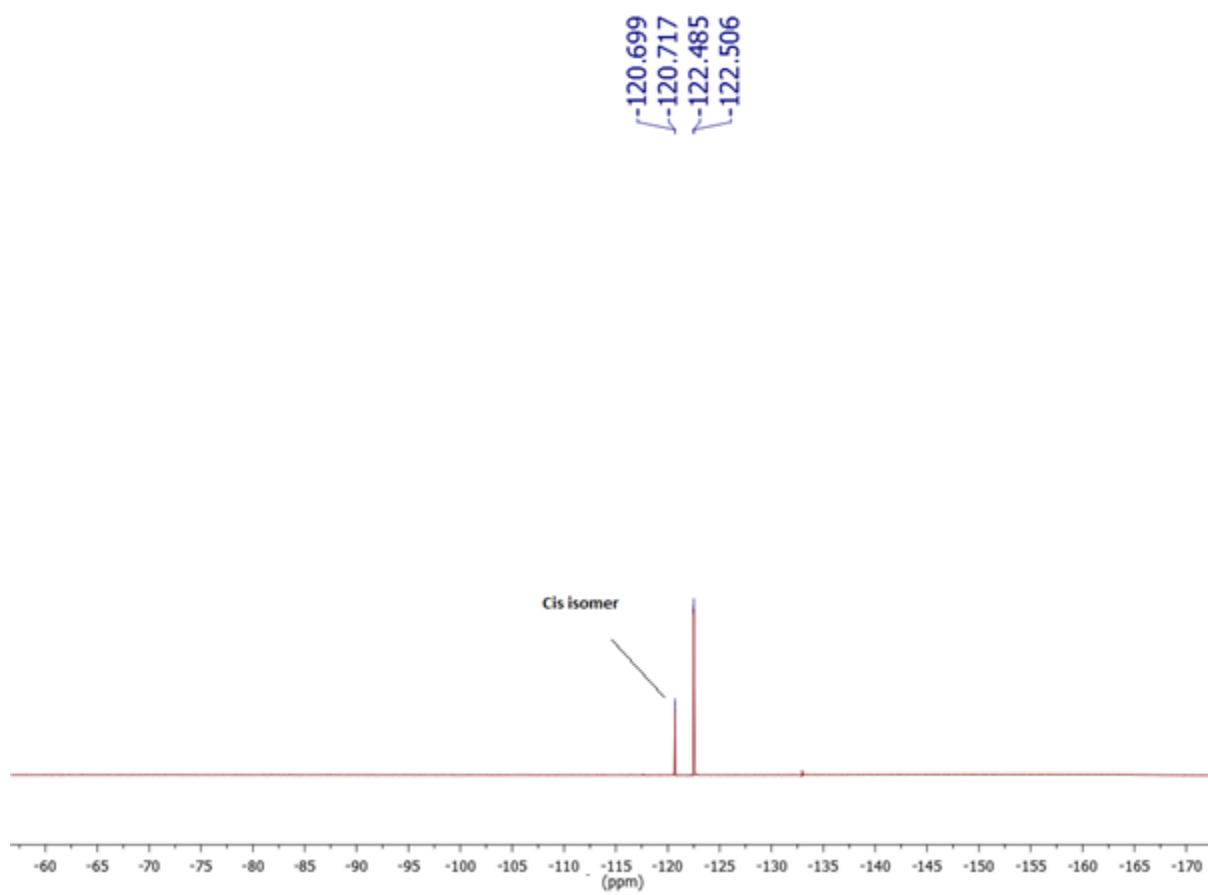
Compound 10



^1H NMR (300 MHz, CDCl_3)

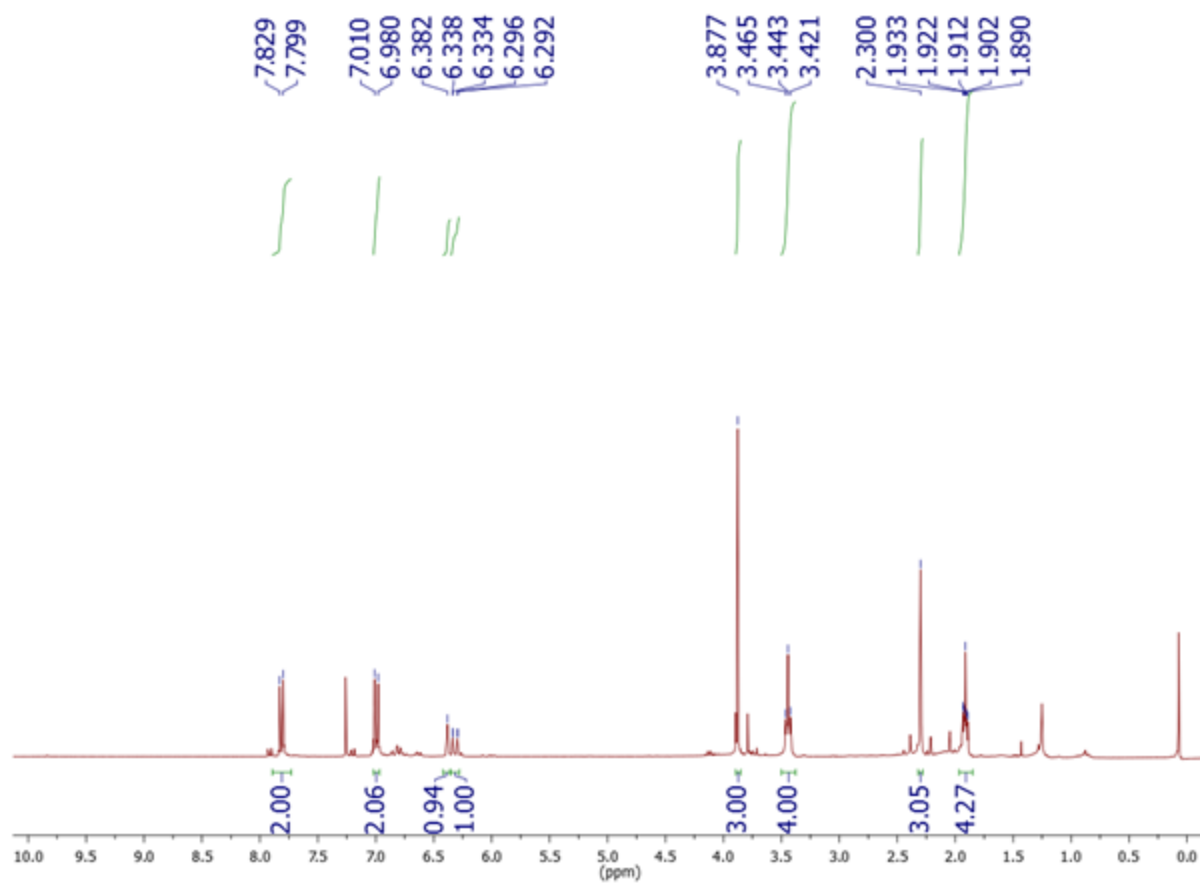
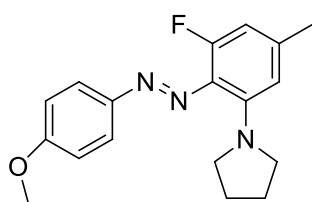


^{13}C NMR (75 MHz, CDCl_3)

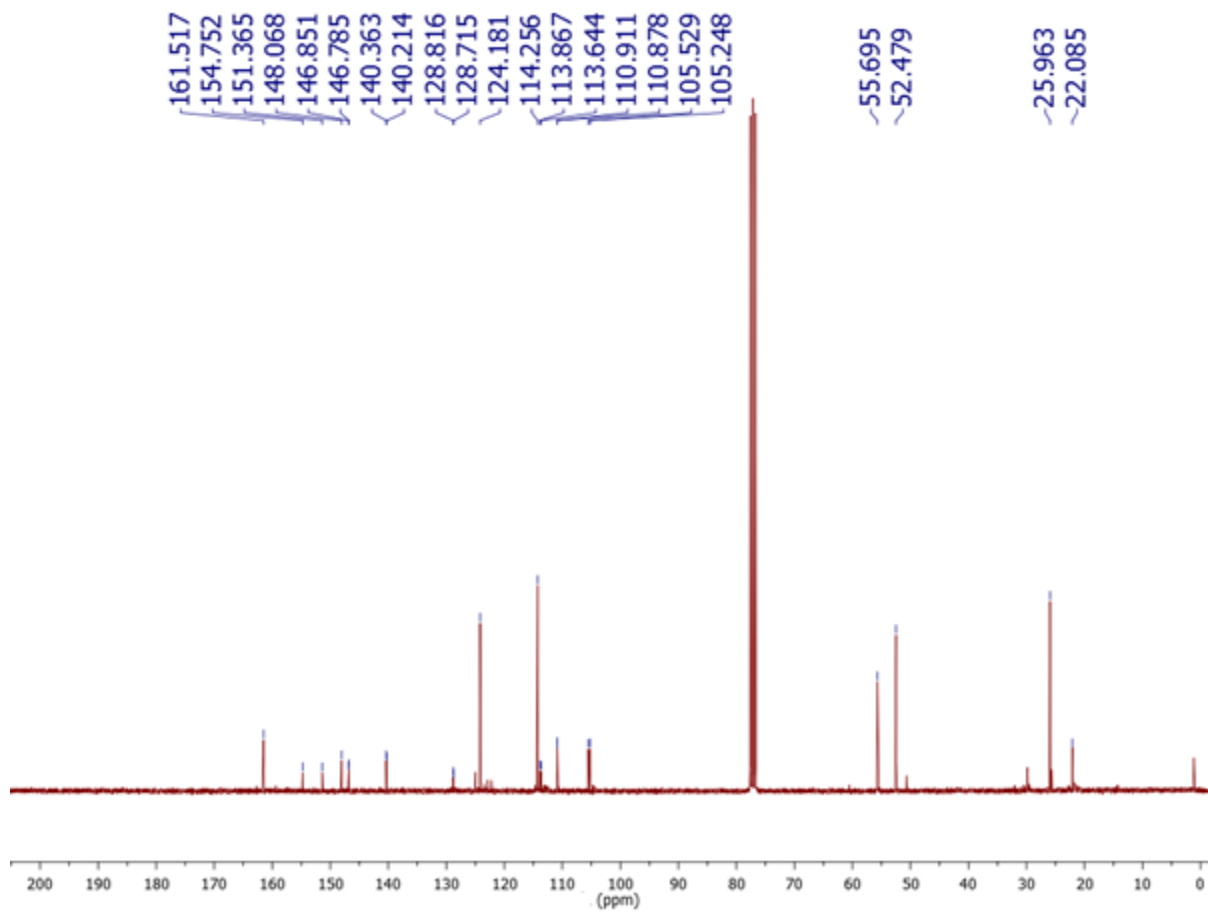


^{19}F NMR (471 MHz, CDCl_3)

Compound **11**

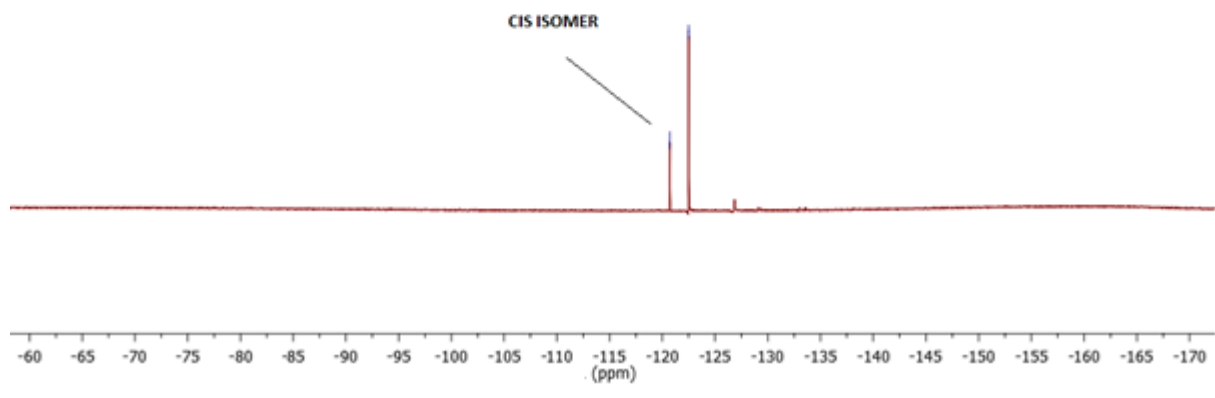


¹H NMR (300 MHz, CDCl₃)



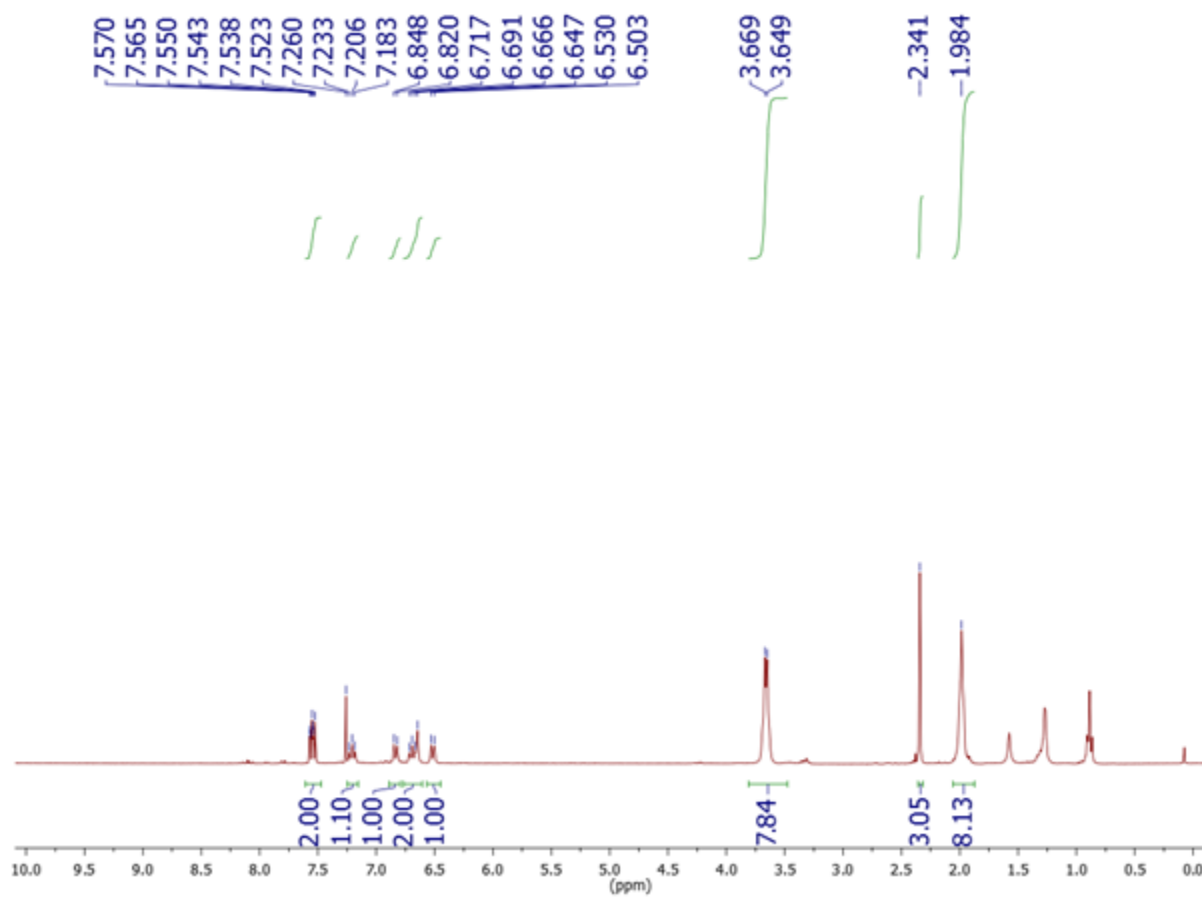
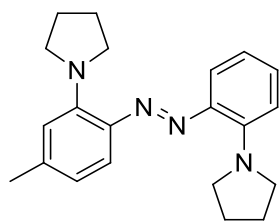
^{13}C NMR (75 MHz, CDCl_3)

-120.700
-120.718
-122.490
-122.511

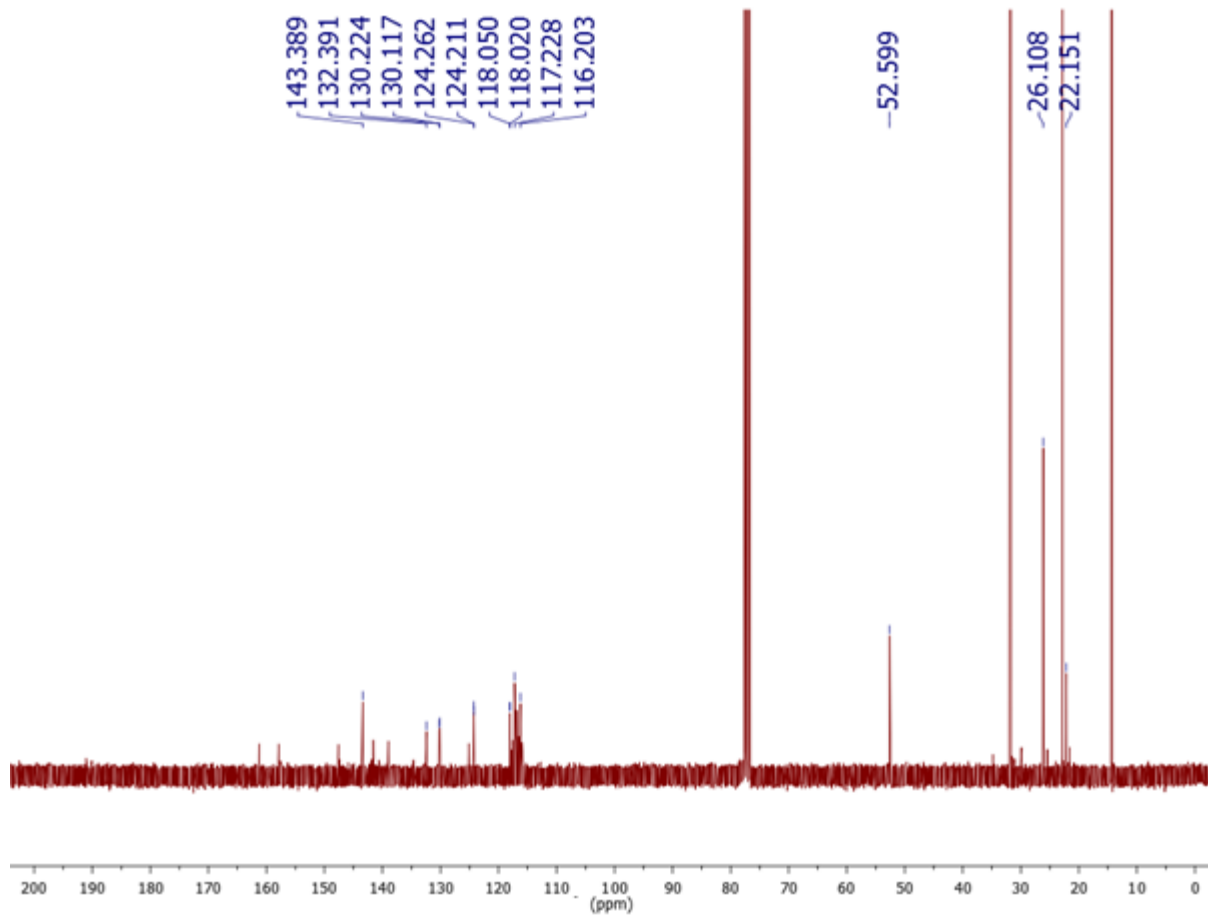


¹⁹F NMR (471 MHz, CDCl₃)

Compound 13

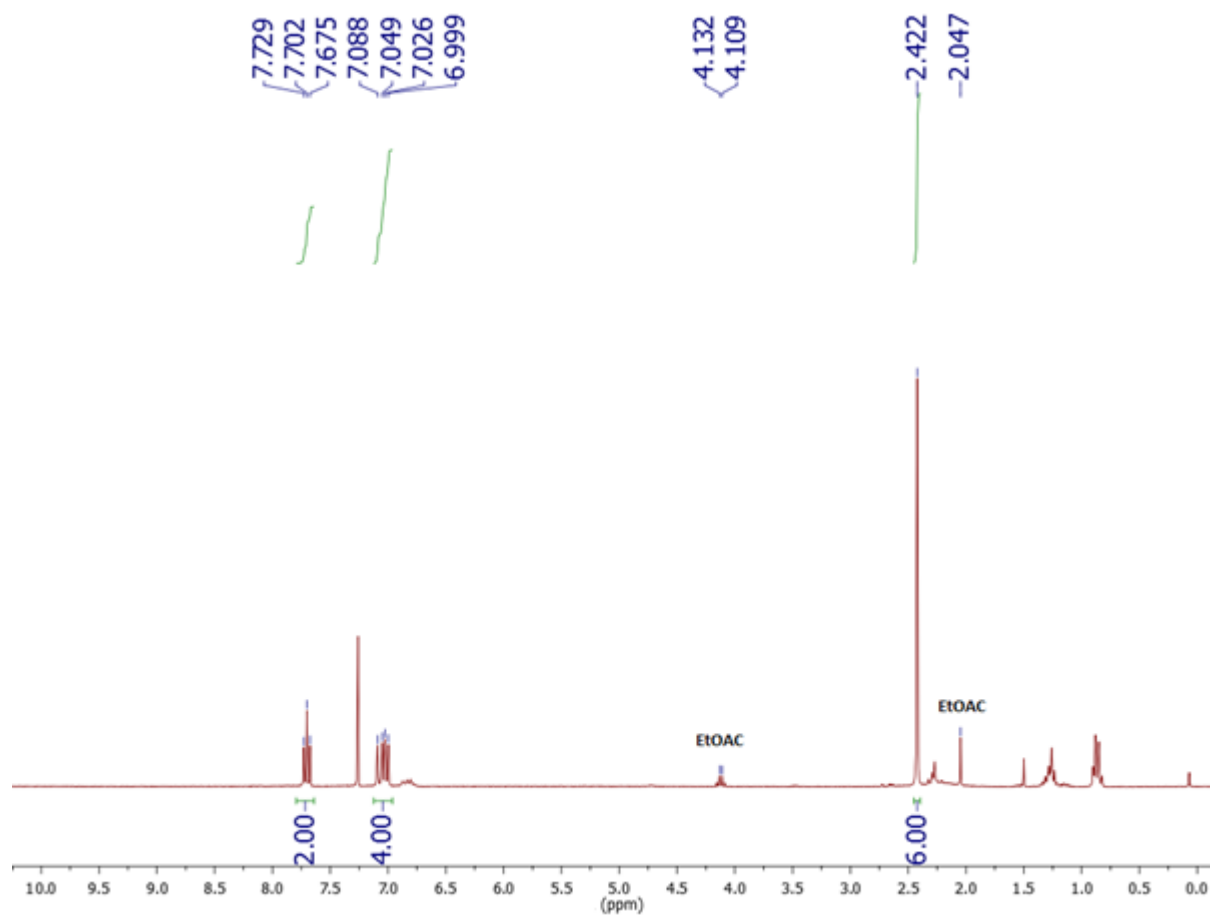
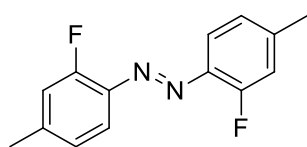


^1H NMR (300 MHz, CDCl_3)

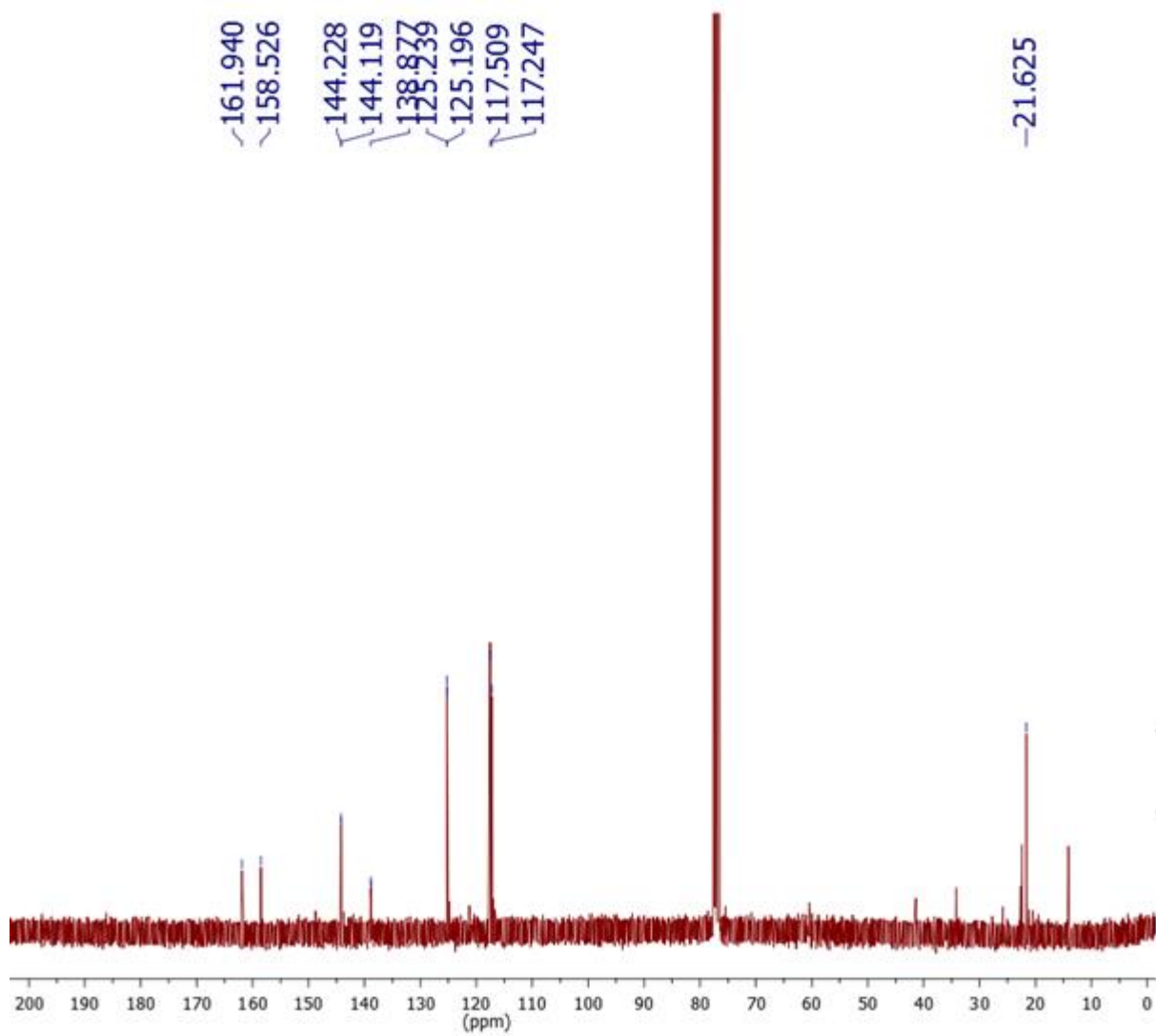


^{13}C NMR (75 MHz, CDCl_3)

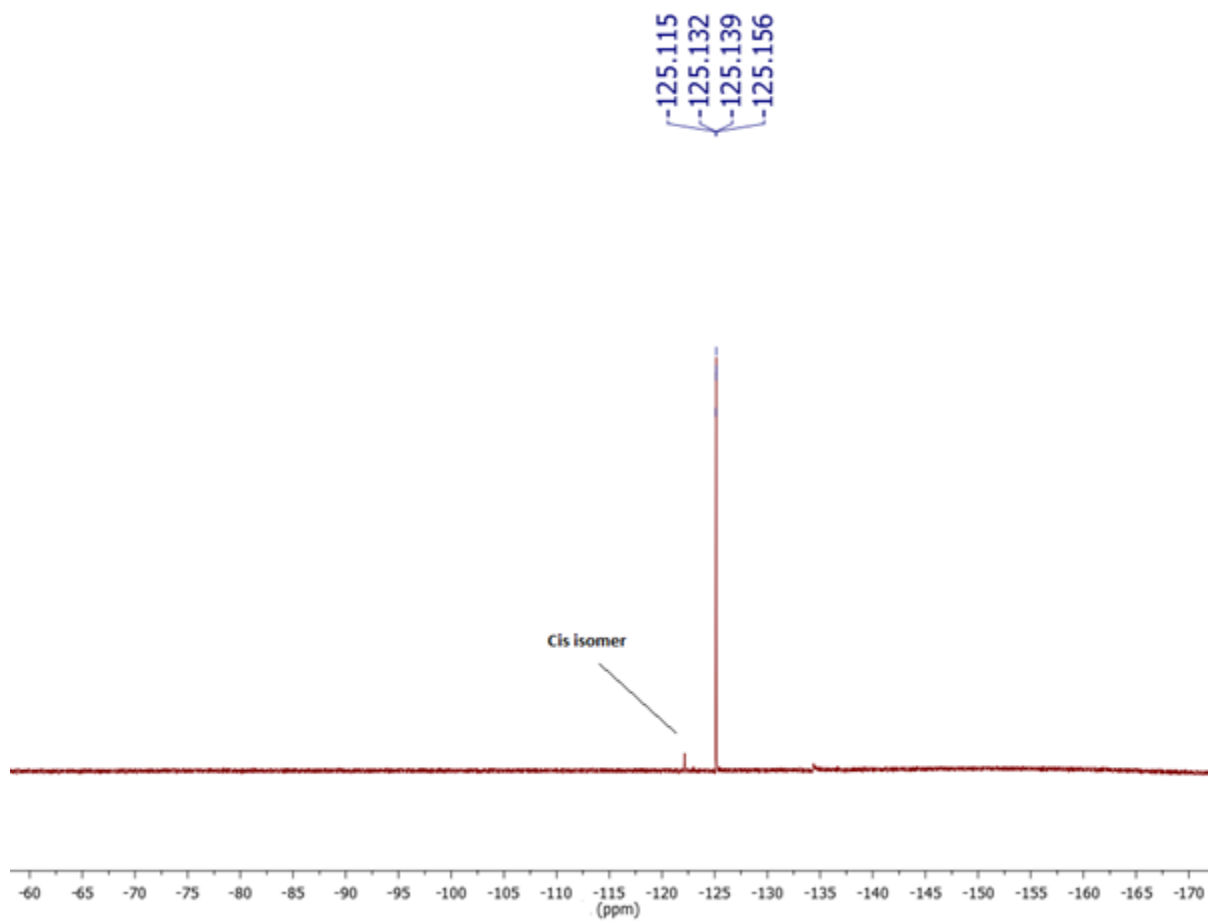
Compound 14



^1H NMR (300 MHz, CDCl_3)

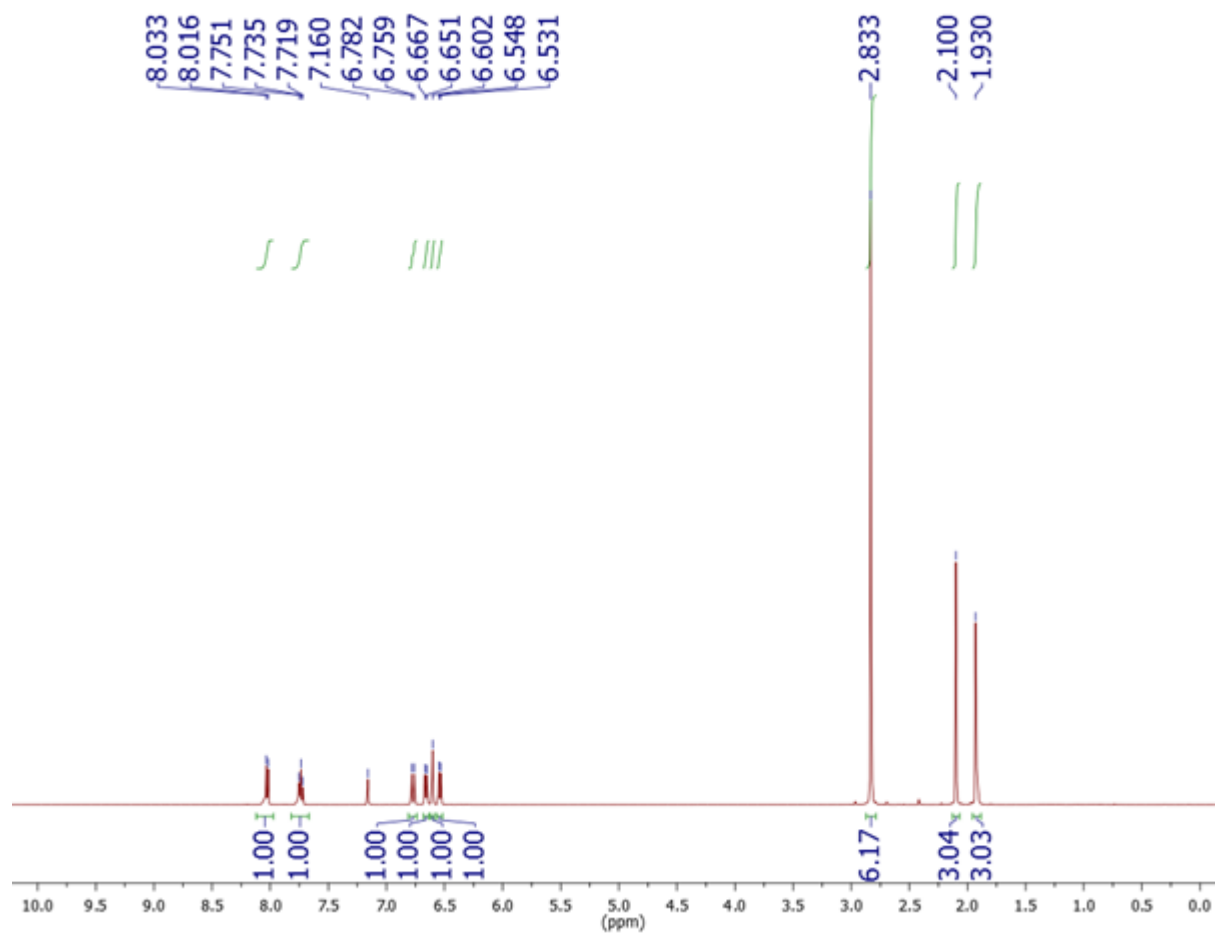
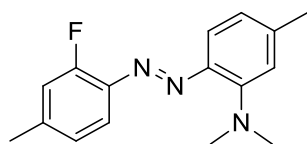


^{13}C NMR (75 MHz, CDCl_3)

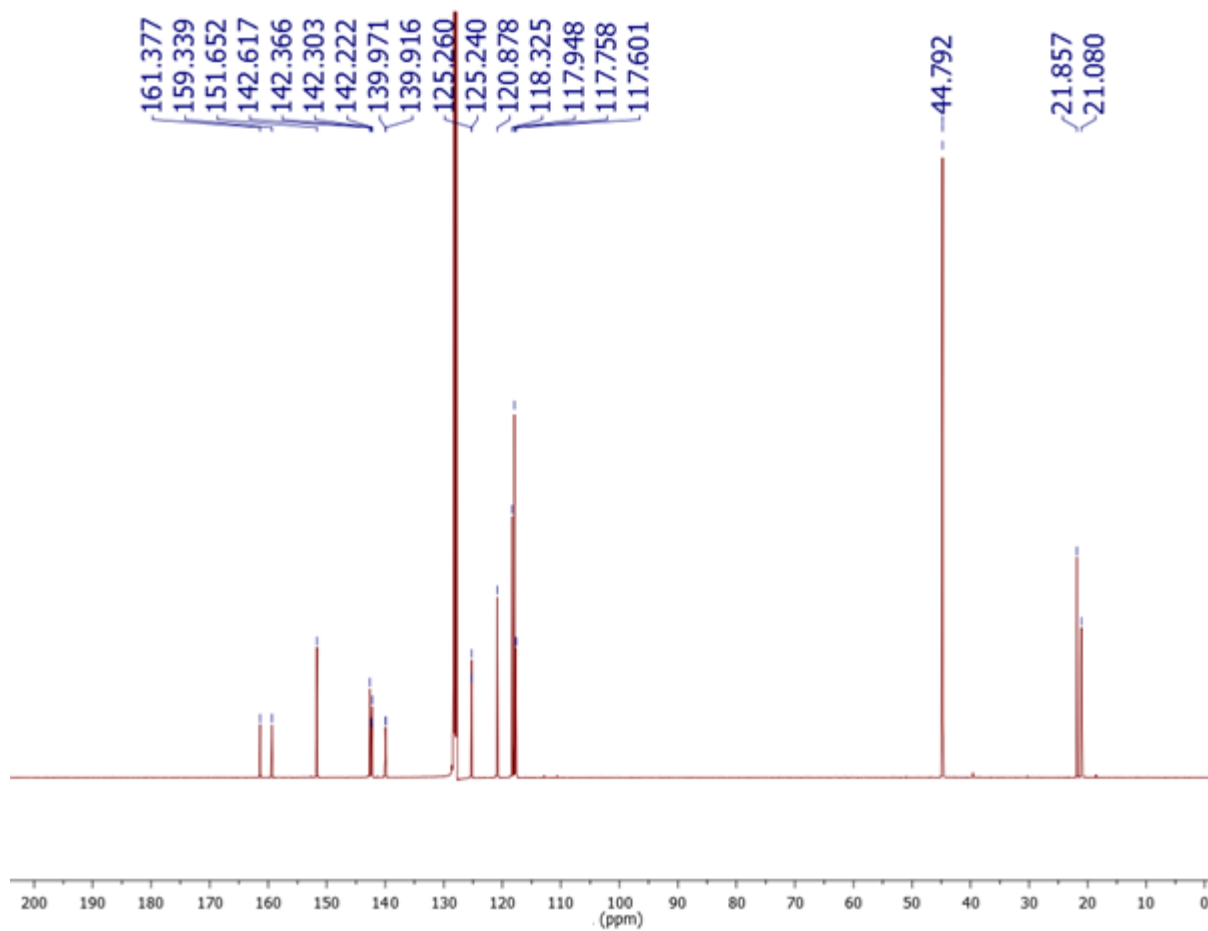


^{19}F NMR (471 MHz, CDCl_3)

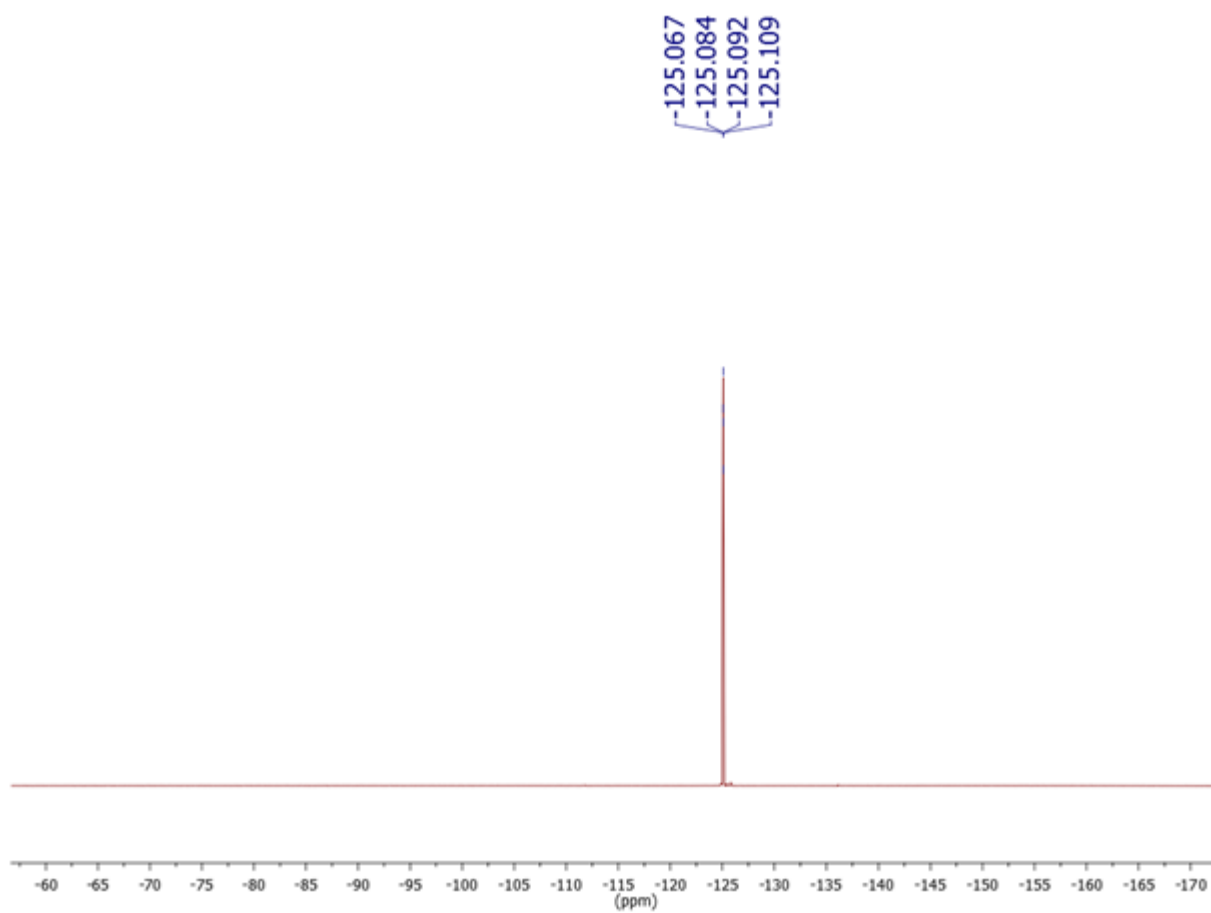
Compound 15



¹H NMR (500 MHz, C₆D₆)

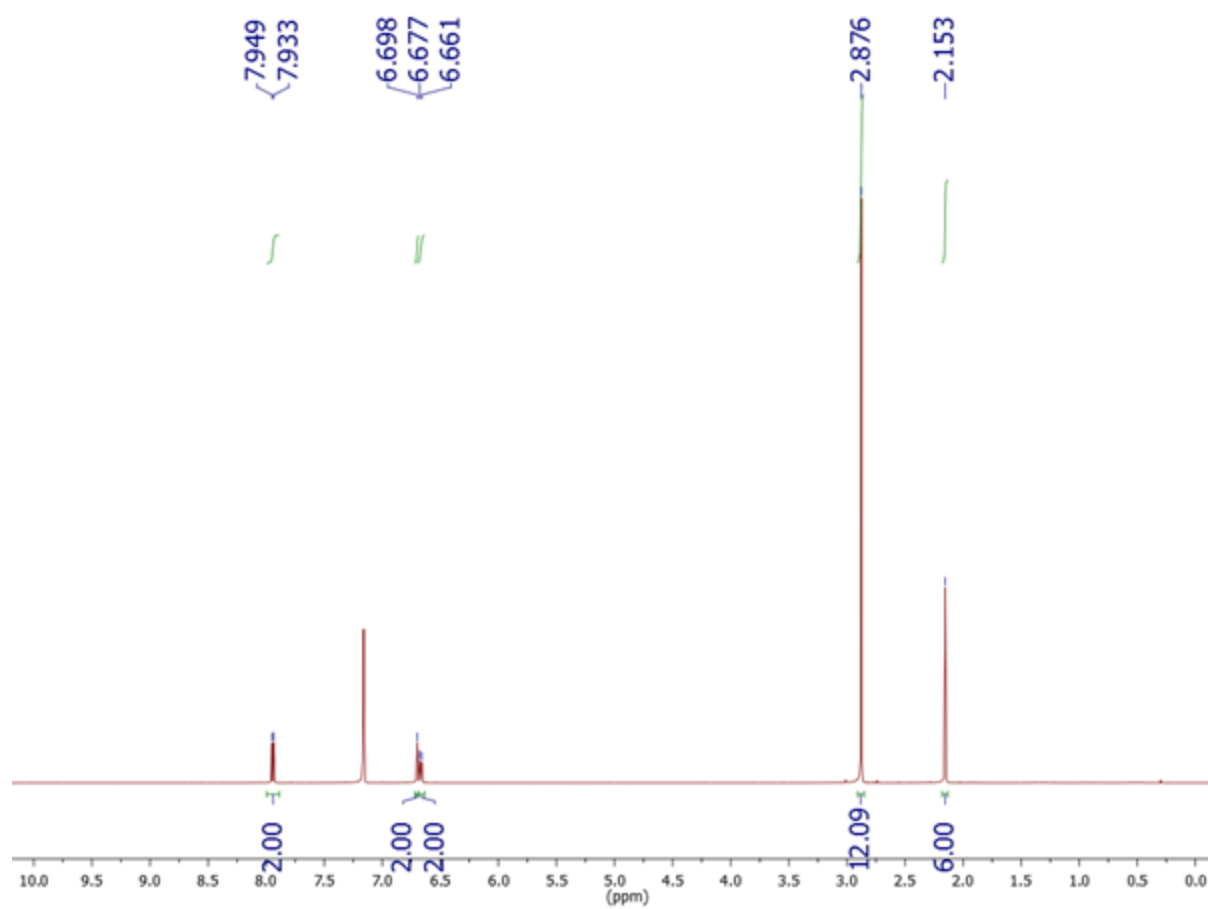
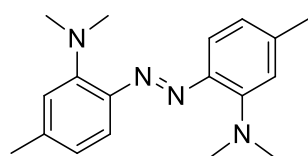


^{13}C NMR (125 MHz, C_6D_6)

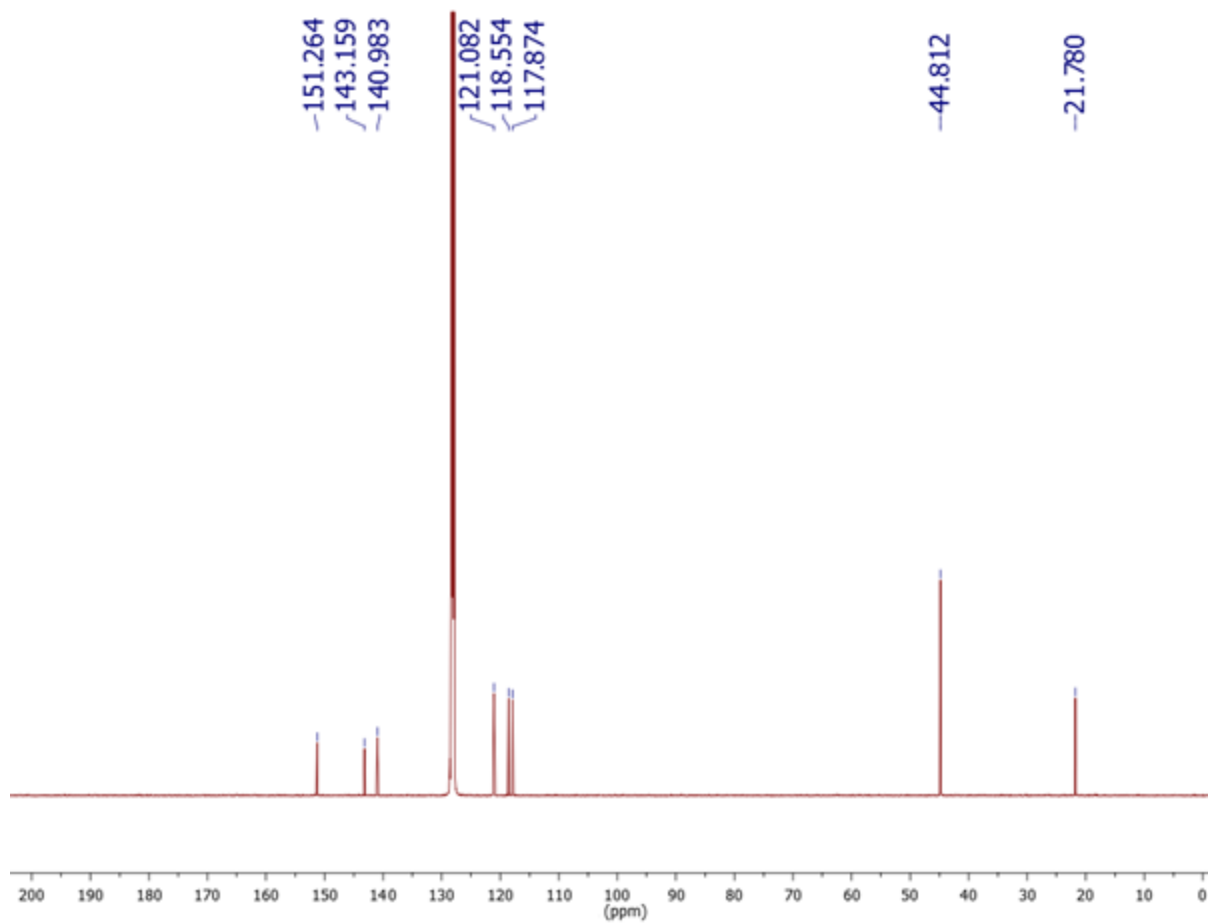


^{19}F NMR (471 MHz, C_6D_6)

Compound 16

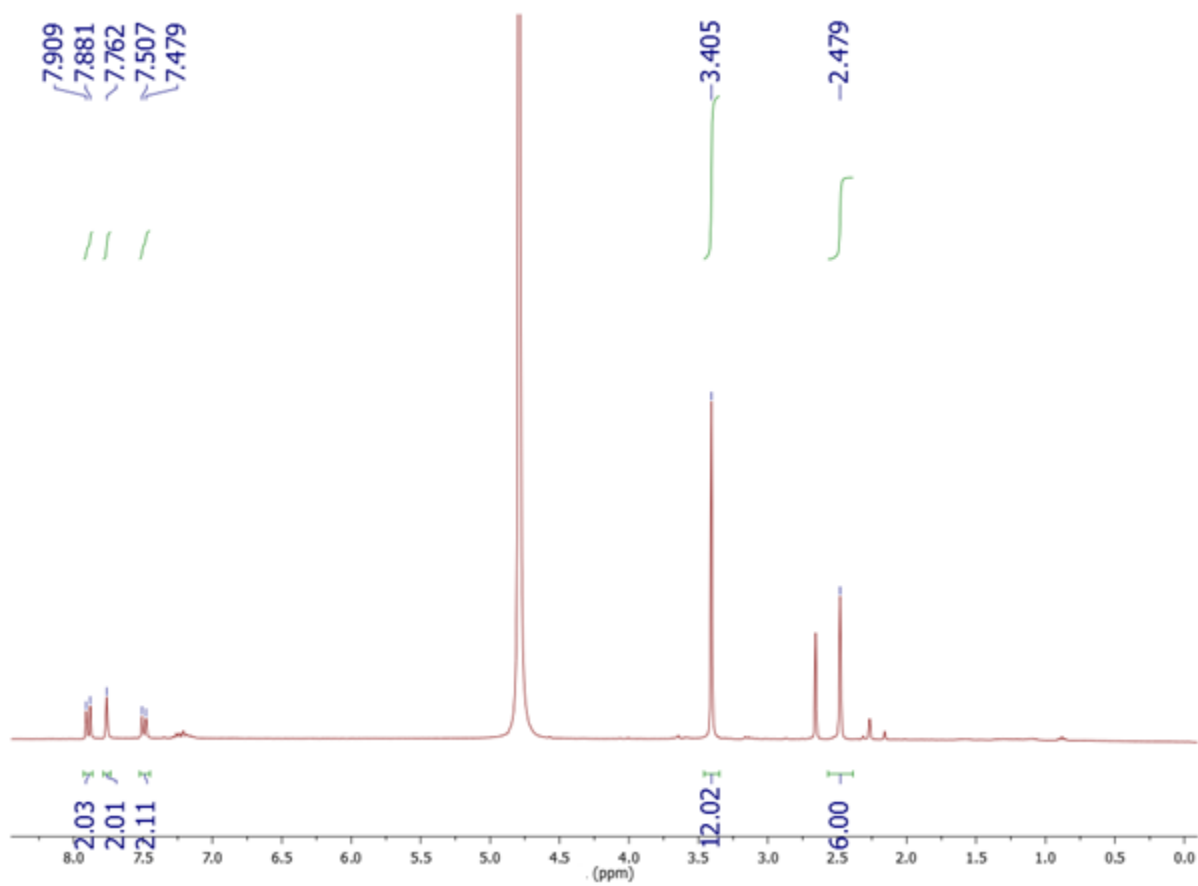


^1H NMR (500 MHz, C_6D_6)



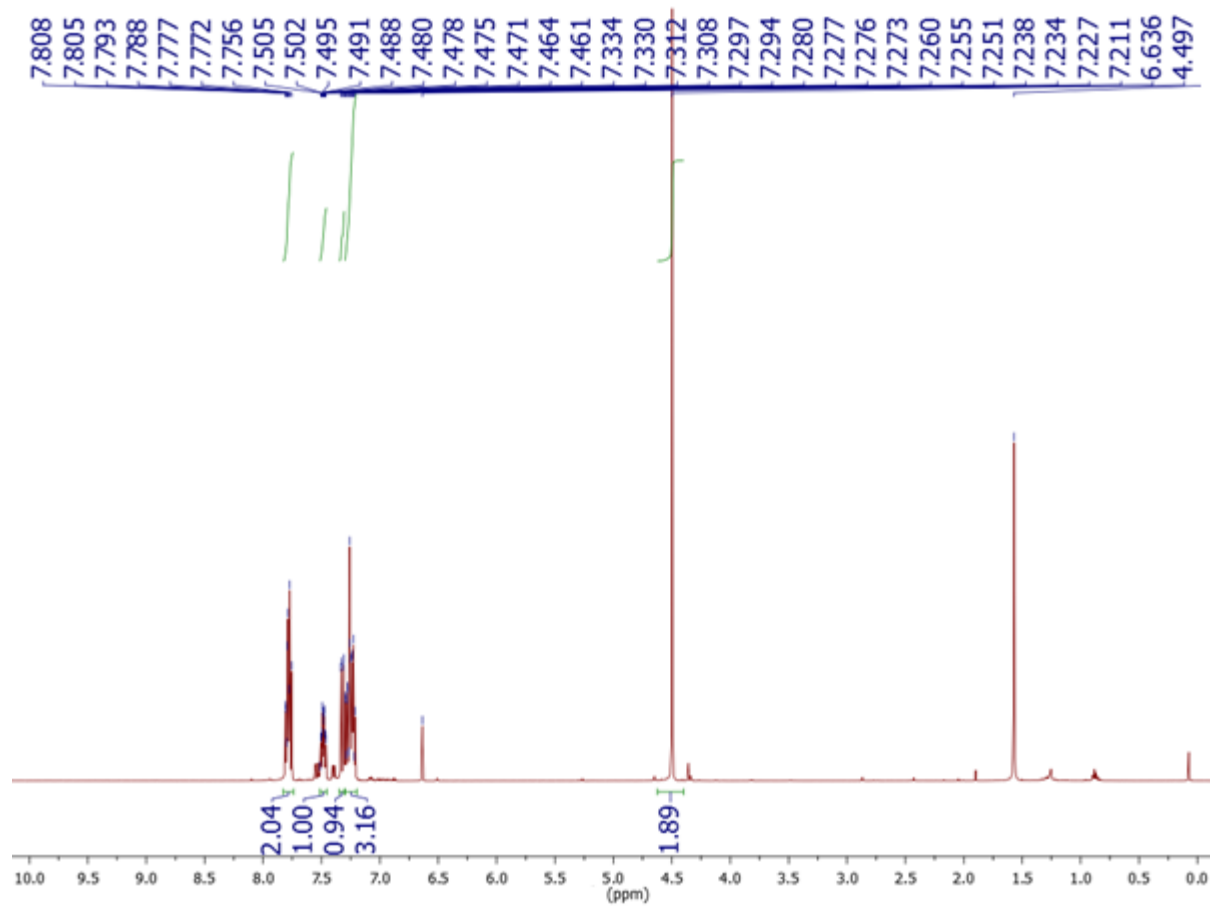
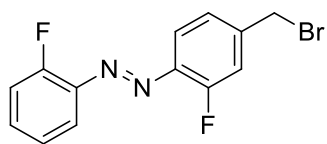
^{13}C NMR (125 MHz, C_6D_6)

Compound 18

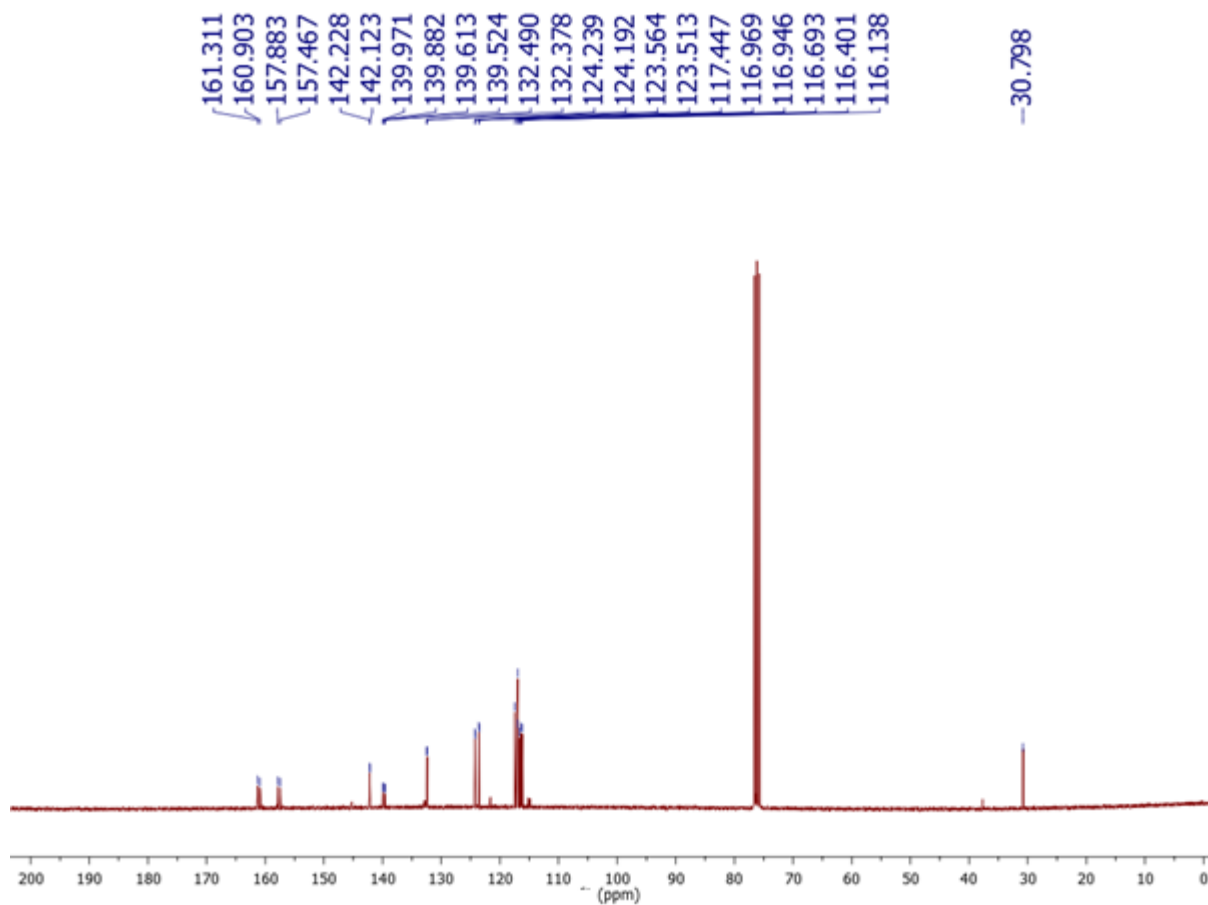


¹H NMR (300 MHz, D₂O)

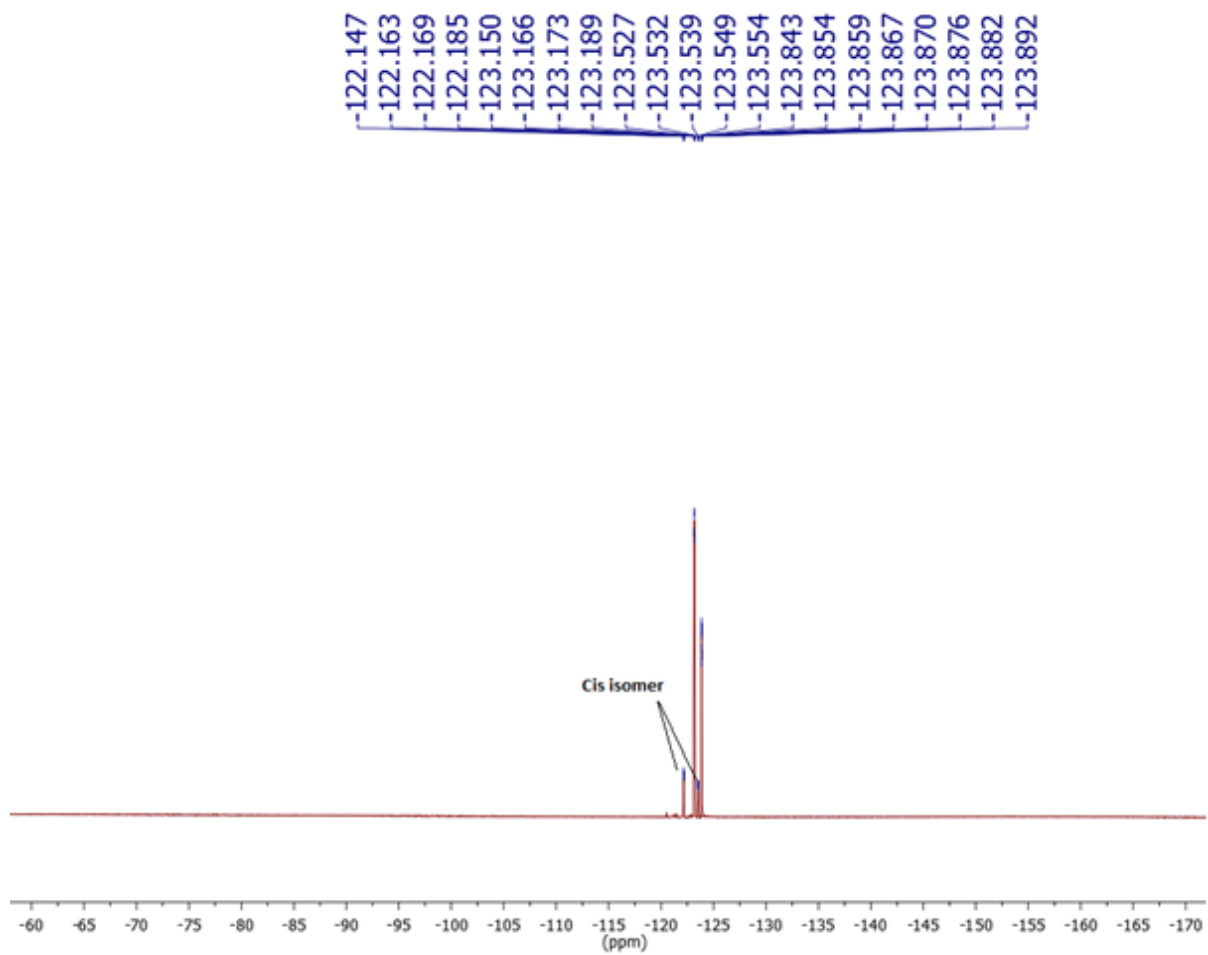
Compound 19



¹H NMR (500 MHz, CDCl₃)

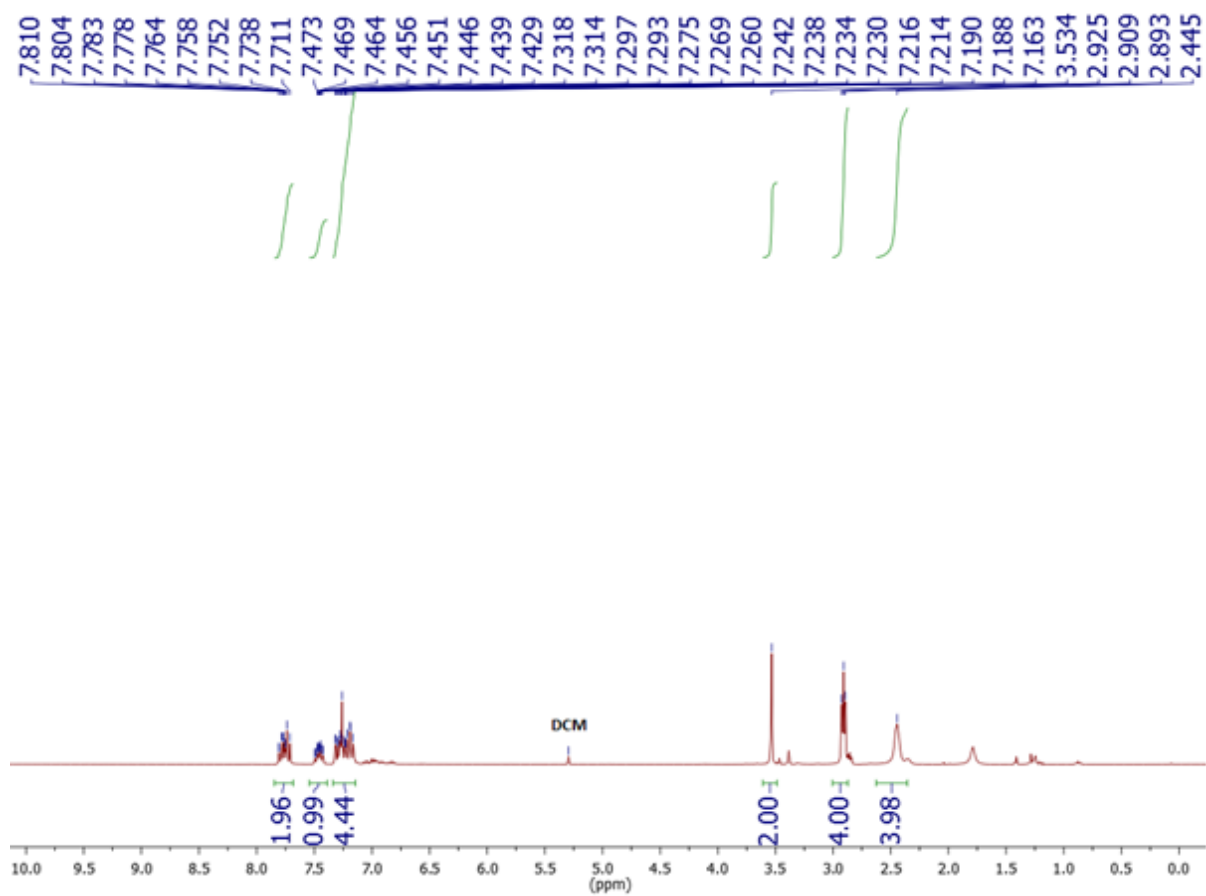
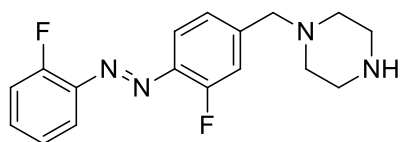


^{13}C NMR (75 MHz, CDCl_3)

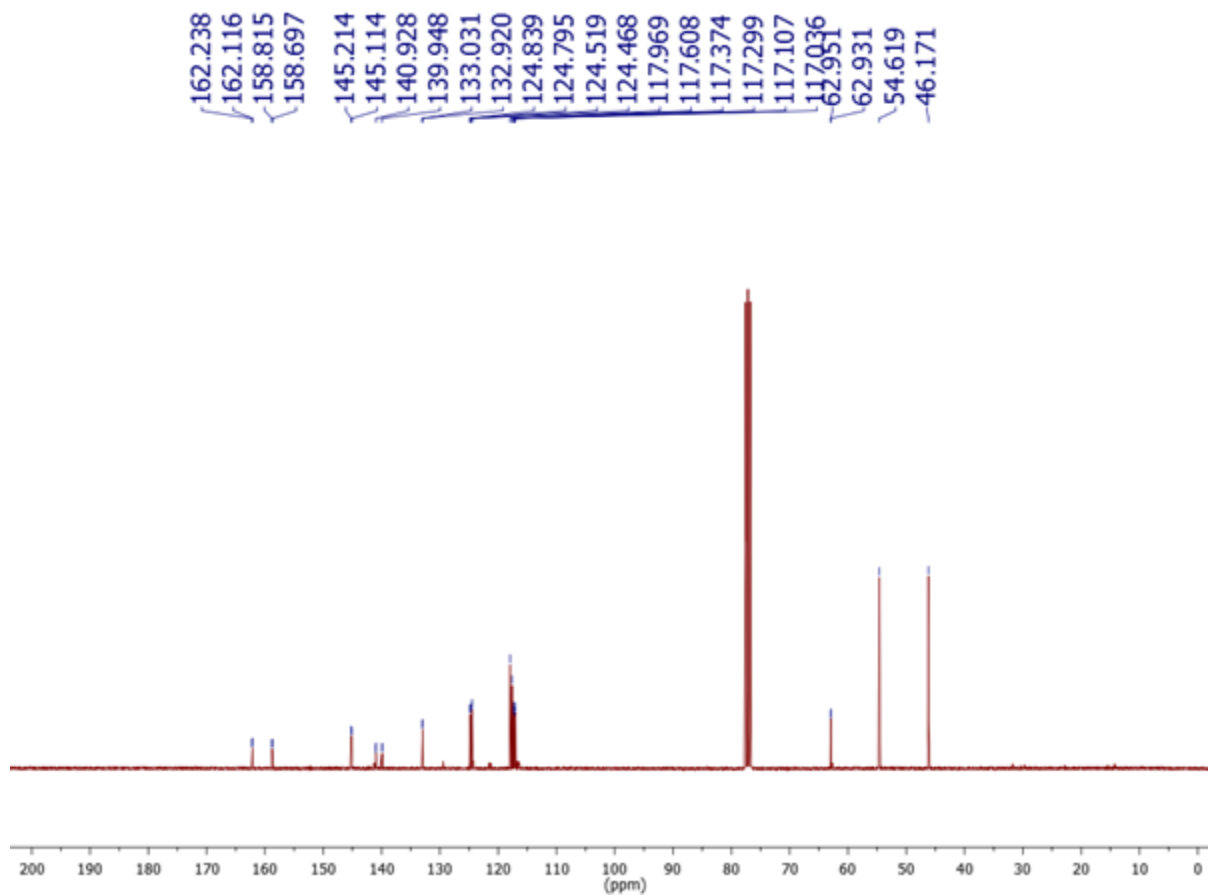


^{19}F NMR (471 MHz, CDCl_3)

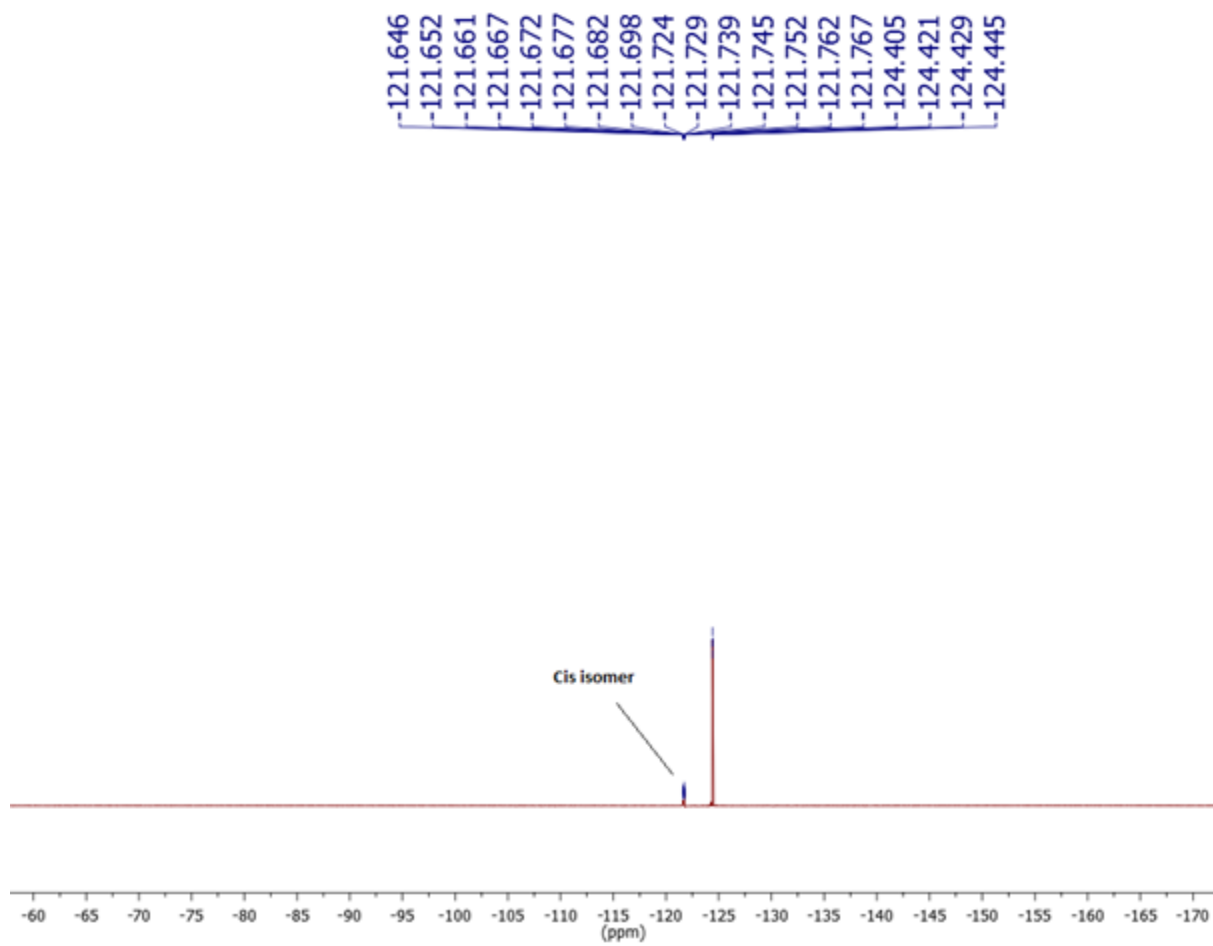
Compound 20



^1H NMR (300 MHz, CDCl_3)

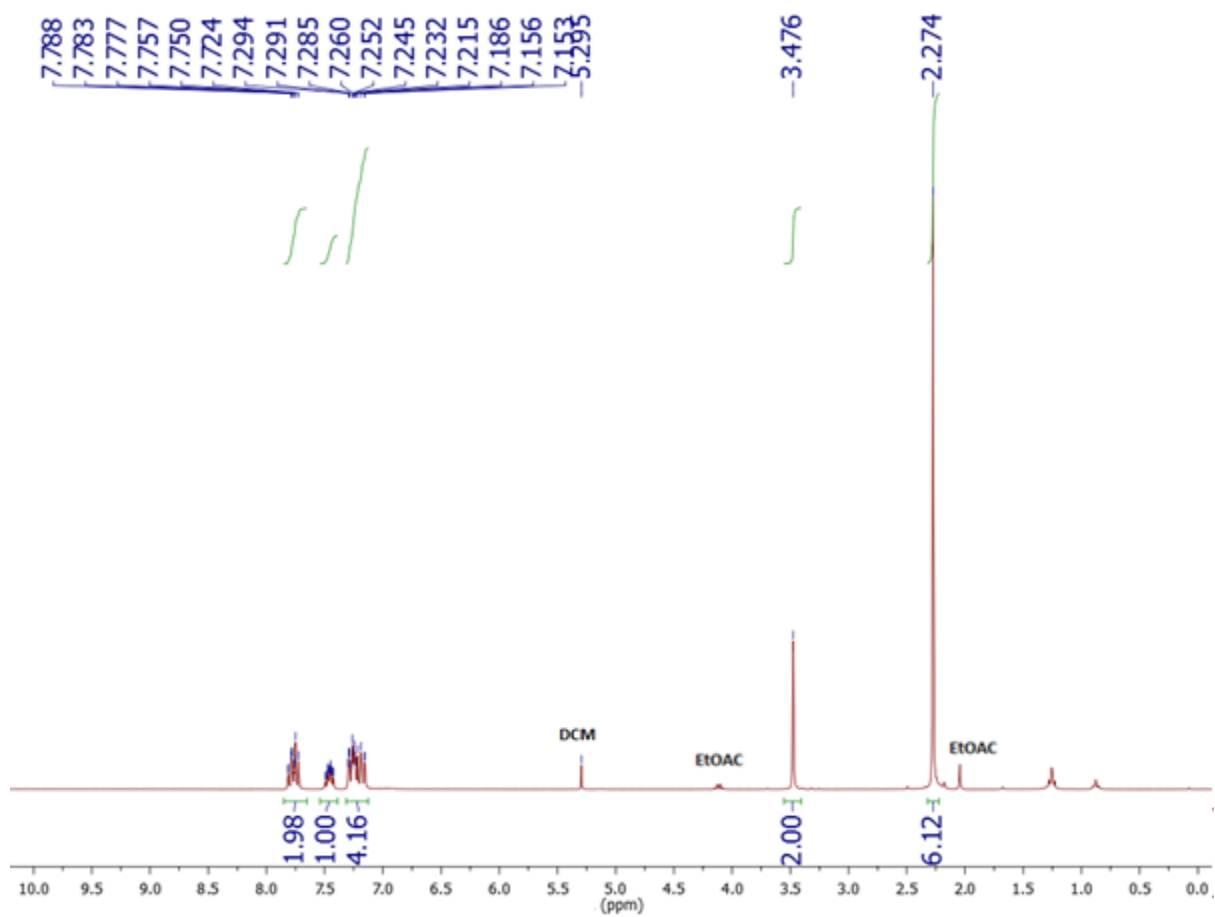
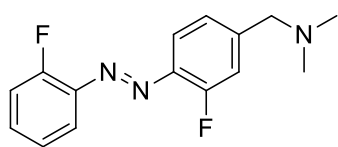


^{13}C NMR (75 MHz, CDCl_3)

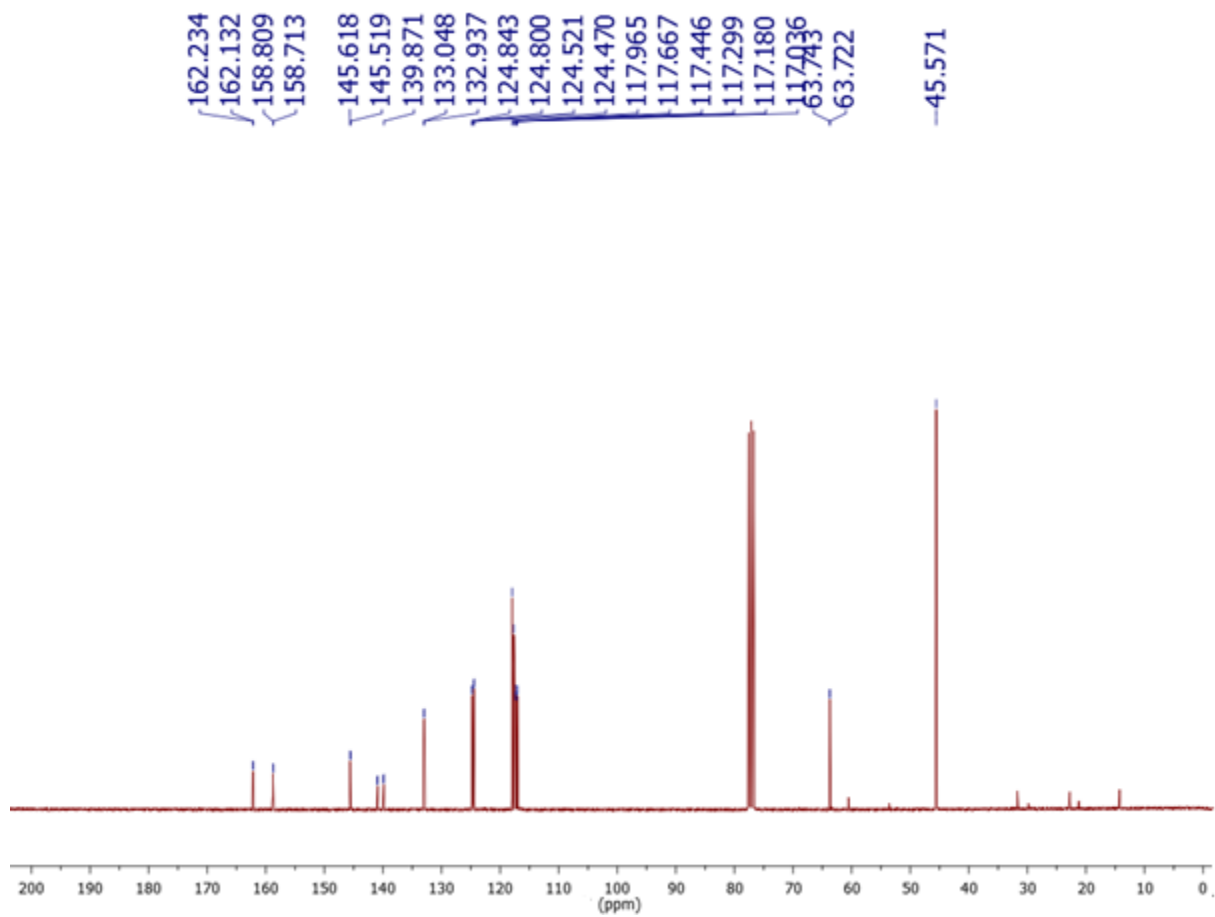


^{19}F NMR (471 MHz, CDCl_3)

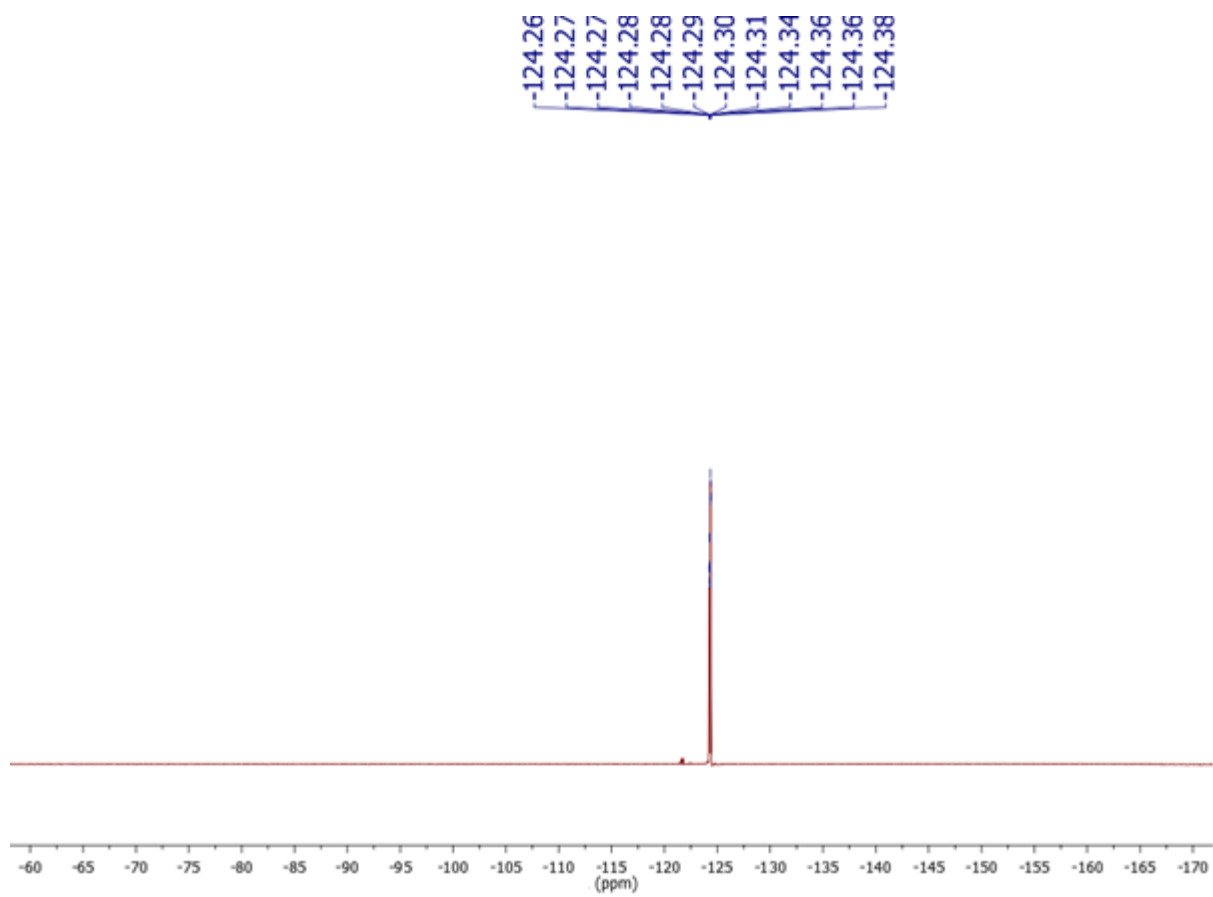
Compound **22**



¹H NMR (300 MHz, CDCl₃)



^{13}C NMR (75 MHz, CDCl_3)



^{19}F NMR (471 MHz, CDCl_3)